NASA CR-159855

CR159855
R80AEG514

NASA

National Aeronautics and
Space Administration

NASA-CR-159855
19810002720

EXPERIMENTAL EVALUATION OF COMBUSTOR CONCEPTS FOR BURNING BROAD-PROPERTY FUELS

by

J.M. Kasper
E.E. Ekstedt
W.J. Dodds
M.W. Shayeson

GENERAL ELECTRIC COMPANY

September 1980

Prepared For

National Aeronautics and Space Administration

1. Report No. NASA CR-159855	2. Government Accession No.	3. Recipient's Catalog No.
4. Title and Subtitle EXPERIMENTAL EVALUATION OF COMBUSTOR CONCEPTS FOR BURNING BROAD SPECIFICATION FUELS		5. Report Date September 1980
		6. Performing Organization Code
7. Author(s) J.M. Kasper, E.E. Ekstedt, W.J. Dodds, M.W. Shayeson		8. Performing Organization Report No. R80AEG514
		10. Work Unit No.
9. Performing Organization Name and Address General Electric Company Aircraft Engine Group Cincinnati, Ohio 45215		11. Contract or Grant No. NAS2-21594
		13. Type of Report and Period Covered Contractor Report
12. Sponsoring Agency Name and Address National Aeronautics and Space Administration Washington, D.C. 20546		14. Sponsoring Agency Code

15. Supplementary Notes
Project Manager: A.L. Smith
NASA-Lewis Research Center
Cleveland, Ohio 44135

16. Abstract

A baseline CF6-50 combustor and three advanced combustor designs were evaluated to determine the effects of combustor design on operational characteristics using broad-property fuels. Three fuels were used in each test: Jet A, a broad-property 13% hydrogen fuel, and a 12% hydrogen fuel blend. Testing was performed in a sector rig at true-cruise and simulated-takeoff conditions for the CF6-50 engine cycle.

The advanced combustors (all double-annular, lean-dome designs) generally exhibited lower metal temperatures, exhaust emissions, and carbon buildup than the baseline CF6-50 combustor. The sensitivities of emissions and metal temperatures to fuel hydrogen content were also generally lower for the advanced designs. The most promising advanced design used premixing tubes in the main stage. This design was chosen for additional testing in which fuel/air ratio, reference velocity, and fuel-flow split were varied.

17. Key Words (Suggested by Author(s)) Combustion Fuels Combustor Design	18. Distribution Statement Unclassified – Unlimited	
19. Security Classif. (of this report) Unclassified	20. Security Classif. (of this page) Unclassified	21. No. of Pages 166	22. Price*

N 81-11228#

FOREWORD

The work described herein was conducted by the General Electric Company, Aircraft Engine Business Group, under Contract NAS3-21594. The work was performed under the direction of the NASA Project Manager, Arthur L. Smith.

Key General Electric contributors to this program were: E.J. Rogala, Program Manager; E.E. Ekstedt, Technical Program Manager; C.C. Gleason, Principal Investigator; W.J. Dodds, Combustor Design; J.M. Kasper, Combustor Design and Evaluation; C.A. Martin, Combustor Testing; and V.M. Cecil, Data Reduction and Graphics.

TABLE OF CONTENTS

LIST OF ILLUSTRATIONS

LIST OF ILLUSTRATIONS (Continued)

LIST OF TABLES

1.0 SUMMARY

The objective of this program was to evaluate the use of advanced combustor concepts as a means of accommodating possible future broad-property fuels.

The evaluations consisted of sector combustor tests using a three-swirl-cup-sector, CF6-50 test rig. The various combustor configurations were evaluated at true cruise and simulated takeoff conditions for the CF6-50 engine cycle. In each test, the combustors were evaluated with three fuels:

- Jet A – 14% hydrogen by weight

- Broad-Property Fuel – 13% hydrogen by weight

- Special Blend – 12% hydrogen by weight

The program included one test of a current-production CF6-50 combustor configuration, to serve as a baseline for comparison; one screening test each of three advanced, double-annular-combustor concepts; and a parametric test of a selected combustor. The three advanced, double-annular-combustor concepts consisted of: (1) a concept employing high-pressure-drop fuel nozzles for improved atomization, (2) a concept with premixing tubes in the main stage, and (3) a concept with the pilot stage on the inside and the main stage on the outside (the reverse of the other two concepts). This last concept was intended to reduce the main-stage length (and, therefore, residence time and NO_x emissions) and to provide an improved exit-temperature radial profile.

The baseline CF6-50 burner was tested first. The baseline burner demonstrated sensitivity to fuel hydrogen content with regard to smoke, NO_x (takeoff), and liner temperatures. Concept 1 produced low smoke levels; it showed little sensitivity to fuel hydrogen content with regard to smoke levels and metal temperatures, and it had no combustion stability problems. NO_x levels were lower than CF6-50 levels but higher than Concept 2 levels. Concept 2 produced the lowest NO_x levels. The dome was very clean with virtually no carbon deposits. Smoke levels were lower than those of the baseline combustor, and no combustion instability was observed at any operating condition. Liner temperatures were low except for a region on the inner liner downstream of the premixing tubes, and the higher temperatures in this region were not considered a major problem. Concept 3 produced the lowest smoke levels and demonstrated that the radial temperature profile could be inverted by reversing the pilot- and main-stage domes in a double-annular combustor. The NO_x levels were between those measured for the other two concepts. However, this combustor encountered combustion resonance and flame-instability problems in the dome at some operating conditions.

Concept 2 was chosen for the parametric test. In the screening tests, Concept 2 had demonstrated the potential of a premixed-prevaporized design in achieving low NO_x levels and clean liners and domes. The Concept 1 test had shown that the use of high-pressure-differential (ΔP) fuel nozzles produced no significant improvement over the low-ΔP fuel nozzles used in similar combustor designs developed in previously conducted programs. Data from the Concept 3 test were considered nonrepresentative of the potential of the concept because of combustion instability and resonance problems. Thus, Concept 2 was chosen for the parametric testing. Although no refinements or development tests to resolve problems were conducted on these advanced designs, they all appear to have potential for use with fuels with broadened properties.

The parametric test demonstrated that the CO emission index increased with reference velocity; however, NO_x emission index, smoke number, and metal temperatures decreased with reference velocity. The CO emission index decreased with increasing pilot/total fuel-flow ratio, but the NO_x emission index increased with increases in this ratio. The parametric-test burner (Concept 2) yielded the least carbon deposits of all burners tested.

2.0 INTRODUCTION

Current fuel specifications for aircraft gas-turbine engines were established when there was an abundance of high-quality, domestic, petroleum resources. Presently, however, the United States is highly dependent upon foreign supplies, and demand is projected to increasingly exceed petroleum availability sometime after 1985 (Reference 1). Because of the projected changes in the composition and quality of petroleum-crude supplies during the next decade and thereafter, together with the expected associated diminishing availability of these crude supplies, it is anticipated that operation of aircraft turbine engines with fuels of broader specification than those presently available will be required. For these reasons, a set of specifications for broad-property fuel (BPF) was evolved during the NASA-Lewis workshop in Jet Aircraft Hydrocarbon Fuels Technology in 1977 (Reference 1). The primary purpose of establishing this test-fuel specification was to define a reference fuel (12.8 ± 0.20% hydrogen by weight) to permit comparisons of test results from different experiments.

As typified by the test-fuel specification, broad-property jet fuels of the future are expected to contain higher aromatic contents (or lower hydrogen contents), higher final boiling points, and lower thermal-stability limits than those allowed with present-day jet fuels. In current-technology combustors, the differences among these key fuel properties can be expected to result in increased carbon deposition and fuel-injector plugging tendencies plus increased smoke, NO_x, and CO/HC emission levels. Any significant increases in carbon deposition can be expected to result in combustor performance deterioration. In addition to objectionable exhaust visibility, any increases in smoke level will be accompanied by increased flame luminosity and, in turn, higher combustor metal temperatures with consequent reduced combustor life. Several recently developed combustor-dome concepts show promise for reduced smoke and NO_x emission levels using currently available fuel. The objective of this program was to evaluate experimentally the effects of broad-property fuels on the carboning tendencies, emissions levels, and metal temperatures of these advanced combustor concepts.

As a result of Government and industry efforts initiated more than 12 years ago, significant advances have been made in the development of smoke-abatement technology for aircraft turbine engines. Modern engines using JP-4 and Jet A fuels, such as the General Electric (GE) CF6, operate with virtually invisible smoke levels and, thus, are already in compliance with current smoke-emission standards of the Environmental Protection Agency (EPA). However, compliance with current EPA standards for gaseous emissions requires large reductions in the emission levels of all current-technology engines. Major advances in combustor-design technology are needed to attain these significant reductions in gaseous pollutant emission levels.

To provide the needed combustor technology advances, the Experimental Clean Combustor Program (ECCP) was initiated by the U.S. National Aeronautics and Space Administration (NASA) in 1972. The overall objective of this major program was to define, develop, and demonstrate technology for the design of low-pollutant-emission combustors for use in advanced, commercial, conventional-takeoff-and-landing aircraft with high-pressure-ratio engines (in the range of 20 to 35). The NASA/GE ECCP was one of a number of subprograms that composed the overall program. As part of this program, staged-combustor design concepts were developed in order to reduce NO_x and smoke emissions. Significant reductions (40 to 90%) in each of the gaseous emissions were demonstrated (Reference 2).

Further work on advanced, double-annular combustors was done during the NASA/GE Quiet, Clean, Short-haul, Experimental Engine (QCSEE) program. The objective of that program was to demonstrate an advanced-technology engine suitable for short-range commercial applications. The QCSEE Clean Combustor Program was part of this engine-development program and dealt specifically with a QCSEE combustor designed to meet the 1979 EPA gaseous-emissions standards for Class T2 engines. A combustor design was evolved which complied with EPA standards. This combustor yielded significant reductions in CO and HC emission levels at low-power operating conditions, along with significant reductions in NO_x emission levels at high-power conditions, compared to the CO, HC, and NO_x emission levels of the reference F101 engine combustor (Reference 3).

As a part of the NASA/GE ECCP, some tests of prototype versions of the advanced combustors tested in this program were conducted with several alternative blends of hydrocarbon fuel. These tests clearly showed that, compared to current-technology combustors such as used in the current-production CF6-50, these low-emissions combustor design concepts can accommodate the use of broad-property fuels with less severe impacts on performance and emissions characteristics. The advanced combustor configurations tested in this program were designed for significantly enhanced capabilities for satisfactorily accommodating broad-property fuels, and they were specifically designed to further improve smoke and carbon suppression relative to the final versions of the combustors that were evolved in the NASA/GE ECCP.

3.0 DESIGN APPROACHES

3.1 COMBUSTOR CONCEPTS

The current-production CF6-50 combustor was chosen as the baseline combustor of this program. The CF6-50 is a modern, high-bypass, turbofan engine that is in commercial service as the power plant for the McDonnell Douglas DC-10 Series 30 Tri-Jet long-range intercontinental aircraft and the Airbus Industrie A300B aircraft. The CF6-50 engine is a dual-rotor, high-bypass-ratio turbofan incorporating a variable-stator, high-pressure-ratio compressor; an annular combustor; an air-cooled, core-engine turbine; and a coaxial front fan with a low-pressure turbine. The major features of the engine are shown in Figure 1. The CF6-50 combustor is very representative of modern-technology combustors used in commercial aircraft. This combustor was designed and developed to operate, using present-day jet fuels, with low smoke levels and without carbon-deposition problems. As a consequence, the primary-combustion-zone design technology evolved from this program is expected to be generally applicable to a variety of modern turbine engine applications.

Several models of the CF6-50 engine are currently in production. The CF6-50C model was selected for combustor design and test conditions. Key, standard-day, combustor-operating conditions for this model are presented in Table I. The high-power operating conditions in Table I are averages from acceptance tests of 17 production engines and are essentially the same as the early cycle data.

The CF6-50 combustor is a high-performance design with demonstrated low exit-temperature pattern factors, low pressure loss, high combustion efficiency, and low-smoke-emission performance at all operating conditions. A cross-sectional drawing of this combustor, as installed in an engine, is presented in Figure 2. Key features are a low-pressure-loss step diffuser, a carbureting swirl-cup dome design, and the short burning length. Additional details of the CF6-50 engine and combustor are contained in Reference 4; the full annular burner is shown in Figure 3.

The three advanced combustor designs are shown in Figures 4 through 6. These designs were all of the double-annular type and drew heavily on experience gained in the NASA/GE ECCP and QCSEE programs. These designs were similar to the ECCP double-annular combustor (Figure 7) except that they included features intended to improve fuel atomization and fuel-air mixing in the dome region. All were sized for the CF6-50 combustor flowpath.

Concept 1, shown in Figure 4, had the pilot dome on the outside with the main or high-power stage on the inside. Each dome employed three swirl cups because the test combustors were 36° sectors; each dome would have 30 swirl cups for a full-annular combustor. The swirl cups were adaptations of designs developed during the QCSEE combustor program. Each QCSEE swirl cup had an axial primary swirler and a radial secondary swirler; ECCP swirl cups had axial primary and secondary swirlers. The radial secondaries are more compact
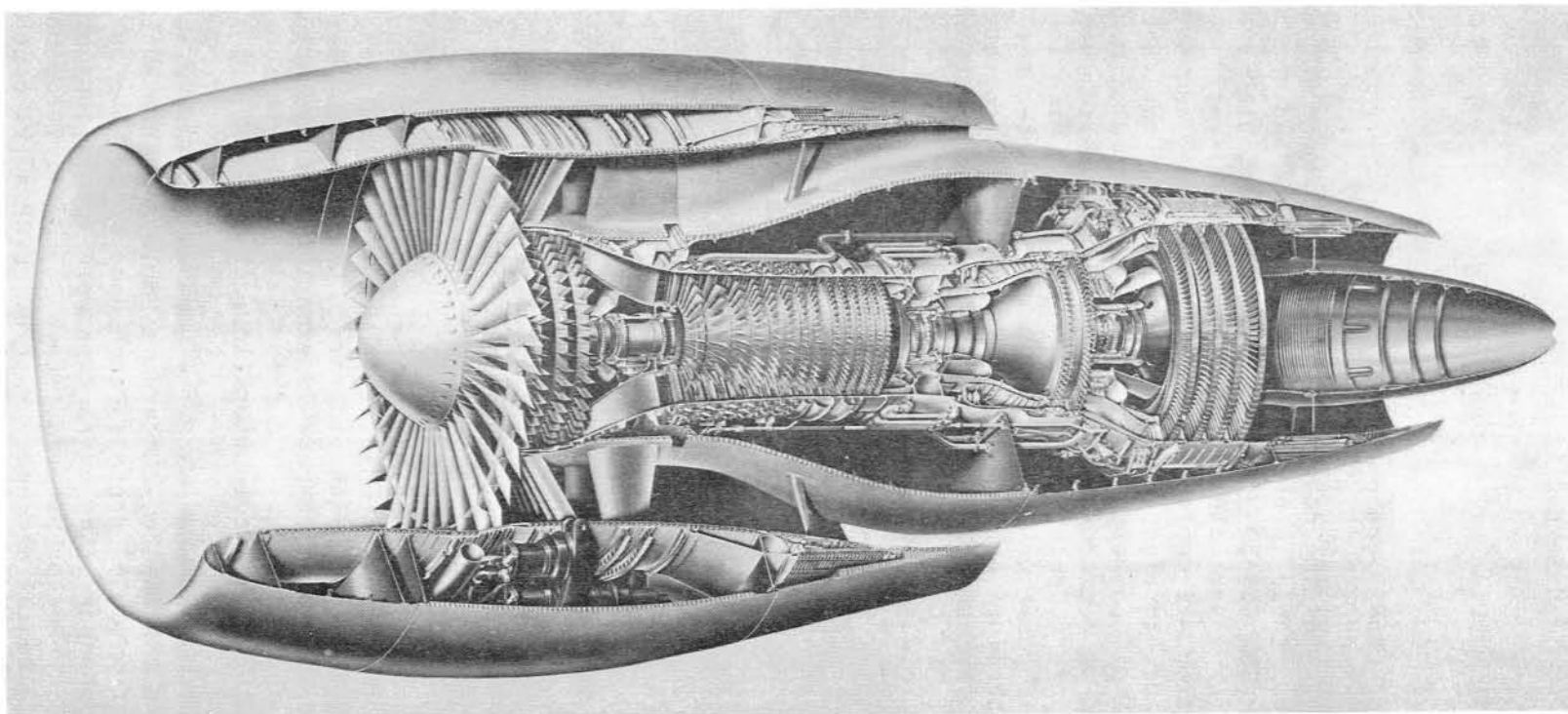
Figure 1. General Electric CF6-50 High-Bypass Turbofan Engine.

Table I. CF6-50 Engine/Combustor Operating Conditions.

- Standard Day Conditions
- No Bleed-Air Extraction
- Jet A Fuel

Parameter	Units	Idle[1]	Approach[1]	Cruise[2]	Climb[1]	Takeoff[1]
Installed Net Thrust	kN	7.53	66.59	47.23	188.66	221.95
Percent Takeoff Thrust	%	3.39	30.0	---	85.0	100.0
High-Pressure-Compressor Physical Speed	rpm	6412	8620	9585	9890	10150
High-Pressure-Compressor Discharge Total Pressure	atm	2.92	11.7	11.4	25.9	29.8
High-Pressure-Compressor Discharge Total Temperature	K	429	630	733	786	820
High-Pressure-Compressor Discharge Airflow	kg/s	16.37	56.7	49.5	109.3	122.0
Combustor Airflow	kg/s	13.81	47.6	41.8	92.1	103.0
Ideal Fuel Flow[3]	kg/hr	547	2395	3159	7104	8573
Combustor Reference Velocity	m/s	15.4	19.5	20.4	21.3	21.5
Combustor Fuel/Air Ratio[3]	---	0.0110	0.0140	0.0210	0.0214	0.0231

[1]Sea Level Static

[2]Altitude = 10.67 km, Flight Mach Number = 0.85

[3]Assumes Combustion Efficiency = 100%

7

Burning Length

Carbureting Dome
Swirl Cups

Diffuser
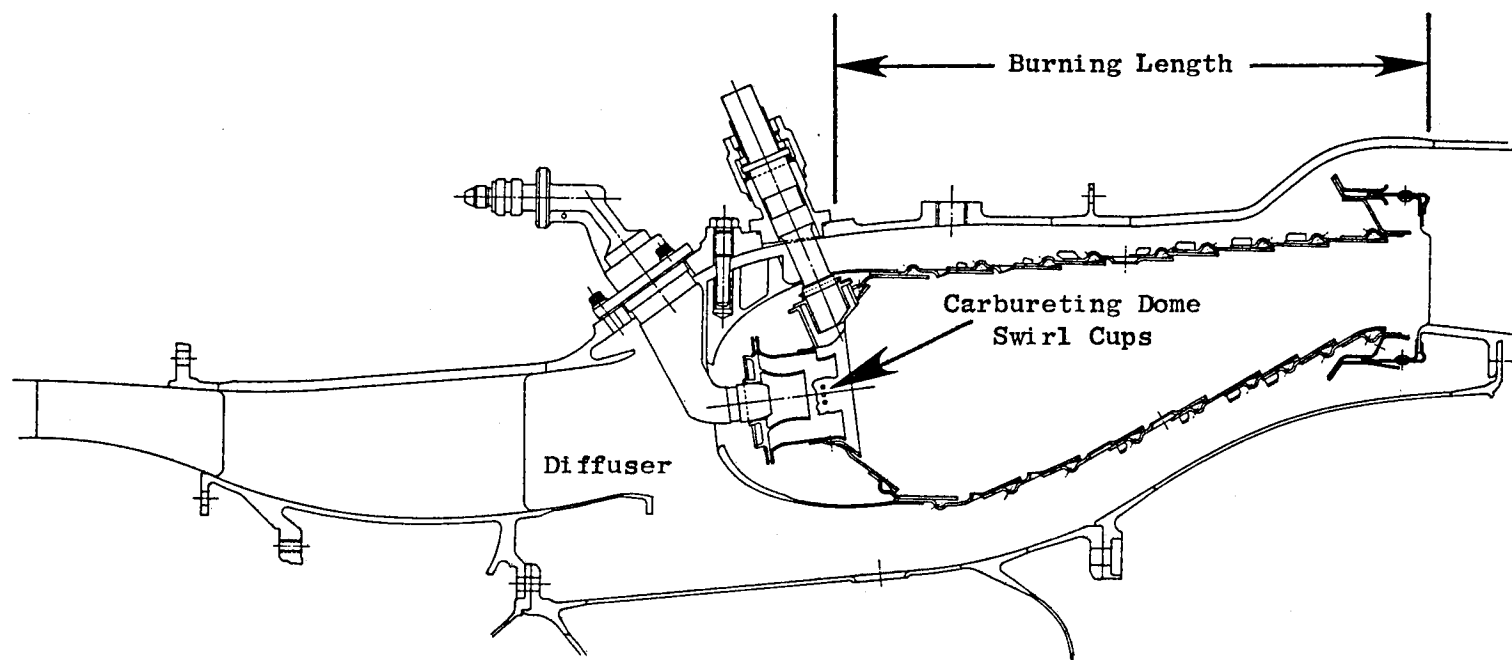
Figure 2. Production CF6-50 Combustor.
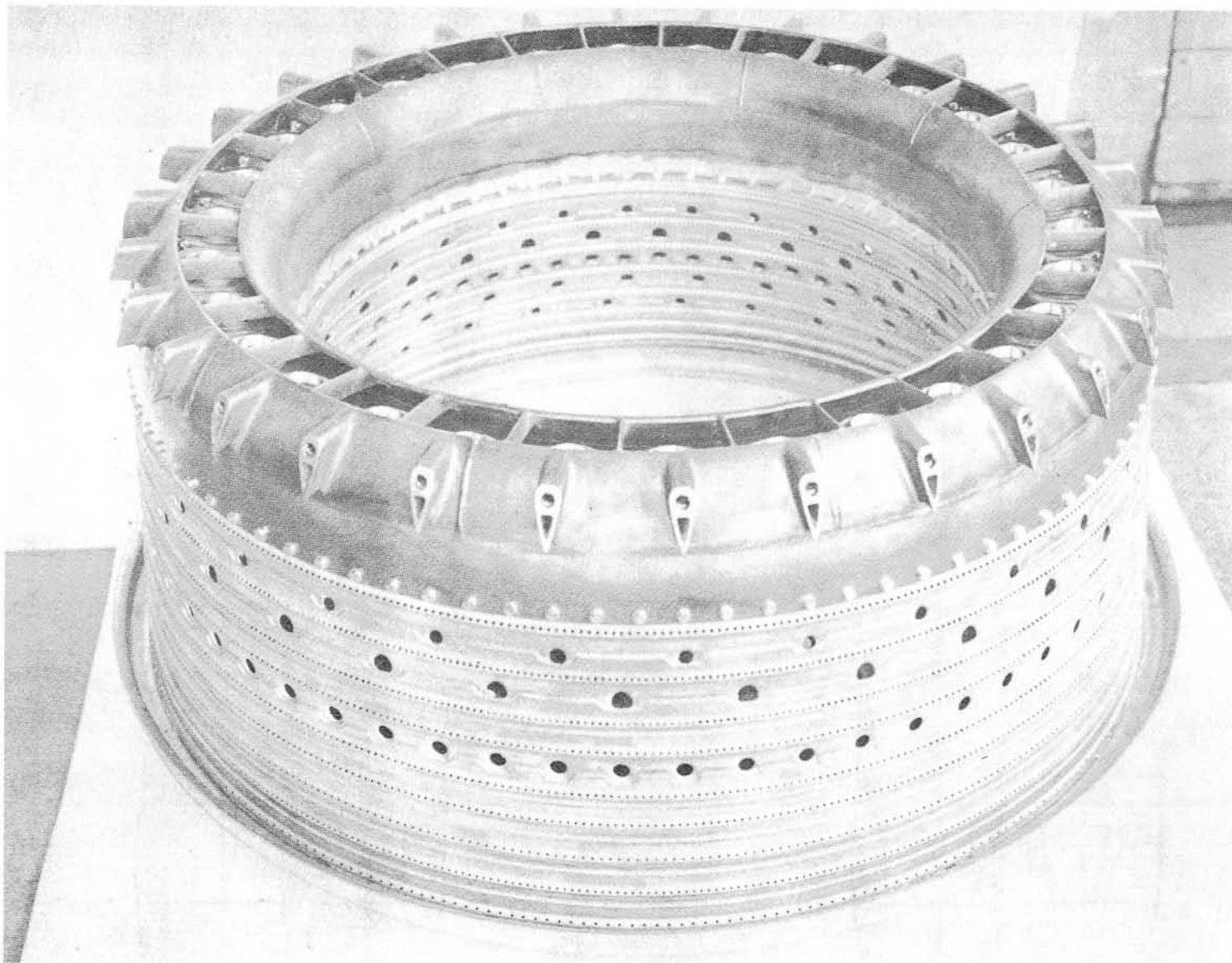
Figure 3. CF6-50 Combustor Assembly.

Pilot Stage

Main Stage
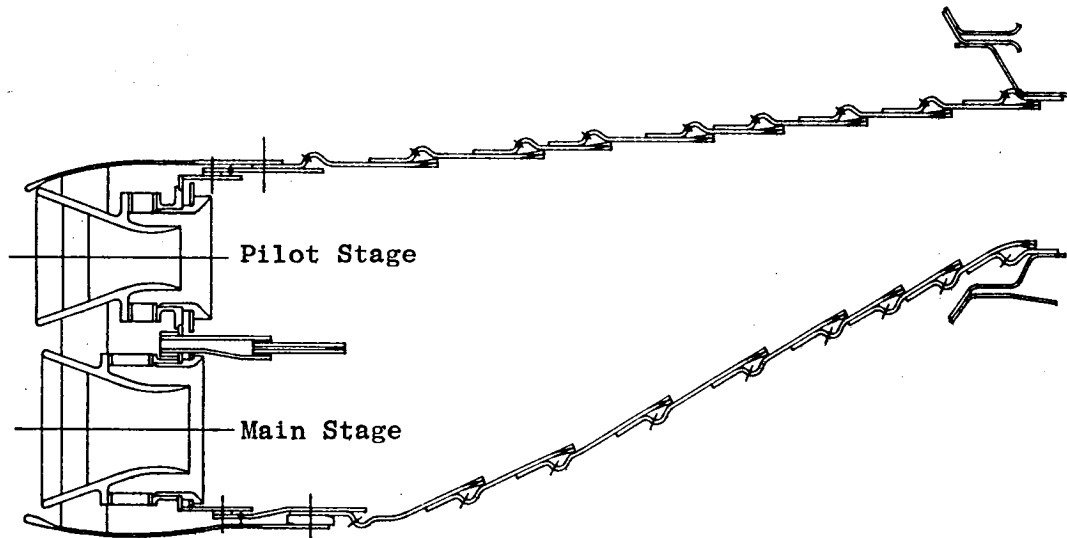
Figure 4.   Advanced Combustor Concept 1.

Pilot Stage

Main Stage
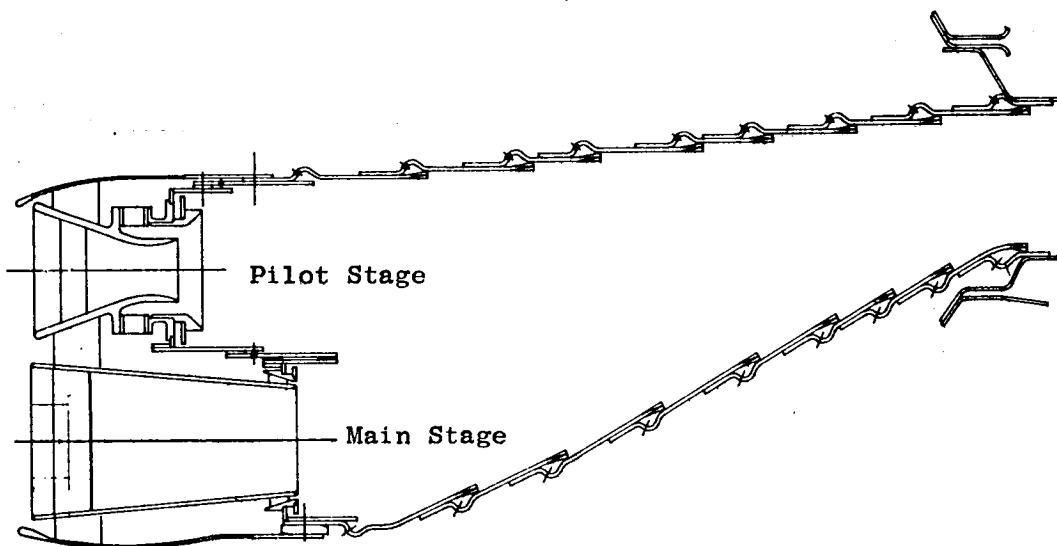
Figure 5.   Advanced Combustor Concept 2.

Corotating Swirlers Between Main Swirlers

View A

A ▷ Main Stage

Pilot Stage
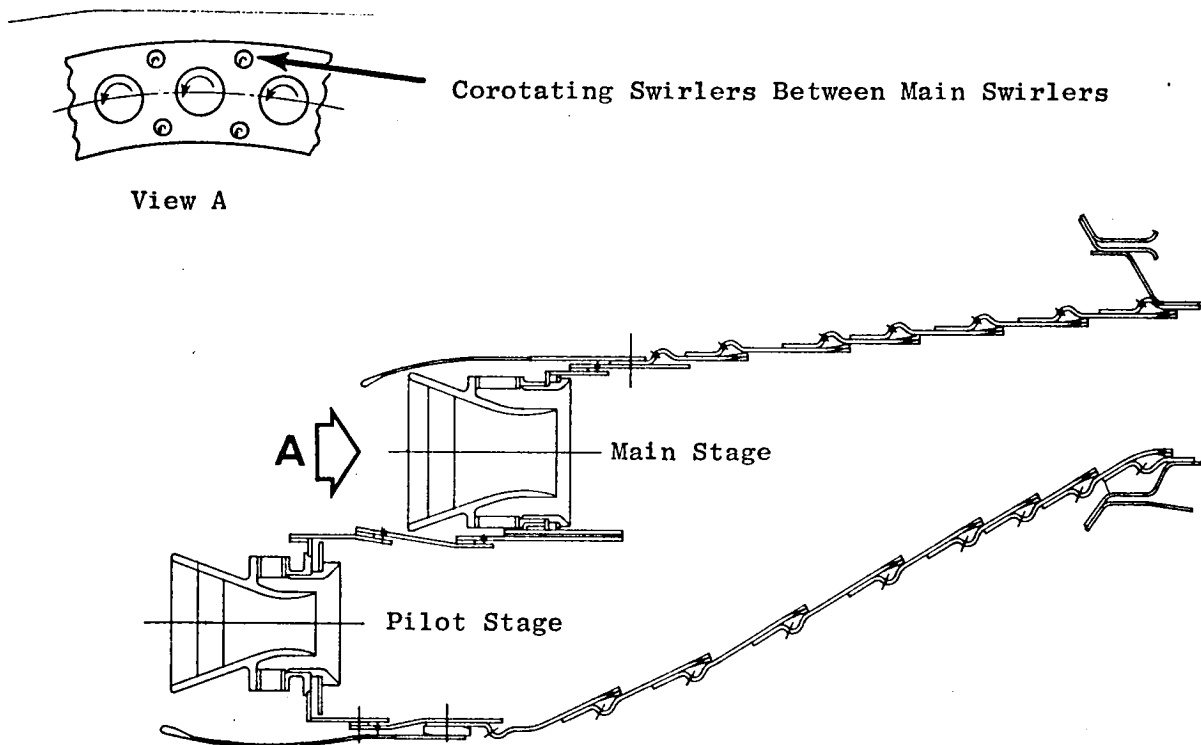
Figure 6.   Advanced Combustor Concept 3.
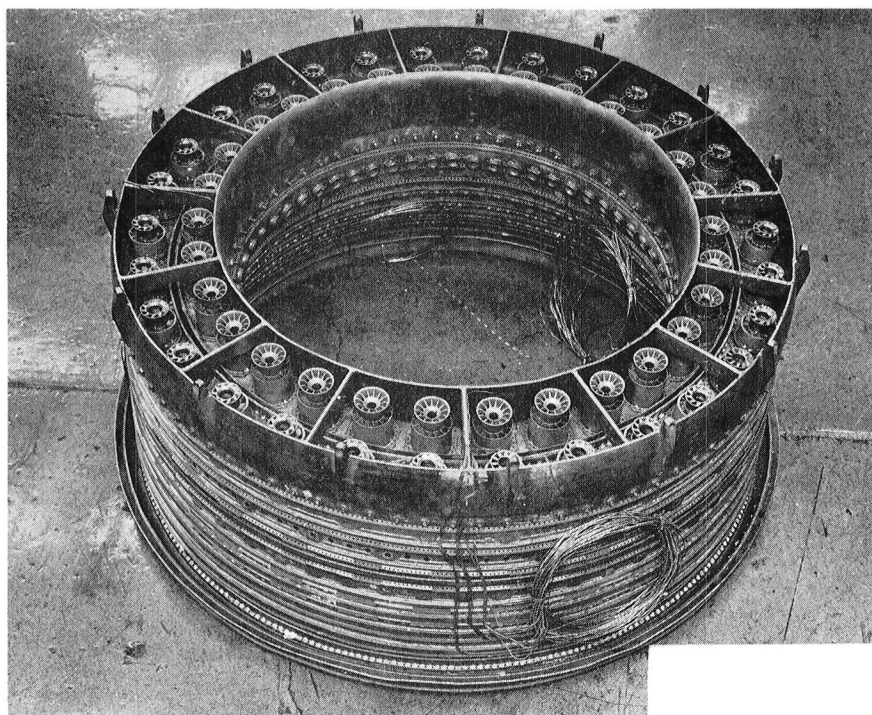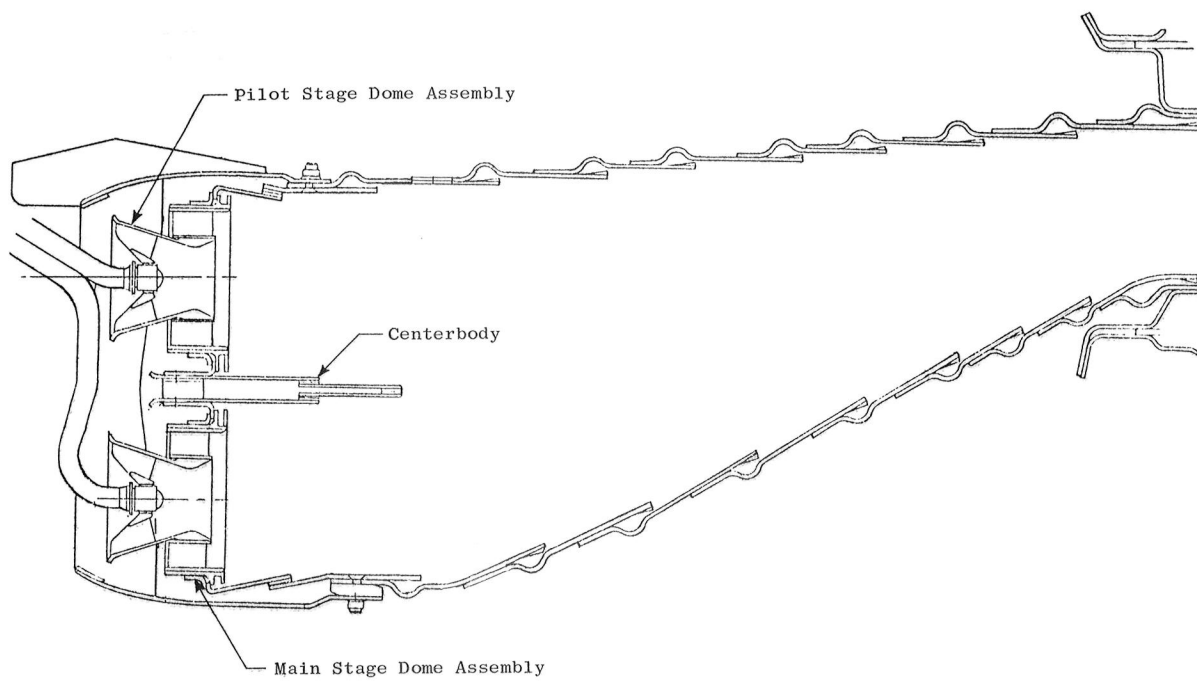
Figure 7. Double-Annular Combustor General Arrangement.

12

than axial secondaries and allow increased swirl to be used. Rig testing during the QCSEE program demonstrated that radial/axial swirl cups yield lower emissions than axial/axial swirl cups. During the QCSEE development program, component spray testing showed that excellent fuel atomization, with no voids or streaks in the spray patterns, was achieved with this type of swirler. Spray-pattern tests conducted as part of this program verified previous results, as shown in Figures 8 and 9. Cross-sectional and exploded views of the QCSEE-type swirl cups used in this program are illustrated in Figures 10 through 13. Features of this design include high secondary-swirler airflow rates (60% of the swirl-cup airflow) and a 90° conical sleeve in the secondary swirler exit.

Another feature of Concept 1 was the use of high-pressure-drop, simplex, pressure-atomizing fuel nozzles. These nozzles were designed for a maximum pressure drop of 8.27 MPa, compared with a maximum pressure drop of 3.45 MPa used in conventional fuel-injection systems. Increasing fuel-nozzle pressure drop while holding fuel flow constant decreases the Sauter Mean Diameter (SMD) of the fuel droplets. In an internal General Electric program studying the combustion characteristics of residual fuels (proprietary General Electric Report R79AEG577), high-pressure-drop simplex fuel nozzles were found to decrease carbon deposition on combustor liners and domes. The tests were run on a CF6 derivative combustor and used fuels with viscosities ranging from 10 to 21 mm^2/s.

The combination of high-pressure-drop fuel nozzles and low-emissions features, such as the double-annular combustor and QCSEE swirl cups, had not been tested prior to this program and were expected to provide significantly improved performance here. A droplet size comparison for the high ΔP nozzles and the baseline CF6-50 dual-cone nozzles is given in Table II. Droplet sizes were calculated using correlations from Reference 5.

Table II. Fuel Nozzle Droplet Size Comparison.

Test Point	Fuel/Air Ratio	Calculated Droplet Size (SMD, μm)		
			High ΔP	
Cruise		Dual Cone	Pilot	Main
1	0.012	118	56	74
2	0.015	114	50	66
3	0.018	113	45	60
4	0.021	109	42	56
5 (Design Point)	0.024	108	40	53
Takeoff				
1	0.015	111	44	59
2	0.018	109	40	54
3	0.021	106	37	49
4	0.024	104	35	47
5 (Design Point)	0.026	102	33	44

- Fuel Pressure: 3.5 MPa
- Air Pressure: 9.0 kPa
- Conventional Fuel Nozzles

Figure 8. Main-Stage Swirl Cup Fuel Spray Pattern.

- Fuel Pressure: 0.48 MPa
- Air Pressure: 20.7 kPa
- Conventional Fuel Nozzles

Figure 9. Pilot-Stage Swirl Cup Fuel Spray Pattern.
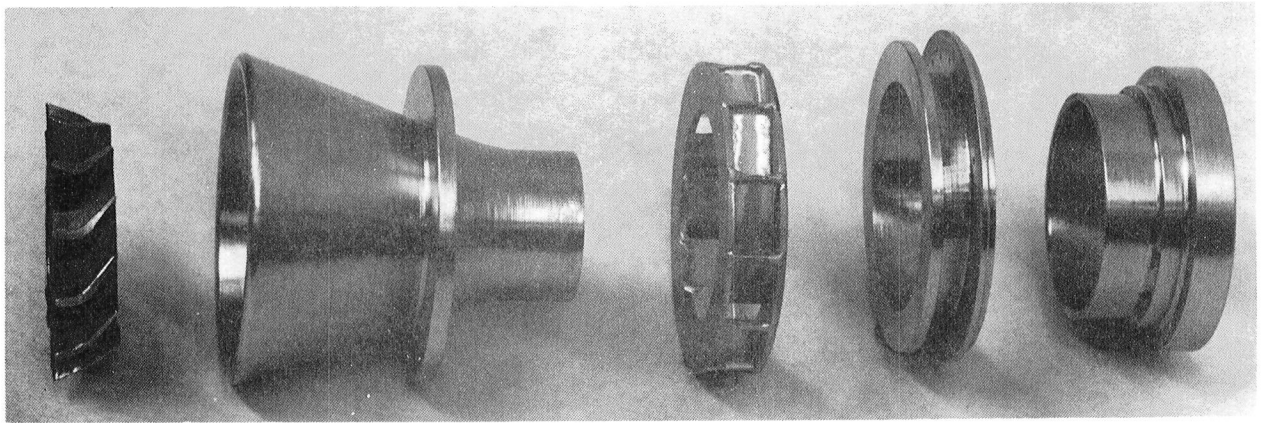
Figure 10.   Pilot-Stage Swirl Cup - Exploded View.

Figure 11.   Assembled Pilot-Stage Swirl Cup.

16
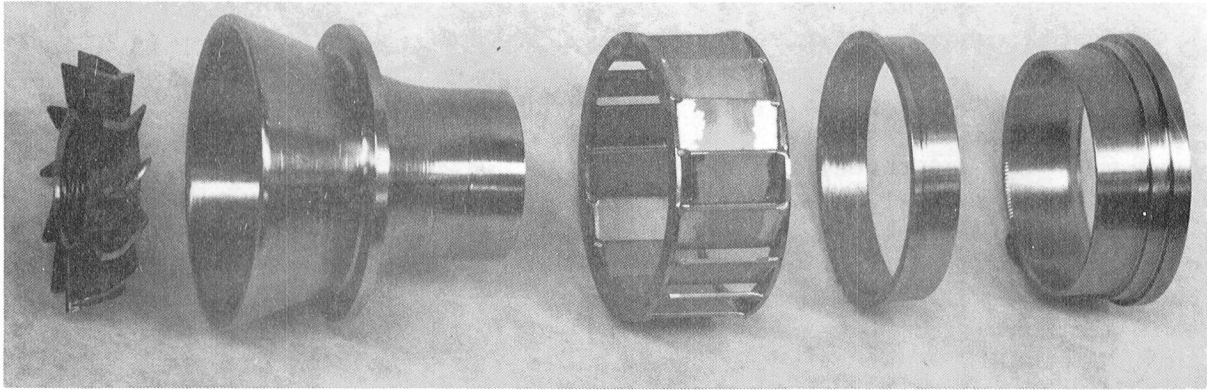
Figure 12.   Main-Stage Swirl Cup - Exploded View.
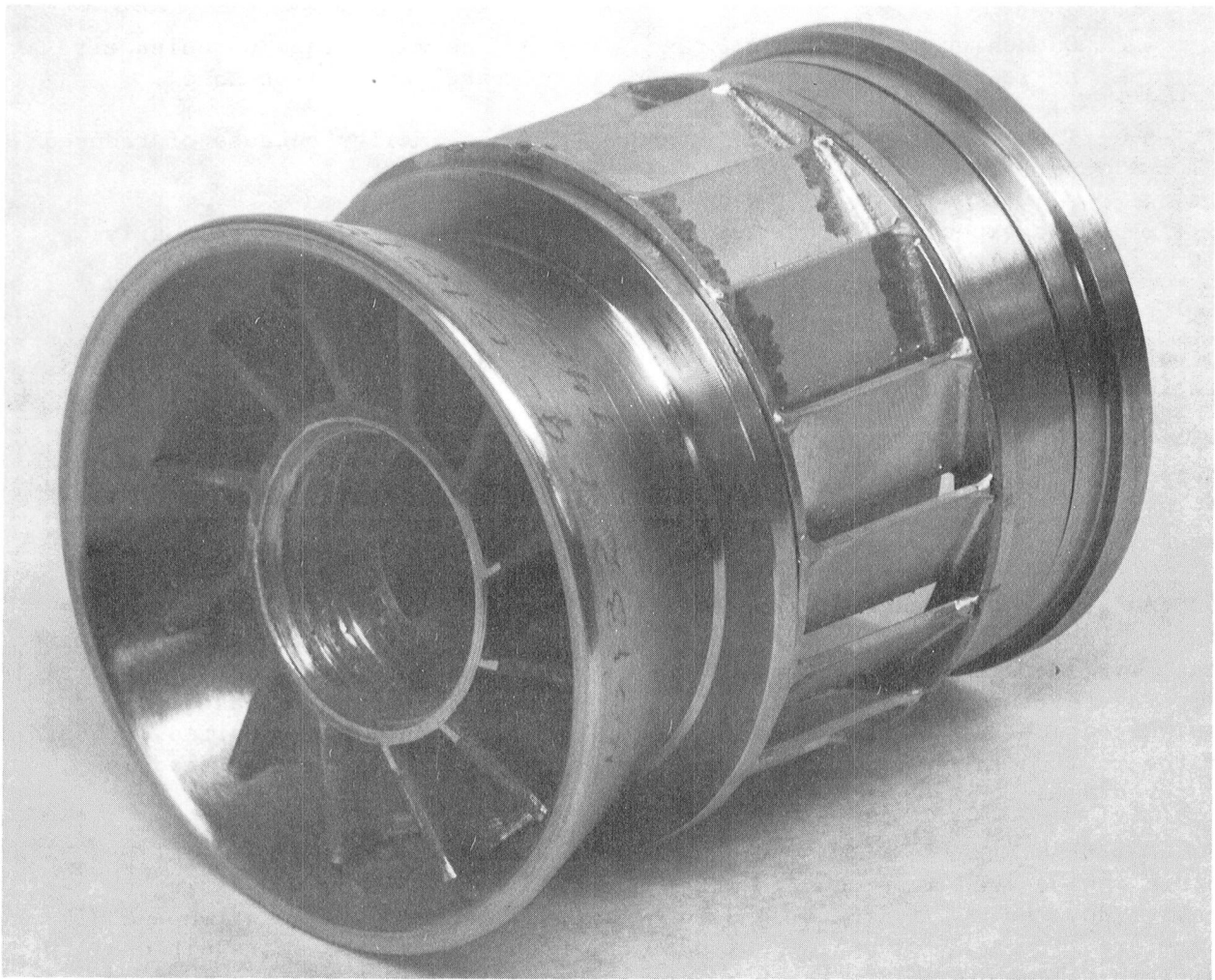
Figure 13.   Assembled Main-Stage Swirl Cup.

17

Concept 2, shown in Figure 5, employed premixing of the main-stage fuel. In this design, the pilot was situated on the outboard side, as in Concept 1, and three counterrotating swirl cups were employed. Conventional (3.45 MPa ΔP) pressure-atomizing simplex fuel injectors were employed in both stages. The second stage had three premixing ducts, shown in Figure 14, that provided approximately 1 ms residence time for mixing and prevaporization of the fuel and air. Pressure-atomizing fuel injectors and 15° swirlers were used at the forward end of the prevaporizing ducts to provide atomization and rapid mixing of the fuel and air. Corotating swirlers with a 35° swirl angle were located at the junction of the premixing ducts and the dome to add additional air and mixing. Figure 15 shows the fuel spray pattern exiting from the premix duct.

Concept 3, shown in Figure 6, featured reversed main and pilot stages with a shortened main stage outboard of the pilot. Some of the reasons for this arrangement are:

- Main-stage residence time is reduced for decreased NO_x production.

- Quenching of the pilot stage gases by the main-stage unfueled air at low-power conditions is prevented (sheltered pilot zone).

- The liner cooling-airflow requirement is smaller because of reduced surface area.

- The expected discharge-gas temperature profile will more nearly match the required turbine profile.

In this design, three QCSEE-type counterrotating swirlers were employed in both the pilot stage and the main stage. Both stages used conventional, simplex, pressure-atomizing fuel injectors.

Because the main-stage dome was moved aft, cooling air required for the outer liner and for one side of the centerbody was reduced. This air was used for dilution and profile trim at the aft end of the liner to reduce pattern factor.

An additional benefit expected from the outboard main stage was profile shape. During the ECCP double-annular program it was experimentally determined that, with main-to-pilot fuel-flow ratios optimized for emissions, the radial temperature profile was tilted inboard. The objective profile based on turbine design considerations is tilted outboard (highest temperature desired outboard of the turbine pitch line). The profile objective should be more readily achieved with Concept 3.

One problem expected with the main stage on the outboard side was how to obtain the desired swirl-cup/primary-zone flow rates without resorting to excessive dome height. Excessive dome height increases residence time and, therefore, increases NO_x production. To overcome this problem, additional swirlers were employed in the triangular-shaped space between the main swirlers and the liner walls, as shown in Figure 6. In addition, main-stage primary-zone dilution was used in the outer liner wall.
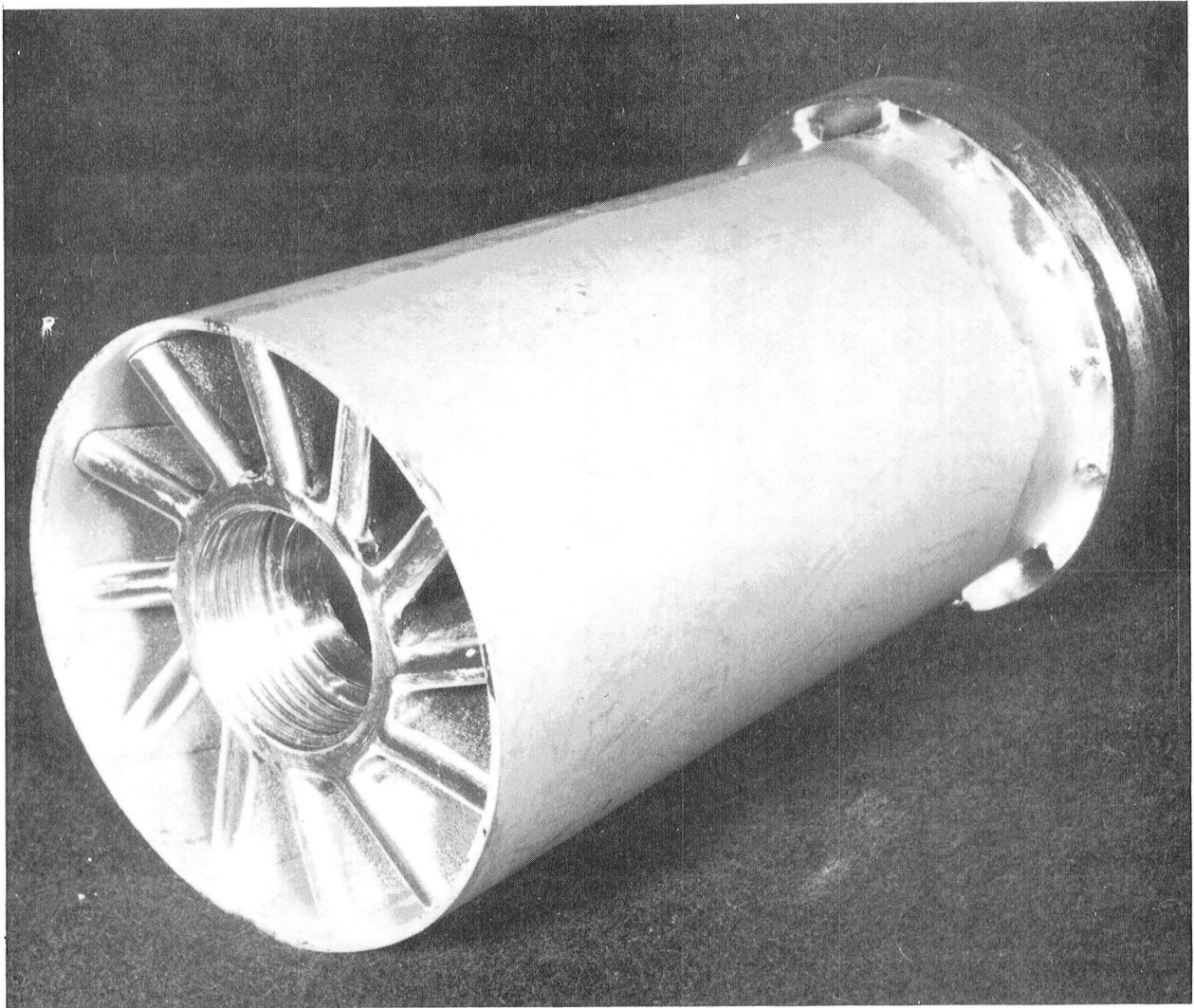
Figure 14. Concept 2 Premix Tube.

- Fuel Pressure: 3.5 MPa
- Air Pressure: 6.9 kPa
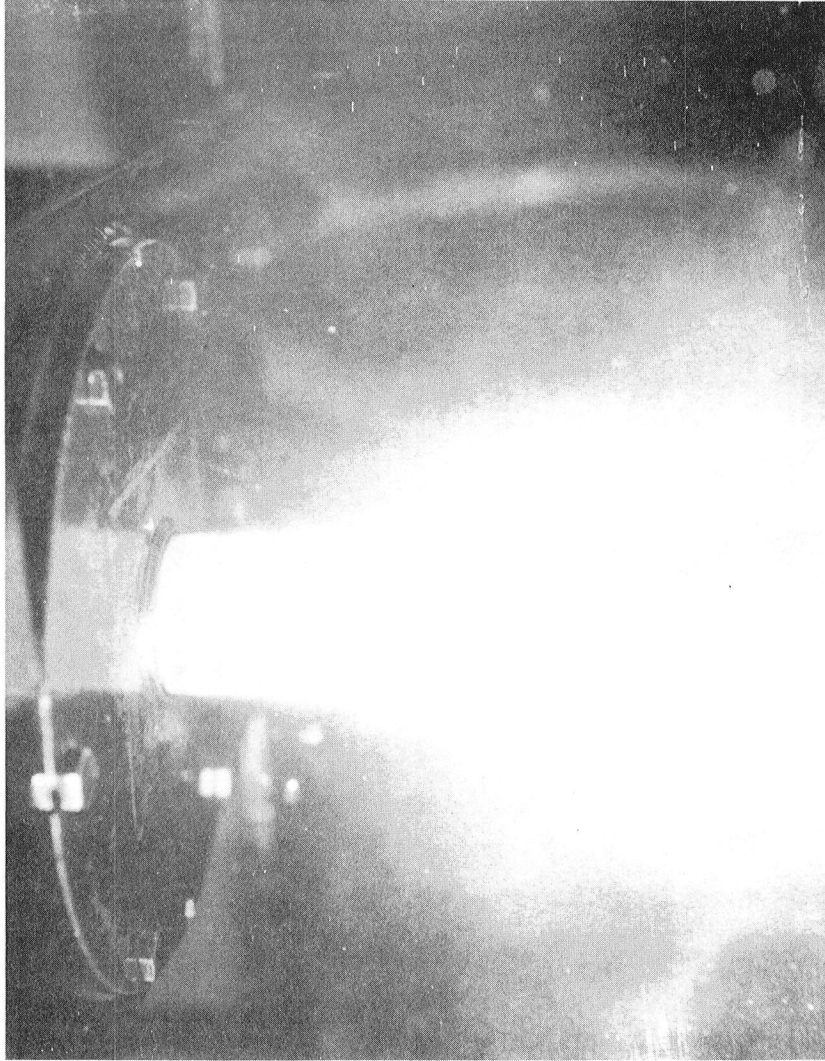
Figure 15. Premix Duct Fuel Spray Pattern.

3.2 COMBUSTOR DETAIL DESIGN

The detail design of the three advanced burners was based on the ECCP-Phase II, Configuration D12, burner. This burner design was very promising and was selected for engine testing. A comparison of design variables is shown in Table III for the ECCP Configuration D12 burner and the four burners tested in this program.

The airflow distributions for the four test combustors are shown in Figures 16 through 19. Pilot-swirler and primary-dilution flows for the three advanced concepts were identical to ECCP Configuration D12 values. Profile trim flows for Concepts 1 and 2 were also identical to those of the ECCP development combustor. Cooling flows were based on ECCP Configuration D12 pilot and main-stage flows, adjusted for liner area. Based on the Phase III ECCP Diesel No. 2 Fuel Addendum engine test results, no increase in cooling level was required for the use of decreased-hydrogen-content fuels for these double-annular burners. The tests indicated no significant change in the lean main-stage liner temperature as the hydrogen content of the fuel was decreased. Some increase in pilot-stage liner temperature was observed, but these temperatures were not life limiting. Cooling-flow requirements for Concepts 2 and 3 were reduced because of decreased cooling-liner surface areas. In Concept 2, the excess cooling flow was added in the premixing tubes. In Concept 3, excess flow was used to increase profile trim air.

The Concept 2 burner was chosen for the parametric test. The inner liner of this burner was modified to reduce liner temperatures on Panels 3 through 5 in line with the premix tubes. These modifications removed the profile trim flow and replaced it with dilution flow on Panels 1 and 3. Airflows for this burner are shown in Figure 20.

Wherever possible, common design features were incorporated into each of the double-annular combustors. Pilot-stage swirl cups were identical for the three concepts, and the main-stage swirl cups for Concepts 1 and 3 were identical. The fuel nozzles used on Concept 2 were also used on Concept 3. All liners were based on CF6-50 production liners; Nichrome patches were used to modify airflows. The outer liners used on Concepts 1 and 2 were identical, and the Concept 1 inner liner was used on Concept 2 (Concept 1 primary dilution holes were covered with Nichrome). The use of these common design features provided a valid comparison of the unique carboning- and emissions-reduction features of each configuration. Pretest photographs of the three advanced dome concepts are shown in Figures 21 through 23.

The Concept 2 premix tubes were designed for a residence time of 1.0 ms assuming no recirculation regions. This is well below the minimum autoignition residence time of 2.6 ms predicted, using data from Reference 6, for the 12% hydrogen fuel.

Table III. Comparison of Combustor Design Parameters.

Combustor Designation	ECCP-D12		Production CF6-50		Concept 1		Concept 2		Concept 3	
Condition	Idle	Takeoff	Idle	Takeoff	Idle	Takeoff	Idle	Takeoff	Idle	Takeoff
Stage	Pilot	Main	Single Stage		Pilot	Main	Pilot	Main	Pilot	Main
Annulus Location	Outer	Inner			Outer	Inner	Outer	Inner	Inner	Outer
Stage Length (L_c), cm	33.3	34.3	35.1		33.5	34.8	33.5	34.5[4]	34.8	26.4
Stage Dome Height (h_d), cm	5.8	5.3	11.4		5.3	5.3	5.3	5.3	6.1	5.3
Injector Spacing (b), cm	7.9	6.4	6.9		7.9	6.6	7.9	6.6	6.6	7.9
L_c/h_d	5.7	6.4	3.1		6.3	6.5	6.3	6.5	5.7	5.0
L_c/b	4.3	5.4	5.0		4.3	5.4	4.3	5.3	5.3	3.3
Reference Area, cm^2 [1]	3729		3729		3706		3706		3706	
Reference Velocity, m/s[2]	16.1	21.5	16.1	21.5	16.2	21.6	16.2	21.6	16.2	21.6
Dome Velocity, m/s[3]	11.0	33.5	11.0	11.0	11.6	27.4	11.6	38.4	11.6	29.6
Space Rate, $MJ/s\text{-}m^3$ atm	---	18.0	---	18.6	---	18.3	---	19.5	---	21.1
Combustor Volume, m^3	0.57		0.060		0.058		0.054		0.049	
Residence Time, ms[3]	---	3.7	---	4.6	---	3.7	---	3.1[5]	---	3.0
Dome Equivalence Ratio[3]	0.85	0.73	0.56	1.21	0.91	0.70	0.91	0.53	0.91	0.56
Dilution Equivalence Ratio[3]	0.20	0.43	0.41	0.89	0.22	0.44	0.22	0.47	0.22	0.46
Outer Passage Velocity, m/s[3]	24.7	34.1	48.8	65.9	15.5	21.3	15.5	21.3	28	38.7
Inner Passage Velocity, m/s[3]	36.6	42.4	49.1	68.3	49.1	67.4	29.6	40.5	12.5	17.4

1. Maximum engine rig combustor flowpath area.
2. Based on compressor exit density at takeoff operating conditions.
3. Main stage evaluated at takeoff operating conditions with 80% of fuel flow to main stage.
4. Pilot stage evaluated at idle operating conditons with 100% of fuel flow to pilot stage.
5. Burning Length, excluding premixing tube: 28.2 cm.
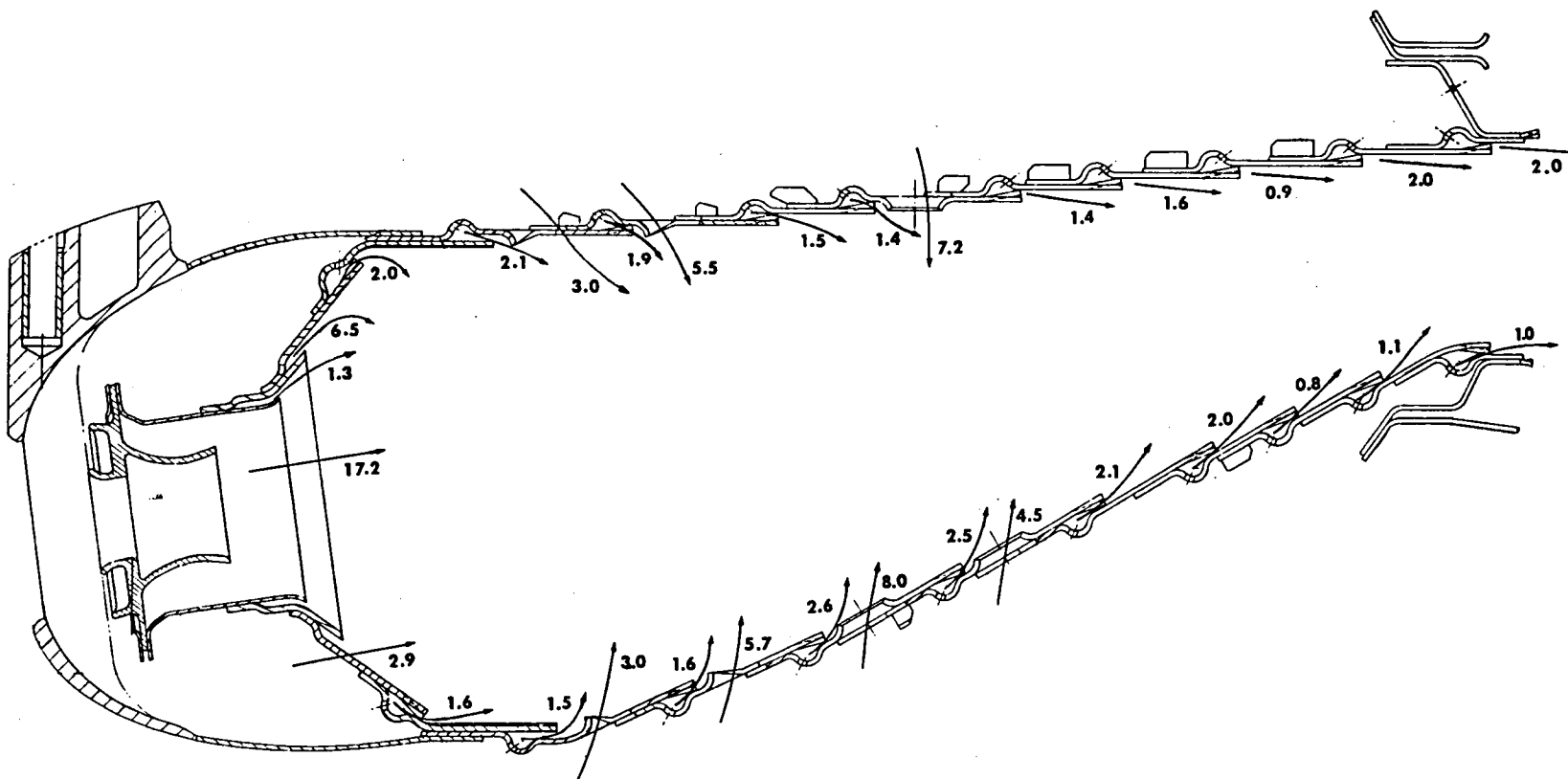
Figure 16. Combustor Airflow Distribution, Baseline CF6-50, Expressed in Percent W_c.
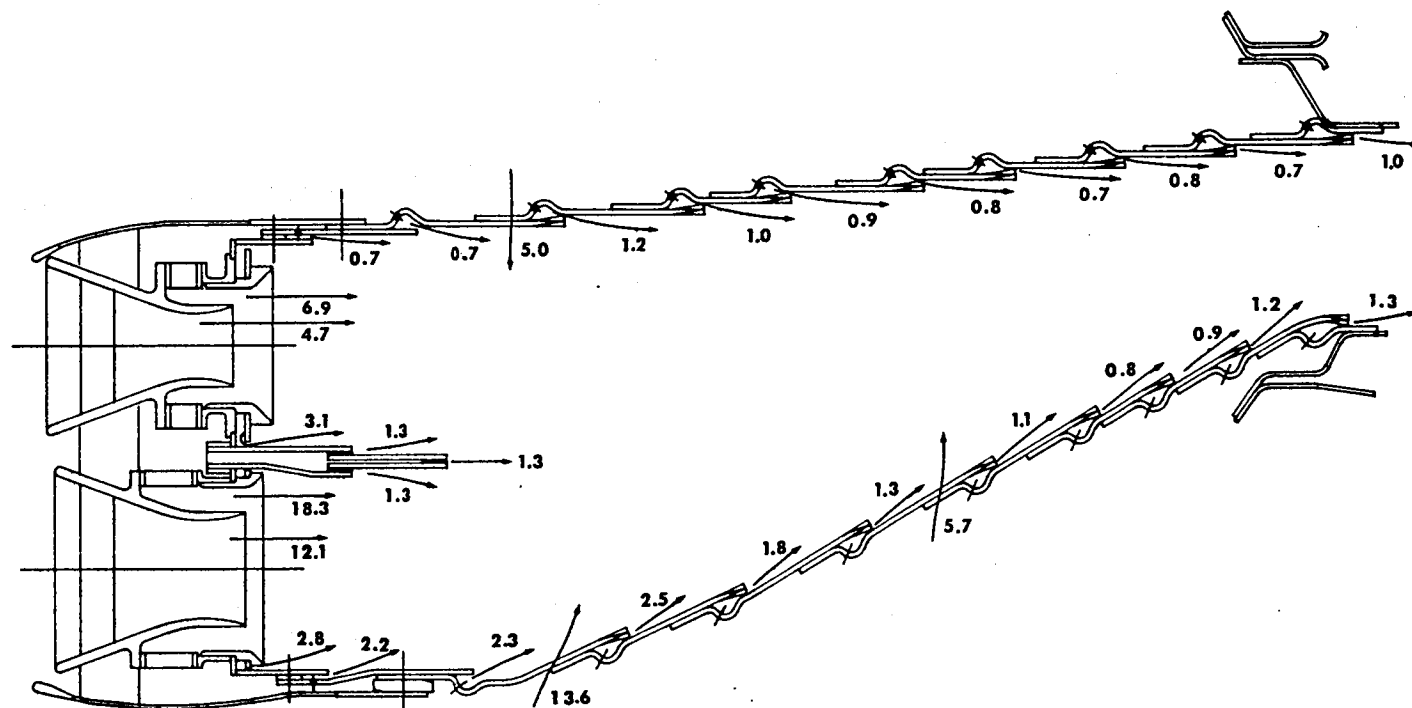
Figure 17. Combustor Airflow Distribution, Concept 1, Expressed in Percent W_c.
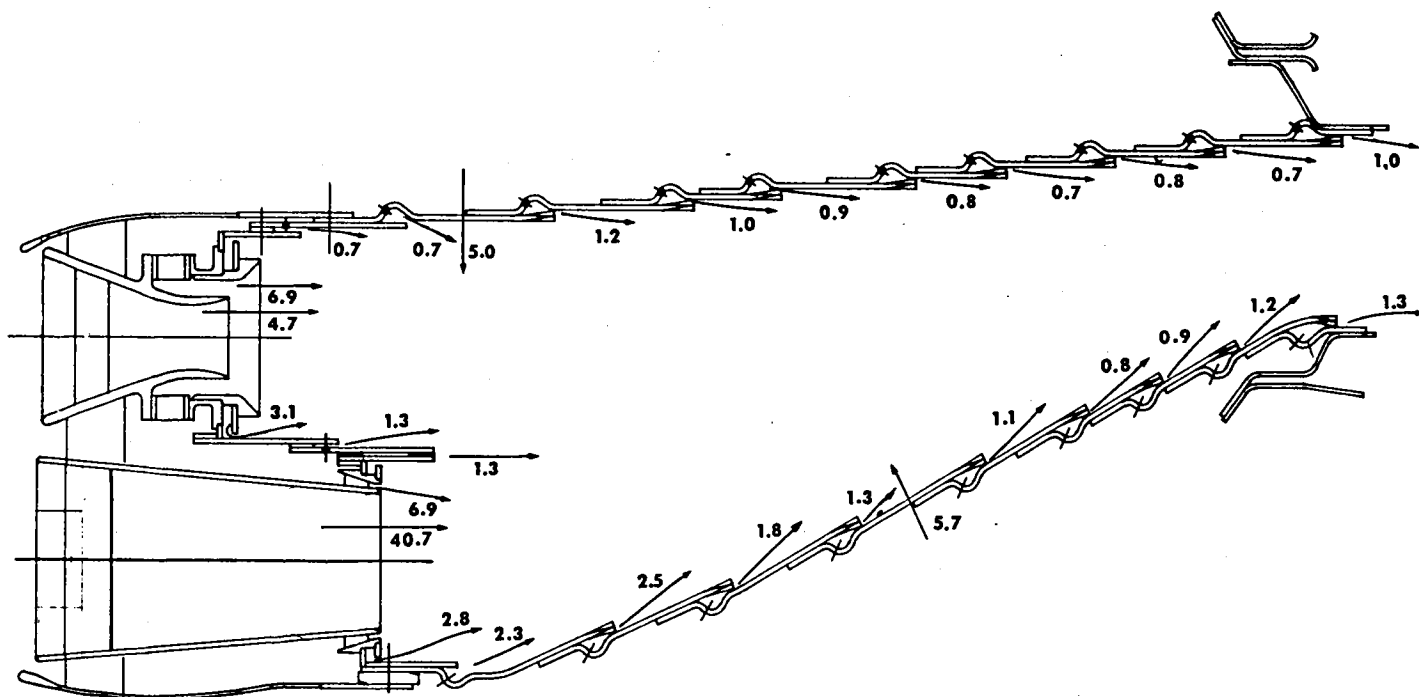
Figure 18. Combustor Airflow Distribution, Concept 2, Expressed in Percent W_c.

Corotating Swirlers Between Main Swirlers, 10% W_c

View A
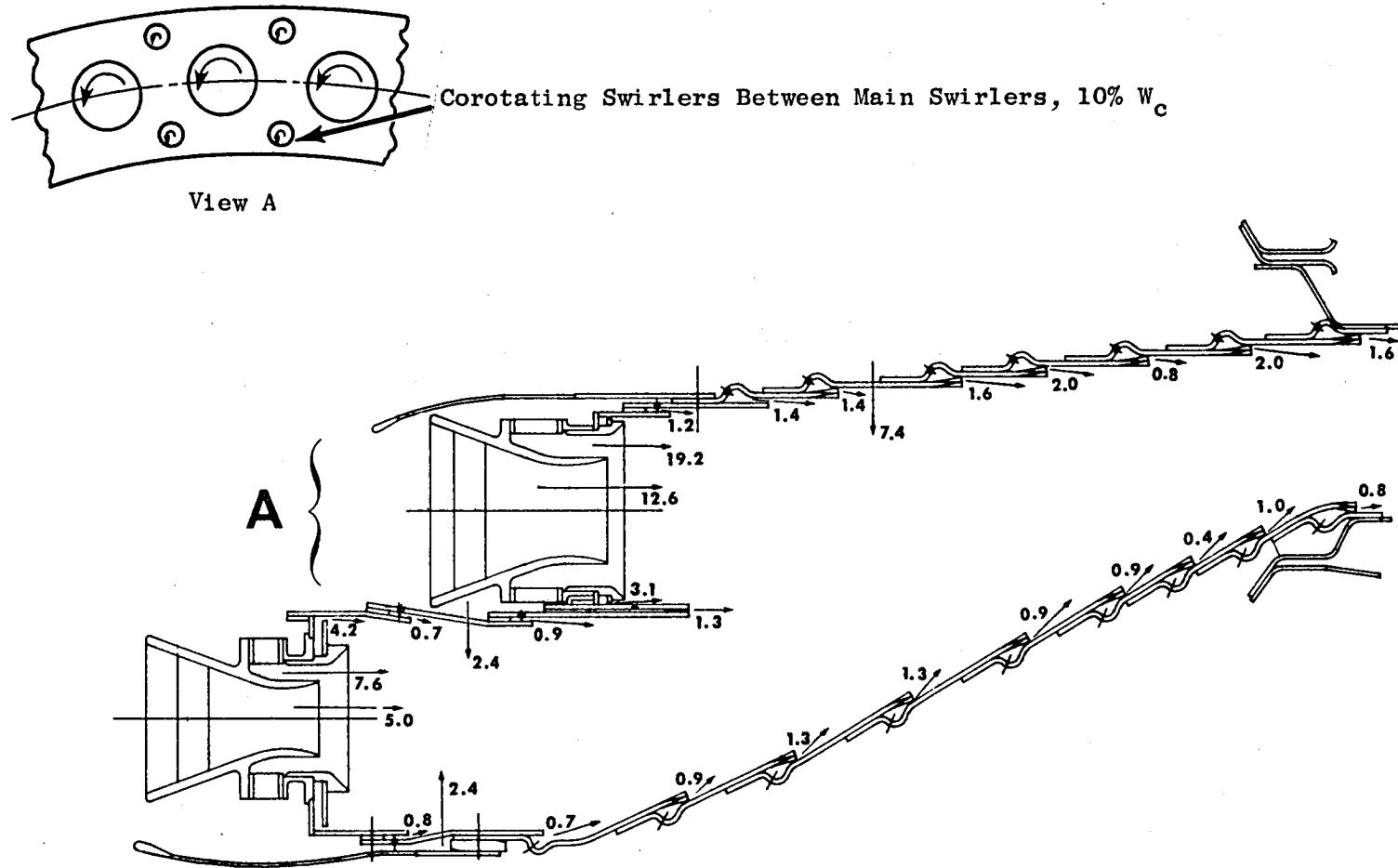
Figure 19. Combustor Airflow Distribution, Concept 3, Expressed in Percent W_c.
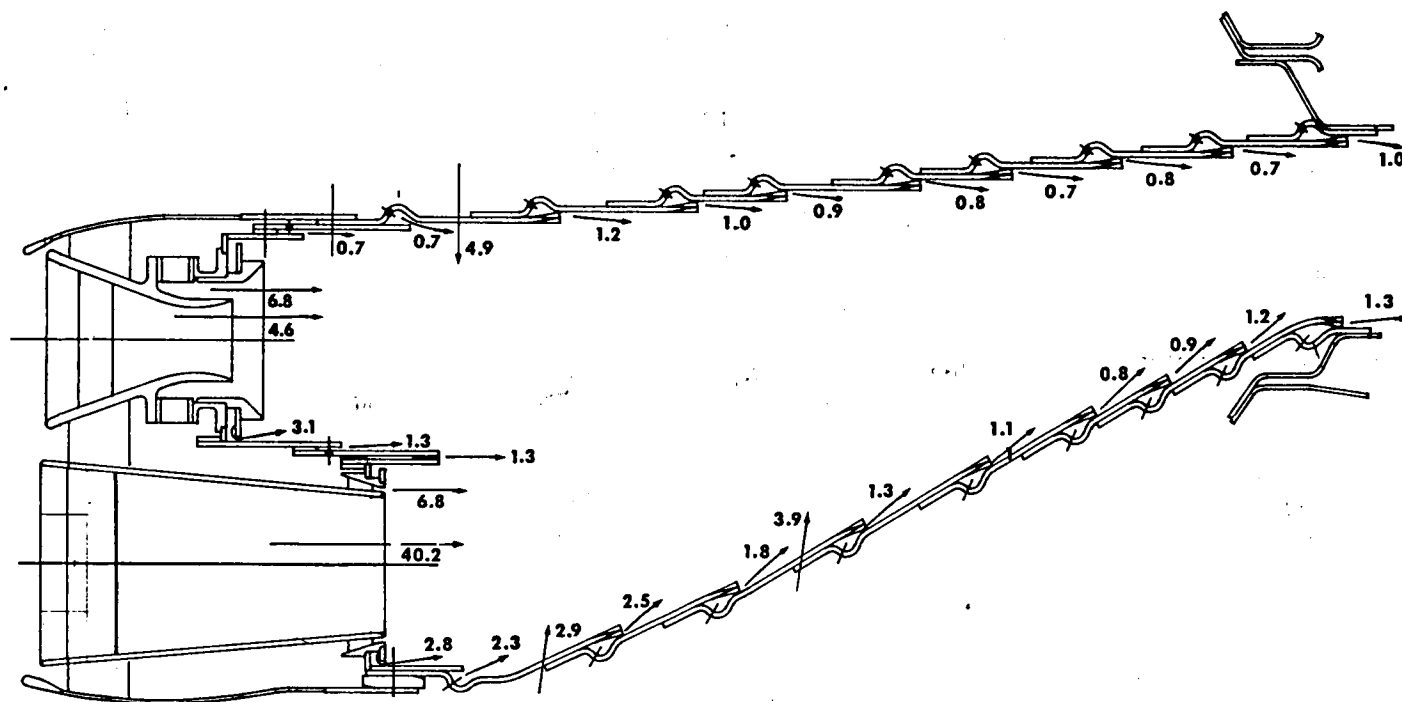
Figure 20. Combustor Airflow Distribution, Paramtric Test, Expressed in Percent W_c.
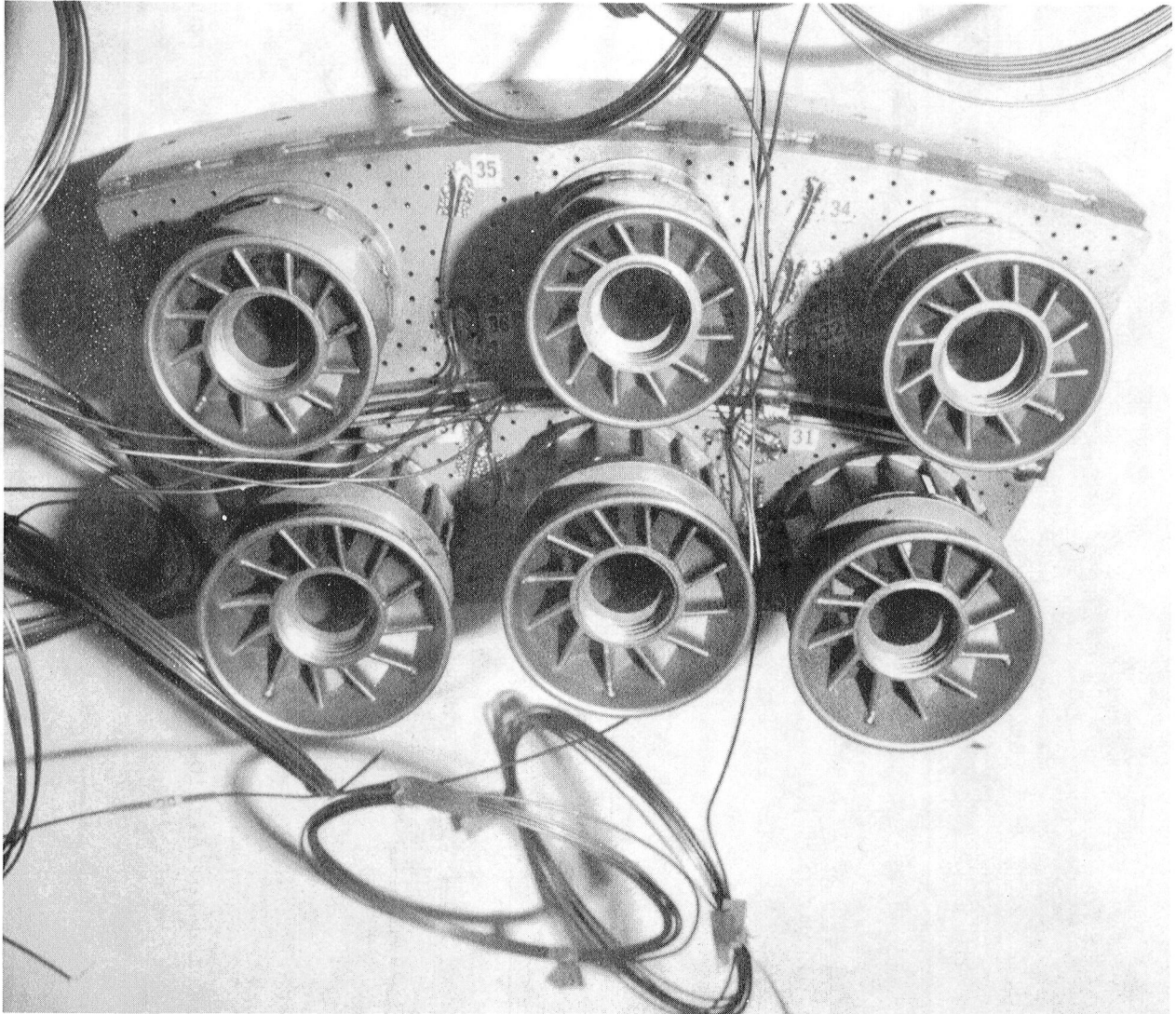
Figure 21. Concept 1 Dome.
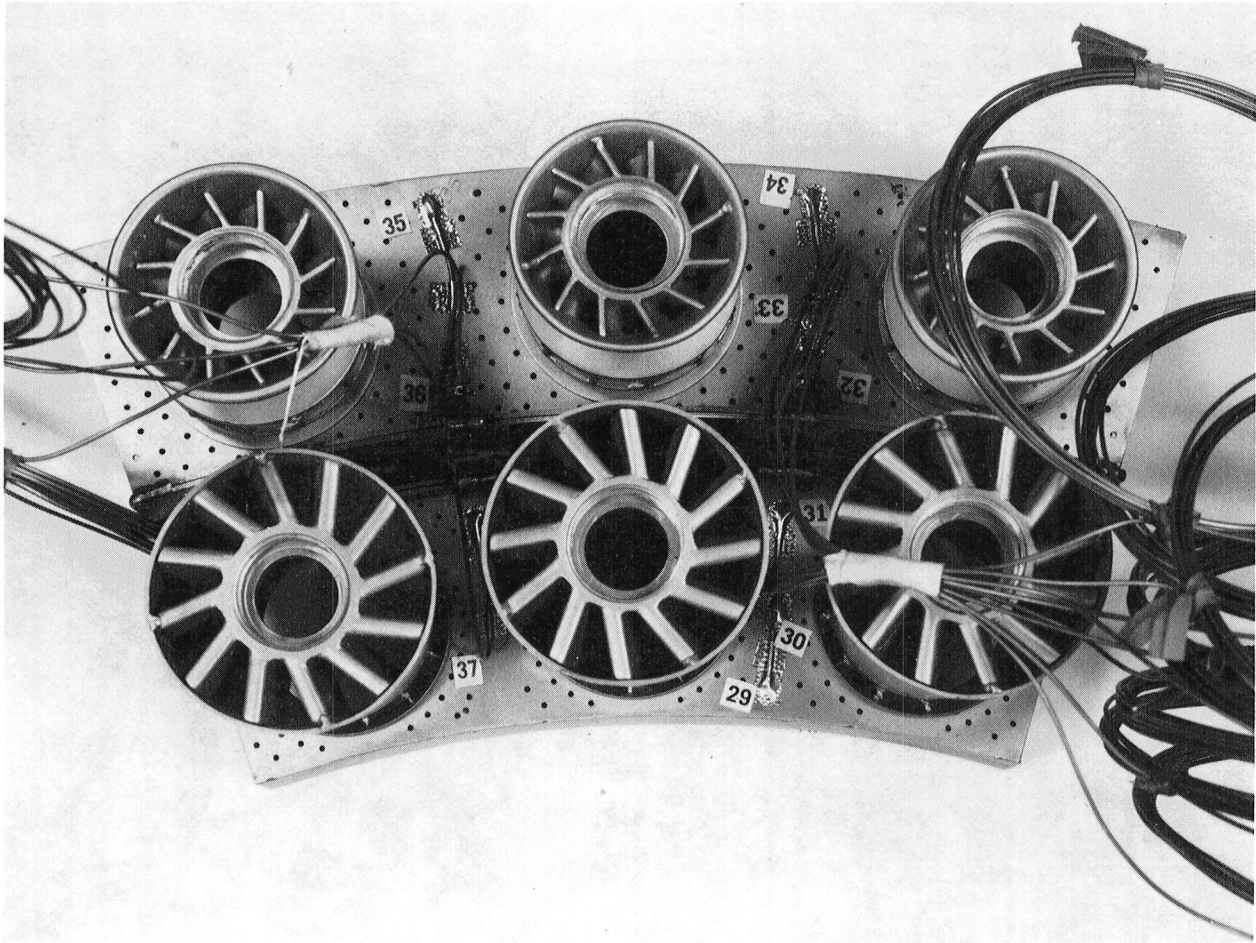
Figure 22. Concept 2 Dome.
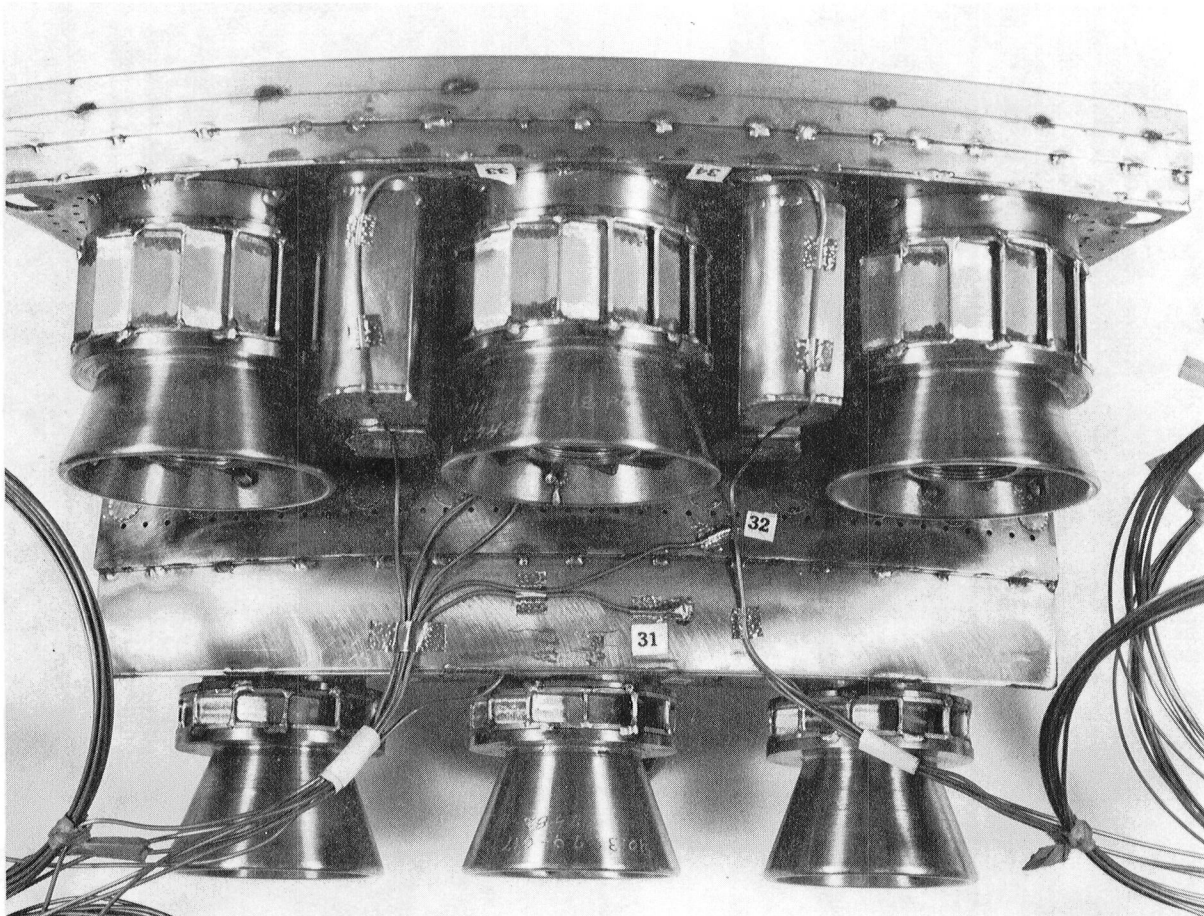
Figure 23.   Concept 3 Dome.

4.0 TEST RIG AND FACILITIES

4.1 COMBUSTOR TEST RIG

The sector combustor tests were conducted in the CF6-50 sector combustor test rig shown in Figure 24. This rig exactly duplicates a 1/10 sector (three fuel nozzles/swirl cups) of the CF6-50 combustor annular flowpath.

The rig simulates the engine flowpath from the compressor-exit plane to the turbine-nozzle-inlet plane, followed by a short combustor-exit instrumentation section. The combustor housing is a thick-walled vessel, shown in Figure 25; it forms the inner flowpath contour and sidewalls. A thick cover plate forms the outer flowpath contour. The sidewalls are air cooled for high-temperature operation. Combustor liners are supported by rails, on the side-plates, that allow for thermal expansion.

Fuel-nozzle mounting pads are located on the test rig coverplate. These pads are positioned exactly as in the engine. This coverplate also contains a spark igniter port positioned as in the engine. However, in order to accommodate the advanced concepts tested in this program, combustor lightoff was effected using torch igniters installed through either the test rig coverplate or (for Concept 3) the bottom wall.

Instrumentation-leadout ports are provided on the coverplate of the combustor housing to provide access for liner thermocouples and pressure taps. The exit instrumentation section has three exit-rake mounting pads located at -9°, 0°, and +9° from the rig centerline, as shown in Figure 26.
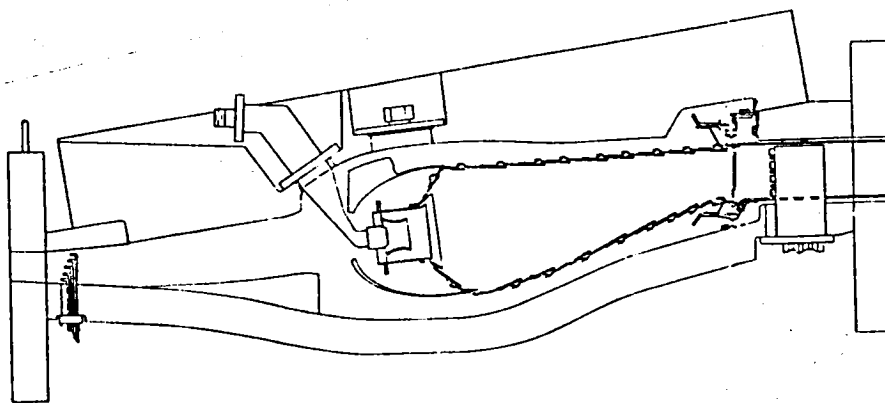
Figure 24. CF6-50 Sector Combustor Flowpath.
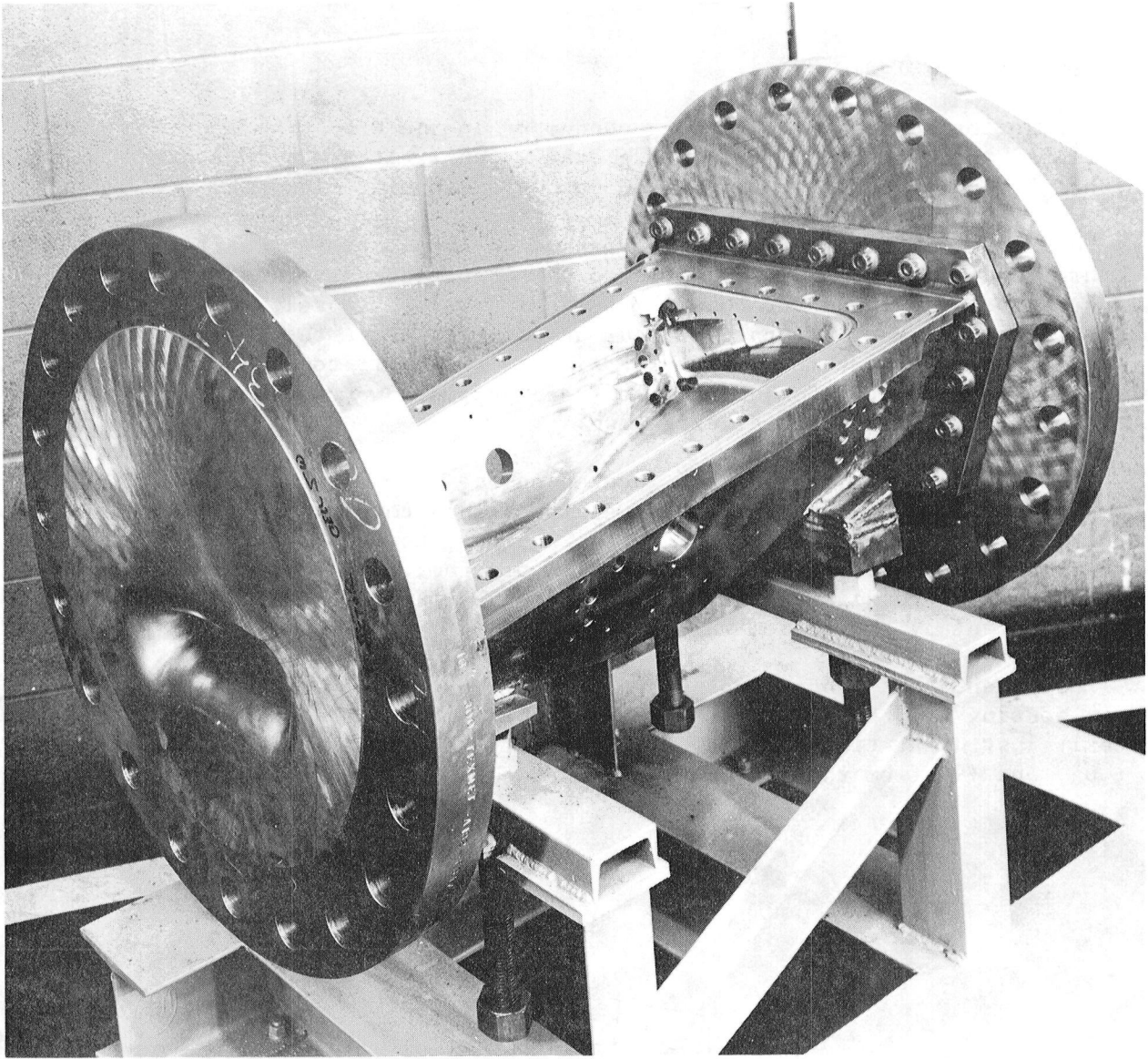
Figure 25. Combustor Housing, 36° Sector.
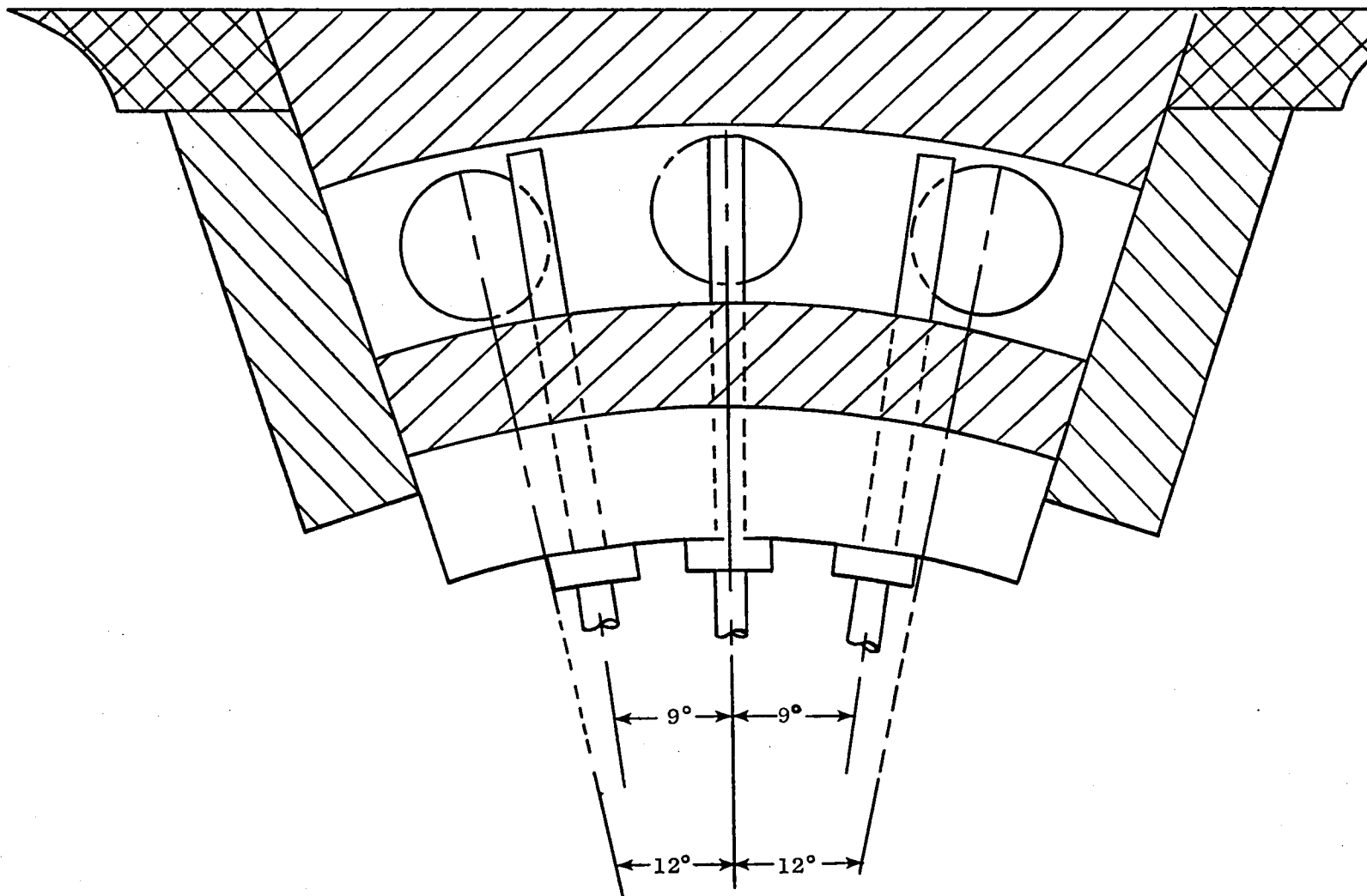
Figure 26. Combustor 36° Sector Exit - Instrumentation Positions.

4.2 COMBUSTOR TEST FACILITY

The sector combustor evaluations were conducted in Combustion Test Cell A5, located at the General Electric Evendale plant. The cell is supplied by air from a central air-supply system rated at 45 kg/s and 2.2 MPa. Combustor inlet air is heated to temperatures typical of actual engine operating conditions by a gas-fired, indirect, air preheater nominally designed to heat 5.44 kg/s of airflow to 922 K. The exact flow/temperature limits are somewhat dependent upon the test setup and procedure.

An interior view of Cell A5, with a typical test vehicle installed, is shown in Figure 27. The cell piping is arranged to accommodate two test vehicles simultaneously, and even greater utilization is effected by mounting test vehicles on portable dollies with quick-change connections; buildup operations are accomplished in another area, and a vehicle occupies the cell only for the duration of actual testing. Instrumentation sensors are prewired to multiple quick-connect-panels to facilitate rig installation. Table IV summarizes available services.

Table IV. Cell A5 Services.

Air

401 Air	18 kg/s at 2 MPa
Shop Air	3 kg/s at 0.7 MPa
Cooper-Bessemer	3 kgs/ at 2 MPa

Fuel Storage Capacity

Tank No. 7	15 m^3
Tank No. 8	3.8 m^3
Tank No. 9	3.8 m^3

Pump Capacity

System No. 1	0.38 kg/s at 4.8 MPa
System No. 2	0.38 kg/s at 4.8 MPa

Water

Quench Capacity	10 kg/s at 2.4 MPa
Jacket Cooling	6 kg/s at 0.5 MPa

Electrical Power Circuits

208 V, 60-cycle, 3-phase
480 V, 60-cycle, 3-phase
120 V d.c.
Control and Lighting: 115 V, 60-cycle, 1-phase
Ignition: 120 V, 60-cycle, 1-phase and 24 V system
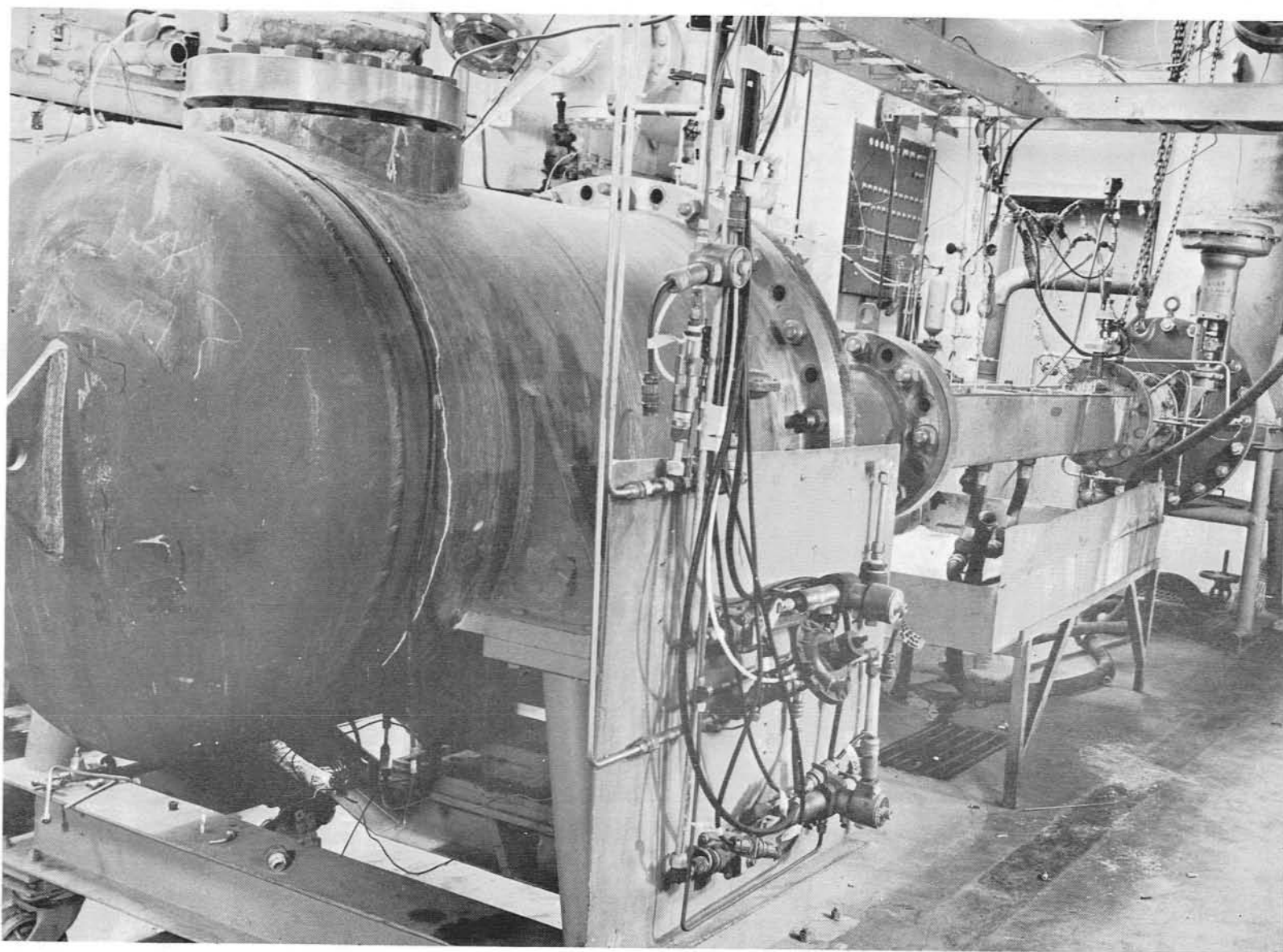
Figure 27.   Cell A5 Small Combustor Test Facility, Interior View.

Airflow rates are measured by standard orifices, of appropriate sizes, conforming to the American Society of Mechanical Engineers (ASME) Measurement Code. Fuel-flow rates are metered by calibrated, turbine-type, flow meters.

The control room is adjacent to the test cell. This is a soundproofed room housing the equipment for test control, monitoring, and data recording. Permanently installed equipment includes a 600-channel, digital-data acquisition system; strip-chart recorders for continuous recording of up to 16 test parameters; displays of 22 pressures, 24 temperatures, and 4 fuel flows for use by the operators in controlling test parameters; and a small, analog computer generally programmed to compute airflows and fuel/air ratios. Portable equipment, available when needed, includes a teletype terminal for time-sharing computers. Emissions-measurement equipment is also located within the control-room complex. In addition, flame radiometers and dynamic pressure, amplitude, and frequency analyzers are available.

4.3 COMBUSTOR AND RIG INSTRUMENTATION

The test duct and test rig assembly are equipped with extensive instrumentation. A complete listing of rig and combustor instrumentation used in these tests is presented in Table V.

Table V. Combustor/Rig Instrumentation.

Parameter	Instrumentation
Total Airflow	Standard ASME Orifice
Bleed Airflow	Standard ASME Orifice
Fuel Flow	Turbine Flow Meters
Fuel Injector Pressure Drop	Pressure Tap in Each Fuel Manifold
Fuel Temperature	Thermocouple in Fuel Manifold
Diffuser Inlet Total Pressure	Two 5-Element Fixed Impact Rakes
Diffuser Inlet Static Pressure	Wall Static Tap
Diffuser Inlet Total Temperature	Two Thermocouples in Inlet Plenum
Combustor Exit Total Temperature Combustor Exit Emissions Levels Combustor Exit Total Pressure	Three Combination Rakes, Each Having Four Gas-Sample/Total-Pressure Elements and Three Thermocouple Elements
Combustor Metal Temperature	Minimum of 30 Surface Thermocouples on Dome and Liners
Inlet Air Humidity Level	Dew-Point Hygrometer
Combustor Dome Pressure Drop	Four Pressure Taps

The combustor inlet-air total pressure was measured with two 5-element impact rakes installed in the combustor inlet diffuser. The inlet rake design is shown in Figure 28. A tap located at the same axial location was used to measure static pressure. Inlet temperature was measured with two single-element, chromel-alumel-thermocouple probes mounted in the inlet plenum, upstream of the diffuser.

Combustor metal temperatures were measured with surface-mounted, chromel-alumel thermocouples located on the dome and liners. As shown in Figure 29, a typical liner thermocouple installation consisted of two or three thermocouples distributed circumferentially at each of four different axial locations, plus several additional thermocouples located on expected liner "hot spots" (for example, just downstream of dilution holes where cooling-film effectiveness is reduced). Ten to twelve additional thermocouples were mounted on the combustor dome (Figure 30) and centerbody (on the advanced designs).

Exit total temperatures and pressures were measured, and exhaust-gas samples were extracted, using an array of three rakes mounted at the combustor exit. The combination pressure/sample/thermocouple rake used for this application is shown in Figure 31. Each of these water-cooled rakes contained four gas-sample/total-pressure elements and three thermocouple elements. These three rakes were mounted at -9°, 0°, and +9°, as shown in Figure 26.

4.4 EMISSIONS ANALYSIS INSTRUMENTATION

Combustor exhaust-gas samples were extracted from the fixed-rake array for smoke and gaseous-composition analysis. The sample lines were connected through a valve panel so that any of the 12 rake elements could be individually analyzed. Normally, however, they were manifolded for a single analysis.

Smoke-emission levels were measured with standard test equipment contained in a portable console, shown in Figure 32, which fully conforms to Society of Automotive Engineers (SAE) Aerospace Recommended Practice (ARP) 1179. This portable console houses a filtering instrument, water trap, vacuum pump, and flow meter. The spot sampler has a filtering area of 3.87 cm^2 and provides a leakproof seal. A water trap is located downstream of the smoke-filtering instrument to remove condensed water vapor and condition the gas for accurate flow measurement. A vacuum pump is used to maintain a constant flow rate at low sample pressures. A rotometer is used to monitor the sample volume. An electromechanical timer is used to measure the time it takes to obtain different sample volumes. The sample volume and time can be used to check flow rates.

The Contaminants Analyzed and Recorded On-Line (CAROL) system was used to measure gaseous emissions. This system conforms to SAE ARP 1256 and consists of four basic instruments: a flame ionization detector (FID) for measuring total HC concentrations, two nondispersive infrared analyzers for measuring CO and CO_2, and a heated chemiluminescent analyzer for measuring NO and NO_2. In the CAROL system, flow through all of the various sampling lines to each of
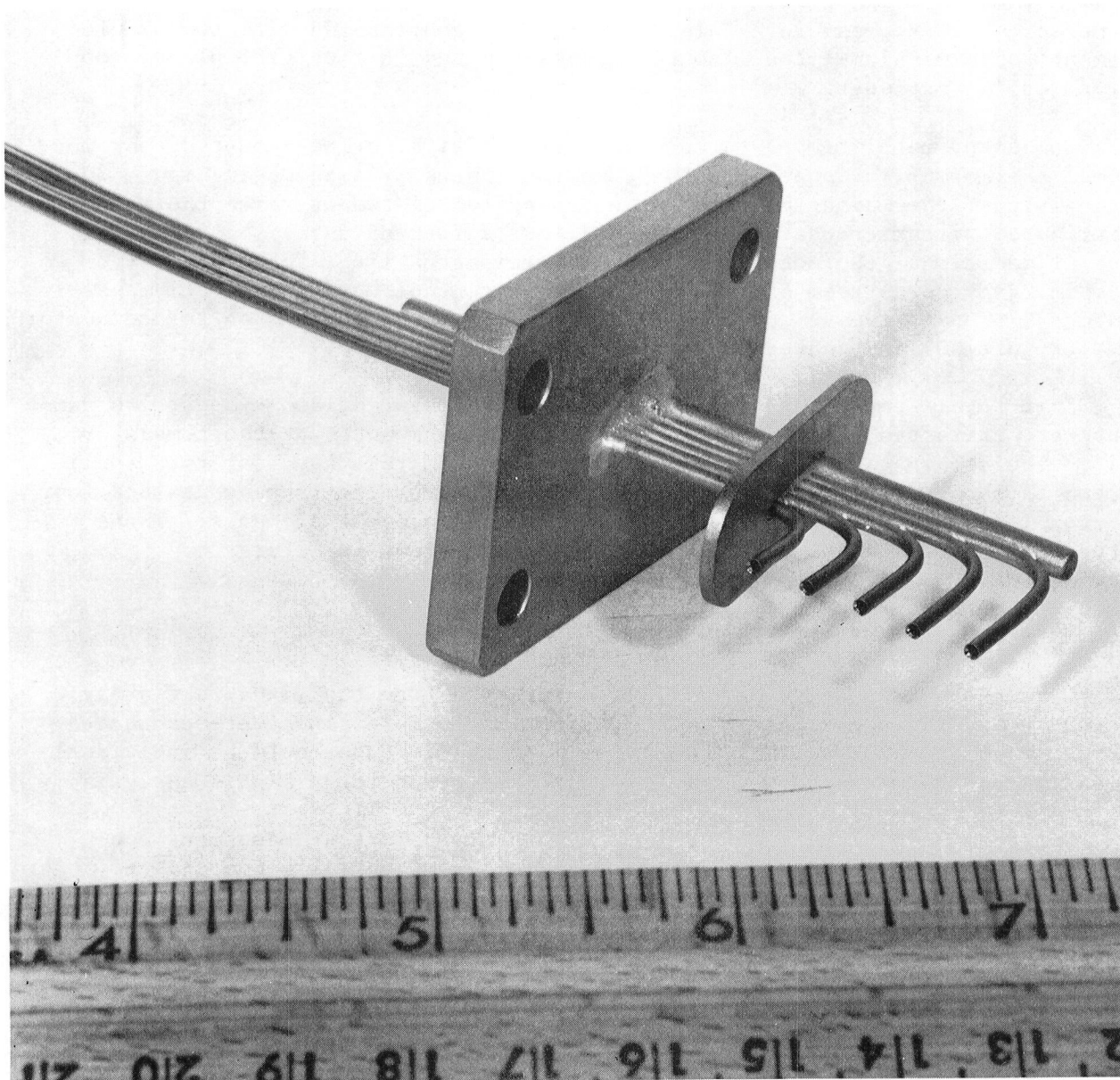
Figure 28. Inlet Total Pressure Rake.

38
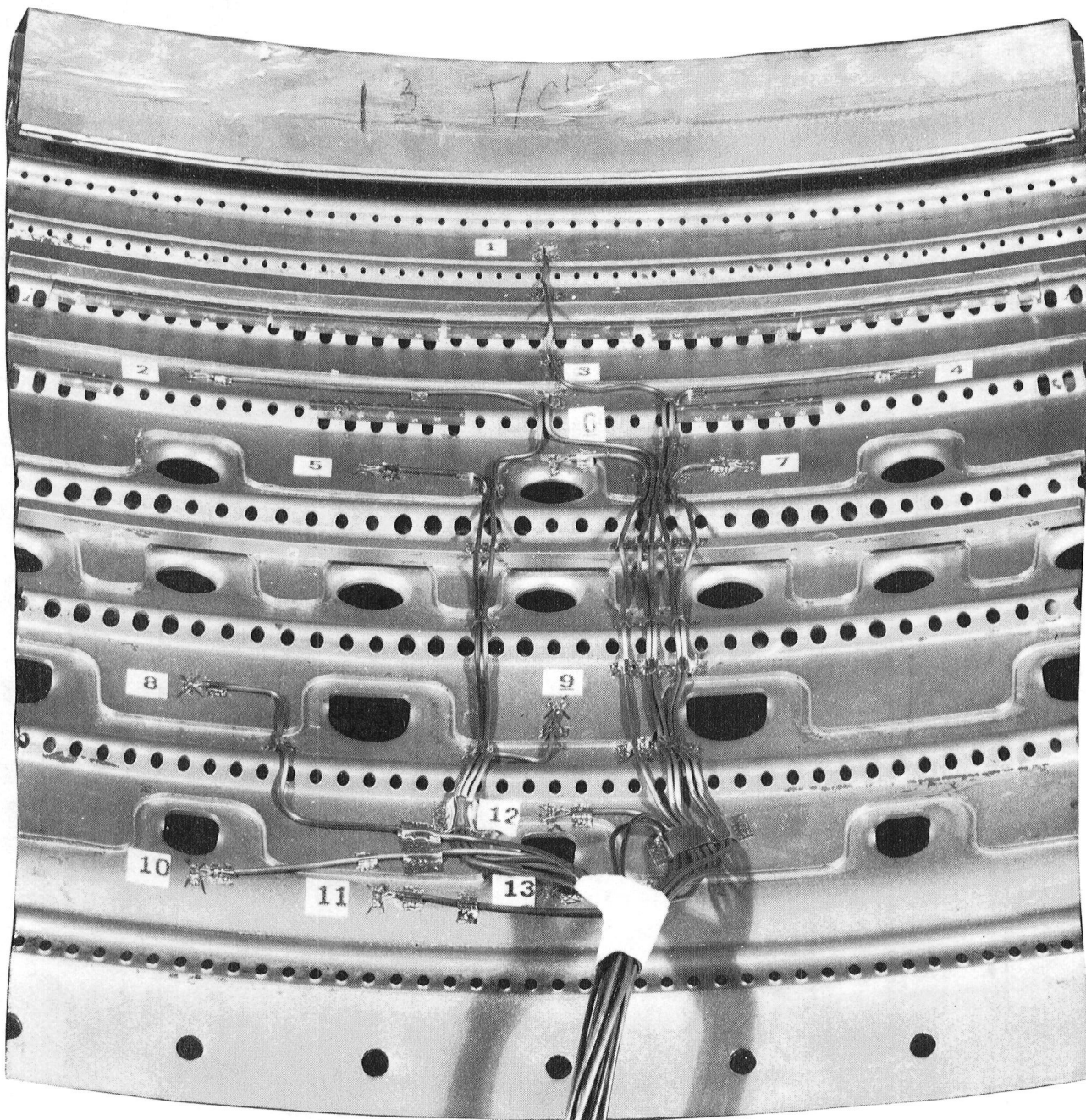
Figure 29. Typical Liner Thermocouple Installation.
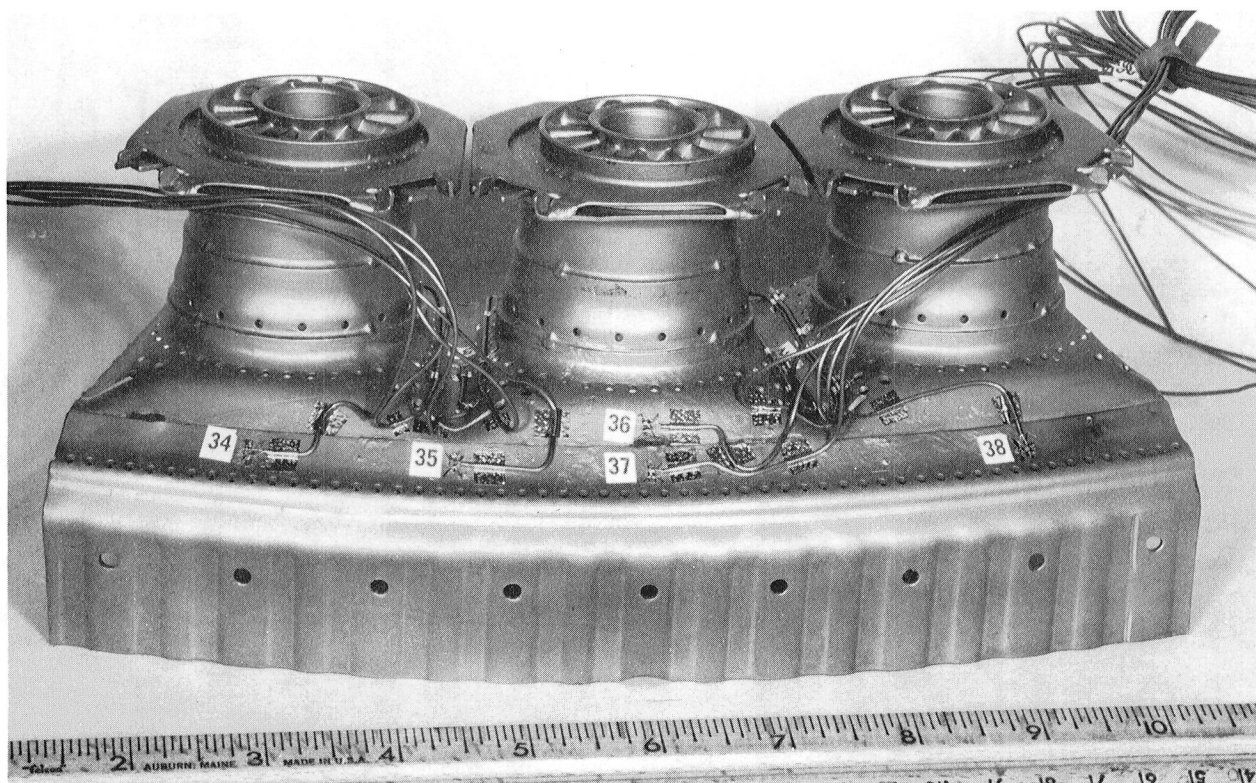
Figure 30. Typical Dome Thermocouple Installation.
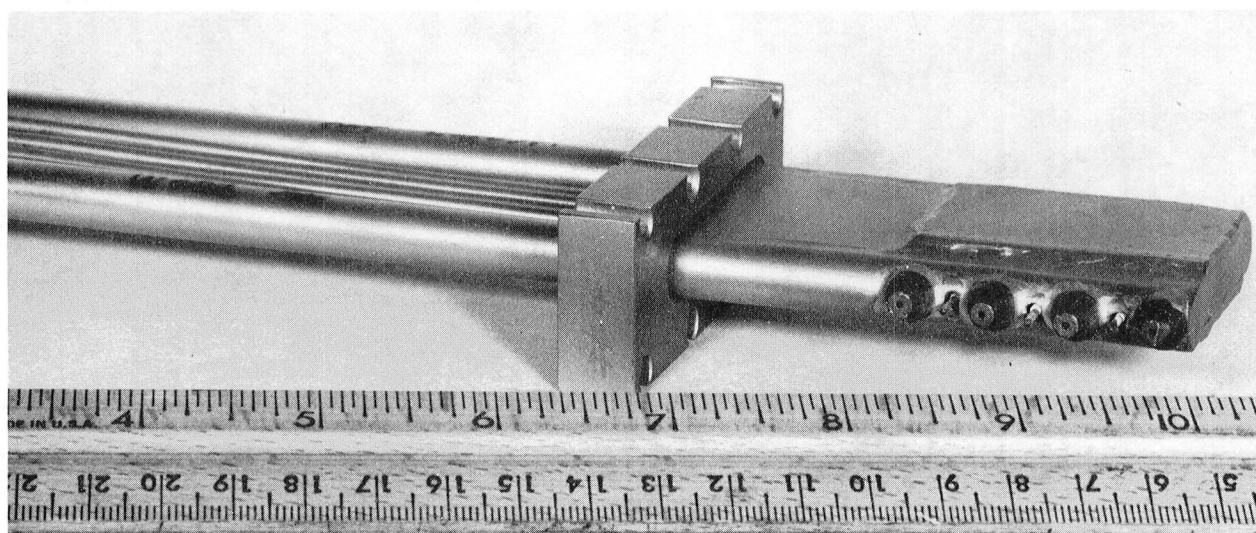
Figure 31. Gas-Sample, Total-Pressure, and Thermocouple Rake
for Combustor Exit.
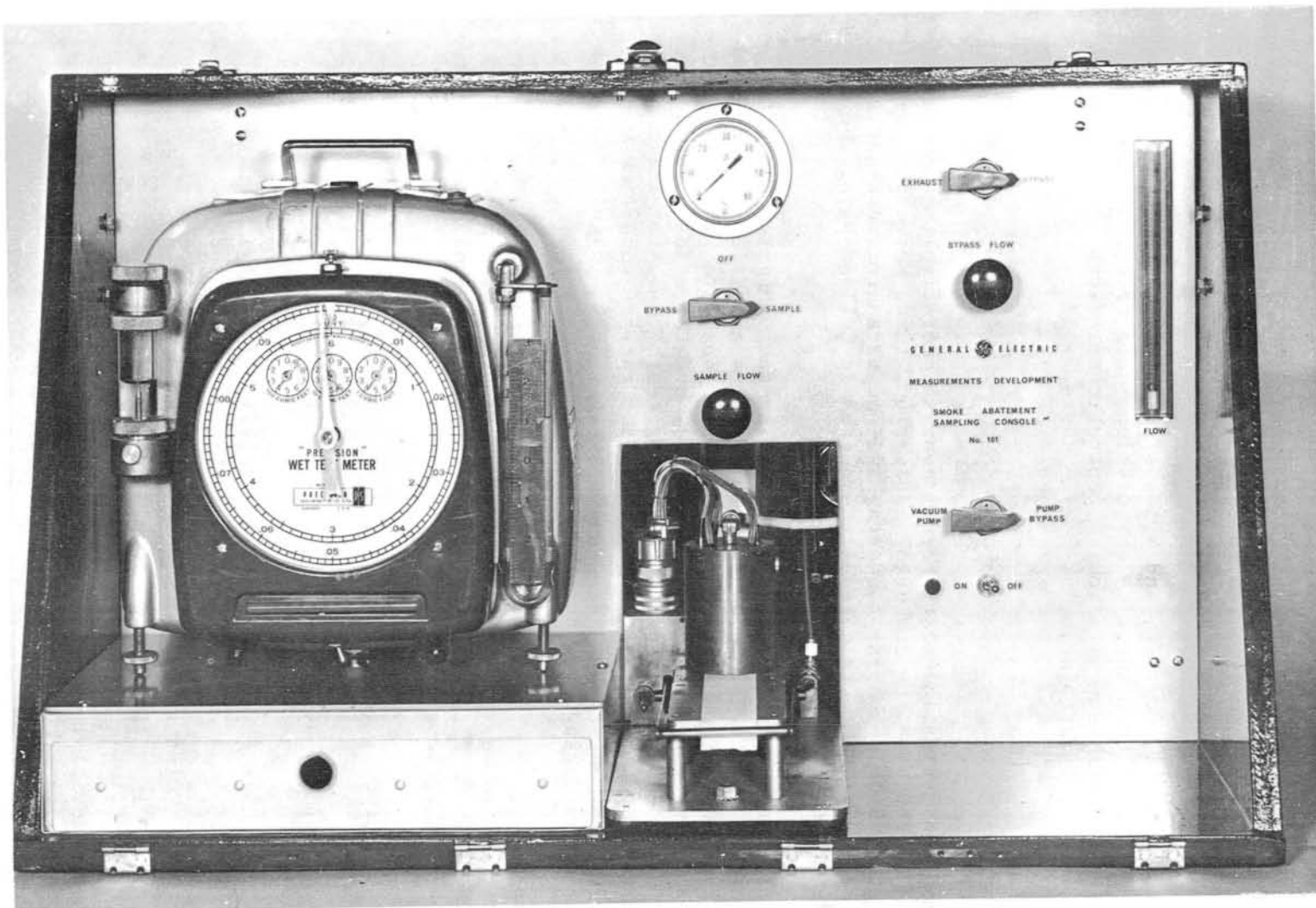
Figure 32. General Electric Smoke-Measurement Console.

the basic instruments is maintained at all times. Three-way valves are used to divert selected sample streams either to an overboard-vent manifold or into the analysis units. Each of the sample lines is maintained at 423 K up to the valve; then the sample is divided into separate streams leading to each of the analysis units. The stream supplied to the FID is maintained at the same temperature all the way to the analyzer.

Output from the CO, CO_2, HC, and NO_x analyzers of the CAROL system were manually recorded for later input to an emissions-data-reduction computer program that calculates exhaust-emission concentrations/indices, combustion efficiency, and sample fuel/air ratio.

4.5 TEST PROCEDURES

The combustor evaluation test program consisted of five test series including: one CF6-50 baseline combustor evaluation, three screening evaluations of advanced double-annular concepts, and one parametric evaluation of a selected concept. These tests were all conducted in Cell A5 using the CF6-50 sector rig described in Section 4.3.

The test point schedule used in the baseline and Concept 1 combustor evaluation is shown in Table VI. This schedule contains actual-cruise and simulated-takeoff combustor operating conditions, five combustor fuel/air ratios (spanning the engine operating fuel/air ratios), and three fuels for a total of 30 test conditions. In subsequent screening tests combustor-inlet temperature, pressure, and maximum fuel/air ratio at the takeoff condition were all decreased to prevent damage to the combustor-exit rakes. (Significant rake damage had occurred during the baseline test.)

All gaseous-emission data were corrected to the true-cruise or simulated-takeoff conditions shown in Table VI. The correlations used were developed as part of the NASA/GE ECCP program (Reference 2). These correlations resulted in the following equations:

$$(EINO_x)_2 = (EINO_x)_1 \ (P_2/P_1)^{0.5} \ (V_{r1}/V_{r2}) \ \exp \ \{[(T_2 - T_1)/195.6] +$$

$$[(H_1 - H_2)/53.19]\}$$

$$(EIHC)_2 = (EIHC)_1 \ (P_1/P_2) \ (V_{r2}/V_{r1}) \ \exp \ [(T_1 - T_2)/58.9]$$

$$(EICO)_2 = (EICO)_1 \ (P_1/P_2)^n \ (V_{r2}/V_{r1}) \ \exp \ [(T_1 - T_2)/82.8]$$

Where   The Subscript 2 indicates a corrected or nominal value

The Subscript 1 indicates a measured (test) value

$EINO_x$ is the nitrogen oxides emission index

EIHC is the unburned hydrocarbons emission index

EICO is the carbon monoxide emission index

H is absolute humidity

P is pressure

T is temperature

V_r is reference velocity

$$n = 0.2 \ [100/(EICO)_1]^{0.7} \leq 2.0$$

A humidity standard was not specified; so an arbitrary value of 2.0 g/kg was chosen, and cruise and simulated-takeoff NO_x data were corrected to this value. Smoke data were also corrected to the conditions shown in Table VI. The smoke data correction for P_3, T_3, and reference velocity was based on a correlation of F101 smoke data from Reference 7. An additional correction was made to account for the turbine-cooling air that would be present in the engine exhaust. The method used to correct for the dilution effect of turbine-cooling air (the same as that used in Reference 8) accounts for the variation of smoke number with carbon concentration.

At each test condition, all of the parameters shown in Table VII were recorded and/or computed. Except for gaseous emissions and smoke, all of the indicated parameters were processed on-line by a time-sharing computer system. Gaseous-emissions analyzer outputs were hand logged and manually input to a time-sharing, data-reduction program immediately following each run. Smoke tapes were also interpreted following the run. In addition to the data indicated in Table VII, photographs of the combustors were taken after each run to record the carboning characteristics.

Table VI. Screening Test Point Schedule.

Test Point Number	Fuel Type	W_{36}, Combustor Airflow, kg/s	P_{T3}, Combustor Inlet Pressure, MPa	T_{T3}, Combustor Inlet Temperature, K	V_r, Combustor(1) Reference Velocity, m/s	W_f, Fuel Flow, kg/s	f_{36} Fuel/Air Ratio, kg/kg	Remarks
1	Jet A	4.21	1.16	733	20.6	0.051	0.0120	
2		4.21	1.16	733	20.6	0.063	0.0150	
3		4.21	1.16	733	20.6	0.076	0.0180	True Cruise
4		5.34	1.59	827	21.6	0.080	0.0150	
5		5.34	1.59	827	21.6	0.096	0.0180	
6		5.34	1.59	827	21.6	0.112	0.0210	
7		5.34	1.59	827	21.6	0.126	0.0236	
8		5.34	1.59	827	21.6	0.139	0.0260	
9	1290 H	5.34	1.59	827	21.6	0.080	0.0150	
10		5.34	1.59	827	21.6	0.096	0.0180	
11		5.34	1.59	827	21.6	0.112	0.0120	
12		5.34	1.59	827	21.6	0.126	0.0236	Simulated Takeoff
13		5.34	1.59	827	21.6	0.139	0.0260	
14	BPF	5.34	1.59	827	21.6	0.080	0.0150	
15		5.34	1.59	827	21.6	0.096	0.0180	
16		5.34	1.59	827	21.6	0.112	0.0210	
17		5.34	1.59	827	21.6	0.126	0.0236	
18		5.34	1.59	827	21.6	0.139	0.0260	
19		4.21	1.16	733	20.6	0.051	0.0120	
20		4.21	1.16	733	20.6	0.063	0.0150	
21		4.21	1.16	733	20.6	0.076	0.0180	
22		4.21	1.16	733	20.6	0.088	0.0210	
23		4.21	1.16	733	20.6	0.099	0.0236	
24	Jet A	4.21	1.16	733	20.6	0.088	0.0210	True Cruise
25		4.21	1.16	733	20.6	0.099	0.0236	
26	12% H	4.21	1.16	733	20.6	0.051	0.0120	
27		4.21	1.16	733	20.6	0.063	0.0150	
28		4.21	1.16	733	20.6	0.076	0.0180	
29		4.21	1.16	733	20.6	0.088	0.0210	
30		4.21	1.16	733	20.6	0.099	0.0236	

(1)Based on W_{36}, P_{T3}, T_{T3}, and 0.371 m^2 Casing Area.

Table VII. Measured and Calculated Combustor Parameters, Sector Combustor Tests.

Parameter	Symbol	Unit	Measured	Calculated	Value Determined From
Inlet Total Pressure	P_{T3}	MPa	X		Average of Measurements from 2 Immersions on 1 Rake
Exit Total Pressure	$P_{T3.9}$	MPa	X		Average of Measurements from 4 Immersions on 3 Rakes (12 Total)
Total Pressure Loss	$\Delta P_T/P_{T3}$	%		X	$100\ (P_{T3} - P_{T3.9})/P_{T3}$
Combustor Airflow	W_c	kg/s		X	ASME Orifice
Reference Velocity	V_r	m/s		X	$W_{36}/(\rho_3 A_{casing})^*$
Total Fuel Flow	W_f	kg/s	X		Turbine Flowmeter
Pilot Fuel Flow	W_{fp}	kg/s	X		Turbine Flowmeter
Main-Stage Fuel Flow	W_{fm}	kg/s	X		Turbine Flowmeter
Overall Metered Fuel/Air Ratio	f	---		X	W_f/W_c
Pilot-Stage Fuel/Air Ratio	f_p	---		X	W_{fp}/W_c
Main-Stage Fuel/Air Ratio	f_m	---		X	W_{fm}/W_c
Inlet Air Humidity	H	g/kg	X		Dew-Point Hygrometer
Inlet Total Temperature	T_{T3}	K	X		Average of Measurements from 2 Immersions on 1 Rake
Exit Total Temperature	$T_{T3.9}$	K		X	Average of Measurements from 3 Immersions on 3 Rakes (9 Total)
Combustor Metal Temperatures	T_c	K	X		Approximately 30 Skin Thermocouples
Gas-Sample Fuel/Air Ratio	f_s	---		X	Manifolded 12-Point Gas Sample
Gas-Sample Smoke Number	SN	---		X	ARP 1179 and 1256 Equations
Gas-Sample CO Emission Index	EICO	g/kg		X	ARP 1179 and 1256 Equations
Gas-Sample HC Emission Index	EIHC	g/kg		X	ARP 1179 and 1256 Equations
Gas-Sample NO_x Emission Index	$EINO_x$	g/kg		X	ARP 1179 and 1256 Equations
Combustion Efficiency	η	%		X	Gas-Sample Analysis
Fuel Injector Pressure Drop	ΔP_f	MPa	X		Fuel-Manifold Pressure Taps

$^*\rho_3$ is the fluid density of the combustor inlet.

5.0 FUEL CHARACTERISTICS

This program showed the effects on the test combustors of three fuels with nominal hydrogen contents of 12, 13, and 14% by weight. The 13% hydrogen fuel was the research BPF. This fuel has been proposed for the development of future combustors because it incorporates characteristics expected in future fuels. The second and third fuels used in this program were required to have hydrogen contents of 14.0 ± 0.2% and 12.0 ± 0.2%. Other requirements were not specified, provided the fuel had physical characteristics similar to those of the BPF. These requirements were met by using Jet A for the 14% fuel and a special blend for the 12% fuel.

It is possible that future fuels will have less desirable combustion characteristics and low-temperature properties because of the diminishing availability of premium crudes for making aviation kerosenes. Currently, the combustion characteristics of Jet A are controlled by aromatics content (25% maximum), smoke point (18 minimum), and naphthalene content (3% maximum). However, present plans are considering the replacement of one or more of the above controls by a requirement for minimum-hydrogen content; this is regarded as a more precise and significant measurement. Average Jet A, today, has a hydrogen content of 13.8%. The BPF was targeted to a substantially lower, but still realistic, level and was established at 12.8%.

The low-temperature properties of Jet A are controlled by the freezing point, 233 K maximum, and the viscosity at 253 K, 8 mm^2/s maximum. The corresponding values established for the BPF were: freezing point, 244 K maximum and viscosity at 253 K, 12 mm^2/s maximum.

The requirements of the BPF specification are shown in Table VIII. Some of the test methods listed were waived for expediency or practicality. For example, in lieu of the NMR (Nuclear Magnetic Resonance) procedure for hydrogen content, GE was authorized to use a macrocombustion method, GE AEG Specification E50TF77-51, with a standard deviation for precision of 0.02% hydrogen. Also, since the American Society for Testing Materials (ASTM) Method D1219 for mercaptan sulfur was withdrawn as a standard in 1979, ASTM Method D3227 (the potentiometric method) was used instead.

Further, the Kjeldahl procedure for nitrogen was not considered suitable for the fuels used in this program because it has a repeatability of 100 ppm, and these fuels were expected to have nitrogen contents in the range of 3 to 100 ppm. Therefore, the procedure used was ASTM Method D3431, the microcoulometric method for trace nitrogen. This method is applicable to fuels containing from 2 to 5000 ppm total nitrogen and has a repeatability of about 3 ppm maximum at a nitrogen level of 40 ppm.

Method D1840, for naphthalenes, is not applicable to fuels containing more than 5% polycyclic compounds or to fuels having end points higher than

Table VIII. Characteristics of Research Broad-Property Test Fuel.

Property	Specification	Test Method	Test Results
Composition			
Hydrogen, Wt %	12.8 ± 0.2	NMR[1]	12.95
Aromatics, Vol %	Report	ASTM D1319	35.0
Sulfur, Mercaptan, Wt %	0.003, Max.	ASTM D1219[1]	0.00052
Sulfur, Total, Wt %	0.3 Max.	ASTM D1266	0.085
Nitrogen, Total, Wt %	Report	Kjeldahl[1]	0.0054
Naphthalenes, Vol %	Report	ASTM D1840[1]	13.15
Volatility			
Distillation Temperature, K			
Initital Boiling Point	Report	ASTM D2892[1]	448
10% Recovered	477 Max.		461
50% Recovered	Report		488
90% Recovered	533 Min.		552
Final Boiling Point	Report		598
Residue, %	Report		1.2
Loss, %	Report		0.3
Flashpoint, K	316 ± 6	ASTM D56[1]	332
Gravity, API[3] (289 K)	Report	ASTM D287	37.4
Gravity, Specific (289/289 K)	Report	ASTM D1298	0.8377
Fluidity			
Freezing Point, K	244 Max.	ASTM D2386	244
Viscosity at 250 K, mm^2/s	12 Max.	ASTM D445	6.52
Net Heat of Combustion, MJ/kg	Report	ASTM D2382	42.51
Thermal Stability			
JFTOT[4] Breakpoint Temp, K (TDR[5] = 13 and ΔP = 25 mm)	511 Min.	ASTM D3241	>511[2]

1. See text for methods actually used
2. Results at 511 K: TDR = 0, ΔP = 0, Visual = 1
3. American Petroleum Institute
4. Jet Fuel Thermal Oxidation Test
5. Tube Deposit Rating

600° F. One or more of the test fuels was expected to exceed these limits, thus casting some doubt on the validity of the results. Therefore, the preferred test procedure for naphthalenes in fuels of this type is gas chromatography; this method can show significantly higher levels than ASTM Method D1840. Gas chromatography was therefore used for determining the naphthalene content of the three test fuels.

The specified distillation test, ASTM Method D2892, is intended primarily for the distillation of crude oils. A high-efficiency, fractionating column is included for the precise separation of the individual hydrocarbons in the original material. The results obtained are not particularly useful in defining engine fuels because established temperatures do not readily relate to those used with the conventional distillation test, ASTM D86. Therefore, ASTM Method D86 was proposed and approved to define the distillation characteristics of the test fuels.

The PM (Pensky-Martens) closed flash-point method, ASTM D93, was approved in lieu of the specified TCC (Tag Closed Cup) procedure, ASTM Method D56, because the former is routinely used by General Electric at Evendale. Available data indicate that PM results average 1.1 K higher than TCC results.

The BPF used in this program was supplied by NASA. The material was reported to be a blend of approximately 35% (by volume) kerosene and 65% hydrotreated catalytic gas oil. An independent analysis of this fuel is given by Prok and Seng (Reference 8). The BPF analysis indicated that the fuel met all the requirements of the research-fuel specification except for the flash point (10 K too high). Because flash point has a negligible effect on performance at cruise and takeoff conditions, the fuel was accepted for use in this program.

The 14% hydrogen content fuel was a commercial Jet A available at the General Electric Evendale plant. The analysis of this fuel is shown in Table IX.

The 12% hydrogen content fuel was prepared by blending 52% (by volume) Jet A fuel from the General Electric Evendale plant supply with 48% light cycle oil (LCO) procured from the Ashland Petroleum Company. The light cycle oil is an internal refinery product high in aromatic content; it is used in blending diesel fuel. The analysis of this fuel blend is shown in Table X.

Distillation curves of the three test fuels are shown in Figure 33.

48

Table IX. Characteristics of Jet A Test Fuel.

Property	Specification	Test Method	Test Results
Composition			
Hydrogen, Wt %	---	E50TF77-51[1]	13.98
Aromatics, Vol %	20 Max.	ASTM D1319	16.7
Sulfur, Mercaptan, Wt %	0.003 Max.	ASTM D3227	0.001
Sulfur, Total, Wt %	0.3 Max.	ASTM D1266	0.01
Nitrogen, Total, Wt %	---		---
Naphthalenes, Vol %	3.0 Max.	Gas Chromatography	1.82
Volatility			
Distillation Temperature, K		ASTM D86	
Initial Boiling Point	---		452
10% Recovered	477 Max.		472
50% Recovered	Report		491
90% Recovered	Report		513
Final Boiling Point	573 Max.		530
Residue, %	1.5 Max.	ASTM D86	1.0
Loss, %	1.5 Max.	ASTM D86	1.0
Flashpoint, K	310.8 Min.	ASTM D93	334
Gravity, API (289 K)	37-51	ASTM D287	42.7
Gravity, Specific (289/289 K)	0.775-0.840	ASTM D1298	0.8123
Fluidity			
Freezing Point, K	233 Max.	ASTM D2386	227
Viscosity at 253 K, mm^2/s	8 Max.	ASTM D445	7.6
Net Heat of Combustion, MJ/kg	42.8 Min.	ASTM D2382	43.13
Thermal Stability			
JFTOT Breakpoint Temp, K (TDR = 13 and ΔP = 25 mm)	---	ASTM D3241	>511[2]

1. GE Specification
2. Results at 533 K: TDR = 0, ΔP = 0, Visual = 1

Table X. Characteristics of the 12% Hydrogen Test Fuel Blend and Light Cycle Oil.

Property	Test Method	LCO/Jet A Blend Test Results	LCO Test Results
Composition			
Hydrogen, Wt %	E50TF77-51[1]	12.06	10.07
Aromatics, Vol %	ASTM D1319	47.0	
Sulfur, Mercaptan, Wt %	ASTM D3227	0.0003	
Sulfur, Total, Wt %	ASTM D1266	0.83	
Nitrogen, Total, Wt %		0.0137	
Naphthalenes, Vol %	Gas Chromatography	23.0	
Volatility			
Distillation Temperature, K	ASTM D86		
Initial Boiling Point		476	
10% Recovered		485	
50% Recovered		515	
90% Recovered		567	
Final Boiling Point		607	
Residue, %	ASTM D86	0.9	
Loss, %	ASTM D86	0.3	
Flashpoint, K	ASTM D93	342	
Gravity, API (289 K)	ASTM D287	31.05	
Gravity, Specific (289/289 K)	ASTM D1298	0.8705	0.9409
Fluidity			
Freezing Point, K	ASTM D2386	250	
Viscosity at 253 K, mm^2/s^2	ASTM D445	11.9	
Net Heat of Combustion, MJ/kg	ASTM D2382	41.81	
Thermal Stability			
JFTOT Breakpoint Temp, K (TDR = 13 and ΔP = 25 mm)	ASTM D3241	<511[2]	

1. GE Specification
2. Results at 511 K: TDR = 14.5, ΔP = D, Visual = 4P
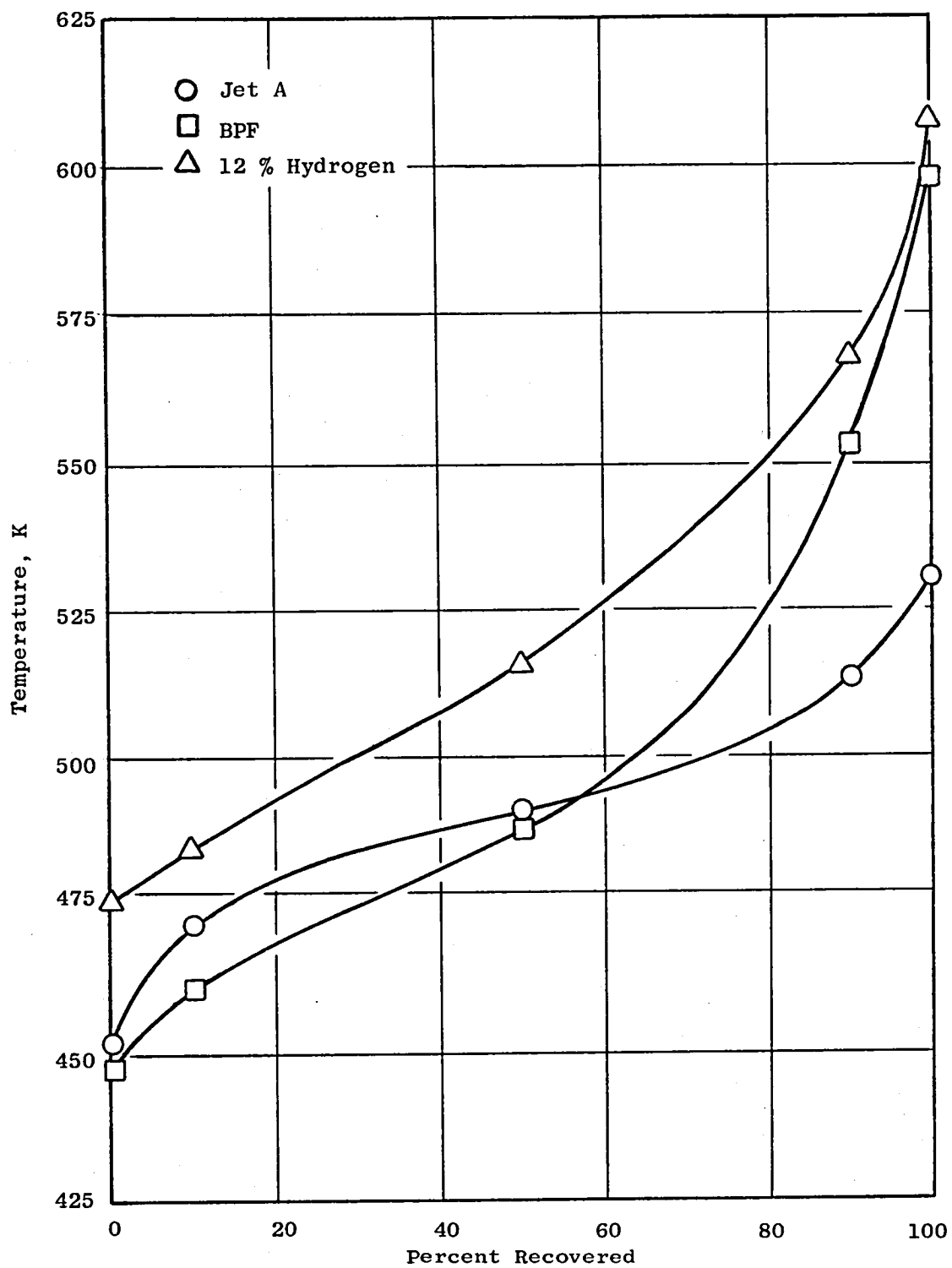
Figure 33. Distillation Curves of the Three Test Fuels.

6.0 EXPERIMENTAL TEST RESULTS

The Experimental evaluation of the test combustors consisted of a screening test of the baseline CF6-50 and three advanced burner concepts and a parametric test of one selected configuration. The screening tests were scheduled for 6 hours each and the parametric test for 12 hours. However, some extra points were run to verify or further explore observed trends, and fuel changes took longer than anticipated. As a result, each test consumed from 18 to 24 hours. In each test, lightoff was accomplished on Jet A fuel, the cruise or takeoff operating condition was set, and fuels were changed while the burner was operating.

6.1 BASELINE TEST RESULTS

The baseline CF6-50 burner was tested first. NO_x emissions levels, liner temperatures, and carbon formation were as expected based on previous full-annular tests of the same combustor configuration. The sector-combustor baseline test also demonstrated that trends with operating conditions for smoke and CO levels were as expected although the absolute levels were higher for these parameters than would occur in full-annular combustor tests. The reasons for the increased levels are test-rig-sidewall cooling and air leakage that could not be completely eliminated between the combustor and test rig. The leakage air quenches combustion reactions at the sides of the burner, thereby increasing CO levels. This side leakage air also increases center-swirl-cup equivalence ratio by reducing dome airflow. This increase in center-swirl-cup equivalence ratio leads to increased smoke. Leakage was minimized by sealing gaps at the burner sides with Nichrome strips, but even with the Nichrome seals leakage was estimated to be on the order of 5 to 10%. Even with the leakage, however, trends with operating conditions were as expected.

Figures 34 and 35 show how liner temperatures for the baseline combustor varied with fuel/air ratio for the three test fuels. Liner temperatures are seen to have increased not only with fuel/air ratio but also with decreasing hydrogen content at both takeoff and cruise. A correlation of maximum liner temperature with fuel hydrogen content is shown in Figure 36 for both takeoff and cruise at a fuel/air ratio of 0.021. The liner temperature decrease of about 30 K/1% hydrogen is in general agreement with results from other test programs. The temperature distribution along the baseline burner is shown in Figure 37.

Posttest inspection of the baseline burner revealed a light (approximately 0.1 mm) and fairly uniform coating of soot on the liners and dome surfaces, with carbon deposits of up to 1.5 mm on the swirl cup venturis (see Figures 38, 39, and 40). There was no carbon buildup on the fuel nozzles (Figure 41). The carbon buildup on the baseline combustor is as expected from previous experience.
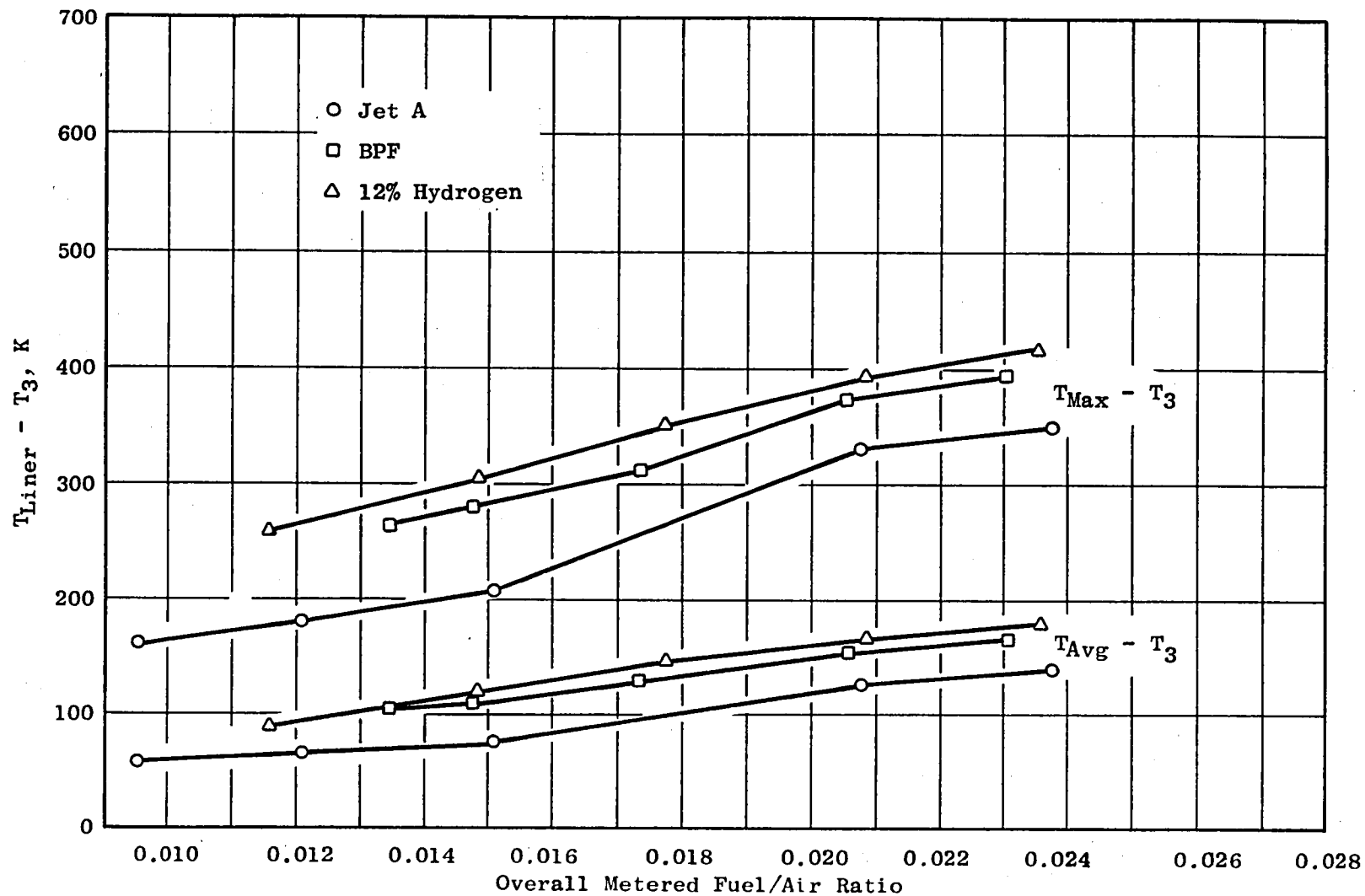
Figure 34. Baseline CF6-50 Liner Temperatures at Cruise Conditions.
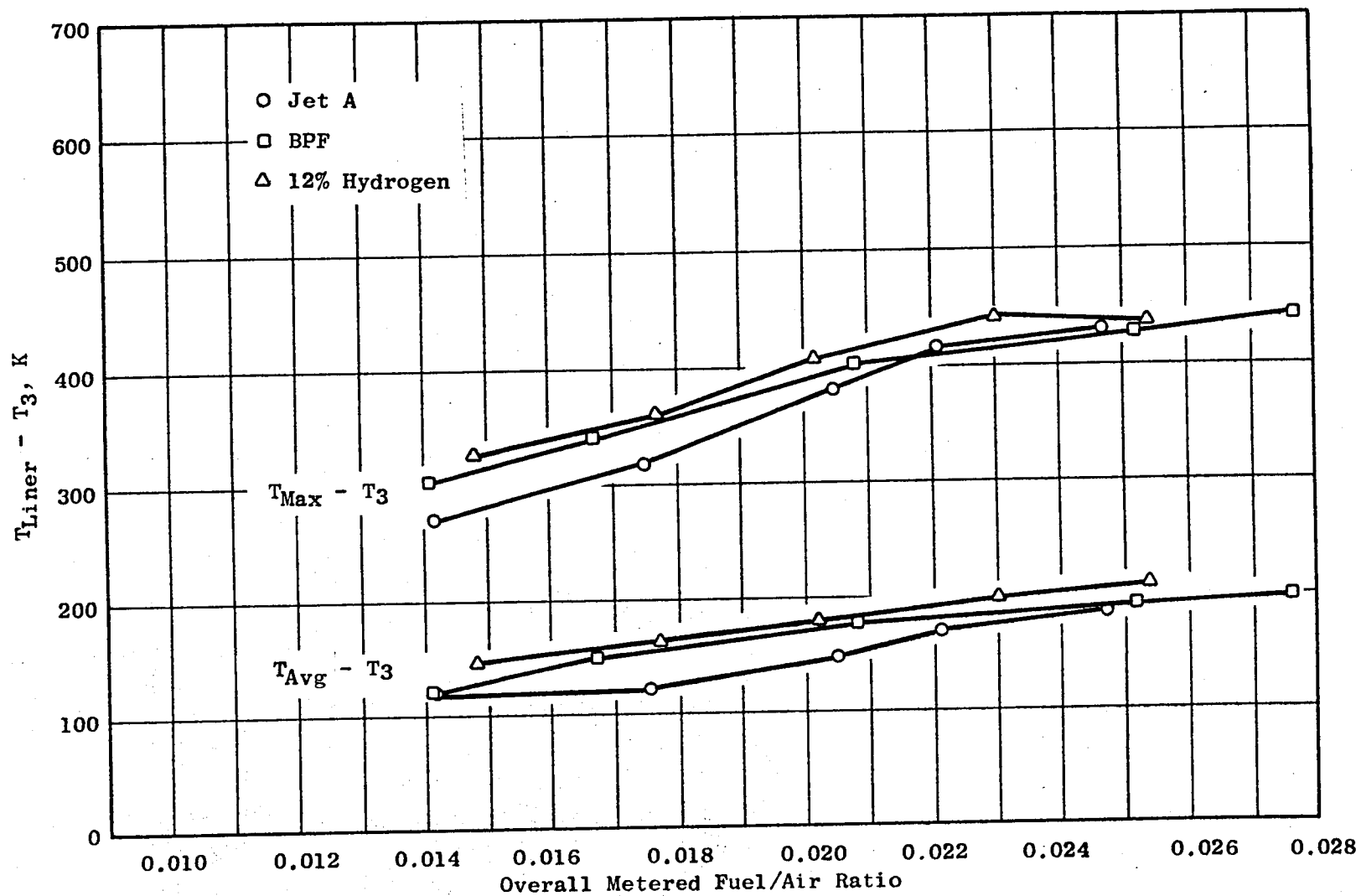
Figure 35. Baseline CF6-50 Liner Temperatures at Simulated Takeoff Conditions.
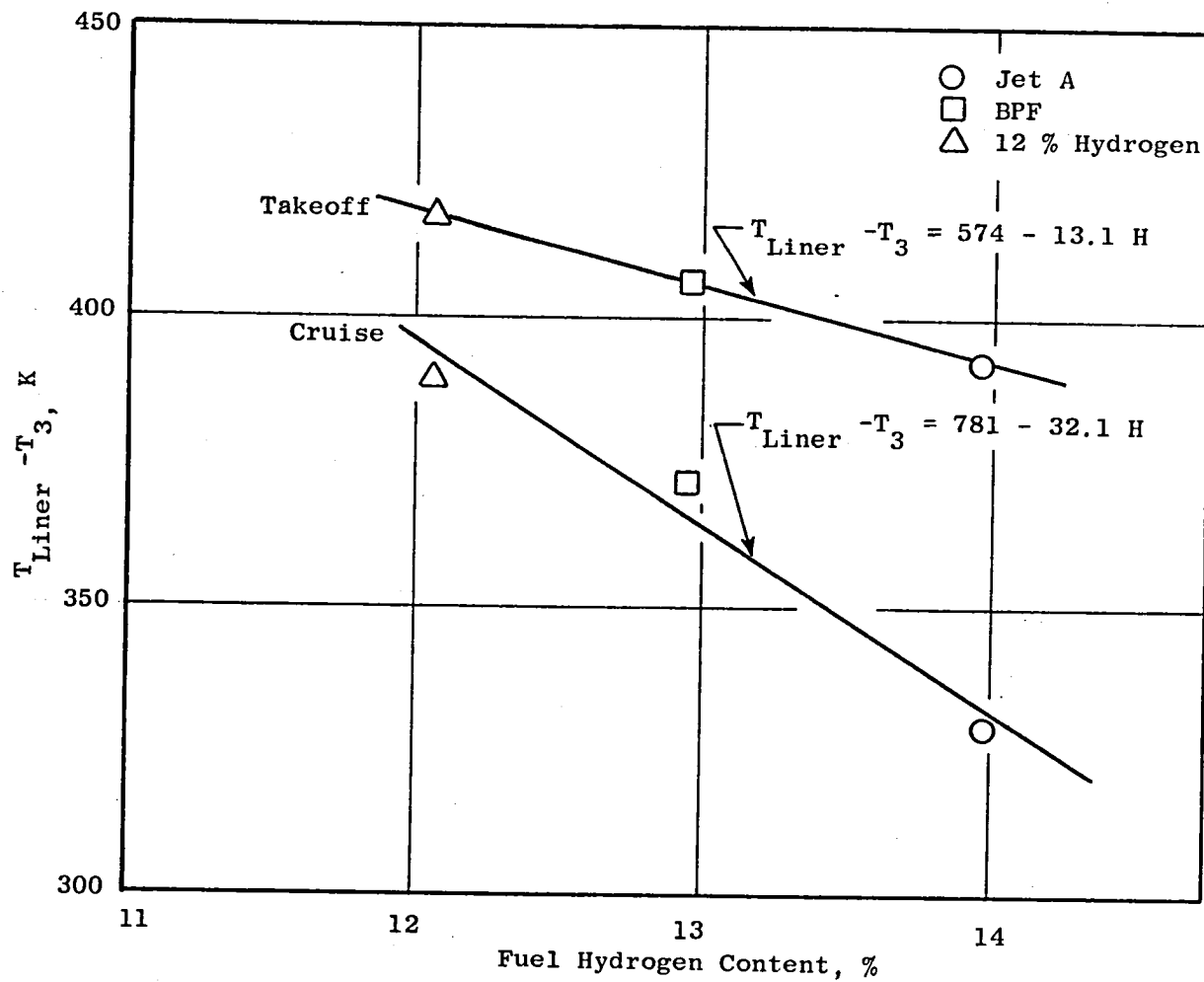
Figure 36. Variation of Baseline CF6-50 Maximum Liner Temperature with Fuel Hydrogen Content, f = 0.021.
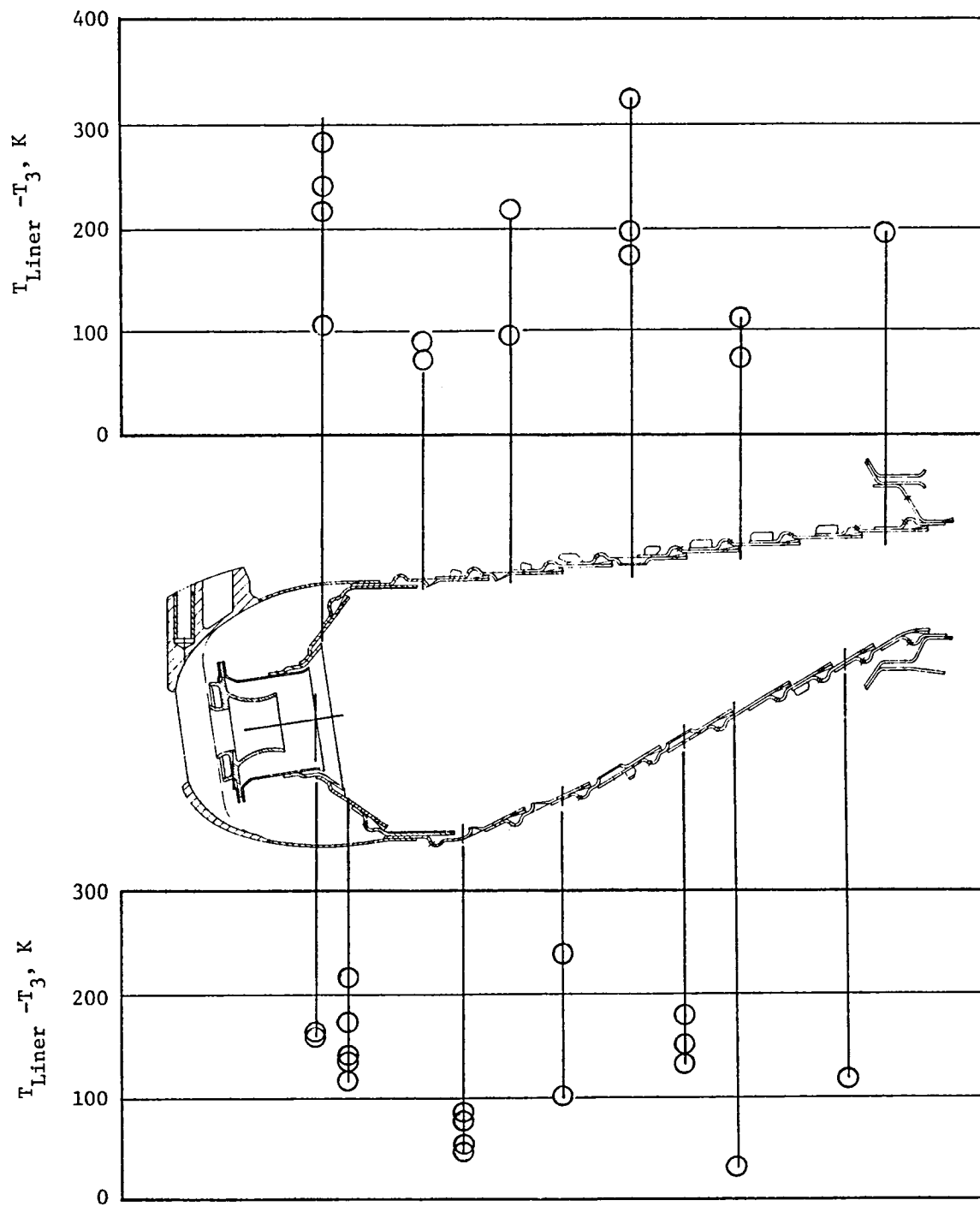
Figure 37. Baseline CF6-50 Liner Temperature Distribution at
Cruise Conditions, Jet A Fuel, f = 0.021.
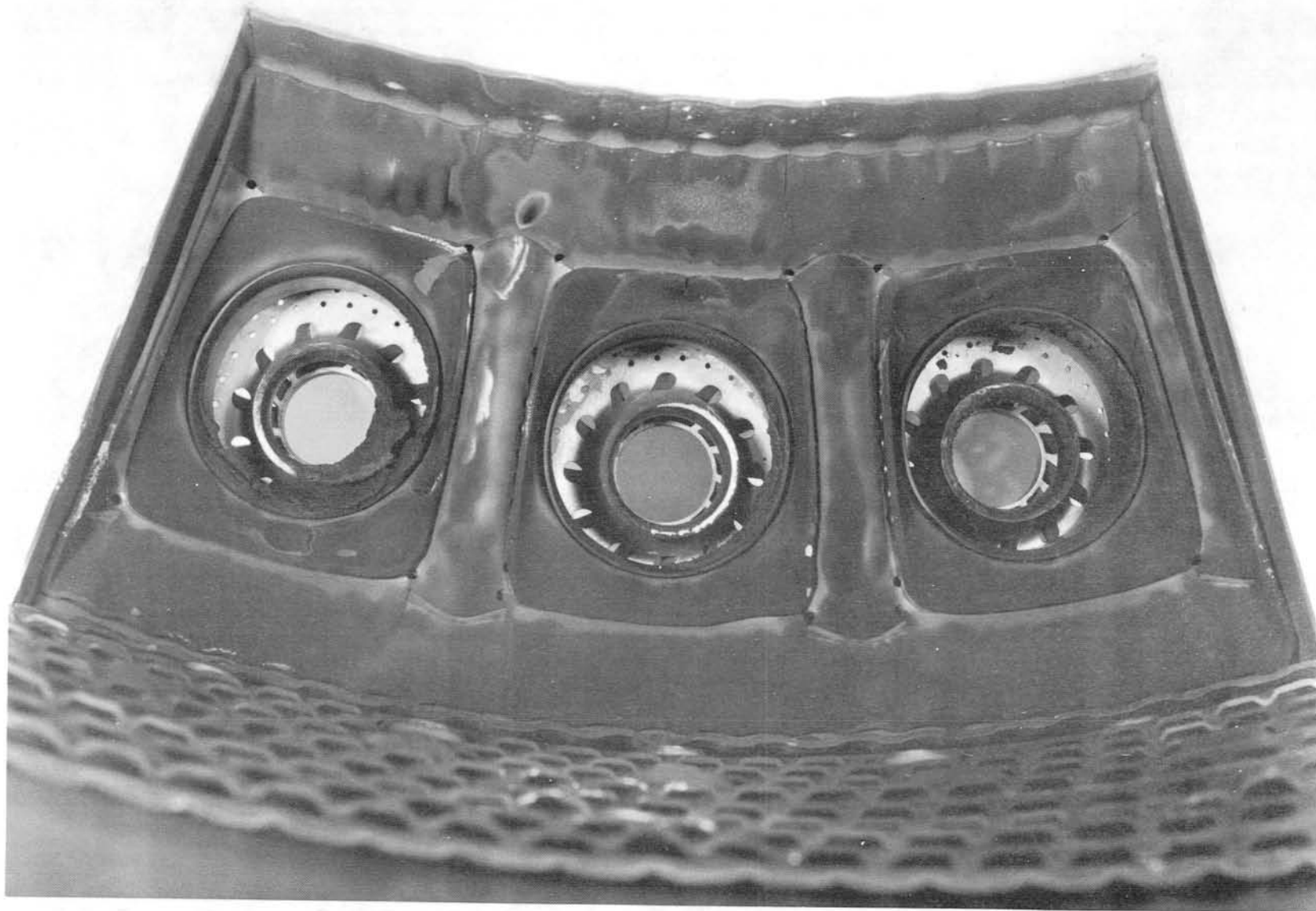
Figure 38.   Baseline CF6-50 Dome and Outer Liner After Test.

57
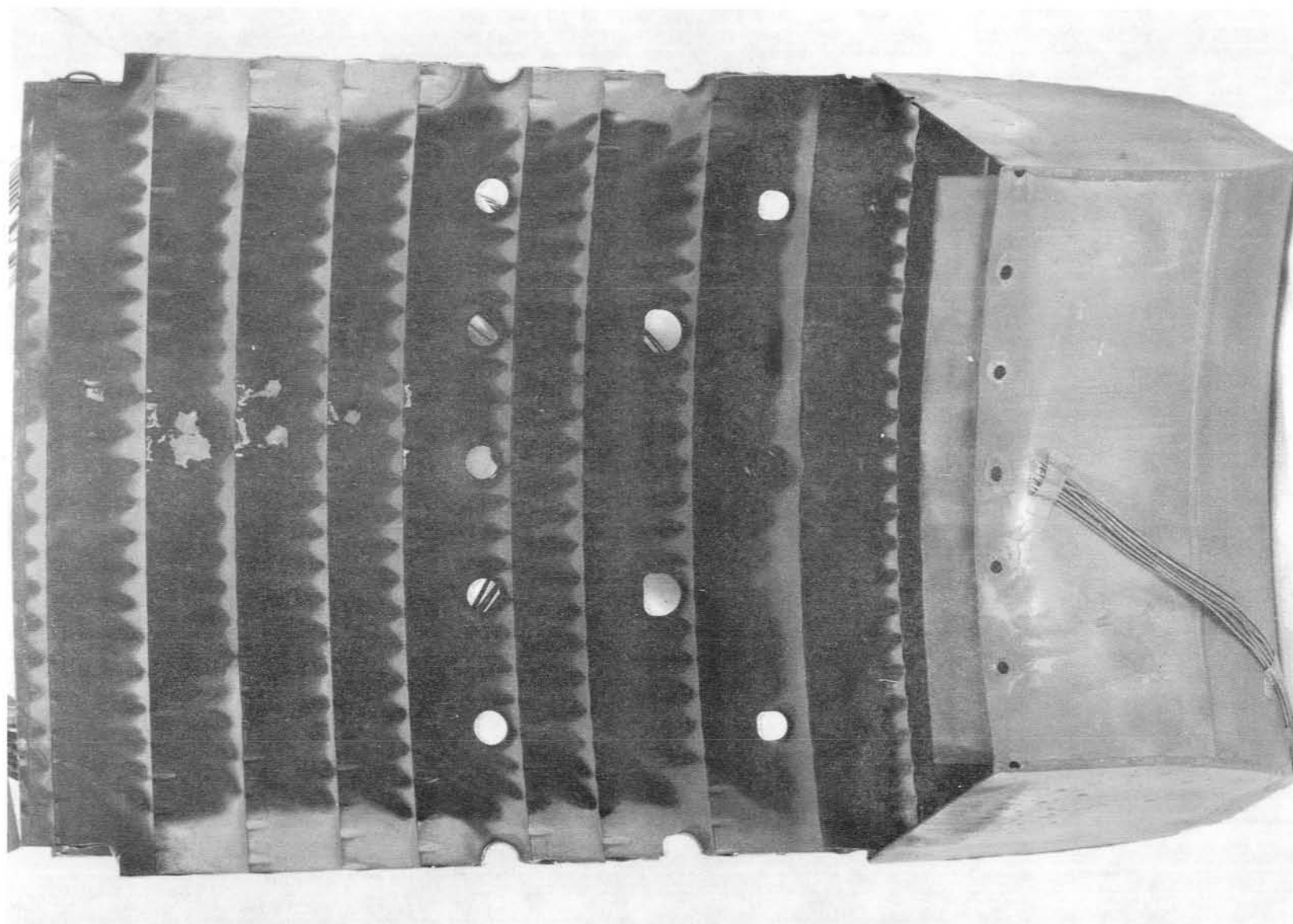
Figure 39.   Baseline CF6-50 Outer Liner After Test.
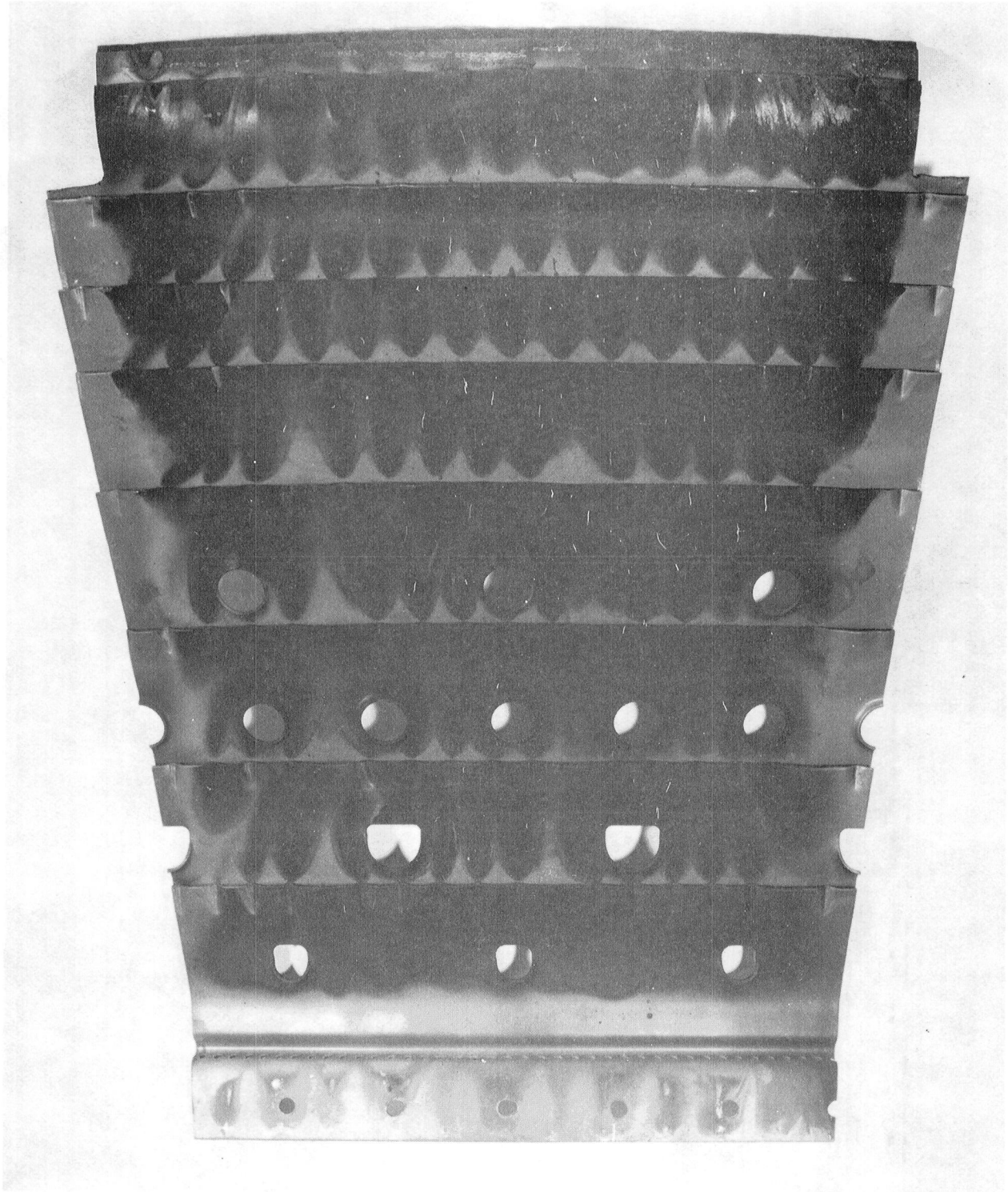
Figure 40.   Baseline CF6-50 Inner Liner After Test.
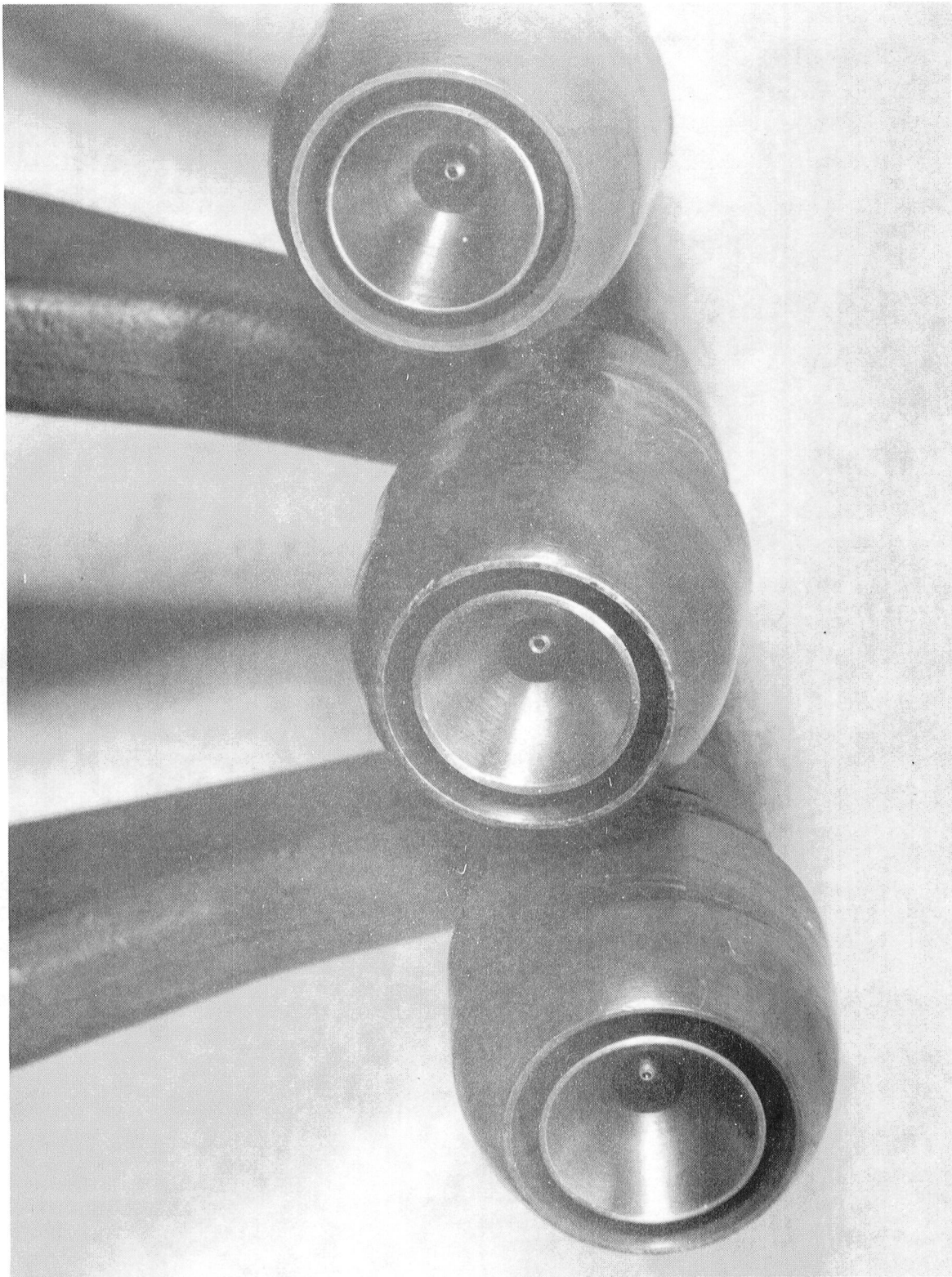
Figure 41. Baseline CF6-50 Fuel Nozzles After Test.

Figure 42 presents the baseline-combustor smoke data as a function of fuel hydrogen content. As anticipated, the smoke level is significantly higher for the fuels with reduced hydrogen content.

NO_x emission indices from the CF6-50 burner are shown in Figures 43 and 44. The decrease with fuel/air ratio is as expected, and the levels measured agree well with expectations based on previous, full-annular combustor tests. The higher NO_x levels at low fuel/air ratio indicate that the dome equivalence ratio is closer to unity, giving higher flame temperatures. NO_x emission indices are also seen to increase with decreasing fuel hydrogen content (Figures 45 and 46).

CO emission indices are shown in Figures 47 and 48. The increase in CO emissions with fuel/air ratio is due to the dome equivalence ratio increasing beyond 1.0. There is no strong correlation between CO emission index and fuel hydrogen content. The CO emission index is believed to be a stronger function of vaporization properties than of fuel hydrogen content.

The unburned hydrocarbon emission index has been correlated with CO emission index by Gleason (Reference 4). These correlations correctly predict very low unburned hydrocarbon emission indices at the low CO emission indices measured here. Unburned hydrocarbon emission indices were all below 0.5 g/kg during this test.

Inspection of the three thermocouple/P_T/gas-sample rakes after the baseline test revealed that 5 of the 12 copper-tipped, gas-sample probes were plugged with either carbon or copper that had eroded from the tips. The rakes were refurbished prior to the next test and modified by drilling a hole in the top of each rake to increase cooling-water flow.

These tests established a set of data to serve as a basis for comparison for the three advanced combustors. The results also verified that the sector test rig provided representative results for NO_x emission levels, liner temperatures, and carbon formation. Further, the trends of smoke and CO emissions with operating conditions were as expected for the baseline burner although the absolute levels were high for the reasons mentioned above.

6.2 CONCEPT 1 SCREENING TEST RESULTS

Concept 1 was the second burner tested. This double-annular combustor produced very low smoke levels and showed little sensitivity to fuel hydrogen content with regard to smoke levels and metal temperatures. The NO_x emission levels were lower than those of the baseline combustor but higher than expected for this design based on previous tests of similar designs. It is suspected that the NO_x emission levels may have been influenced somewhat by the loss of some Nichrome patches on the combustor during the test. Loss of the patches resulted in a slight change in air distribution and an increase in dome equivalence ratio.
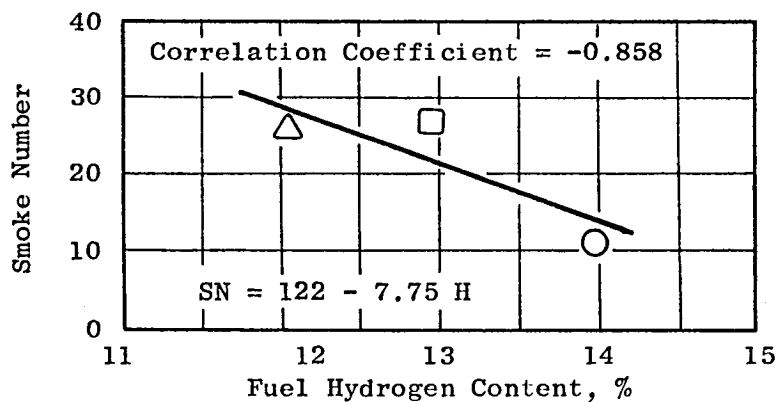
Figure 42. Variation of Baseline CF6-50 Smoke
Number with Fuel Hydrogen Content at
Simulated Takeoff Conditions, f = 0.018.
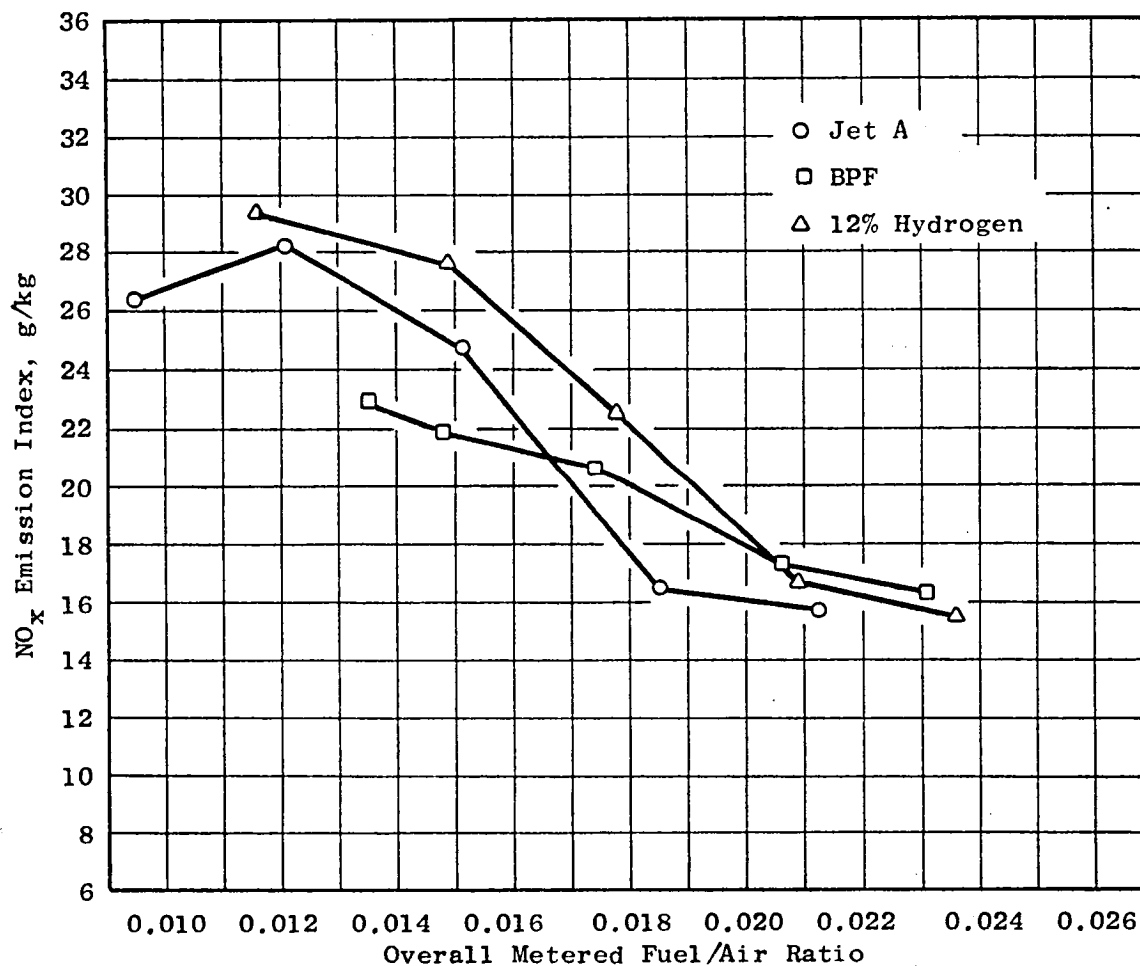
Figure 43. Baseline CF6-50 NO_x Emission Index at Cruise Conditions.
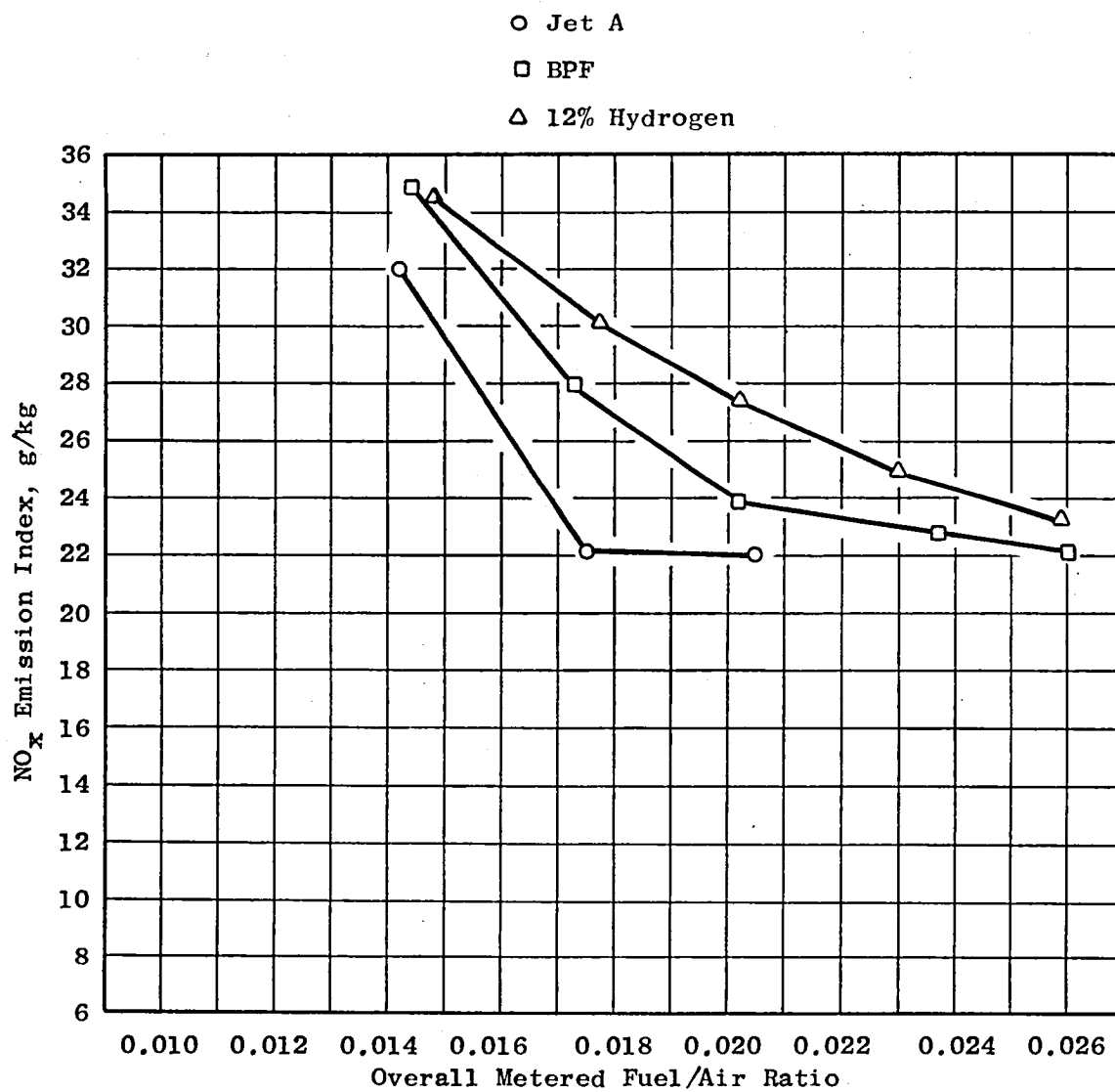
Figure 44. Baseline CF6-50 NO_x Emission Index at Simulated Takeoff Conditions.
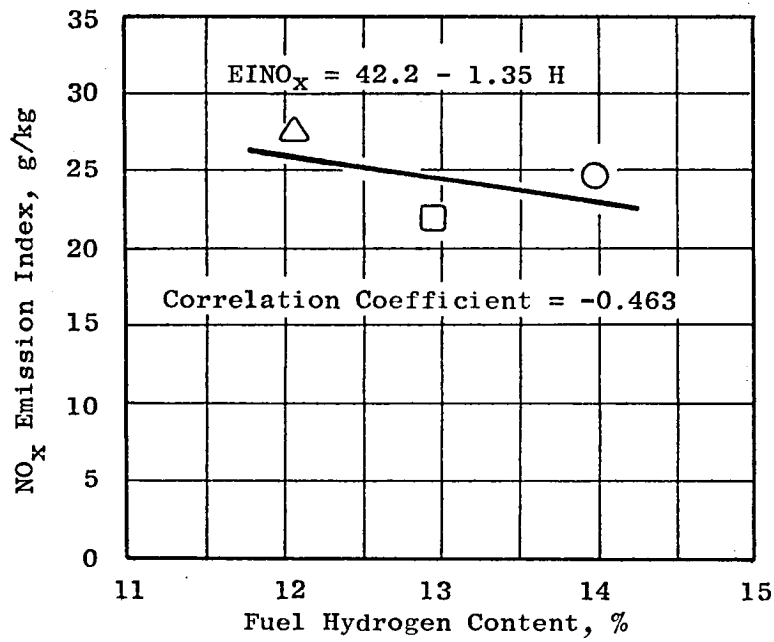
Figure 45. Variation of Baseline CF6-50 NO_x
Emission Index with Fuel Hydrogen
Content at Cruise Conditions, f = 0.015.
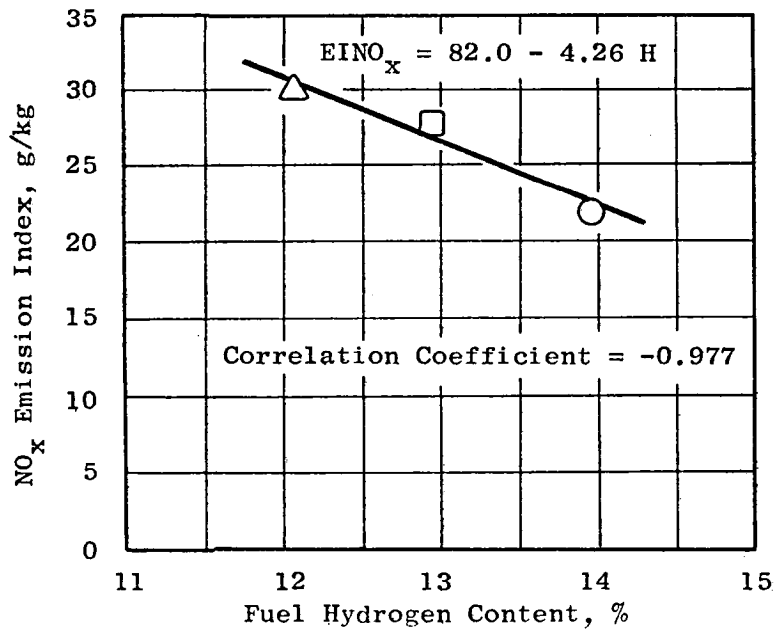
Figure 46. Variation of Baseline CF6-50 NO_x
Emission Index with Fuel Hydrogen
Content at Simulated Takeoff
Conditions, f = 0.018.
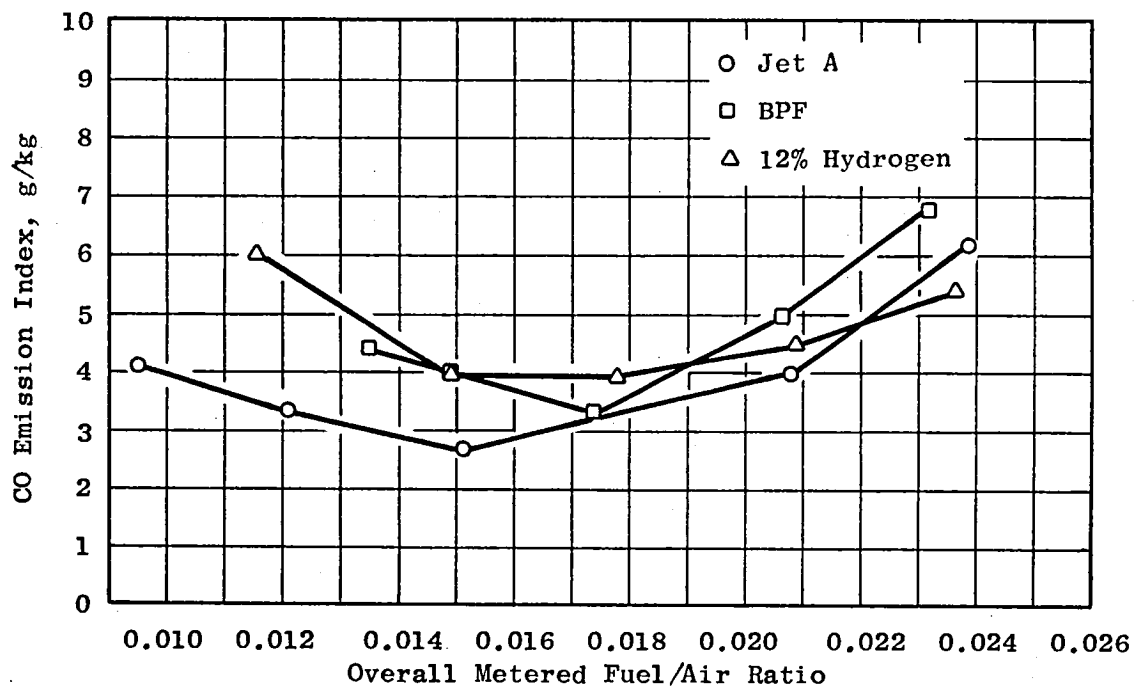
Figure 47. Baseline CF6-50 CO Emission Index at Cruise Conditions.
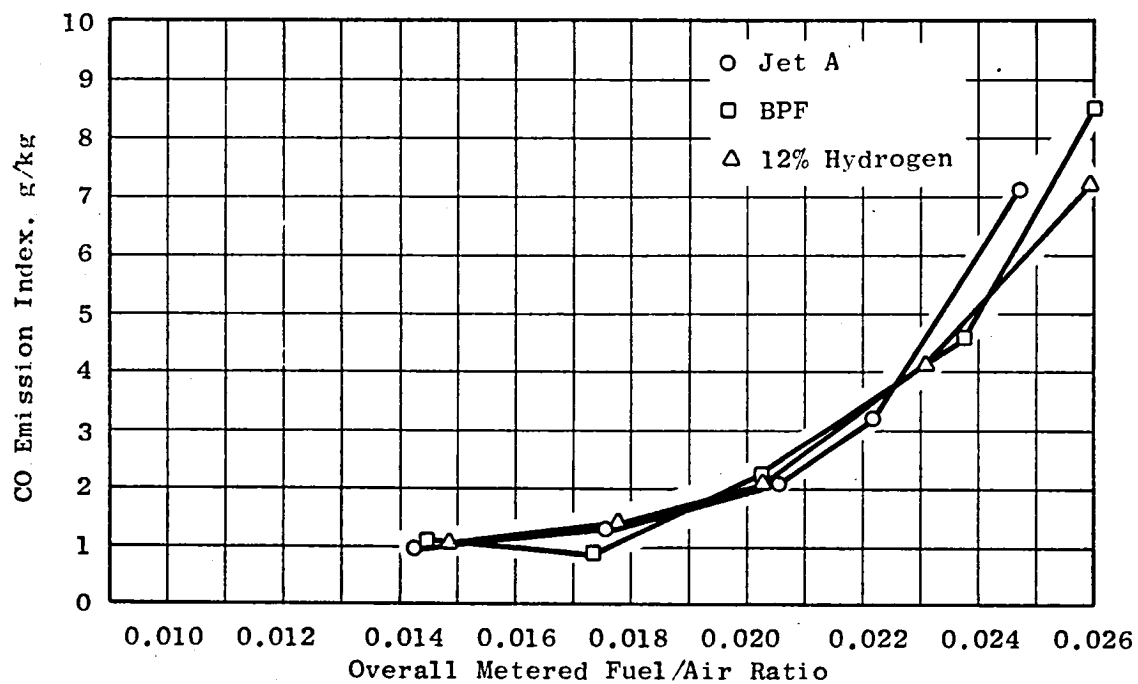
Figure 48. Baseline CF6-50 CO Emission Index at
Simulated Takeoff Conditions.

The Concept 1 combustor utilized high-pressure-drop fuel nozzles (9.65 MPa tip pressure drop at maximum fuel flow) intended to provide very fine atomization of the fuel. The fact that the measured NO_x levels were no better than those of previous combustors of similar dome design implies that little benefit was realized from the use of high-pressure-drop nozzles. However, Concept 1 was not tested with standard-pressure-drop fuel nozzles for a direct comparison. Concepts 2 and 3 (discussed below) were tested with standard-pressure-drop nozzles, and both had lower NO_x emission levels than Concept 1.

The manner in which maximum and average liner temperatures varied with fuel/air ratio for the three test fuels is shown in Figures 49 and 50. As shown in these figures, the double-annular combustor is quite insensitive to fuel hydrogen content. Figure 51 illustrates the variation of liner temperature along the combustor. Correlations of liner temperatures for selected inner- and outer-liner thermocouples are shown in Figures 52 and 53. For the outer liner, the temperature levels were quite low and exhibited little variation with fuel type. For the inner liner the absolute temperature levels were considerably higher than for the outer liner because the main stage was adjacent to the inner liner. However, there was little sensitivity to fuel type. This is attributed to the nature of lean combustion. The equivalence ratios in this dome are considerably lower than for the baseline combustor. Note, also, that none of the advanced combustors had the benefit of cooling-air adjustments. It is likely that the peak temperatures could be significantly reduced, by cooling-air redistribution, without increasing the total amount of cooling air. The inner liner for Concept 1 utilized only 13.2% cooling air versus 15.2% for the baseline combustor.

Carbon buildup on the Concept 1 domes, liners, and fuel nozzles is shown in Figures 54 through 57. The dome surfaces are cleaner than the baseline combustor dome, but the swirl cup venturis have similar carbon buildup, and the liners have the same thin layer of soot as the baseline. The Concept 1 fuel nozzles exhibit some thin carbon deposits. This is believed to be caused by a bluff area, between the primary axial swirler and the fuel nozzles, that existed because of the fuel nozzle mounting arrangement selected for these prototype combustors. The fuel nozzles were held in place in the swirlers by the nuts illustrated in Figure 58. This bluff area would be eliminated on future versions of this combustor in order to provide nozzles that are as free of carbon as the baseline nozzles.

The Concept 1 burner yielded low smoke numbers for both cruise and take-off conditions (Figures 59 and 60). Correlations between smoke number and fuel hydrogen content are presented in Figures 61 and 62. As shown in these figures, the Concept 1 burner is less sensitive to fuel hydrogen content than the baseline burner; the only time it varied with fuel hydrogen content was at simulated takeoff conditions. In general, smoke numbers did not vary with fuel/air ratio for Concept 1. This characteristic is similar to that of the ECCP double-annular burner on which this concept is based (Reference 2).
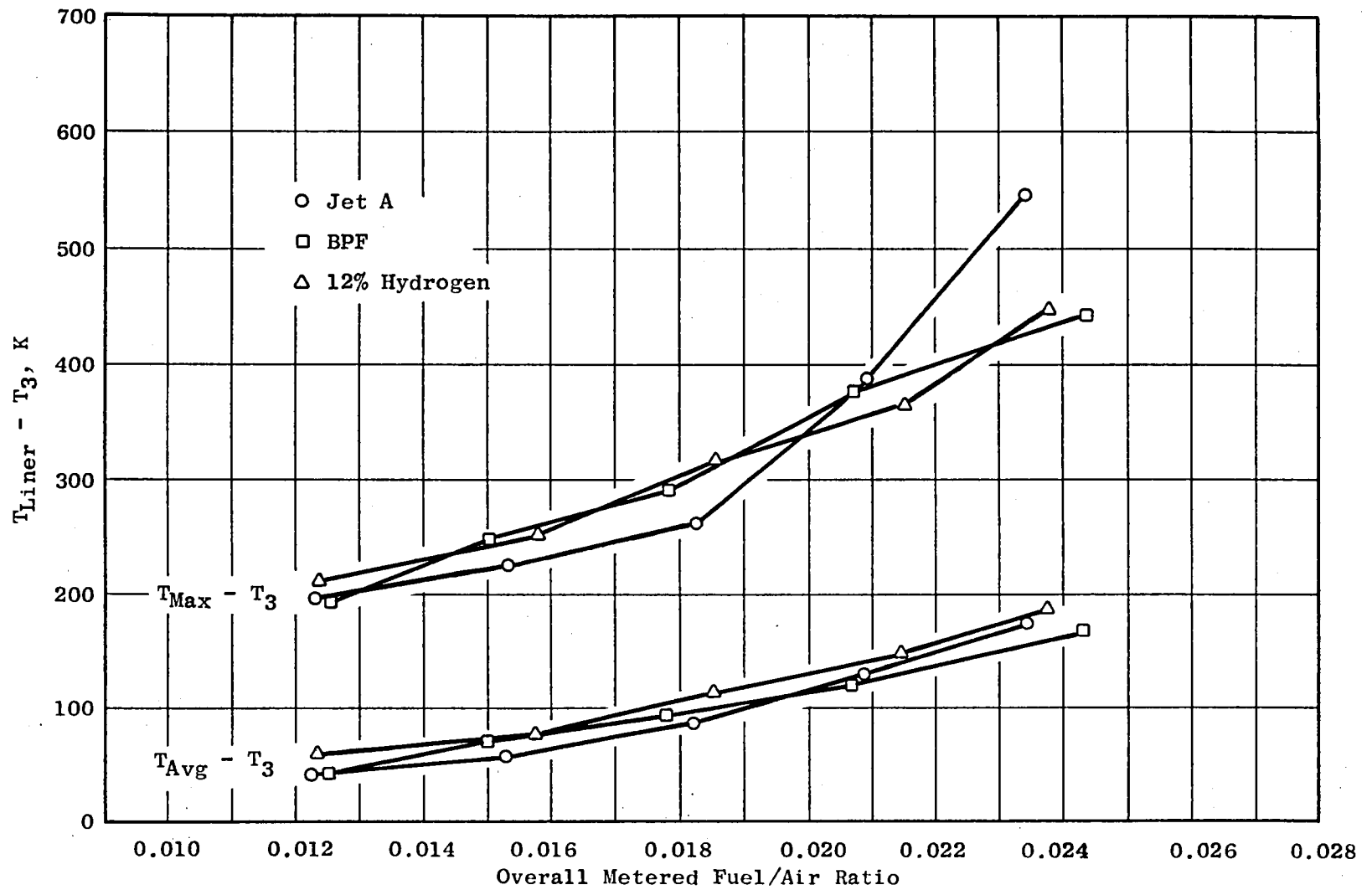
Figure 49. Concept 1 Liner Temperatures at Cruise Conditions.
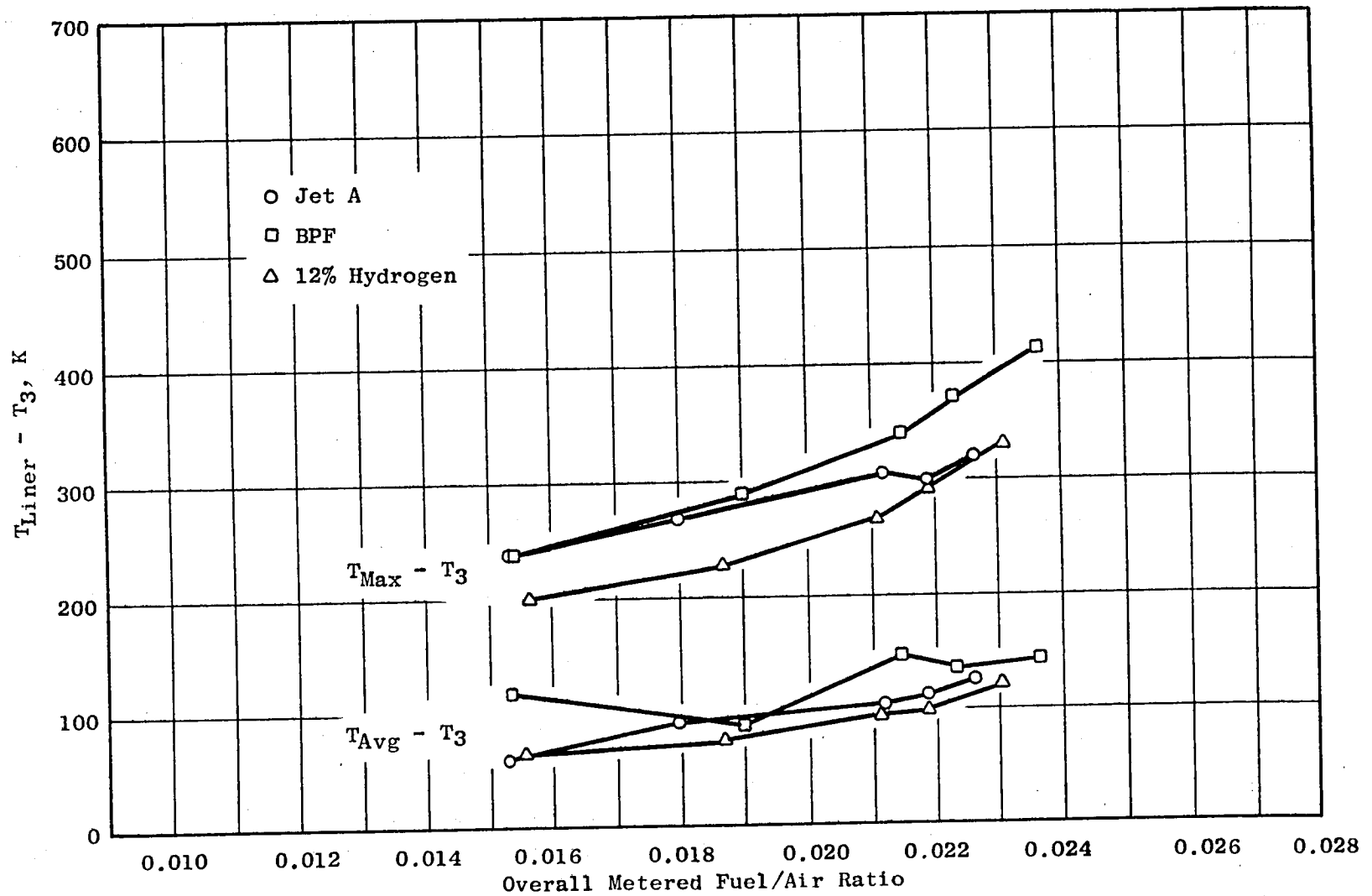
Figure 50. Concept 1 Liner Temperatures at Simulated Takeoff Conditions.
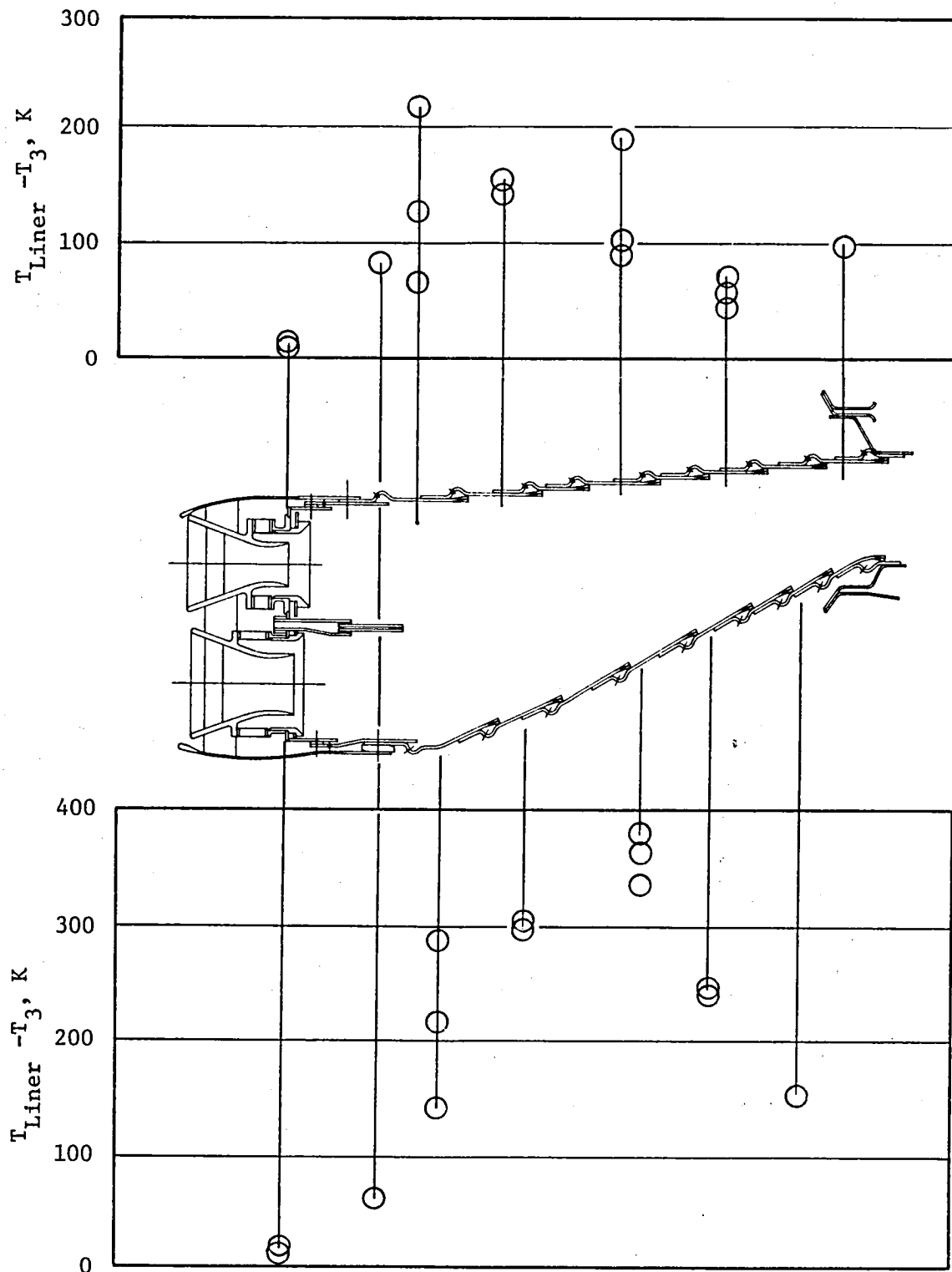
Figure 51.   Concept 1 Liner Temperature Distribution at Cruise
Conditions, Jet A Fuel, f = 0.021

Figure 52. Variation of Concept 1 Outer Liner Temperature with Fuel Hydrogen Content at Cruise Conditions, f = 0.021.

Figure 53. Variation of Concept 1 Inner Liner Temperature with Fuel Hydrogen Content at Cruise Conditions, f = 0.021.

Figure 54. Concept 1 Dome After Test.

Figure 55.   Concept 1 Outer Liner After Test.
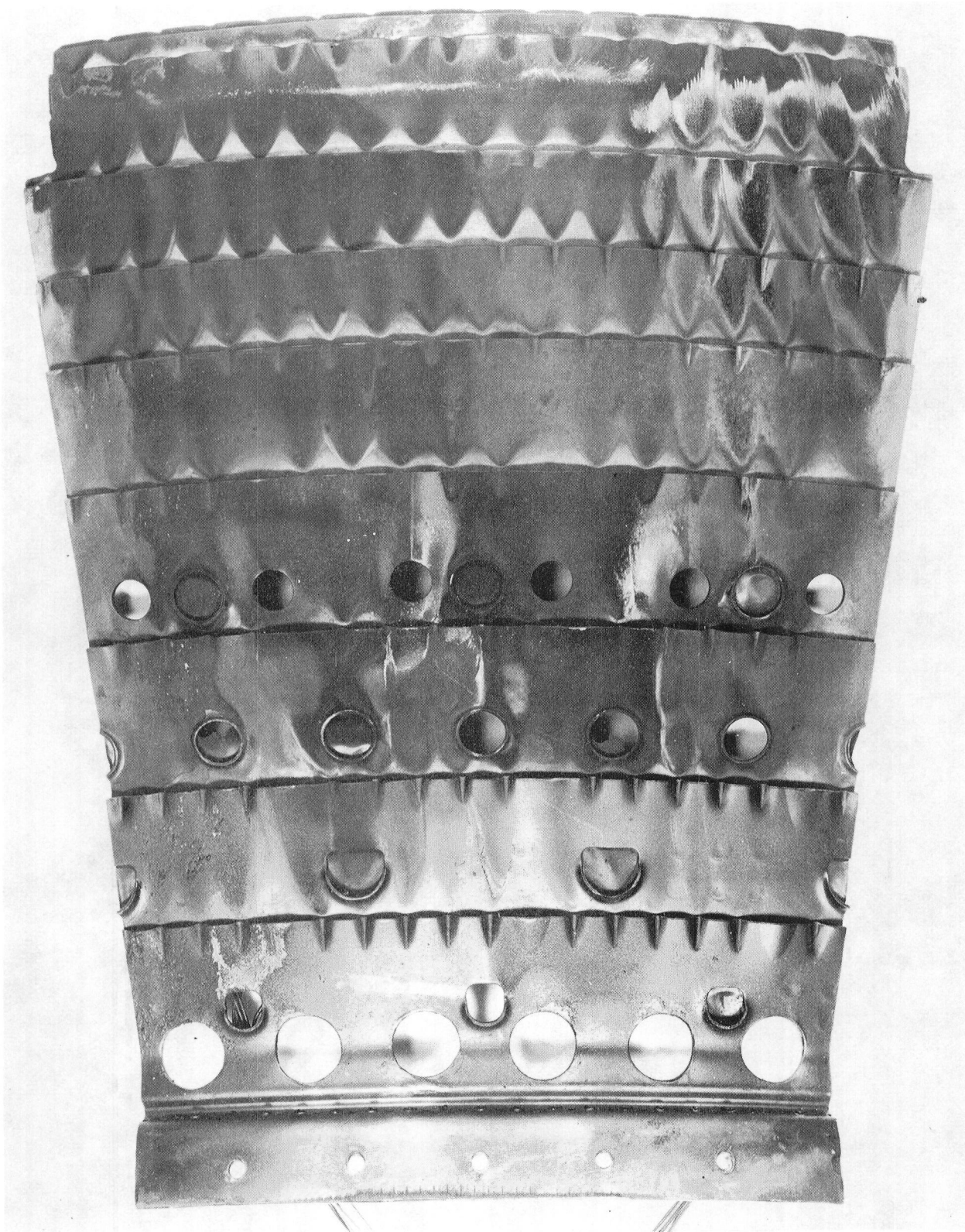
Figure 56.   Concept 1 Inner Liner After Test.
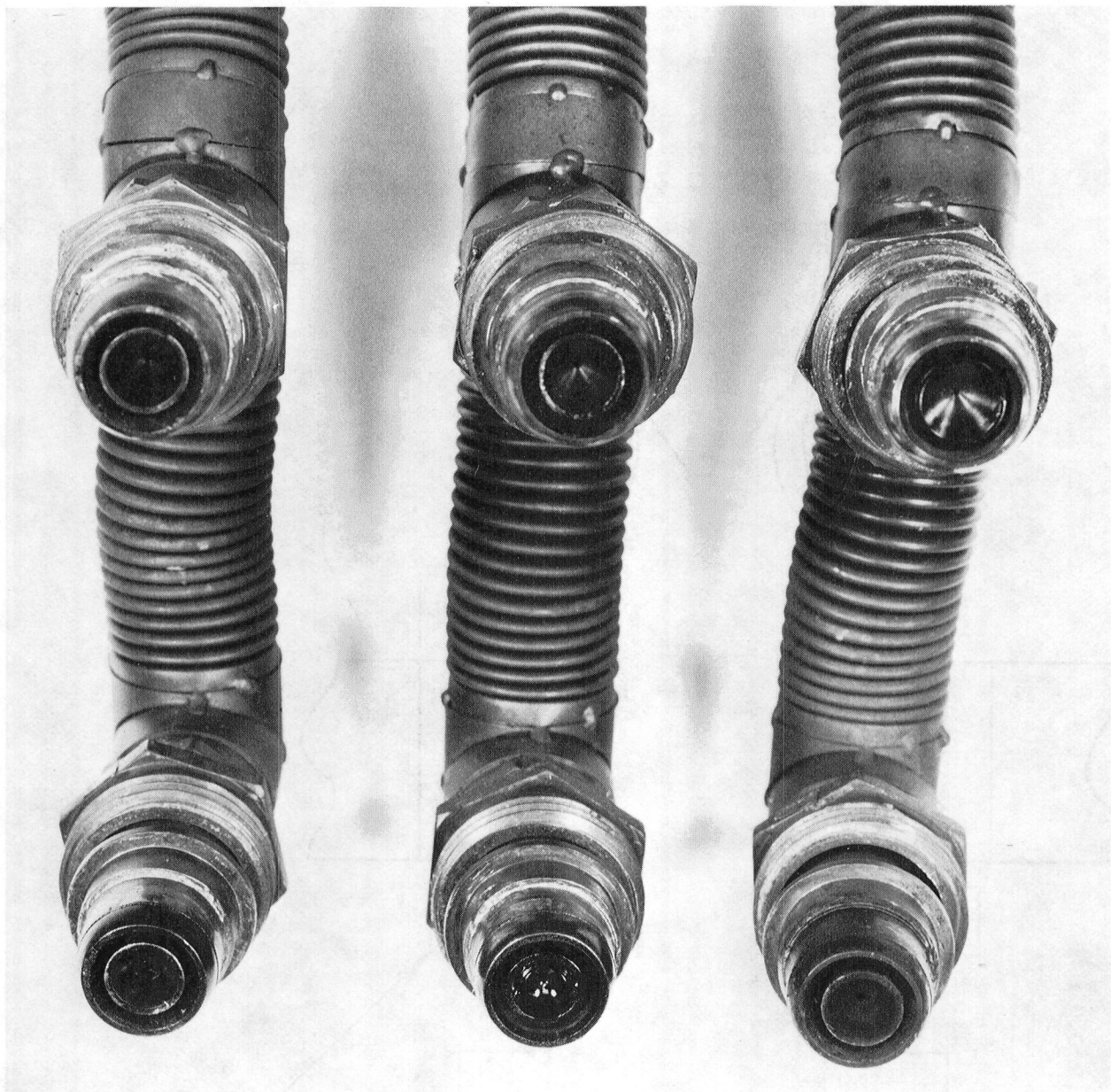
Figure 57. Concept 1 Fuel Nozzles After Test.
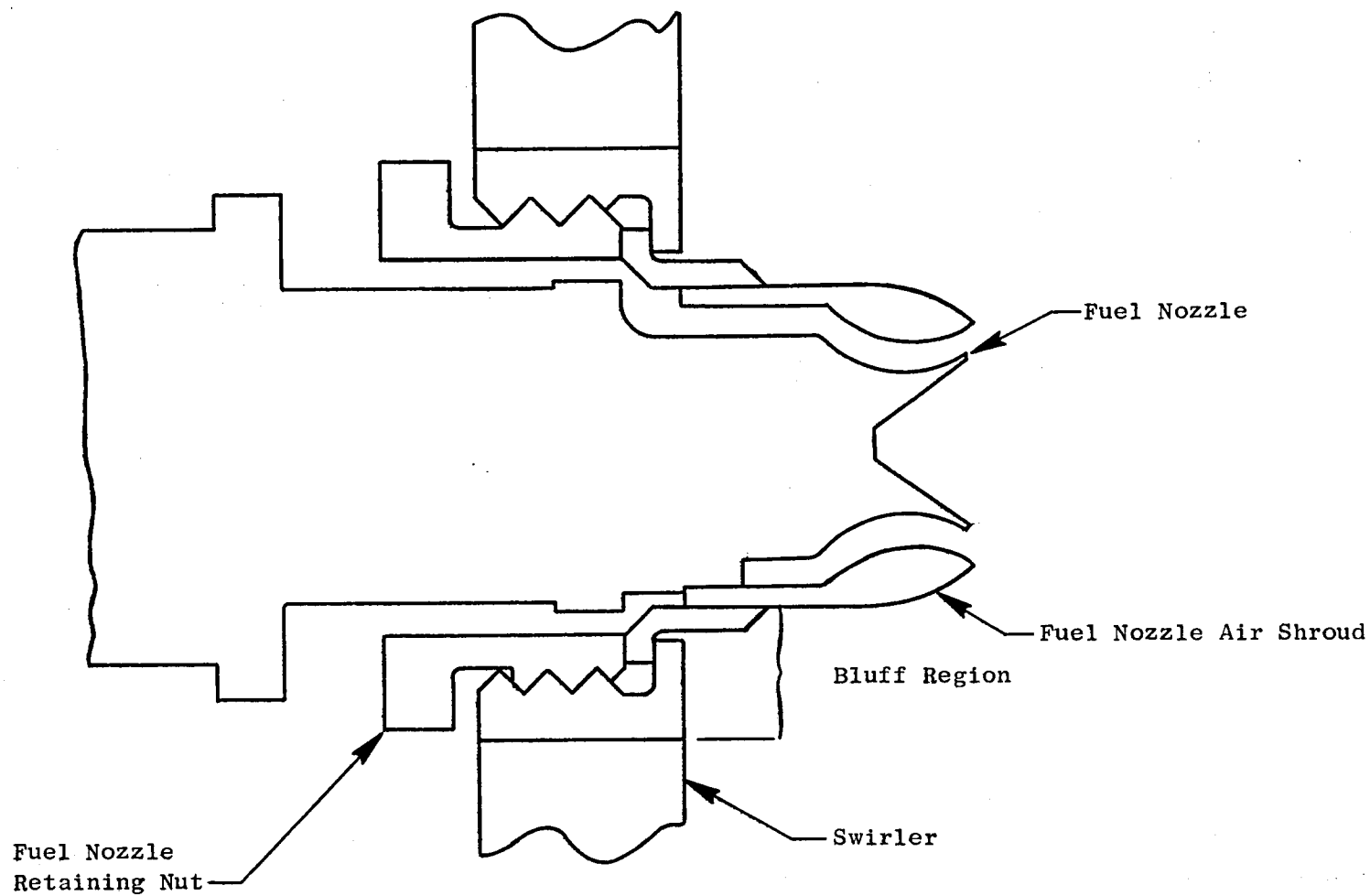
Figure 58. Fuel Nozzle Positioning Arrangement for Concepts 1, 2, and 3.
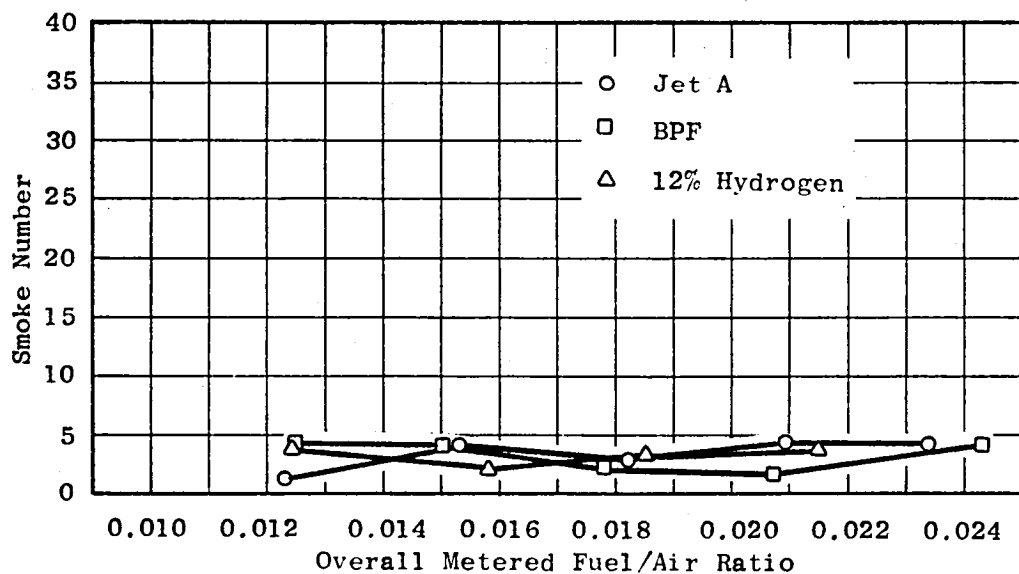
Figure 59. Concept 1 Smoke Numbers at Cruise Conditions.
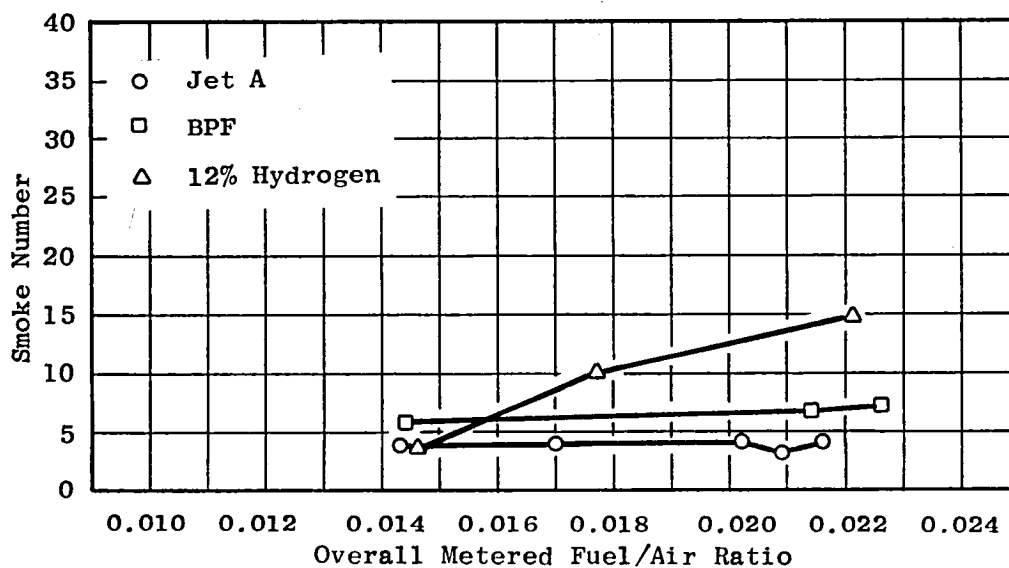
Figure 60. Concept 1 Smoke Numbers at Simulated Takeoff Conditions.
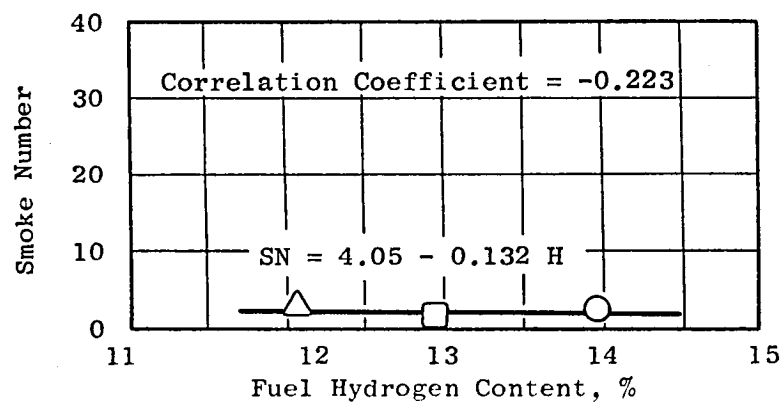
Figure 61. Variation of Concept 1 Smoke Number
with Fuel Hydrogen Content at Cruise
Conditions, f = 0.018.

Figure 62. Variation of Concept 1 Smoke Number
with Fuel Hydrogen Content at Simu-
lated Takeoff Conditions, f = 0.014.

The variation of Concept 1 NO_x emission index with fuel/air ratio is shown in Figures 63 and 64. The NO_x emission index trends are characteristic of a lean-dome design (dome equivalence ratios less than unity) and are similar to NO_x index variations resulting from earlier tests of lean-dome combustors. NO_x emission indices for lean-dome designs characteristically are low for low fuel/air ratios, increase at somewhat moderate fuel/air ratios, and flatten out at higher fuel/air ratios (Reference 4). All of the advanced concepts tested are lean-dome designs. Correlations of NO_x emission index versus fuel hydrogen content are presented in Figures 65 and 66.

The variation of CO emission index with fuel/air ratio for the Concept 1 burner using the three test fuels is shown in Figures 67 and 68. The trends in these results are similar to previous ECCP results, but the levels are higher here. This is believed to be due to the leakage in the sector rig mentioned earlier. Correlations of CO emission index versus fuel hydrogen content are shown in Figures 69 and 70. This concept, like the baseline CF6-50, exhibits a CO emission index that is very insensitive to fuel hydrogen content. Unburned hydrocarbon emission indices were generally below 1.0 g/kg and followed the CO emission index as expected.

At the end of the Concept 1 test, the exit-rake, gas-sample probes were checked; some plugging and erosion were found. To reduce probe erosion in subsequent tests, it was decided to reduce inlet pressure to 1.16 MPa. Emissions results were then corrected using the correlations described in Section 4.5.

6.3 CONCEPT 2 SCREENING TEST RESULTS

The third test was a screening evaluation of Concept 2. This concept, like Concept 1, was a double-annular combustor, but it employed a premixing main-stage dome. Of the four burners tested, Concept 2 had the lowest NO_x levels. It also demonstrated a very clean dome with virtually no carbon deposits, lower smoke levels than the baseline combustor, low dome temperatures, and no combustion instability at any operating condition. Liner temperatures were low except for a region on the inner liner downstream of the premixing tubes. This liner-temperature problem would be relatively easy to remedy by the use of hole-pattern adjustments and preferential cooling; therefore, these high temperatures were not considered a major problem.

The variation of Concept 2 NO_x emission index with fuel/air ratio for the test fuels is shown in Figures 71 and 72. These results are correlated with fuel hydrogen content in Figures 73 and 74. The figures show that, relative to the baseline combustor, the Concept 2 burner had significantly lower NO_x emission index levels and lower sensitivity to fuel hydrogen content.

Figure 75 shows that the Concept 2 dome is very clean; there is none of the carbon buildup that was found in the swirl cup venturis in the other burners. This was the cleanest dome of all the concepts tested. The clean main-stage dome is attributed to the premixing of the fuel and air so that no rich fuel/air mixture could come into contact with the dome.
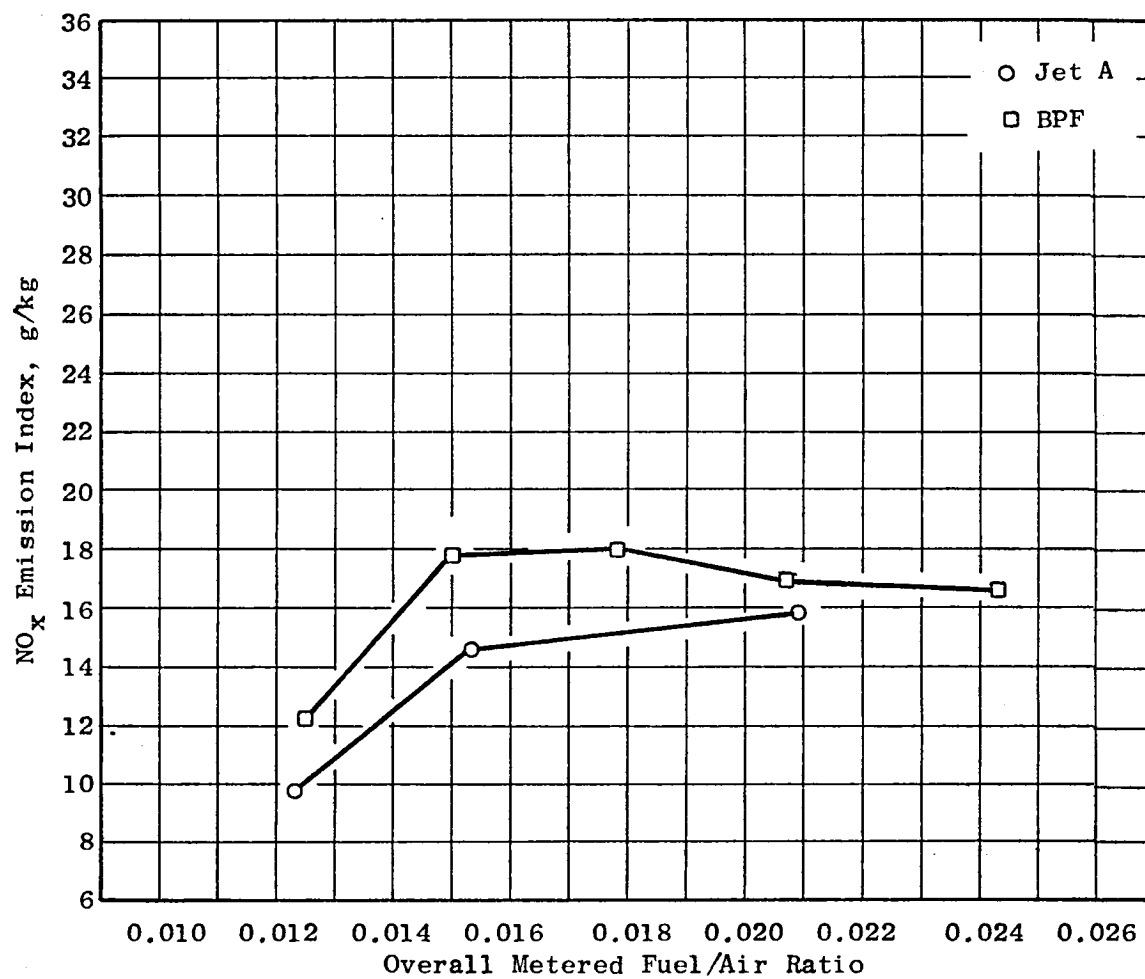
Figure 63. Concept 1 NO_x Emission Index at Cruise Conditions.
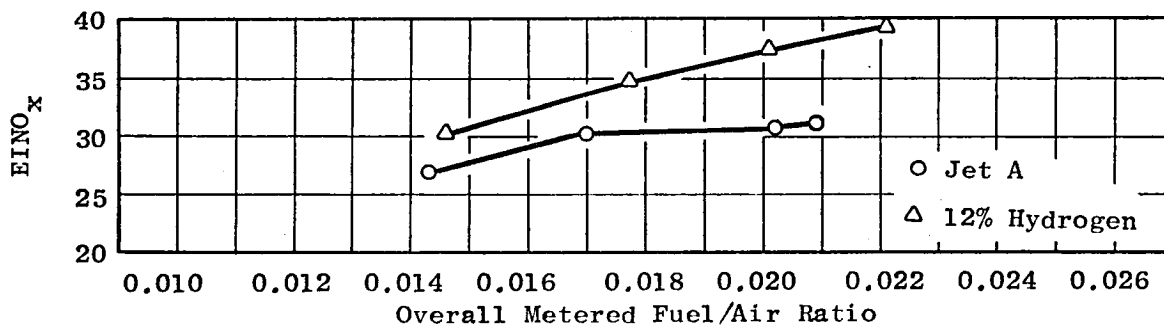
Figure 64. Concept 1 NO_x Emission Index at Simulated Takeoff Conditions.
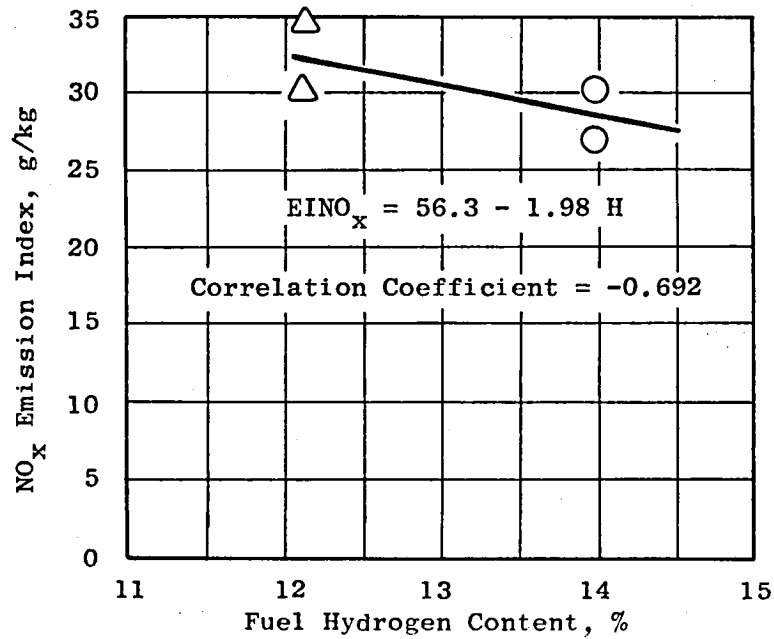
Figure 65. Variation of Concept 1 NO_x Emission
Index with Fuel Hydrogen Content at
Cruise Conditions, f = 0.016.
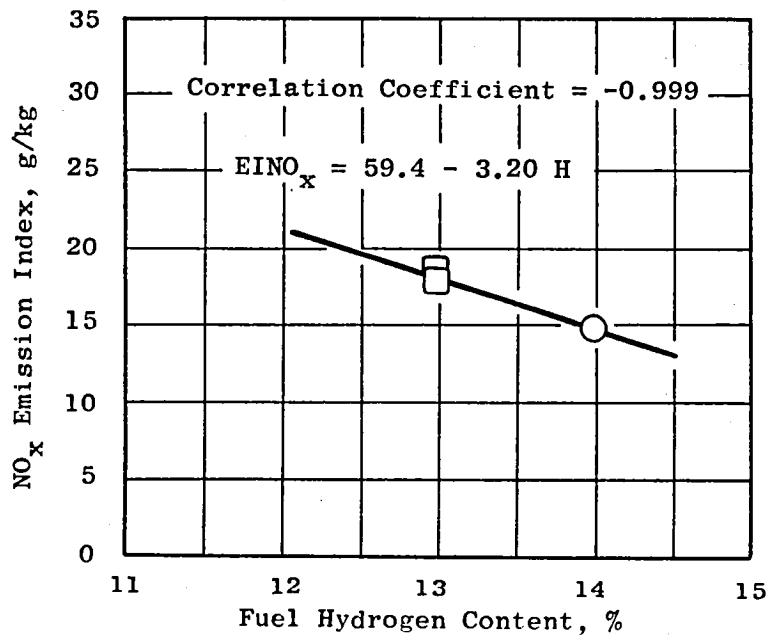
Figure 66. Variation of Concept 1 NO_x Emission
Index with Fuel Hydrogen Content at
Simulated Takeoff Conditions, f = 0.016.
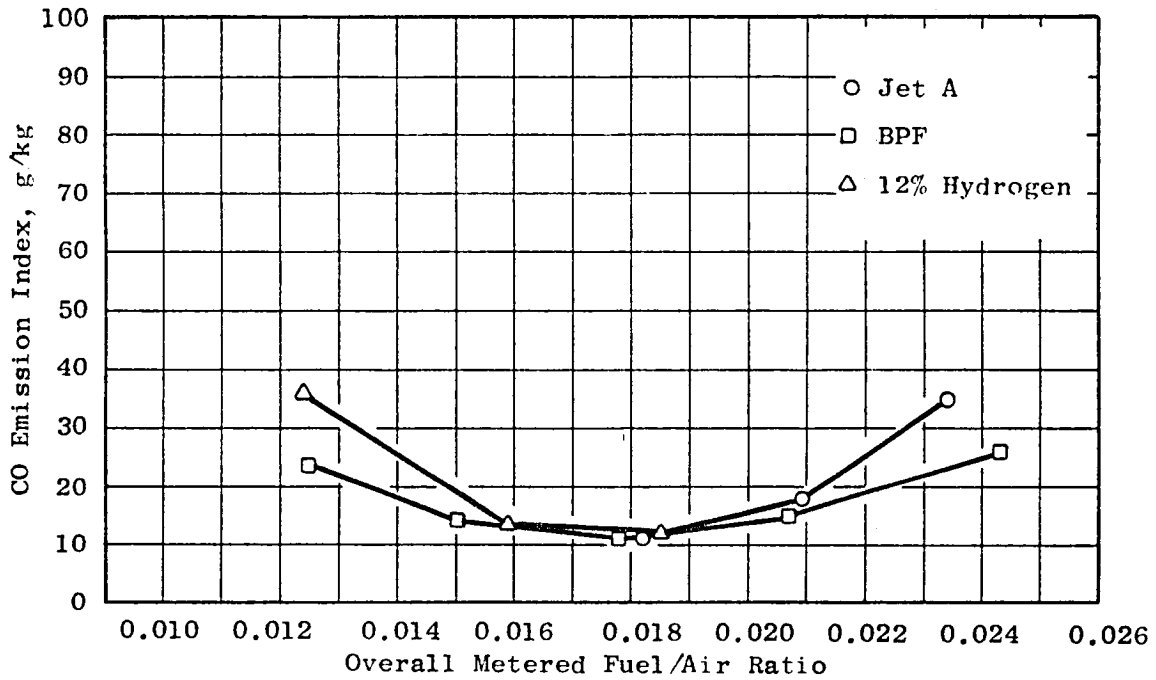
Figure 67. Concept 1 CO Emission Index at Cruise Conditions.
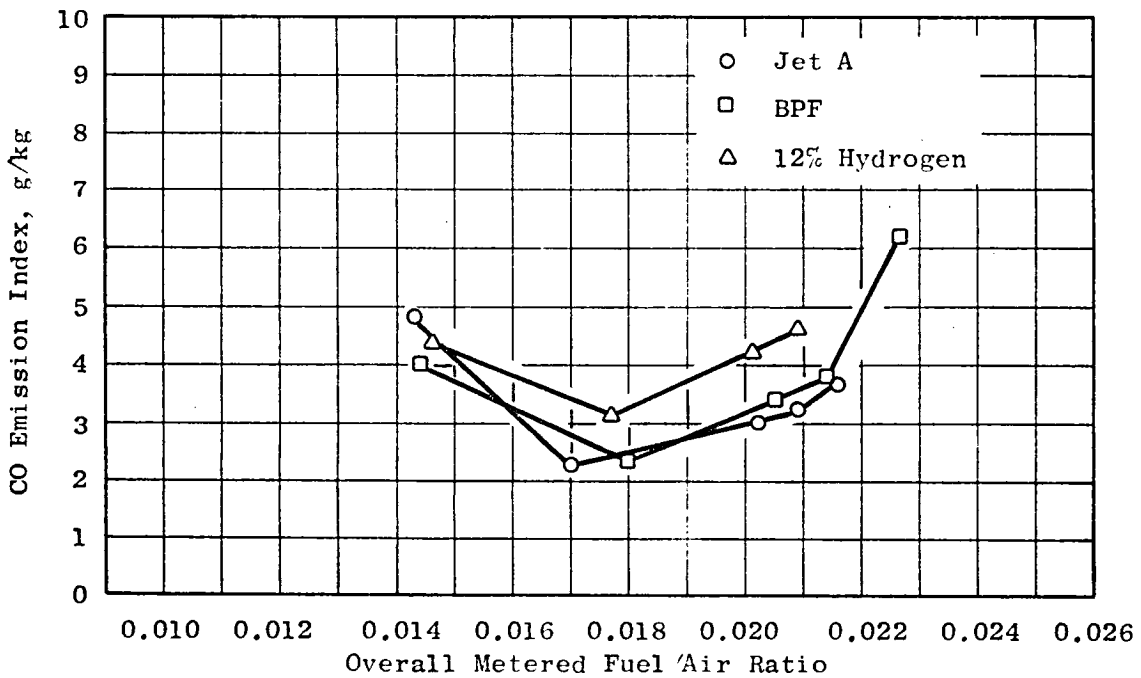
Figure 68. Concept 1 CO Emission Index at Simulated
Takeoff Conditions.

82
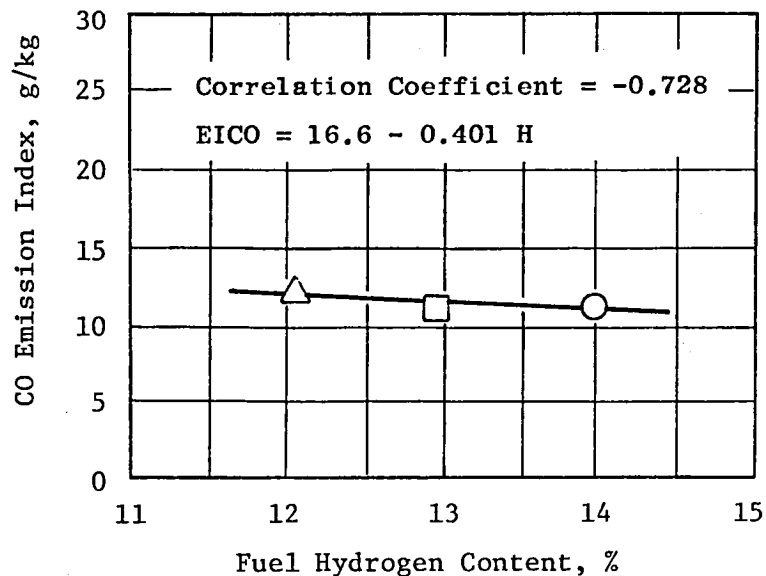
Figure 69. Variation of Concept 1 CO Emission Index with Fuel Hydrogen Content at Cruise Conditions, f = 0.018.
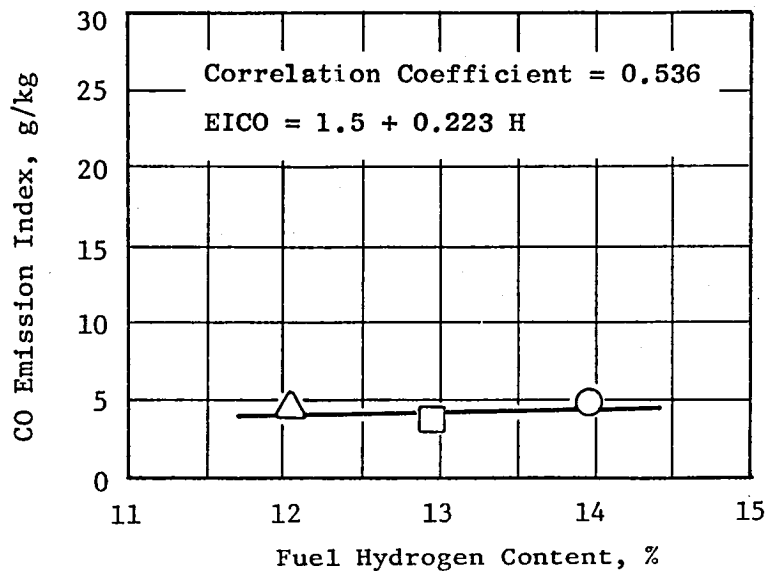
Figure 70. Variation of Concept 1 CO Emission Index with Fuel Hydrogen Content at Simulated Takeoff Conditions, f = 0.014.
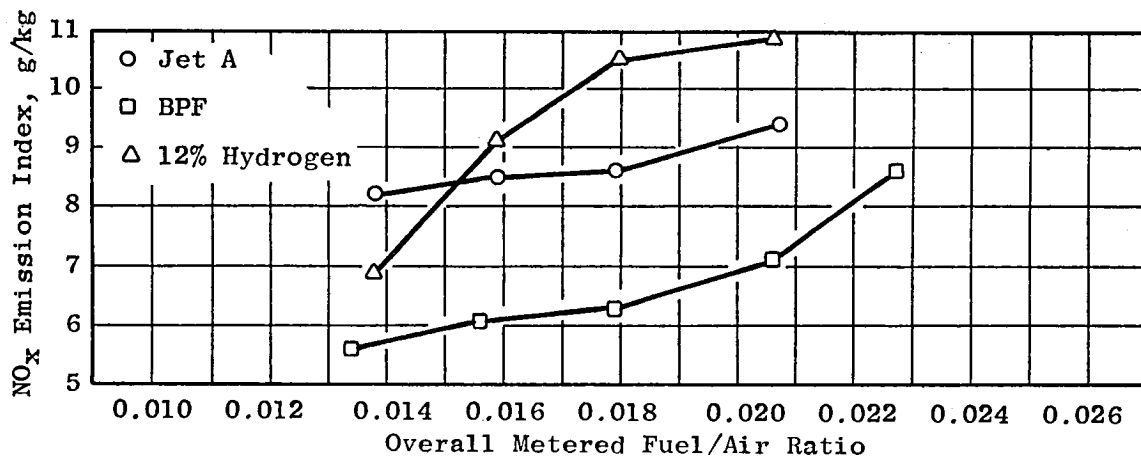
Figure 71. Concept 2 NO_x Emission Index at Cruise Conditions.
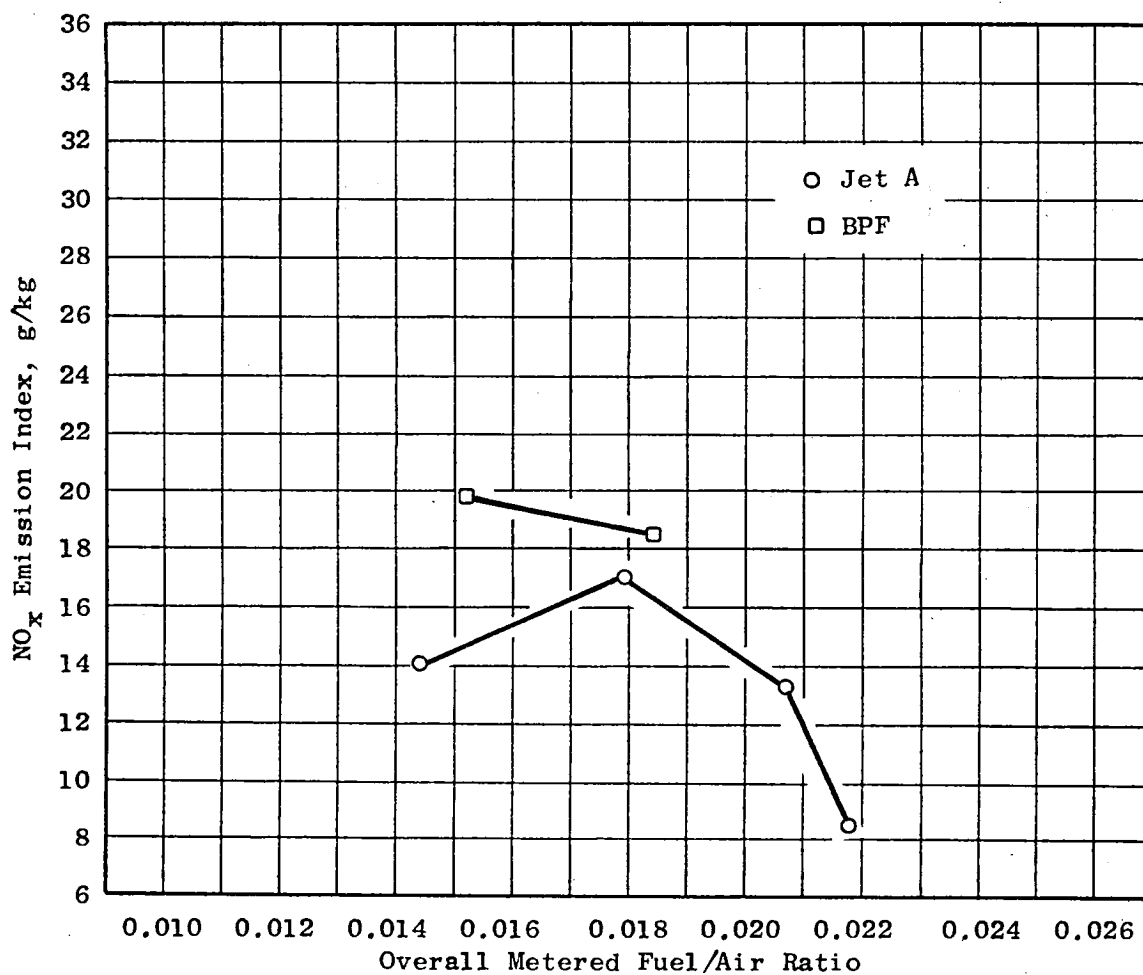
Figure 72. Concept 2 NO_x Emission Index at Simulated Takeoff Conditions.

84
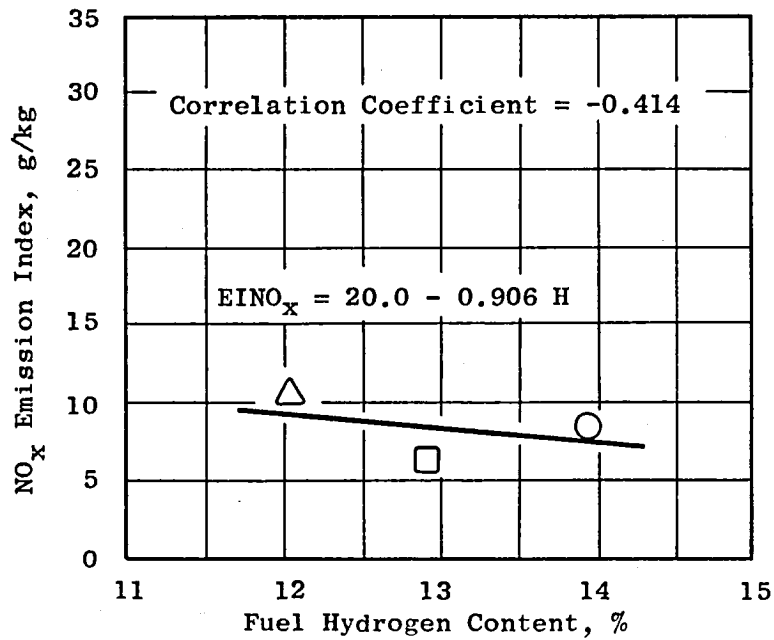
Figure 73. Variation of Concept 2 NO_x Emission
Index with Fuel Hydrogen Content at
Cruise Conditions, f = 0.018.

Correlation Coefficient = -0.414

$EINO_x = 20.0 - 0.906\ H$
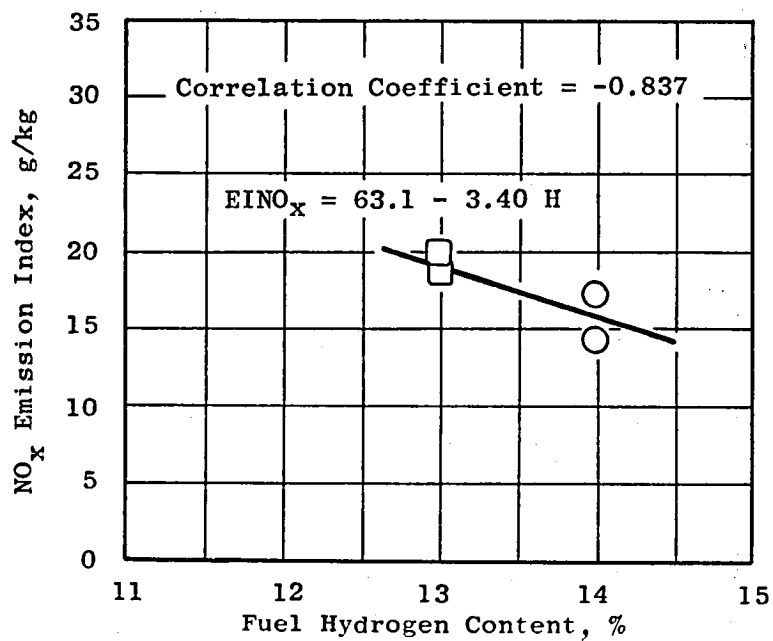
Figure 74. Variation of Concept 2 NO_x Emission
Index with Fuel Hydrogen Content at
Simulated Takeoff Conditions, f = 0.016.

Correlation Coefficient = -0.837

$EINO_x = 63.1 - 3.40\ H$

85
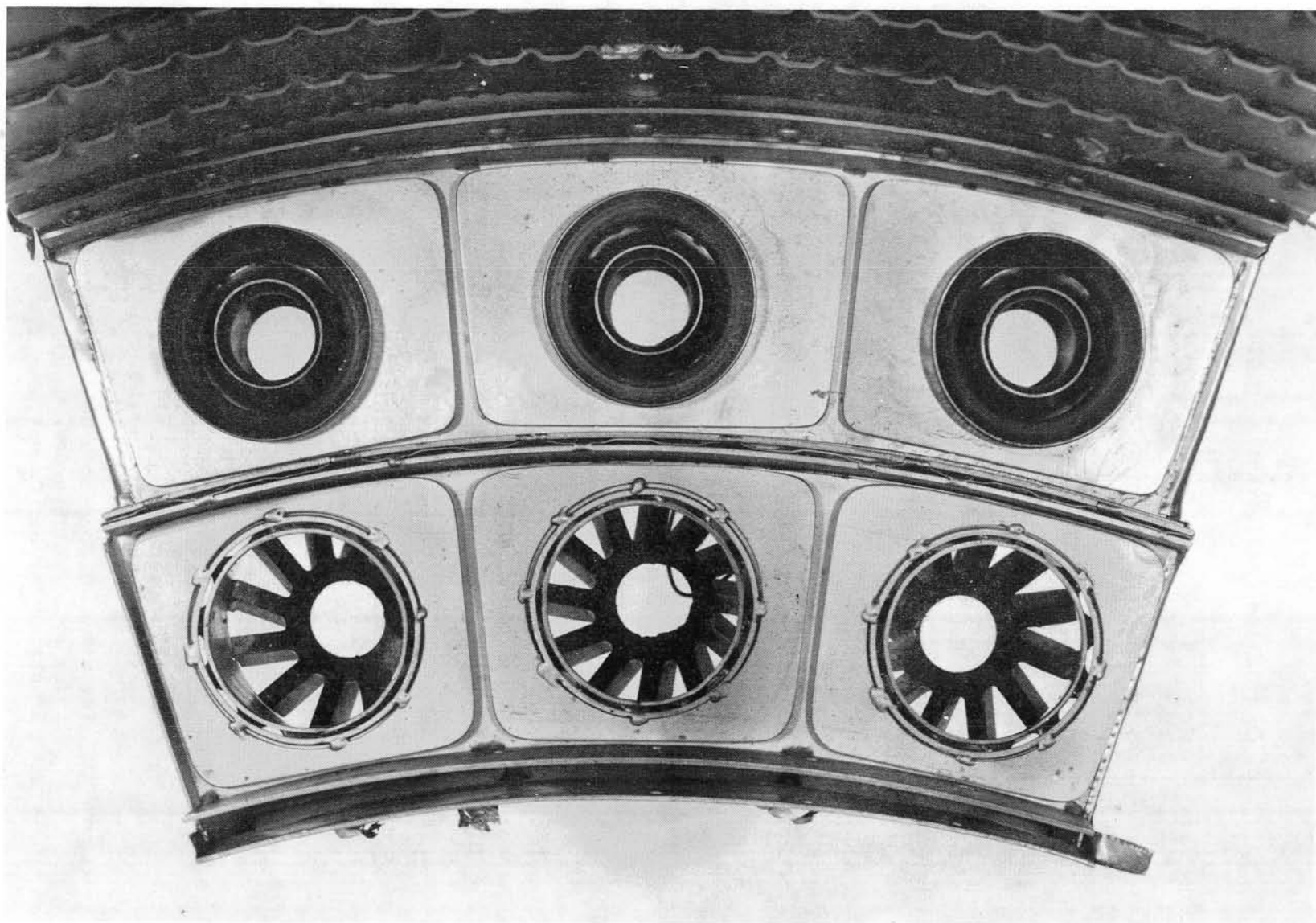
Figure 75. Concept 2 Dome After Test.

Figure 76 shows that the Concept 2 outer liner has the same light, uniform coating of soot as was seen on the baseline and Concept 1 outer liners. Figure 77 shows carbon buildup on the fuel nozzles. This carbon formed in a bluff region behind the swirler (mentioned above) and would be eliminated on future designs. In any case, the bluff regions would be minimized to lessen the risk of autoignition in premixing-prevaporing designs.

Combustor liner temperatures were very low for the outer liner, dome, and premixing tubes for Concept 2. The inner liner exhibited local high temperatures, and the posttest inspection revealed liner damage (Figure 78). The liner overheating was aggravated by disruption of the cooling film by unused dilution hole "thimbles" in this concept - that is, dilution holes that have been drawn to form a rounded entrance on the cold side and a protruding lip on the hot side of the liner. The liners were fabricated from existing combustors, and unused thimbles were closed with Nichrome patches. For a test conducted later, these thimbles were ground smooth and their openings were closed by disks welded into place.

The distribution of temperatures along the combustor is shown in Figure 79. The inner liner has high local temperatures and would benefit from an axial and circumferential cooling redistribution. Note that this combustor uses only 13.2% inner liner cooling versus 15.2% for the baseline combustor. A second improvement for future combustors using this concept might be achieved by inclining the premix tube to direct the combustion gases more directly at the turbine nozzle diaphragm. The main stage is intentionally designed with high flow rate for low residence time. This results in high velocities for the gases turned by the inner liner wall. A third possible means of improvement would be to recontour the inner liner.

Maximum liner temperatures and average liner temperatures are shown as functions of fuel/air ratio in Figures 80 and 81. The maximum temperatures were always on the inner liner. Selected panel temperatures for the inner and outer liners are shown in Figures 82 and 83 as functions of fuel type. The inner liner shows less sensitivity to fuel hydrogen content than the baseline even though the cooling level was 7.8% for Concept 2 versus 14.8% for the baseline. The metal temperature of the center premix tube was monitored during the test. Thermocouples located on the outside of the premix tube, 2.5 and 5.0 cm downstream of the primary swirler, read approximately 45 and 40 K above T_3, respectively, throughout the test.

One of the three nozzles from the main stage showed evidence of high temperatures, apparently the result of autoignition within the premix tube, at some time during the test. This nozzle had a Nichrome shim on the outer surface that was found to be oxidized after the test (see Figure 84). The high temperatures were apparently intermittent; the nozzle had a coating of light, sooty carbon at the conclusion of the test, and the other two nozzles did not show any signs of local burning. This apparent autoignition within the premix tube was probably the result of the bluff region on the swirler base and would be eliminated in future designs.
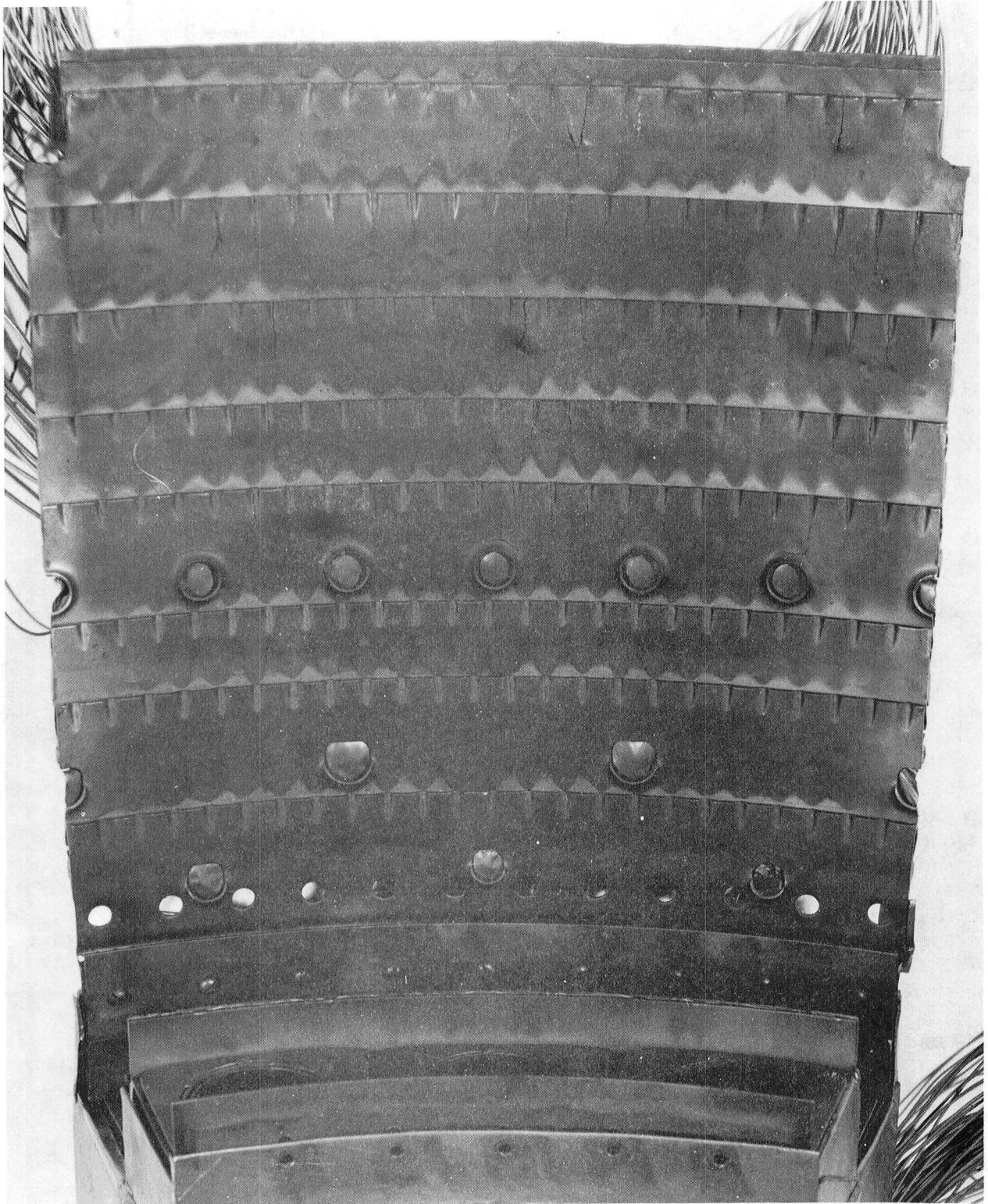
Figure 76. Concept 2 Outer Liner After Test.
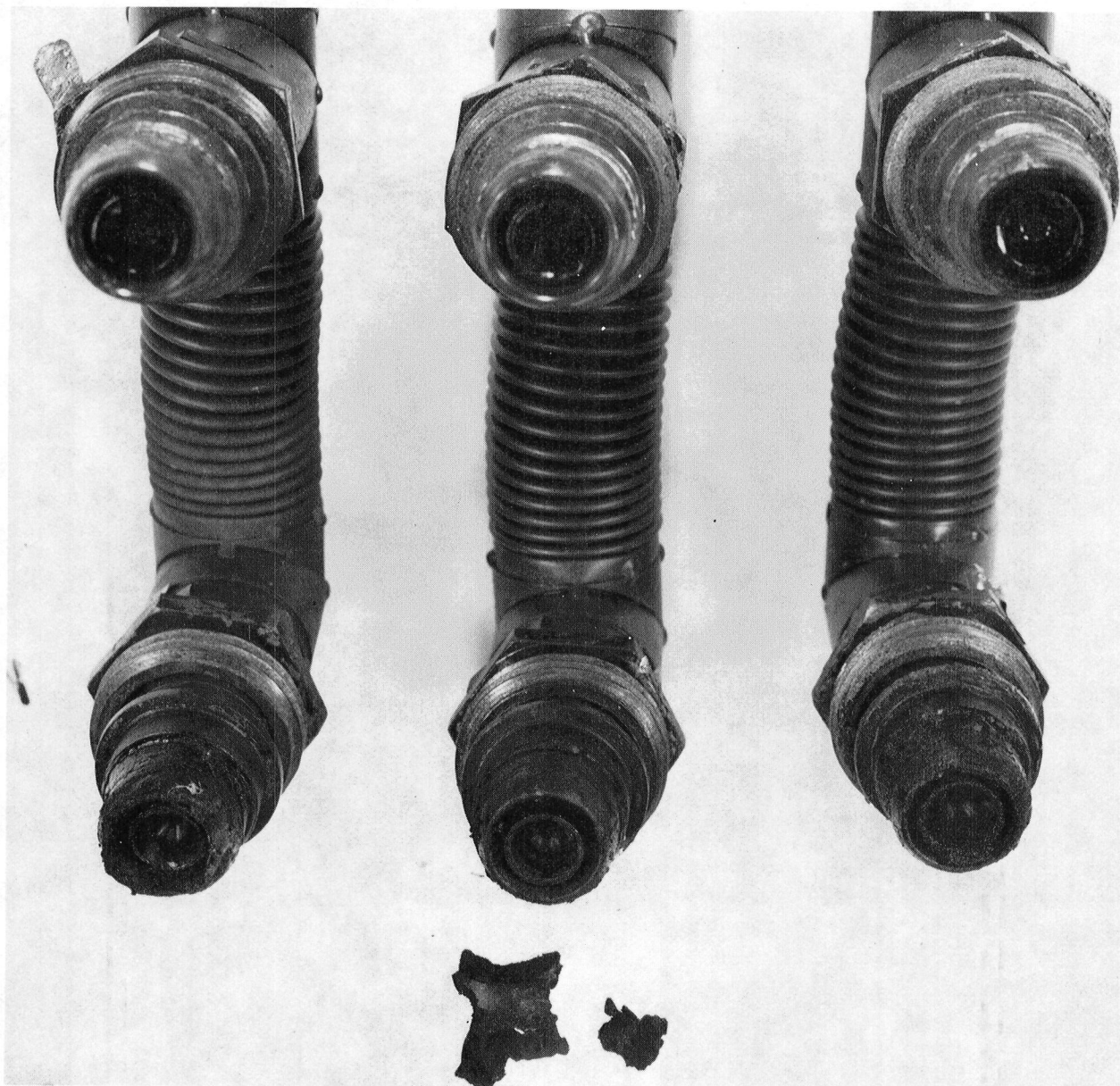
Figure 77.   Concept 2 Fuel Nozzles After Test.
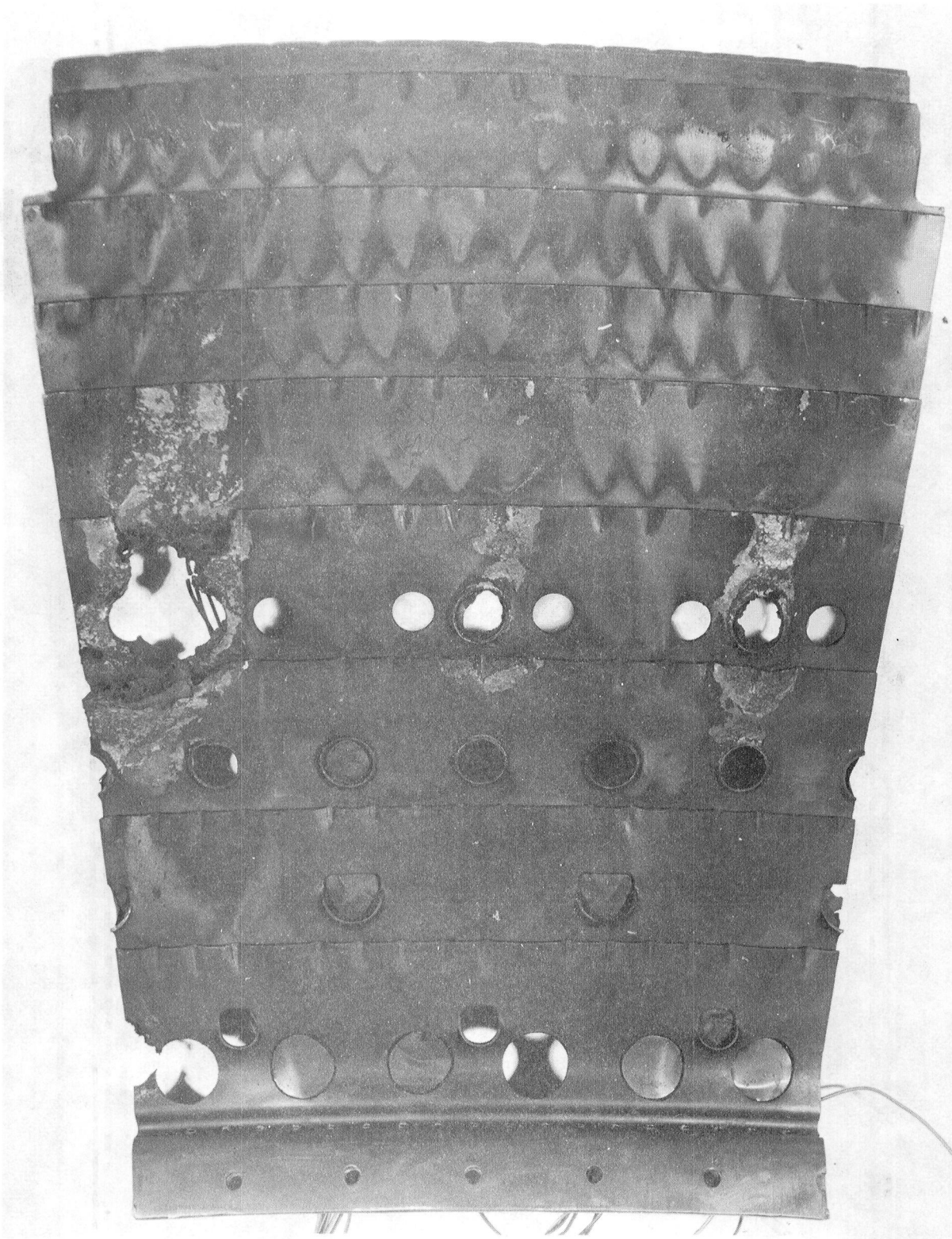
Figure 78. Concept 2 Inner Liner After Test.
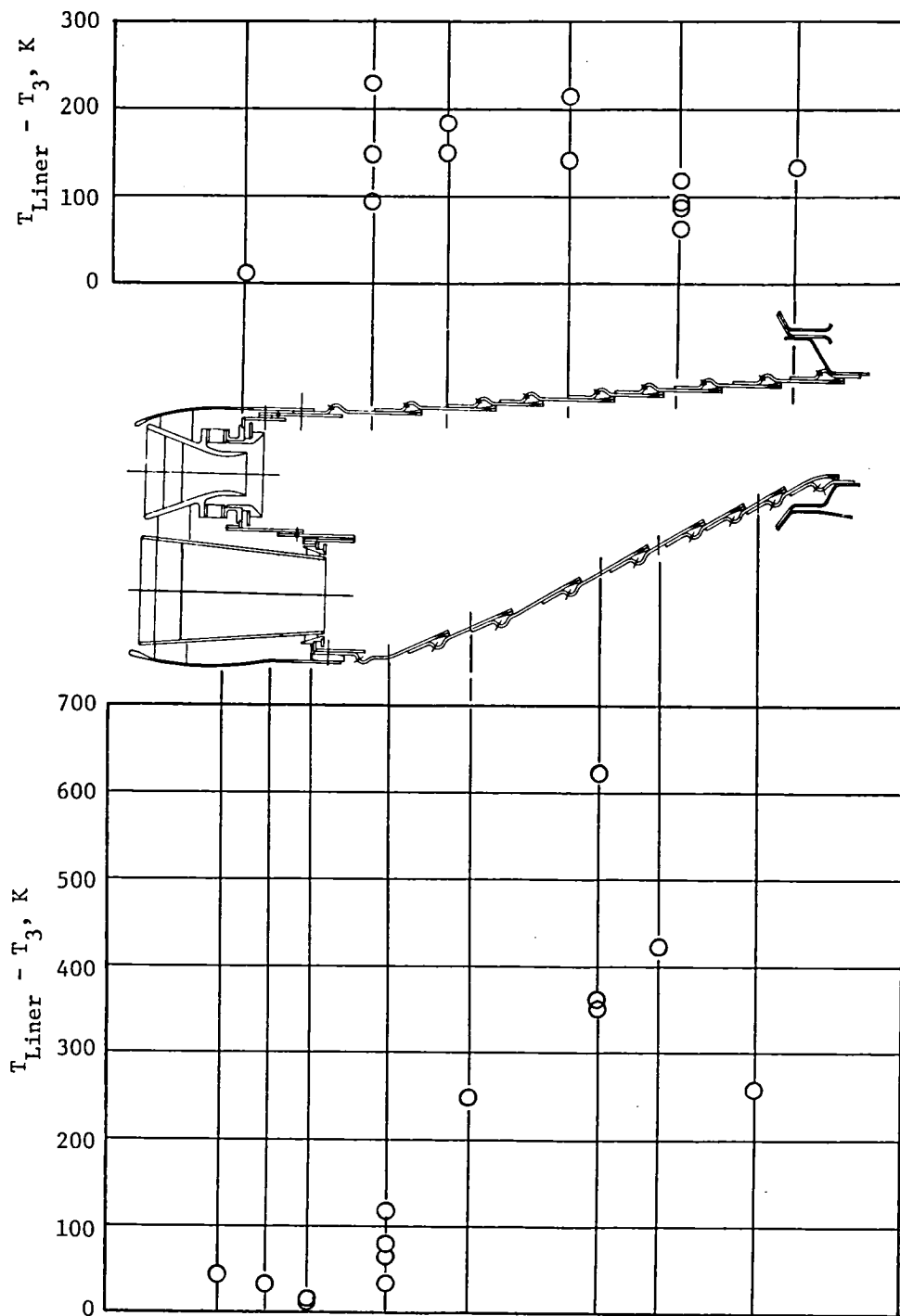
Figure 79. Concept 2 Liner Temperature Distribution at
Cruise with Jet A Fuel, f = 0.021.
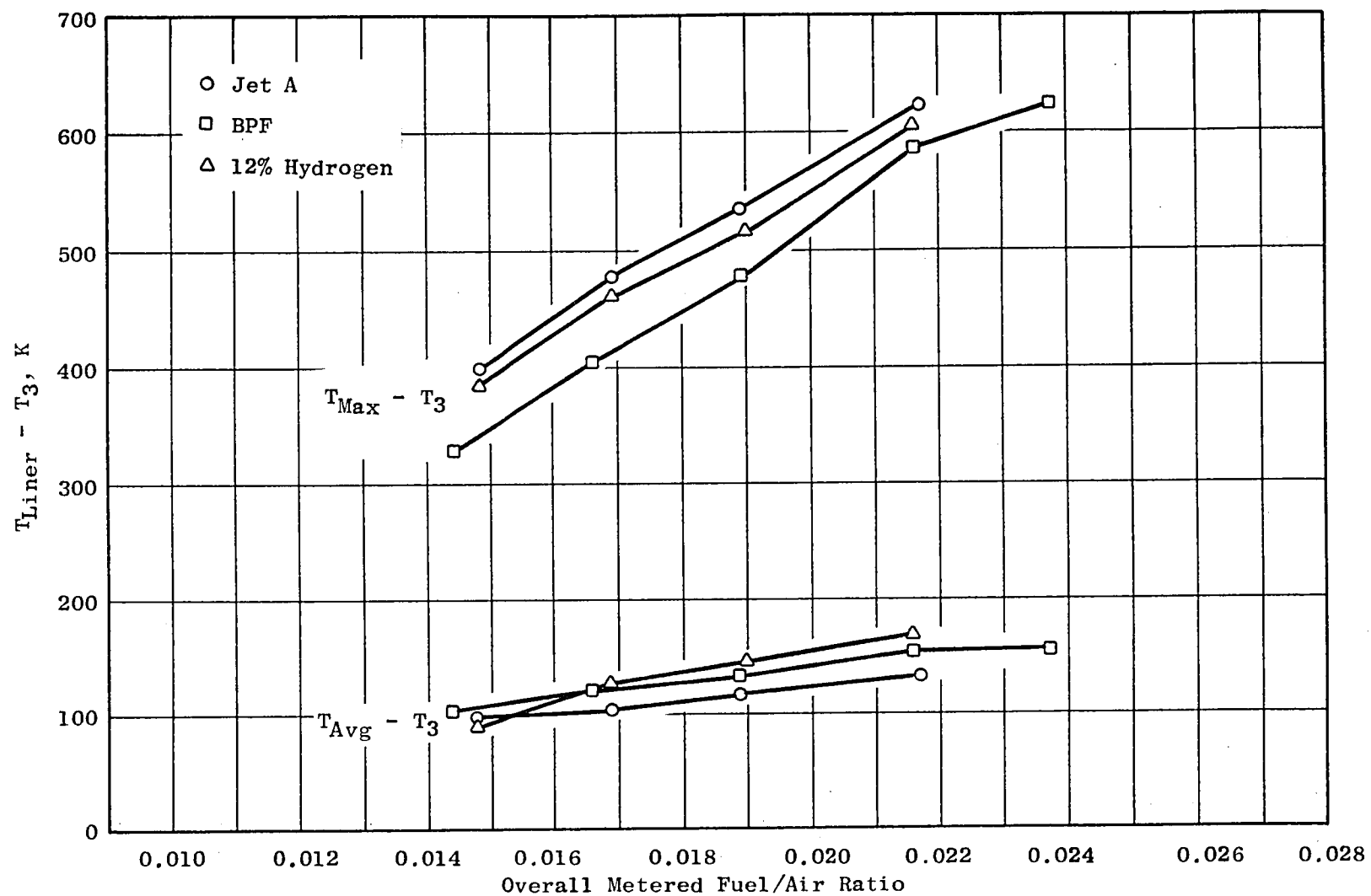
Figure 80.   Concept 2 Liner Temperatures at Cruise Conditions.
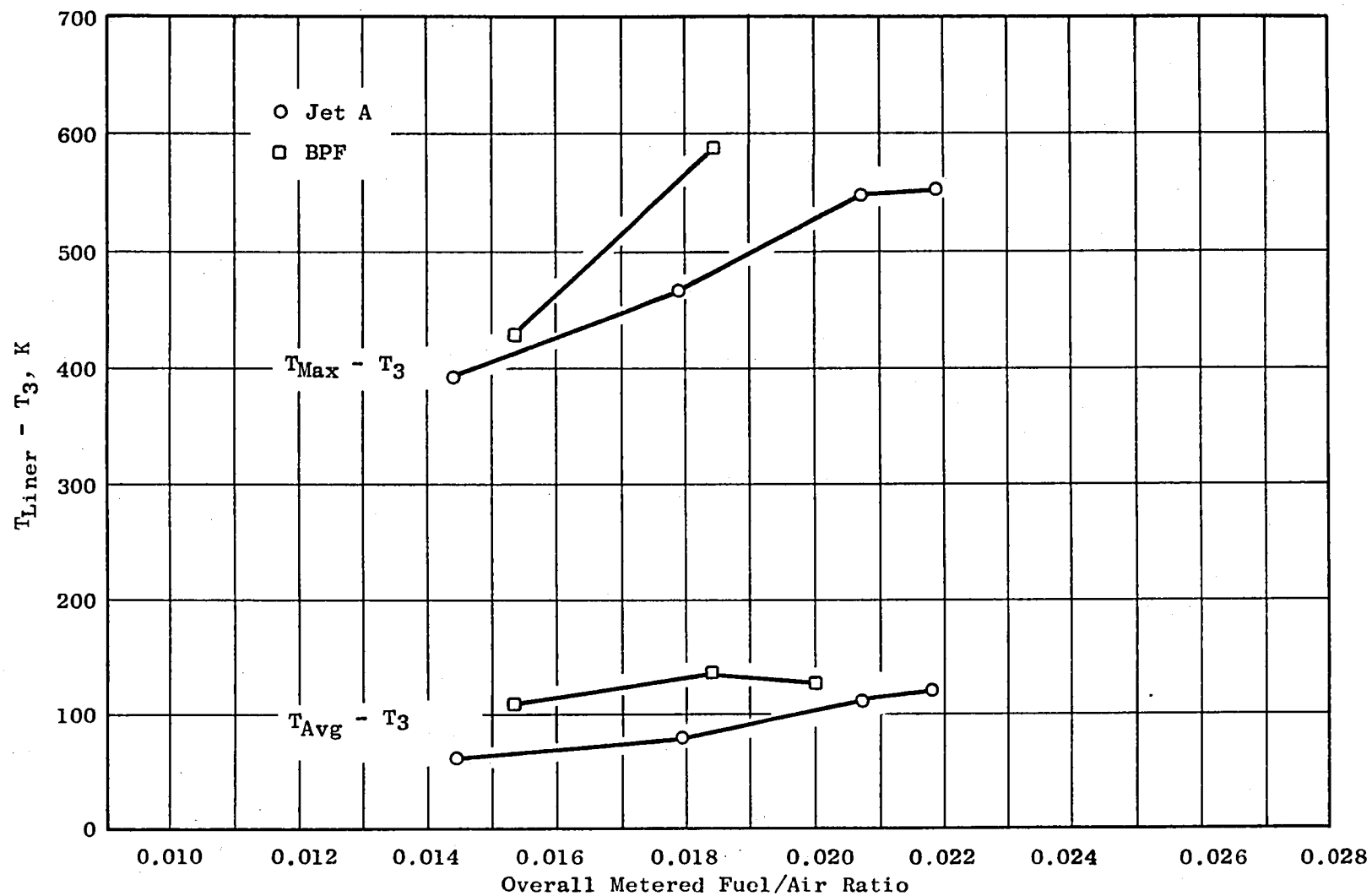
Figure 81. Concept 2 Liner Temperatures at Simulated Takeoff Conditions.
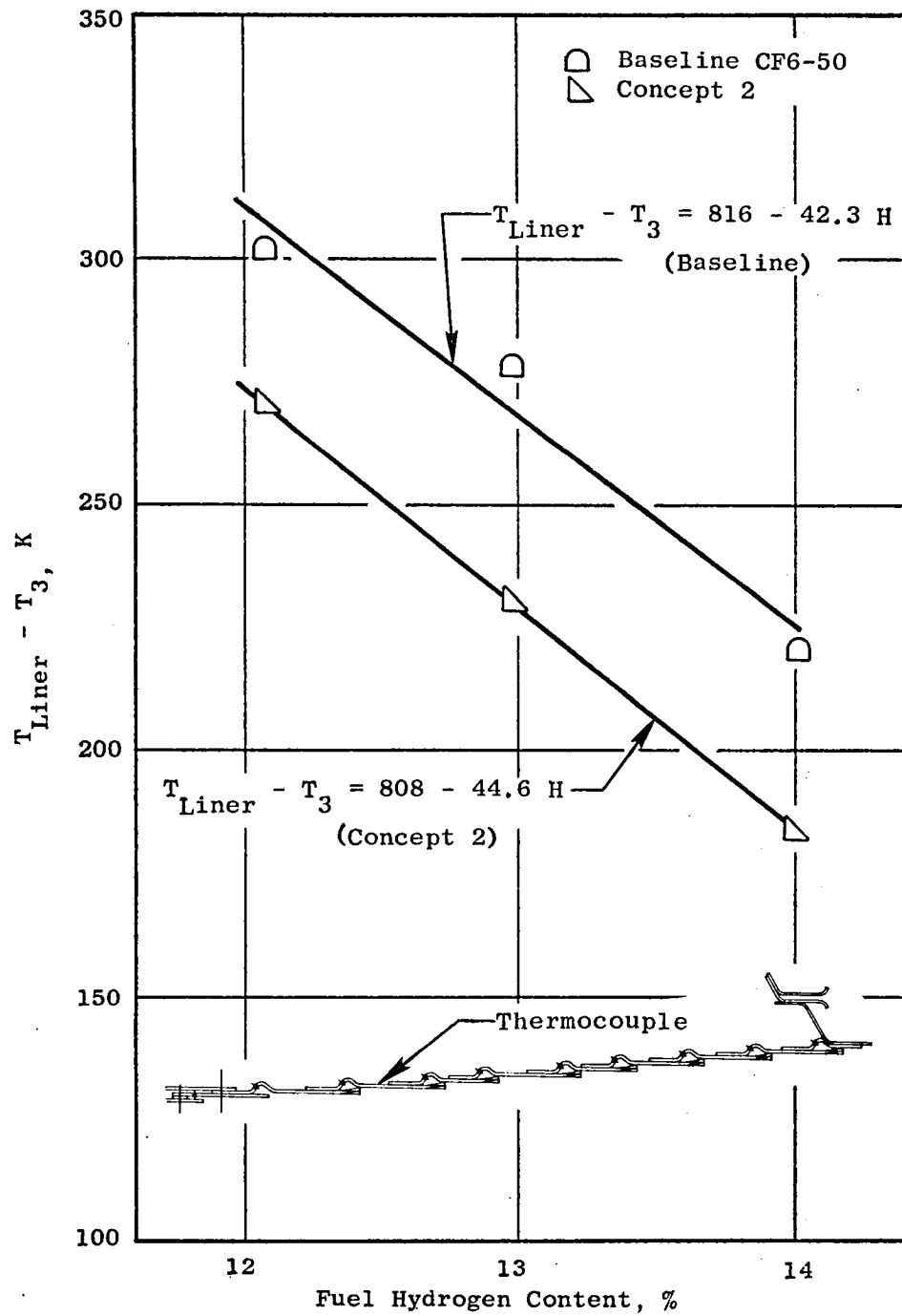
Figure 82. Variation of Concept 2 Outer Liner Temperature with Fuel Hydrogen Content at Cruise Conditions, f = 0.021.

$$T_{Liner} - T_3 = 815 - 41.4 \text{ H} \quad \text{(Baseline)}$$

$$T_{Liner} - T_3 = 564 - 22.4 \text{ H} \quad \text{(Concept 2)}$$

⌂ Baseline CF6-50
◺ Concept 2

Thermocouple

Fuel Hydrogen Content, %

$T_{Liner} - T_3$, K
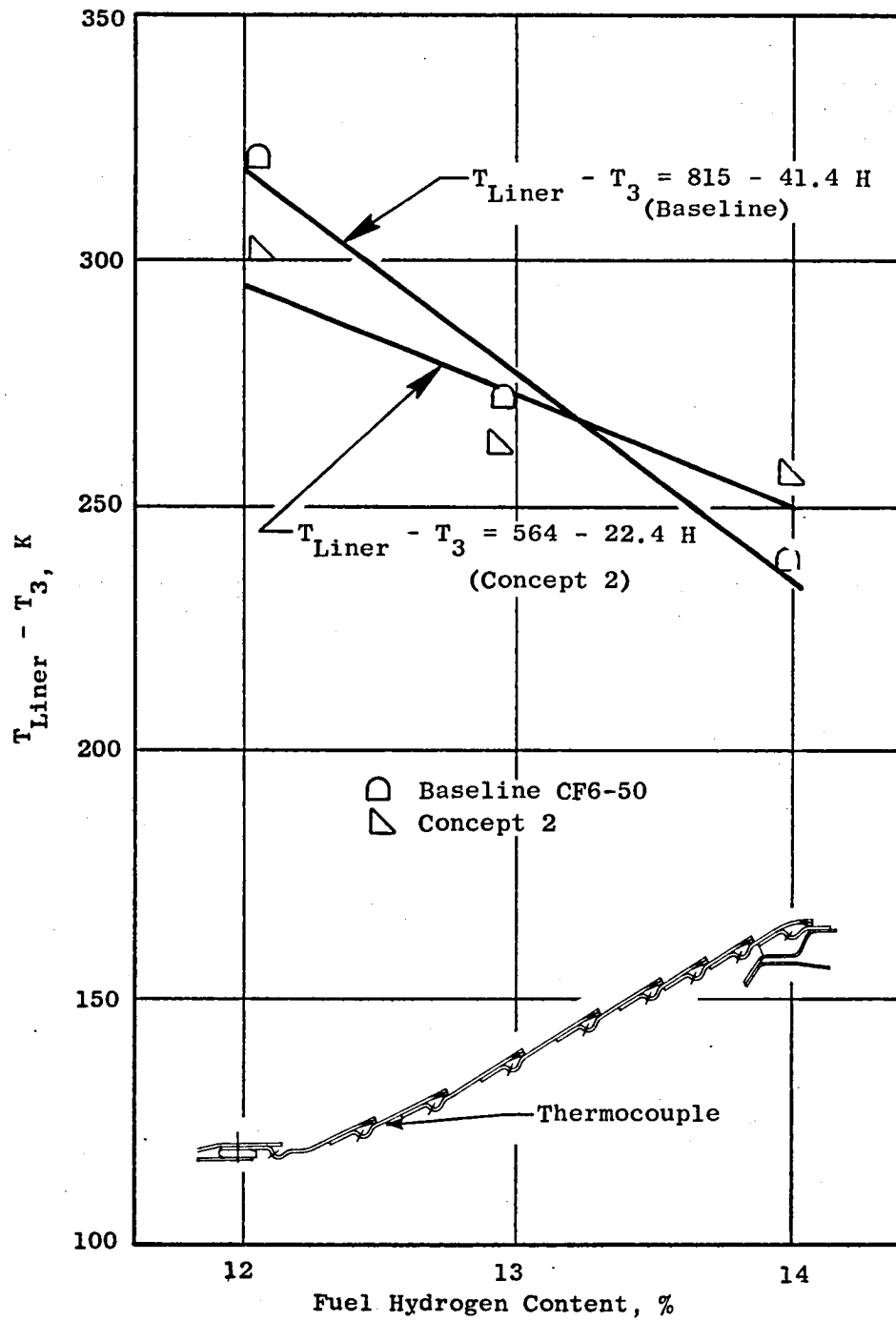
Figure 83. Variation of Concept 2 Inner Liner Temperature
with Fuel Hydrogen Content at Cruise Conditions,
f = 0.021.

Figure 84.   Concept 2 Main-Stage Fuel Nozzle Air Shroud After Test.

The variation of Concept 2 smoke number with fuel/air ratio for the test fuels is shown in Figures 85 and 86. These results are correlated with fuel hydrogen content in Figure 87. This burner yielded higher smoke numbers than those for Concept 1 but lower than those for the baseline combustor. Since premixing combustors would be expected to have the potential for very low smoke, it is possible that some nonuniformity in the fuel distribution existed at the exit of the premix duct. This would lead to locally rich burning and produce smoke. Spray tests of the premix ducts and fuel injectors were conducted at ambient inlet conditions. Additional development of the premixing tubes and fuel-injection system would likely result in improved performance of this concept.

Figures 88 and 89 show the variation of CO emission index with fuel/air ratio for the test fuels. As with the baseline configuration, there is very little effect from the fuel variation. The high level of CO emission index at the lowest fuel/air ratio for the 12% hydrogen blend is due to incomplete combustion near the lean stability limit with this fuel. The unburned-hydrocarbon emission index, Figure 90, follows the CO emission index.

Posttest examination of the exit gas-sample probes indicated that they were in good condition, verifying that the change in test procedures was effective.

6.4 CONCEPT 3 SCREENING TEST RESULTS

The last screening test was the one conducted for Concept 3. The main and pilot stages were reversed for this concept.

Concept 3 produced the lowest smoke levels of all the combustors tested and demonstrated that the radial temperature profile could be inverted by reversing the pilot- and main-stage domes in a double-annular combustor. The NO_x levels were between those measured for the other two concepts. However, this combustor encountered combustion resonance and dome flame-stability problems at some operating conditions. It is believed that, during a portion of the test, the flame was not seated in the pilot dome. It is likely that the observed resonance and dome instability were caused by leakage between the three-cup sector and the test-rig sidewalls.

The pilot instability problem is illustrated by the data in Figure 91; the data points are connected in the sequence in which they were run. Low combustion efficiencies were initially observed at low fuel/air ratios. After setting high fuel/air ratios, the efficiencies increased and remained high even when the fuel/air ratios were reduced to the previous levels. Figure 92 illustrates that the problem was associated with the inner dome. For two points with the same fuel/air ratio, but different combustion efficiencies, the inner-liner temperatures are significantly different. This indicates that the inner dome was not operating properly at one set of conditions. The outer-liner temperatures were unaffected. The combustor also encountered combustion resonance at the higher fuel/air ratio points at
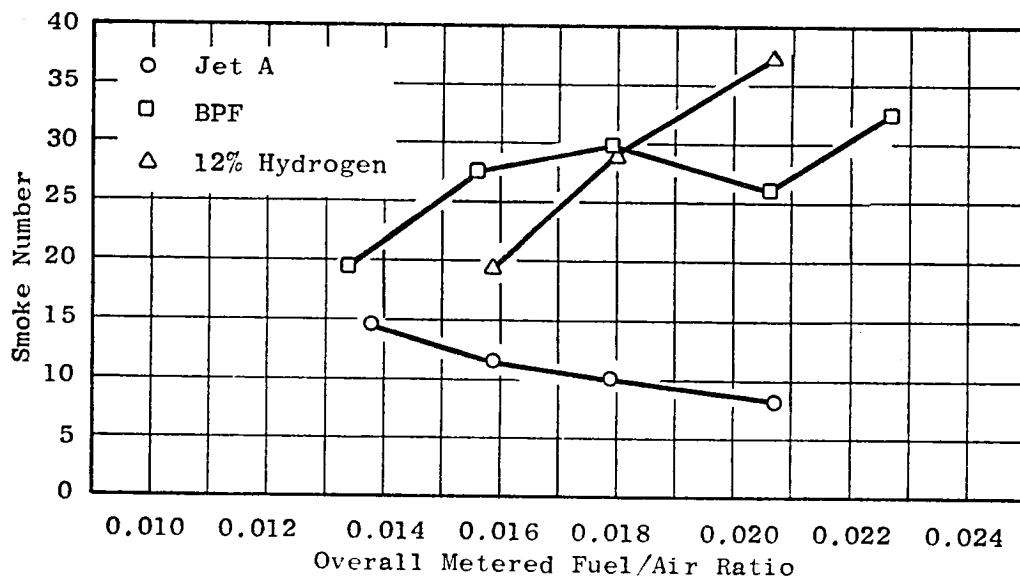
Figure 85. Concept 2 Smoke Numbers at Cruise Conditions.
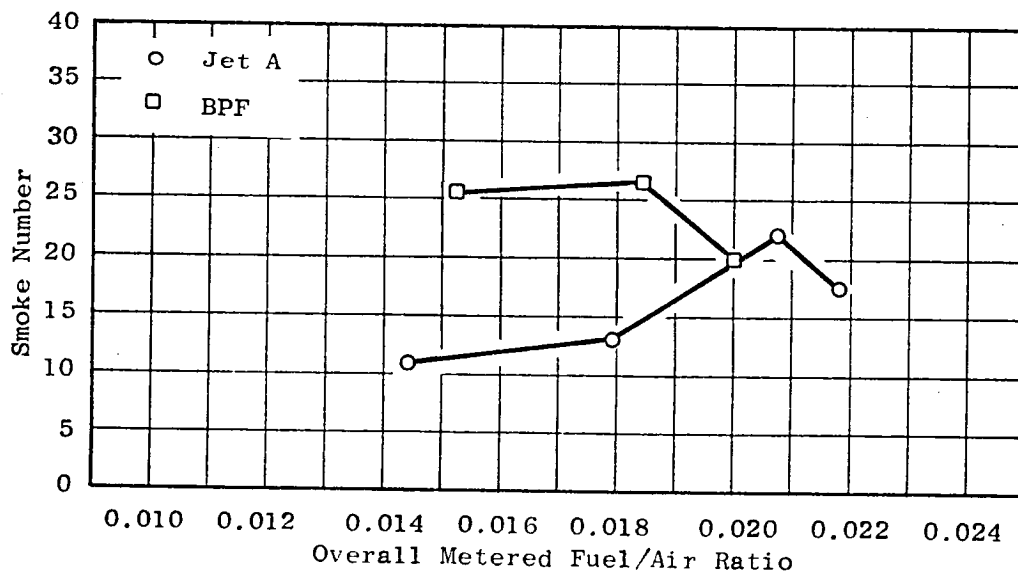
Figure 86. Concept 2 Smoke Numbers at Simulated Takeoff Conditions.

98
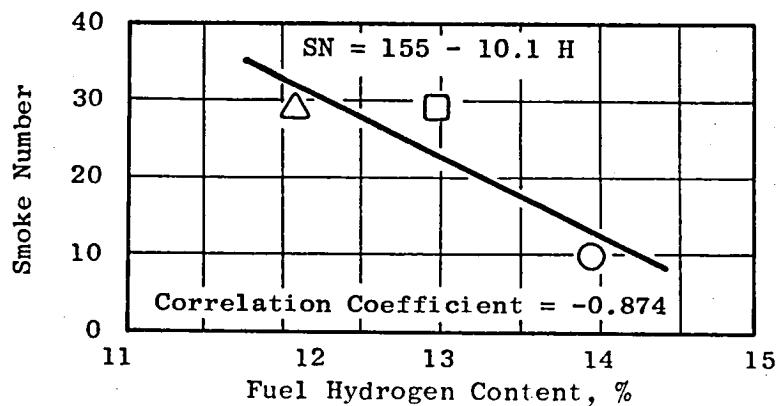
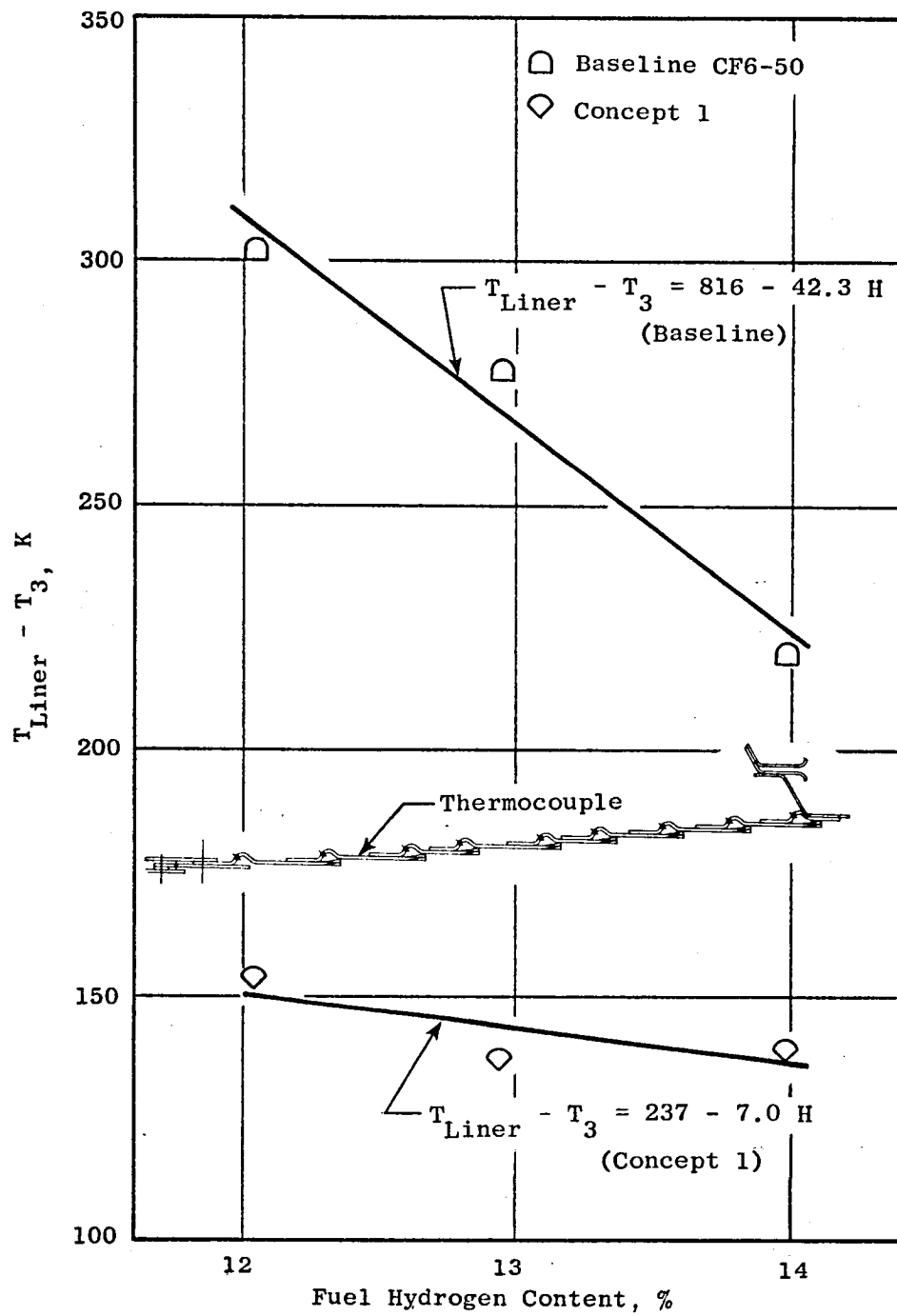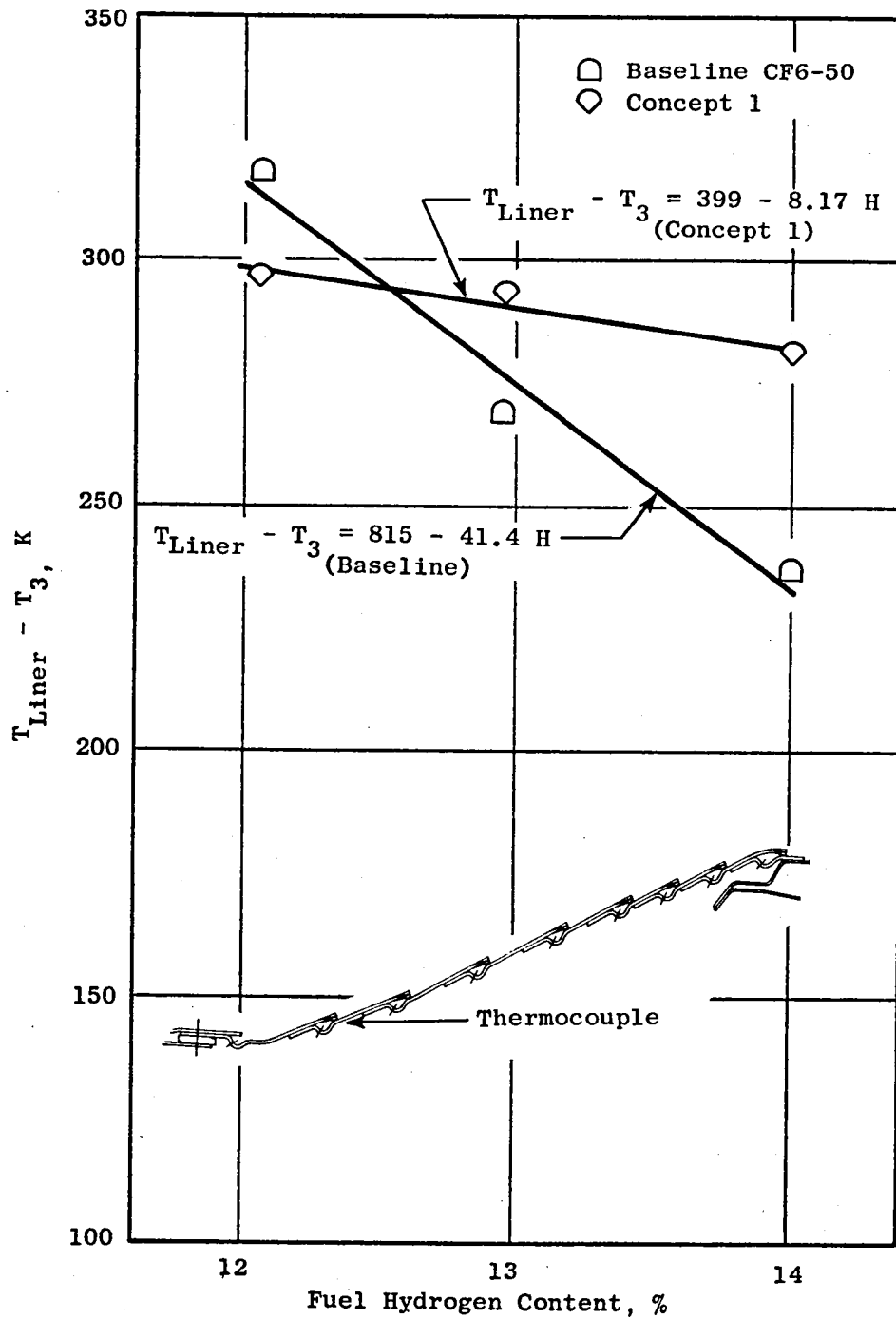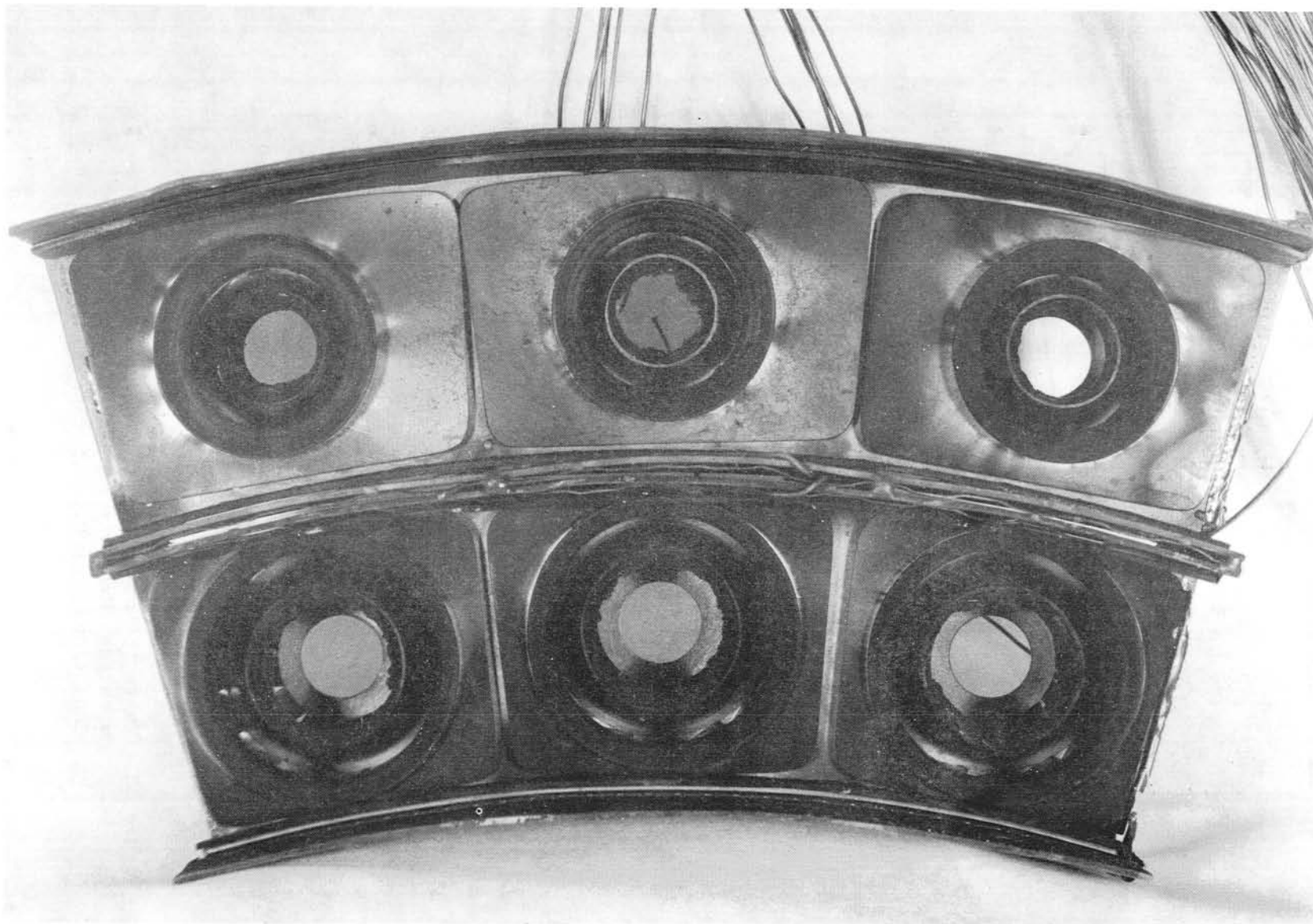Figure 87. Variation of Concept 2 Smoke Number
with Fuel Hydrogen Content at Cruise
Conditions, f = 0.018.
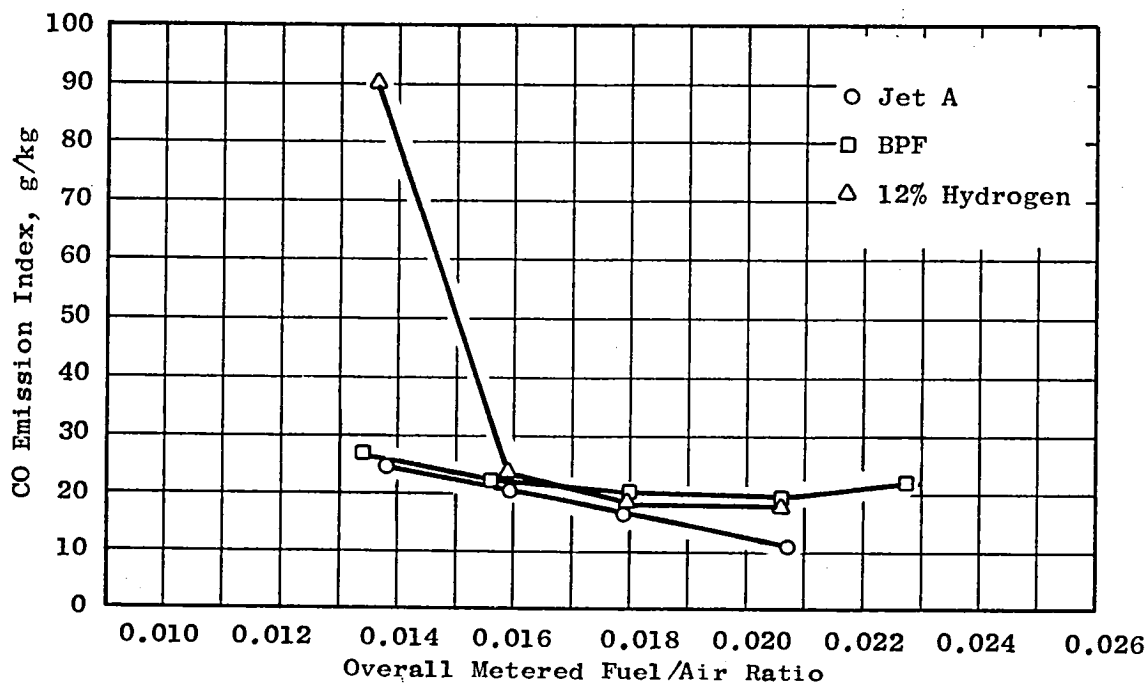
Figure 88. Concept 2 CO Emission Index at Cruise Conditions.
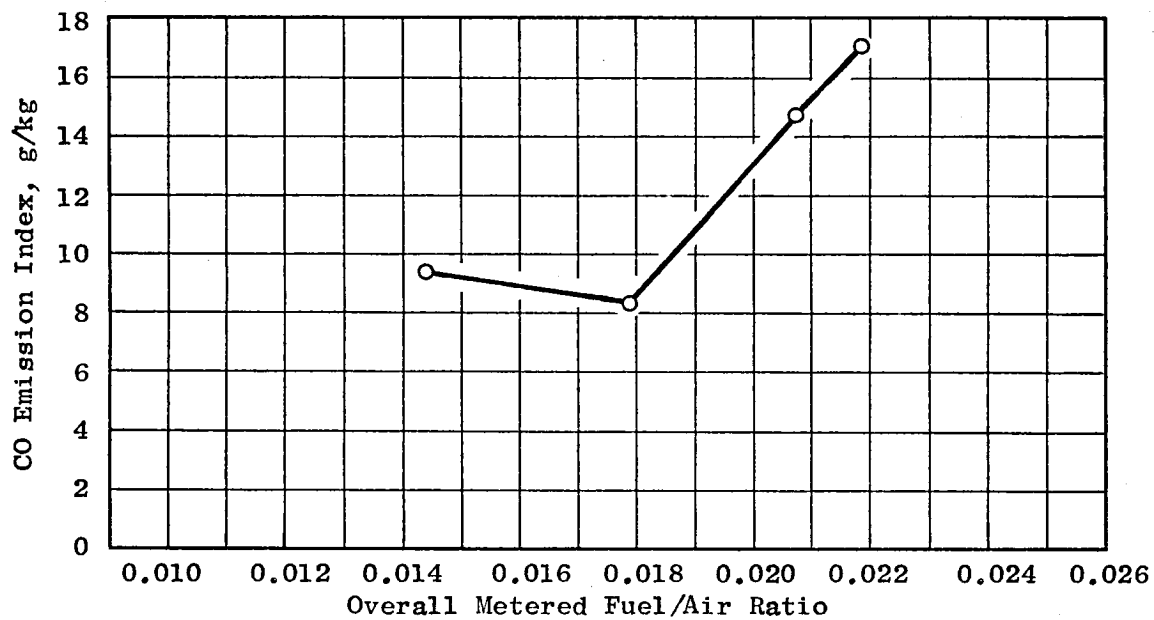
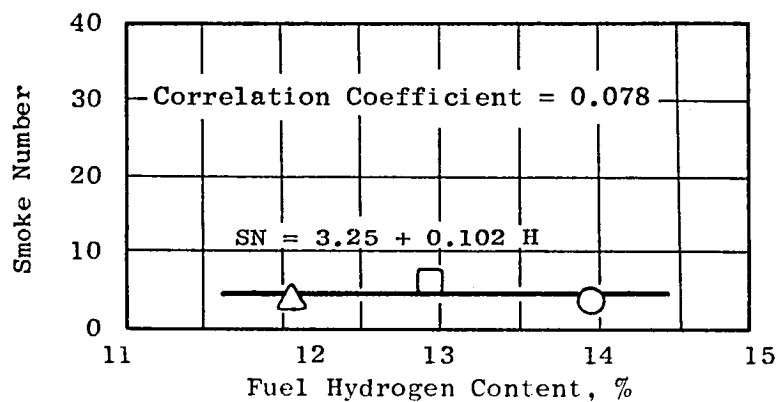Figure 89. Concept 2 CO Emission Index at Simulated Takeoff Conditions, Jet A Fuel.
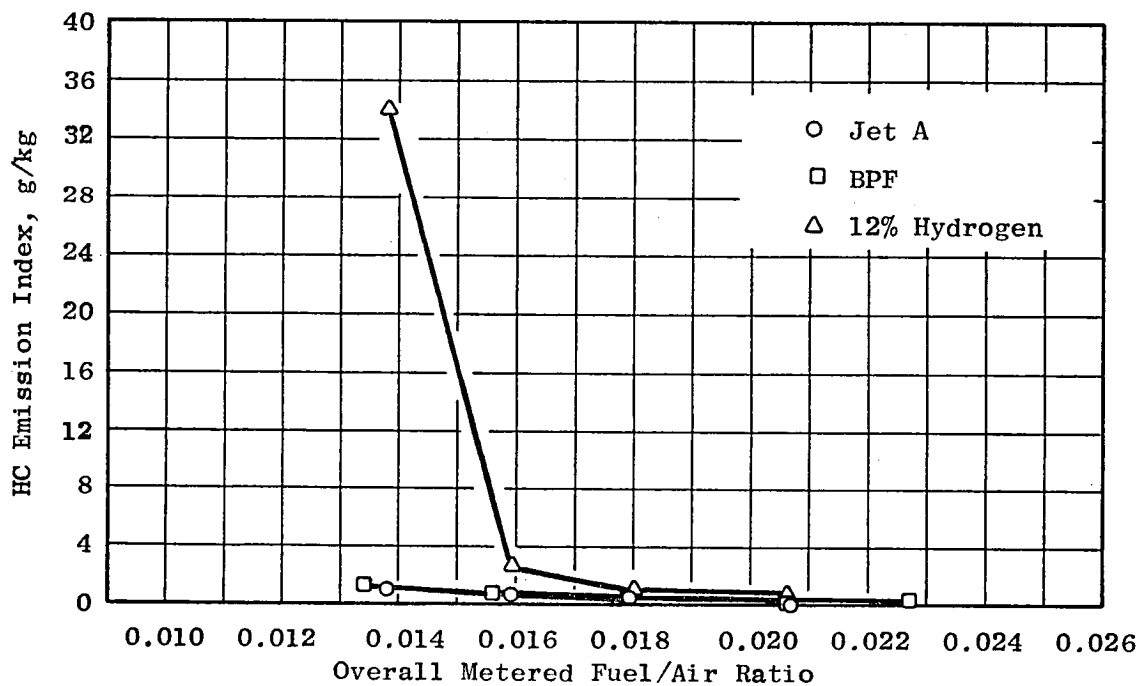
Figure 90. Concept 2 Unburned Hydrocarbon Emission Index at Cruise Conditions.
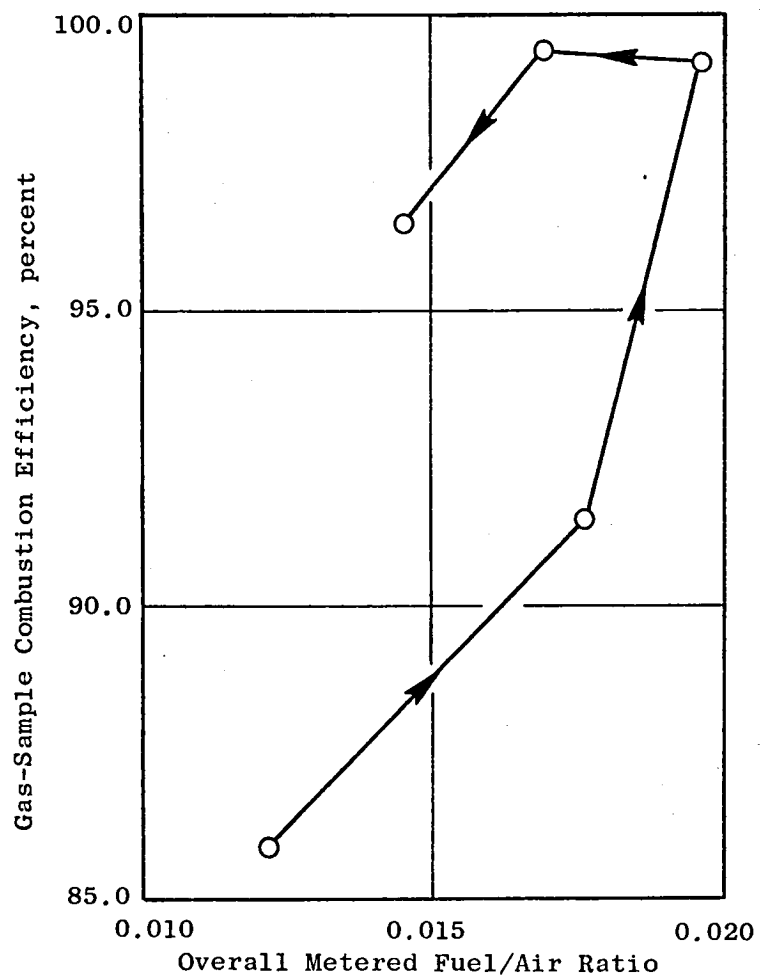
Figure 91. Variation of Concept 3 Combustion
Efficiency with Fuel/Air Ratio at
Cruise Conditions Illustratiing
Bimodal Pilot Dome Flame Holding
with Jet A Fuel.
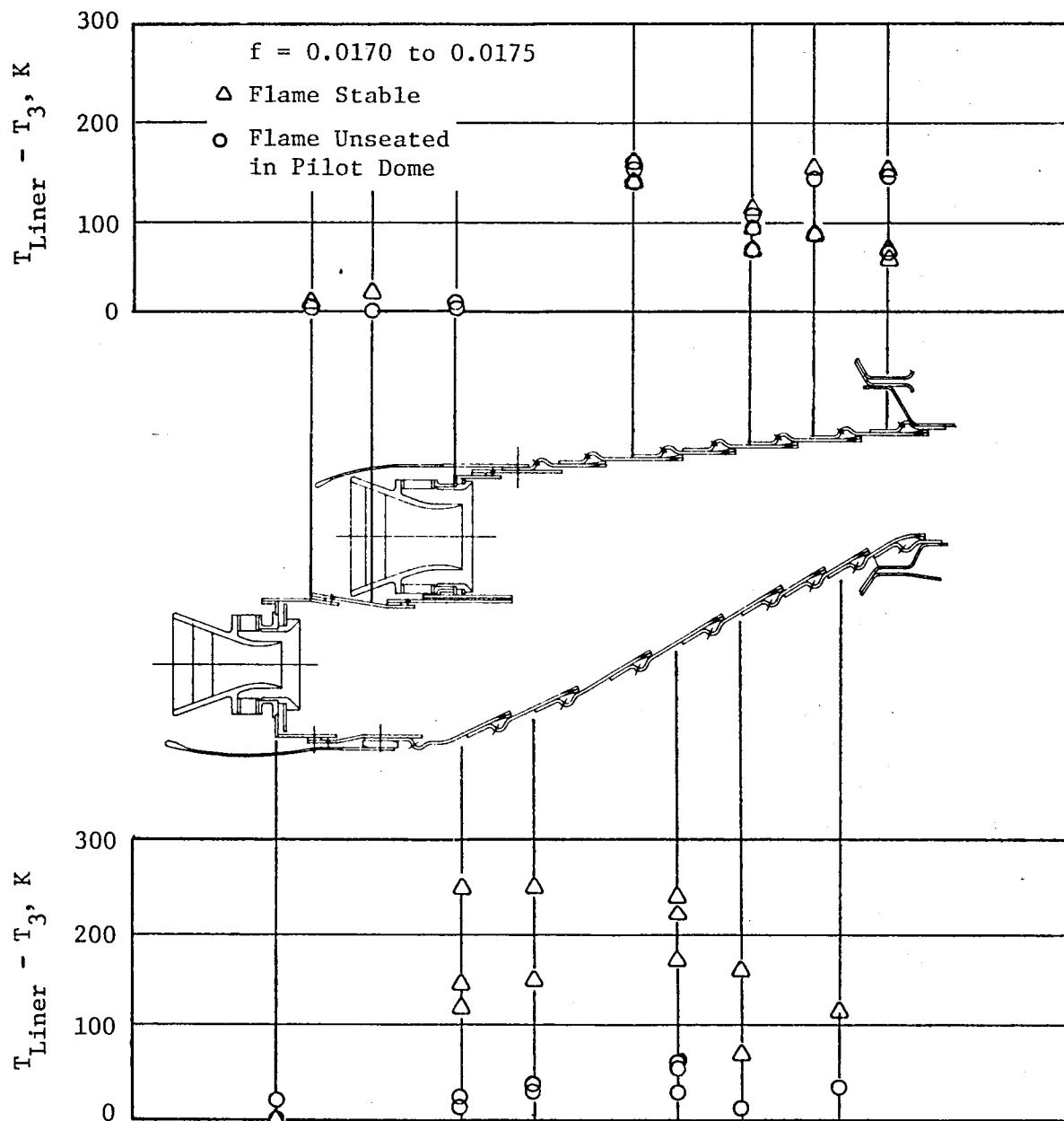
Figure 92.   Concept 3 Liner Temperature Distributions During Bimodal Operation.

cruise conditions. These problems may be attributed to excessive sidewall leakage around the inner dome. Despite these difficulties, a complete set of representative data was accumulated on Jet A fuel, and the outer-liner temperatures are believed to have been unaffected.

Carbon buildup and soot deposits in the Concept 3 burner are shown in Figures 93 through 96. This combustor had characteristics similar to Concept 1; the pilot dome was very clean, and the main-stage dome had moderate carbon deposits. The liners had soot deposits similar to those found on the other burners, including the baseline. The fuel nozzles appeared to be somewhat cleaner than those used for the other two advanced designs.

Only general trends for radial exit temperature profiles are obtainable from sector tests; however, the Concept 3 combustor exhibited a significant shift in the exit temperature pattern relative to Concept 2, which had the main stage on the inboard side. Some gas-sample, exit-fuel/air-ratio profiles (equivalent to temperature profiles) are in Figure 97. These data indicate that, for Concept 2, the profile peak occurred near the 30% point of the radial blade height. For the baseline, and for Concept 3 with the main stage on the outside, the peaks occurred at approximately 55% radial height or further outboard. Shifting the radial profile peak outboard was one of the objectives of the Concept 3 design.

Concept 3 produced very low smoke levels. The smoke data for Jet A fuel are presented in Figures 98 and 99 along with results for the other two double-annular combustors. The reduced smoke levels, relative to Concepts 1 and 2, may be traceable to the use of additional pairs of dome swirlers (unfueled) between the fueled swirlers. These are the dome swirlers shown in Figure 6. The Concept 1 and 2 domes are shown in Figures 4 and 5 respectively.

The NO_x emissions level for Concept 3 is shown in Figure 100 for Jet A fuel. The levels achieved were below those for Concept 1 but not as low as for Concept 2. The improvement over Concept 1 is attributed to the reduced residence time in the main stage. Concept 2 had premixing of the fuel and air. A comparison of the results for the three combustors is presented in Figure 101.

Concept 3 liner temperatures are presented in Figure 102. In general, temperatures were low both for the inner and for the outer dome structures. The outer-liner temperature levels (Figure 103) were only 167 K, maximum, above the inlet temperature with Jet A fuel. The baseline outer-liner temperature peaked at approximately 280 K above inlet temperature. Concept 3 had lower temperatures even though only 10.8% cooling is used for Concept 3 versus 14.8% for the baseline. This improvement is attributed to the lean dome operation of the advanced design and also to the shortened outer liner. The effect of fuel type is considerably reduced relative to the baseline combustor.

The outer liner of Concept 3 is cooler than the inner liner of Concept 2 and the baseline, as shown in Figure 103. On Concepts 1 and 2 the main-stage
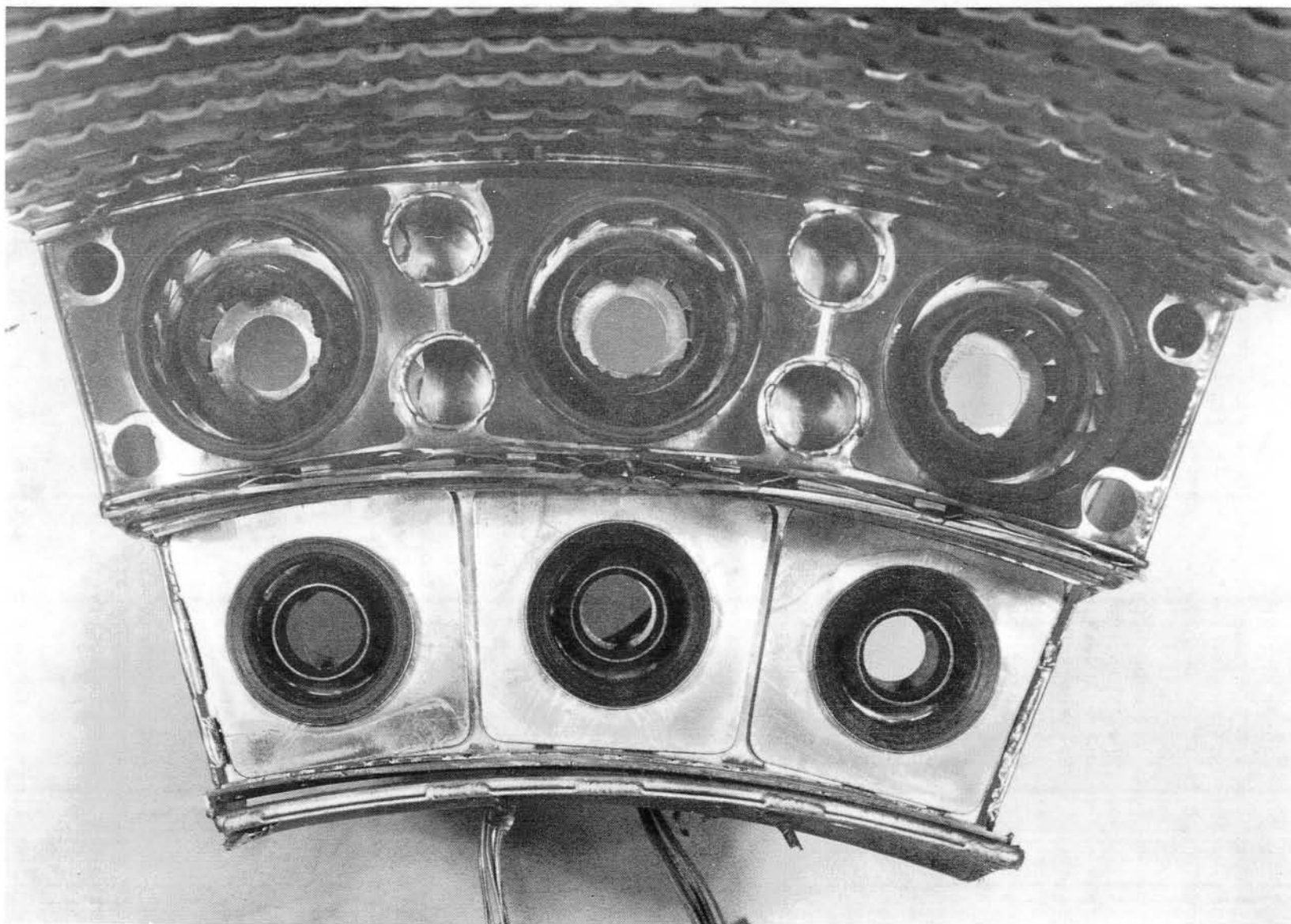
Figure 93. Concept 3 Dome After Test.
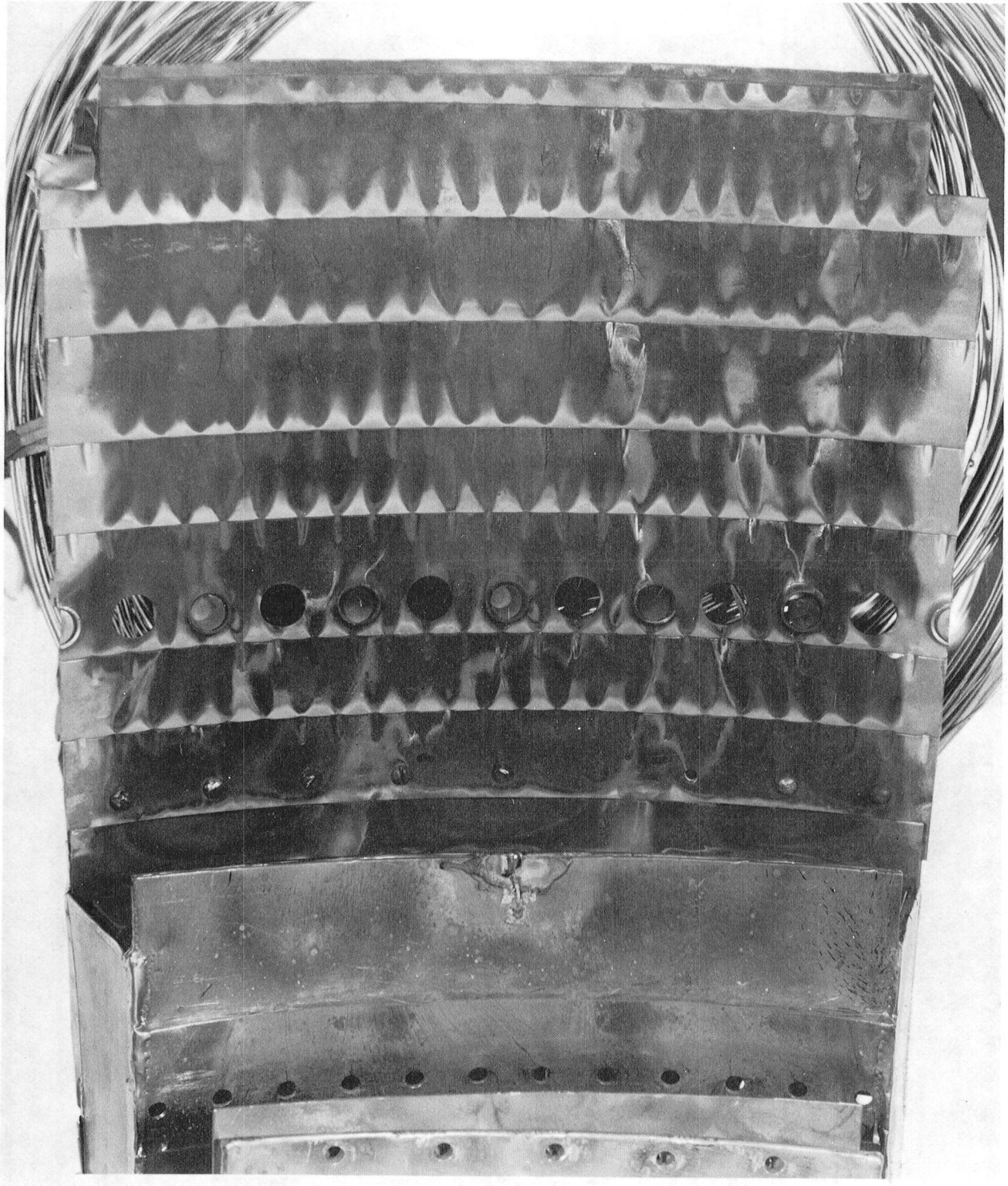
Figure 94.   Concept 3 Outer Liner After Test.
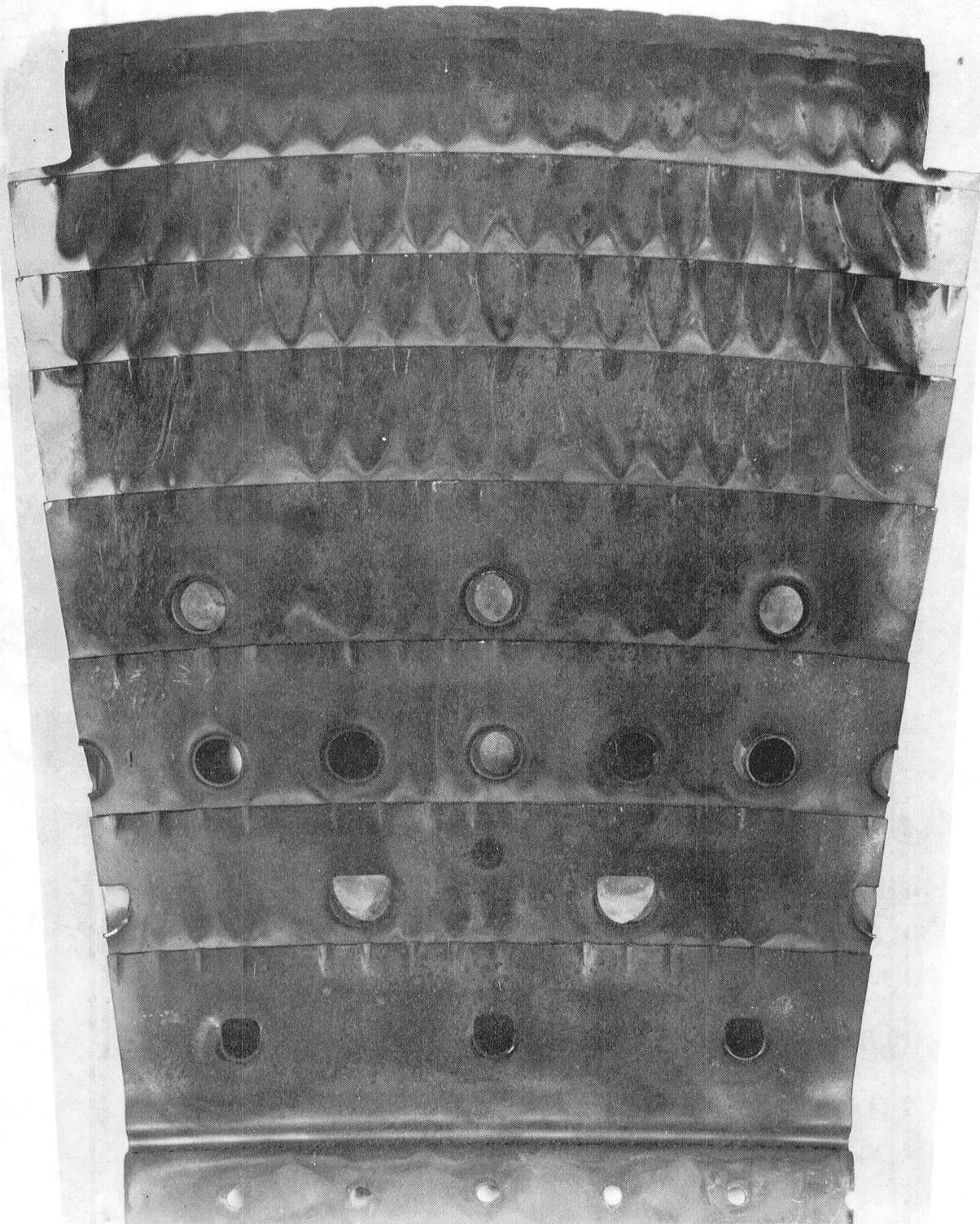
Figure 95. Concept 3 Inner Liner After Test.

Figure 96. Concept 3 Fuel Nozzles After Test.
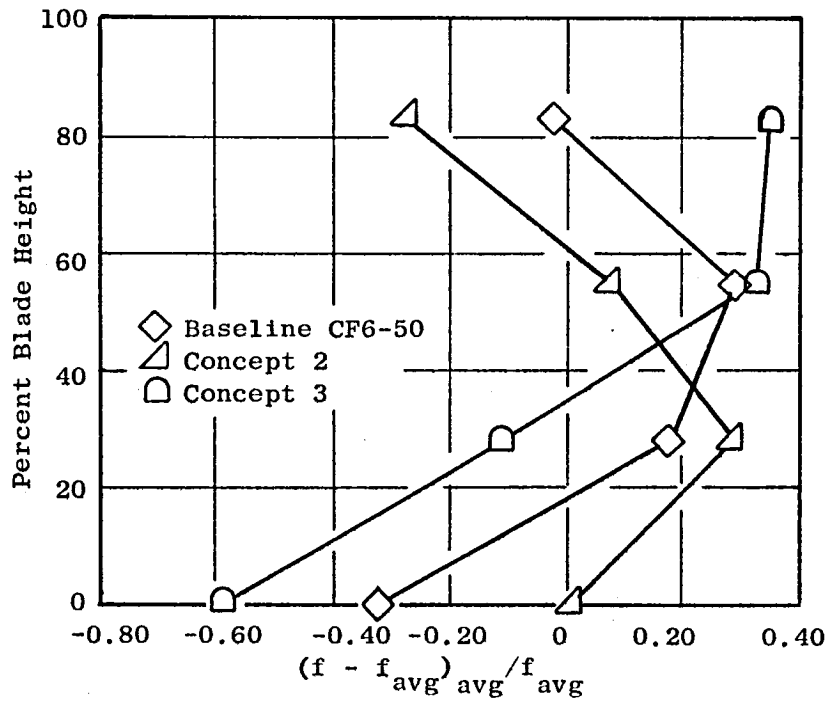
Figure 97. Combustor Exit Fuel/Air Ratio Profile
Shapes Based on Gas-Sample Data.
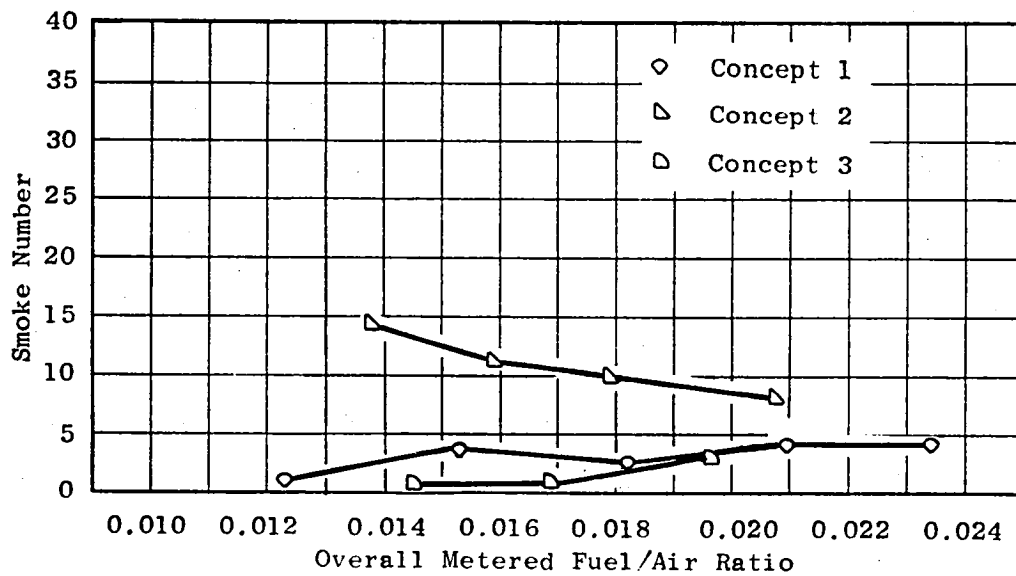
Figure 98. Concept 3 Smoke Numbers at Cruise Conditions, Jet A Fuel.
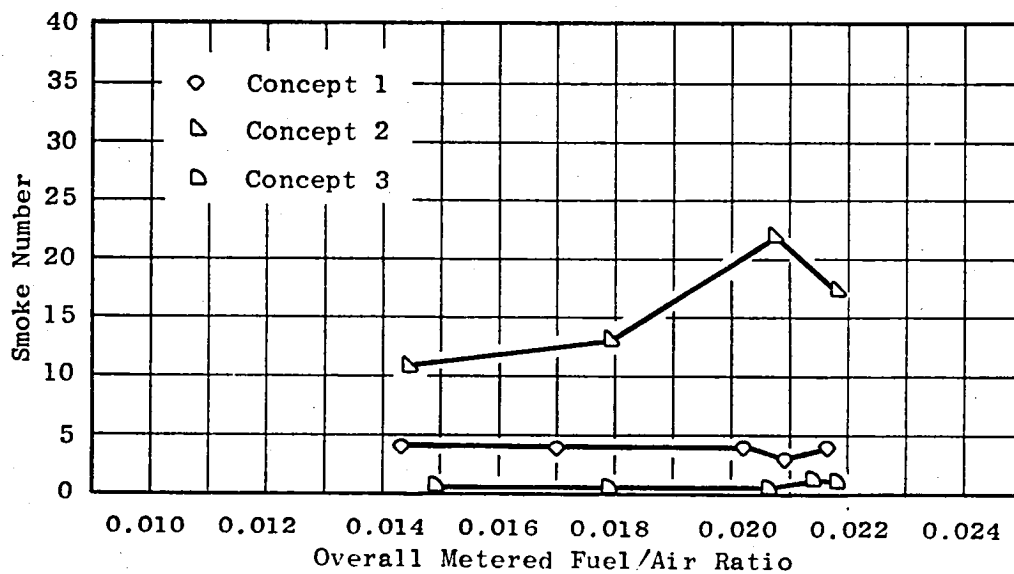
Figure 99. Concept 3 Smoke Numbers at Simulated Takeoff Conditions, Jet A Fuel.
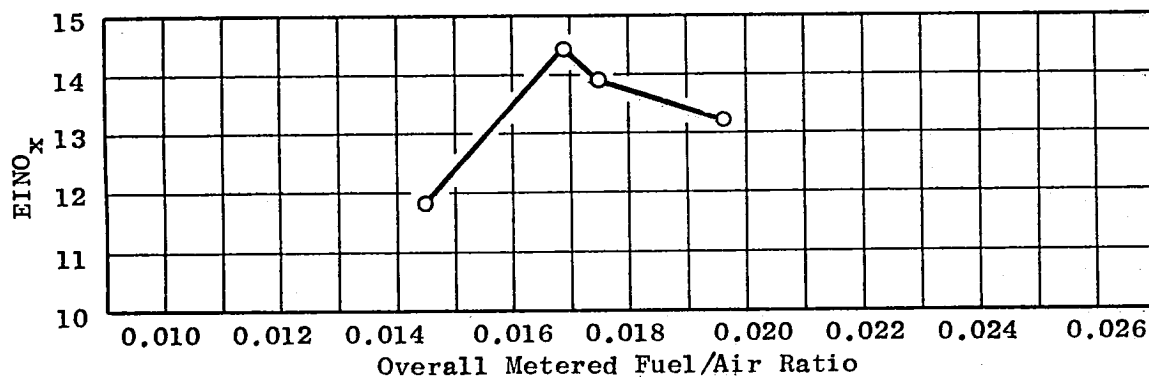
Figure 100. Concept 3 NO$_x$ at Cruise Conditions, Jet A Fuel.
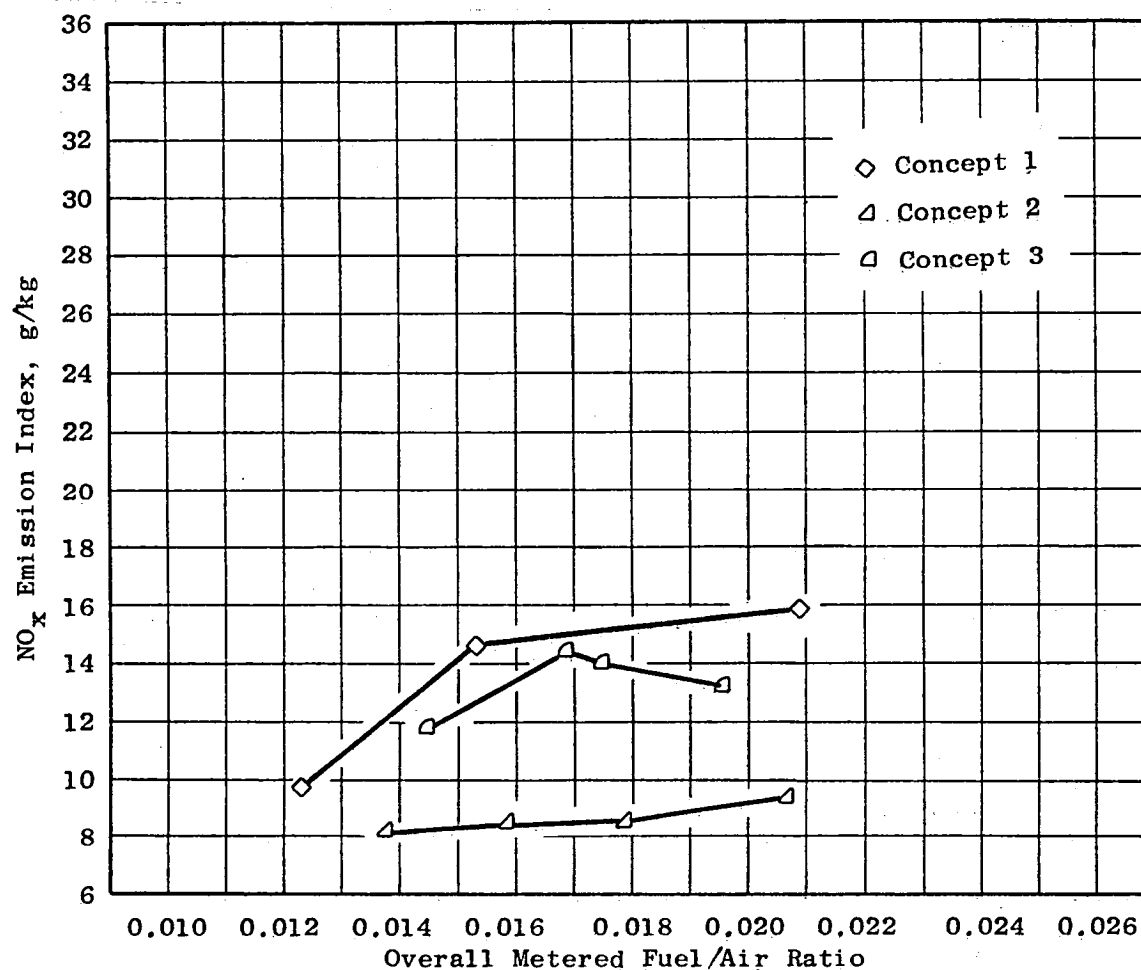
Figure 101. Comparison of NO$_x$ Emission Index for the Three
Advanced Combustor Concepts, Jet A Fuel.
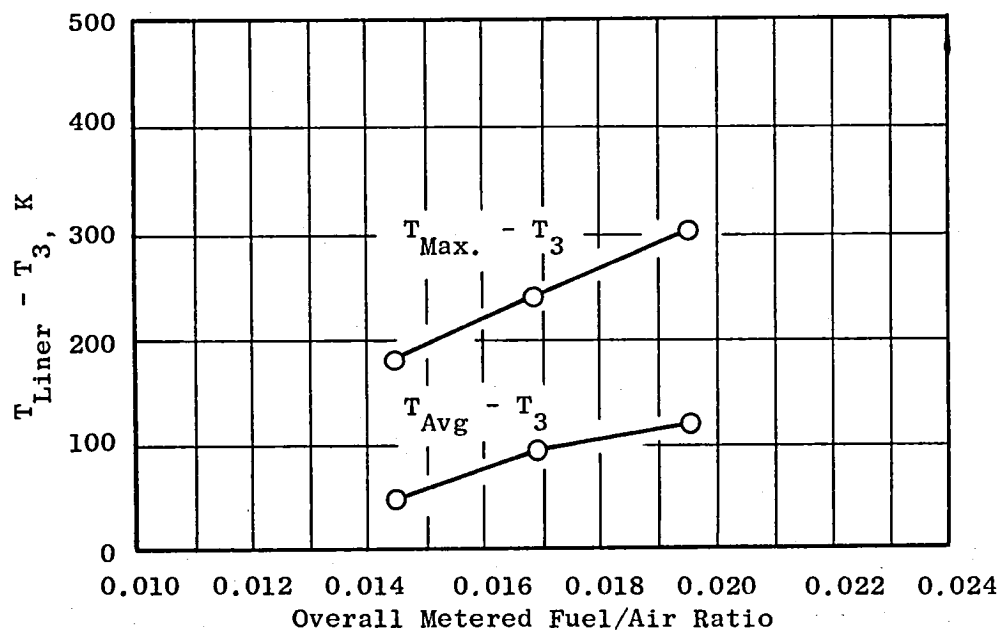
Figure 102. Concept 3 Liner Temperature at
Cruise Conditions, Jet A Fuel.
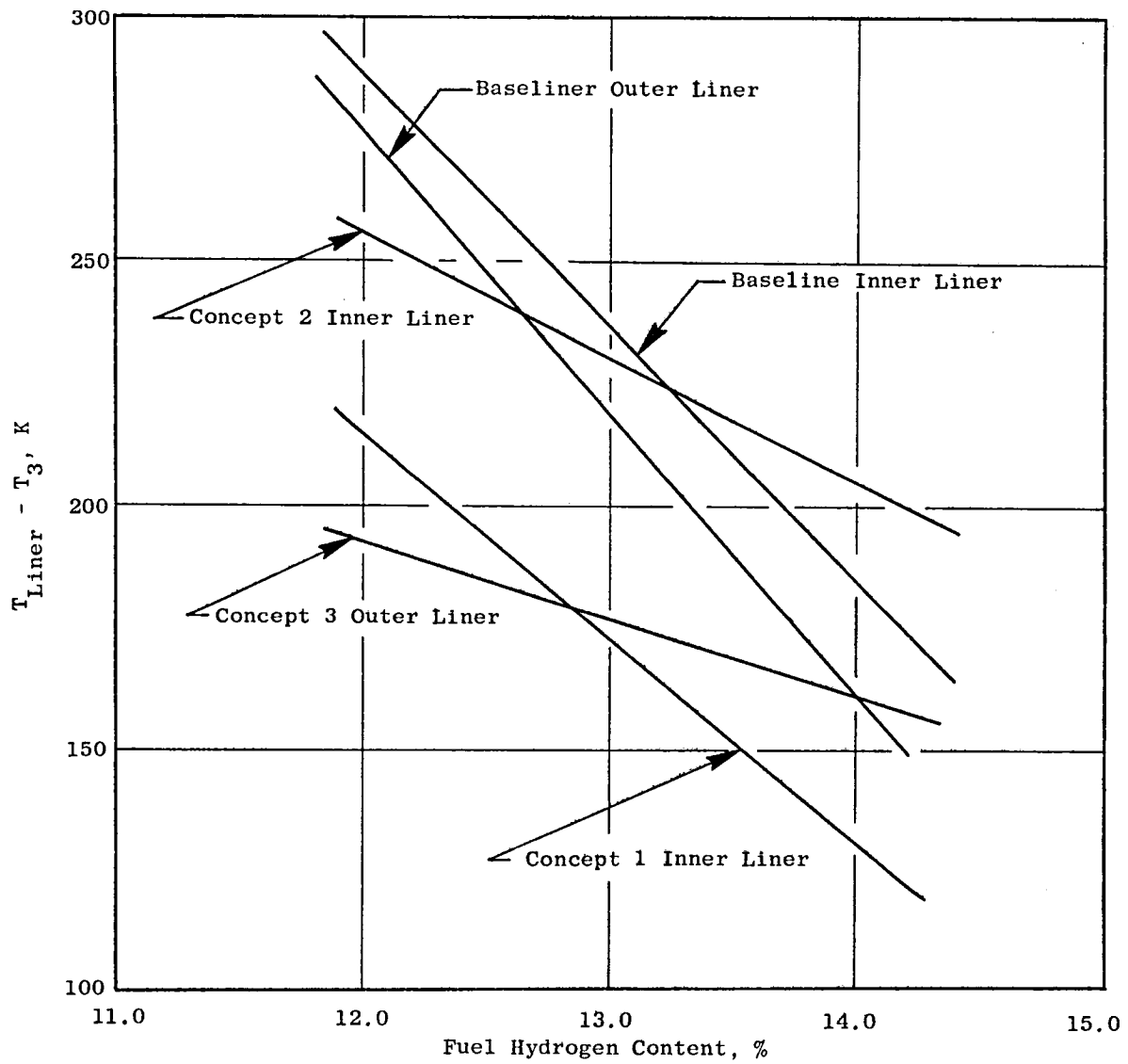
Figure 103. Comparison of Liner Temperatures Adjacent to Main Stage for Baseline and Advanced Concepts, Cruise Conditions, f = 0.0175.

dome is adjacent to the inner liner, and the higher velocity gases from the main stages must be turned outward by the inner liner. It appears that there is less of a cooling problem for the liner adjacent to the main stage if the main stage is on the outboard side of the pilot stage.

For the inner liner, when the flame is properly seated in the dome, the liner temperatures appear comparable to those measured for the baseline combustor even though the cooling level was reduced from 15.2% for the baseline to 8.2% for Concept 3.

6.5 PARAMETRIC TEST RESULTS

The Concept 2 burner demonstrated the potential of a premixing-prevaporizing design in achieving low NO_x levels and clean liners and domes. The Concept 1 test showed that high ΔP fuel nozzles give no significant improvement, using the three test fuels, over the conventional, simplex, fuel nozzles tested in similar combustor designs during the ECCP program. The Concept 3 burner demonstrated lower smoke and the benefits of positioning the main stage on the outboard side. However, the combustor had some combustion instability and resonance problems in the existing configuration. The Concept 2 burner design was chosen for the parametric test for the above reasons and because advanced burner designs using premixing-prevaporizing technology could utilize a broader data base provided by additional testing.

The parametric test-point schedule was designed to explore the effects of pilot/main-stage fuel-flow ratio variations, using Jet A and the 12% hydrogen fuel, and reference velocity variations using the 12% hydrogen fuel only. The inner liner was modified by adding two dilution holes in line with each premix tube and deleting the six profile-trim holes. Liner effective area was increased approximately 2%. Existing holes in the CF6-50-derived liner were filled by welding plugs into the holes. This was done to reduce the liner-temperature problems believed to be caused by the loss of some Nichrome patches in earlier tests. In addition, a thermocouple was added to the inside of all three premix tubes, 5 cm upstream of the tube exits, to detect possible autoignition. These three thermocouples were monitored continuously throughout the test. The locations of thermocouples on the oxidized panel of the Concept 2 burner were moved to the highest temperature location observed during the screening tests. All other thermocouple locations remained the same.

The variation of liner temperatures with fuel/air ratio for the parametric test is shown in Figures 104 and 105. The liner temperatures in these figures cannot be compared directly with the Concept 2 liner temperatures because three more thermocouples were used, and some locations were varied for the parametric test. Individual thermocouples which can be compared are shown in Figures 106 and 107. These two thermocouples were in the same
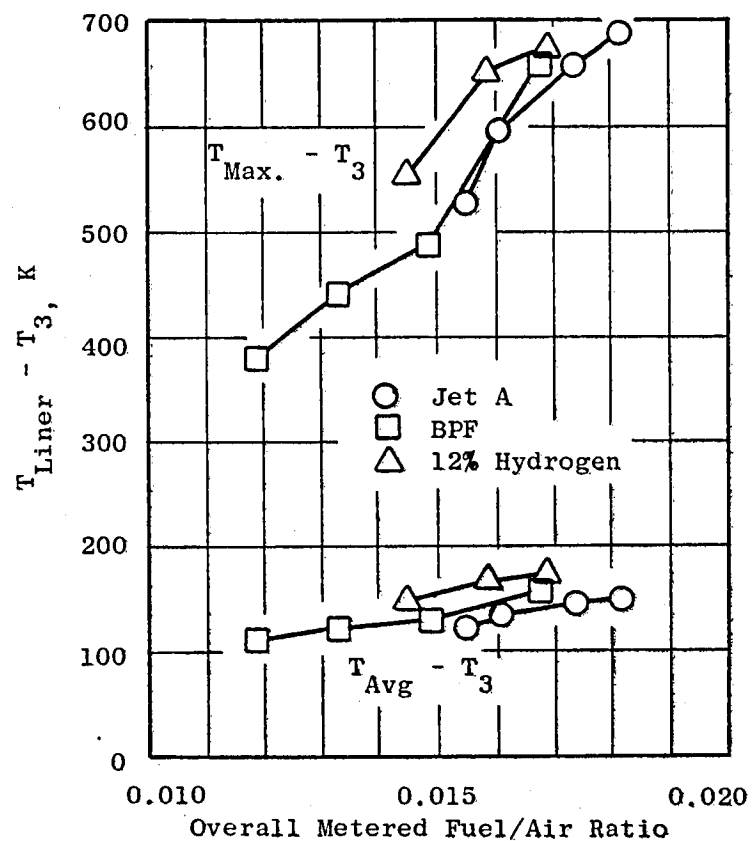
Figure 104. Parametric-Test Liner Temperatures at Cruise Conditions.
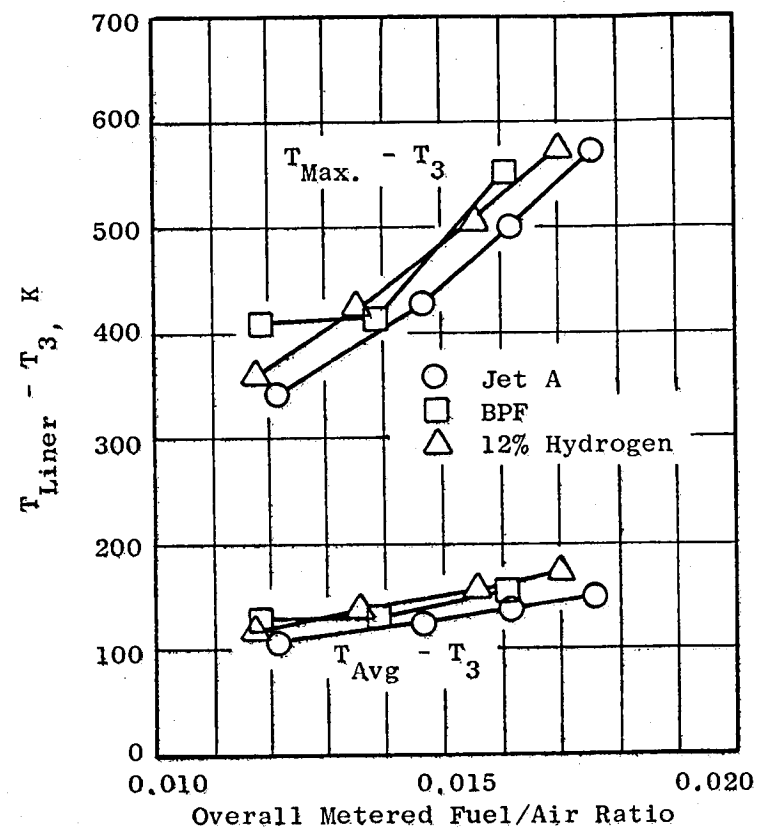
Figure 105. Parametric-Test Liner Temperatures at Simulated Takeoff Conditions.
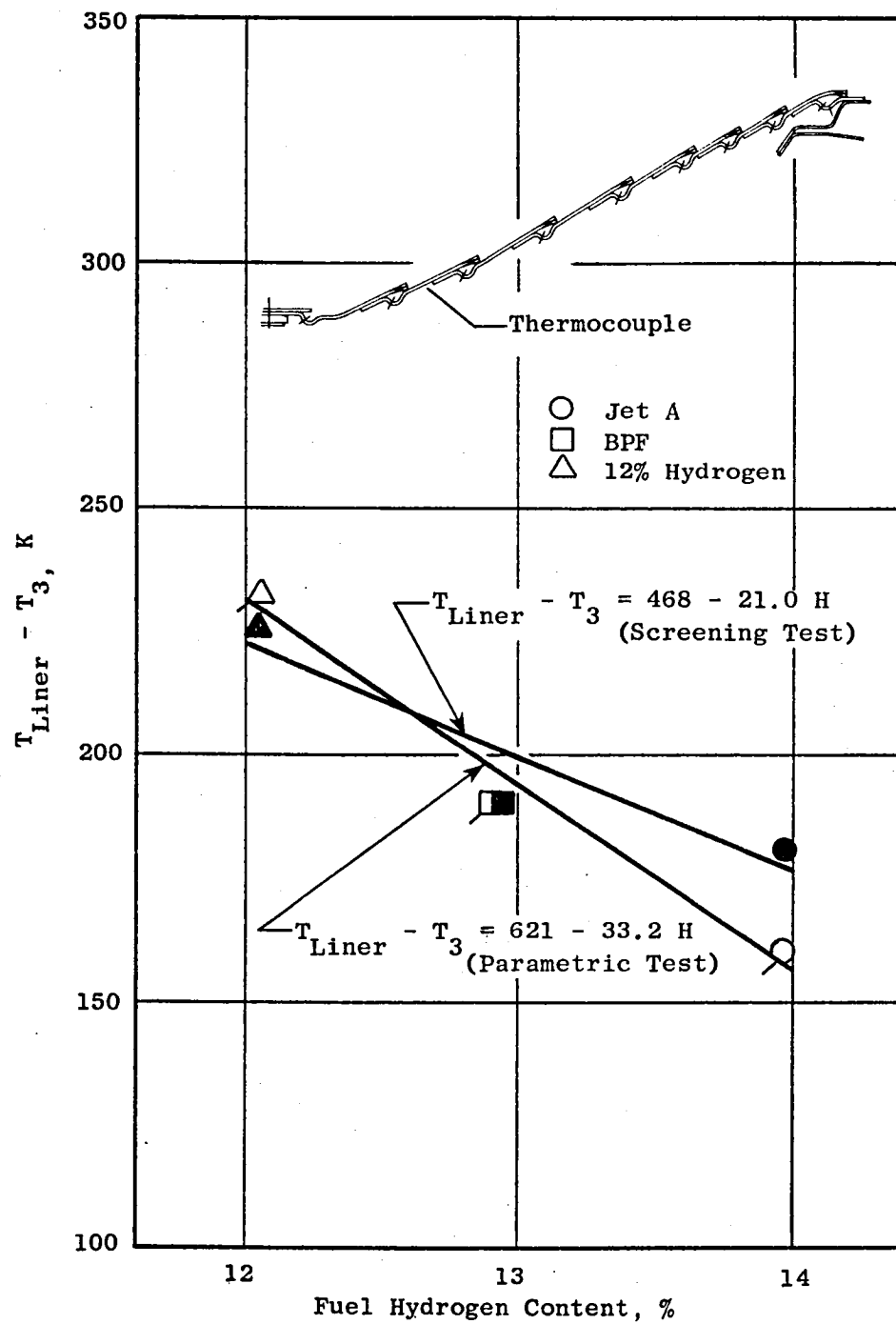
Figure 106. Comparison of Inner Liner Temperatures for Parametric and Screening Tests at Cruise Conditions, f = 0.016.
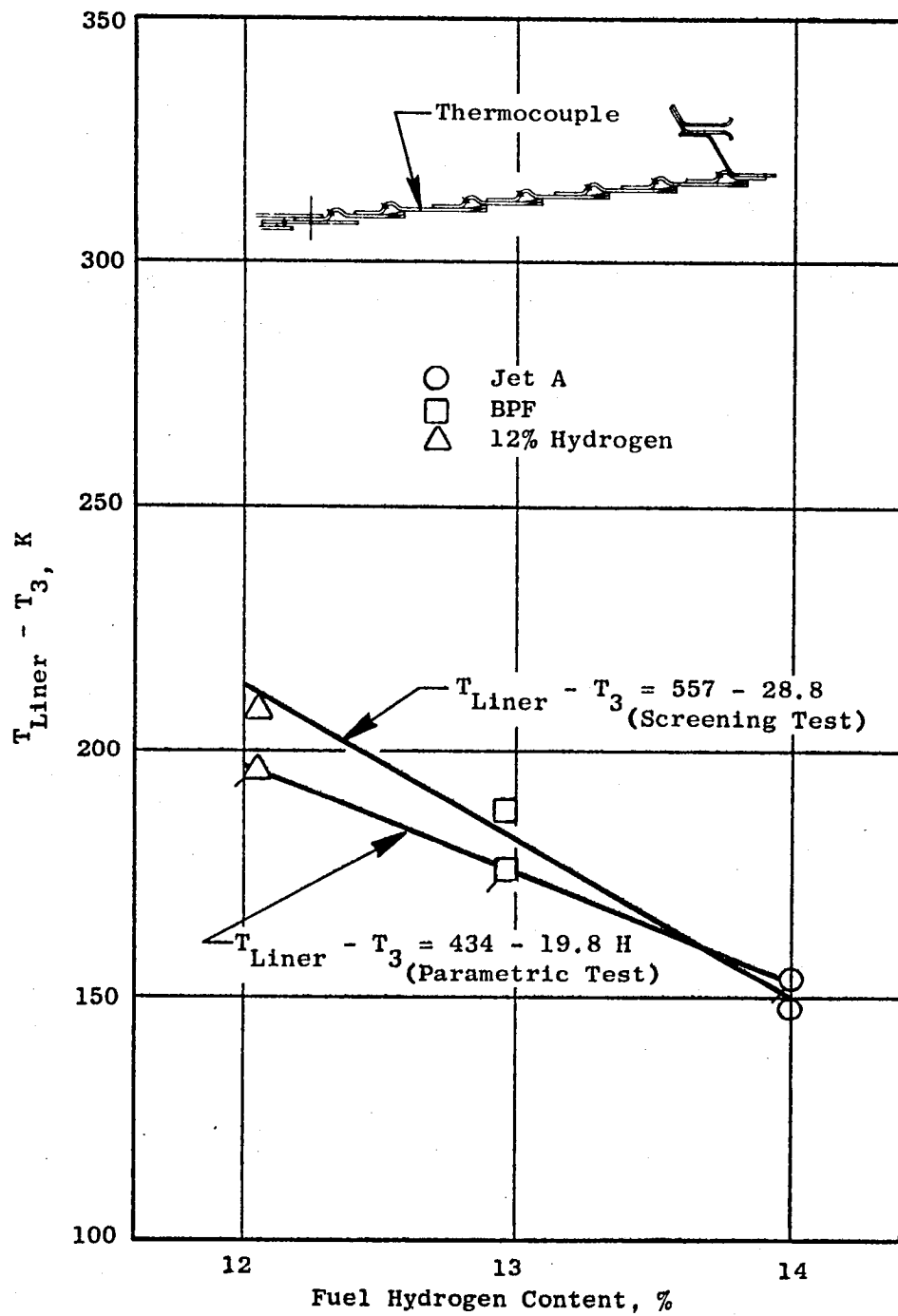
Figure 107. Comparison of Outer Liner Temperatures for Parametric and Screening Tests at Cruise Conditions, f = 0.016.

location, in the hot streak, for both tests. It is seen that the parametric-test liner temperatures were slightly lower. The liner-temperature distribution is shown in Figure 108. This figure is similar to Figure 79 where Concept 2 burner temperatures recorded during the screening test were presented. The maximum temperatures were measured on the same inner panel for both tests. These data indicate that some cooling air should be shifted from the cooler panel to the fourth panel on the inner liner.

The premix-tube thermocouples read approximately 30 to 50 K above T_3 during the test. Whether this was due to radiation from the primary zone or localized autoignition could not be determined.

The variation of maximum, inner-liner temperature (along the centerline) with reference velocity is shown in Figure 109. The location of maximum temperature along the centerline remains unchanged as reference velocity varies, as shown in Figure 110. This figure also shows that all temperatures along the inner-liner centerline decrease with reference velocity. Outer-liner temperatures decreased in a similar manner; the very low dome temperatures remained virtually unchanged.

A posttest inspection of the parametric-test burner revealed that it was in good mechanical condition. Elimination of the thimble protrusion and Nichrome patches relieved the liner burning problem that occurred during the screening tests. A redistribution of the cooling air would significantly improve the liner temperature levels. As shown in Figures 111, 112, and 113, there was only a light soot deposit on the liners, and the dome was very clean as in the screening test. Figure 114 shows the soot-like buildup on the faces of the fuel nozzles. Figure 115 shows the fuel nozzles and carbon deposits from the downstream side of the premix-tube primary swirlers. These deposits formed in the bluff region around the fuel-nozzle air shroud. These regions could be smoothed aerodynamically, so that only a minimum of carbon would be formed, on future test combustors. There were no signs of the high temperatures, on the fuel nozzle or swirlers, that occurred during the screening of this combustor. Apparently the burning that occurred during the screening test was a marginal condition and can be precluded by eliminating the bluff region.

The variation of smoke number with fuel/air ratio for the parametric test is shown in Figures 116 and 117. These data illustrate the trends with fuel/air ratio and fuel type. The smoke data are correlated with fuel hydrogen content in Figures 118 and 119. These data are in general agreement with data from the previous test.

The variation of smoke number with reference velocity is shown in Figure 120. The decrease in smoke number with reference velocity may be due to more intense mixing generated by the increased pressure drop. Decreasing smoke number indicates decreasing flame luminosity and, hence, lower radiant-heating load on the liners and lower metal temperatures. Thus the decrease in liner temperature with increasing reference velocity, illustrated in Figure 110, is
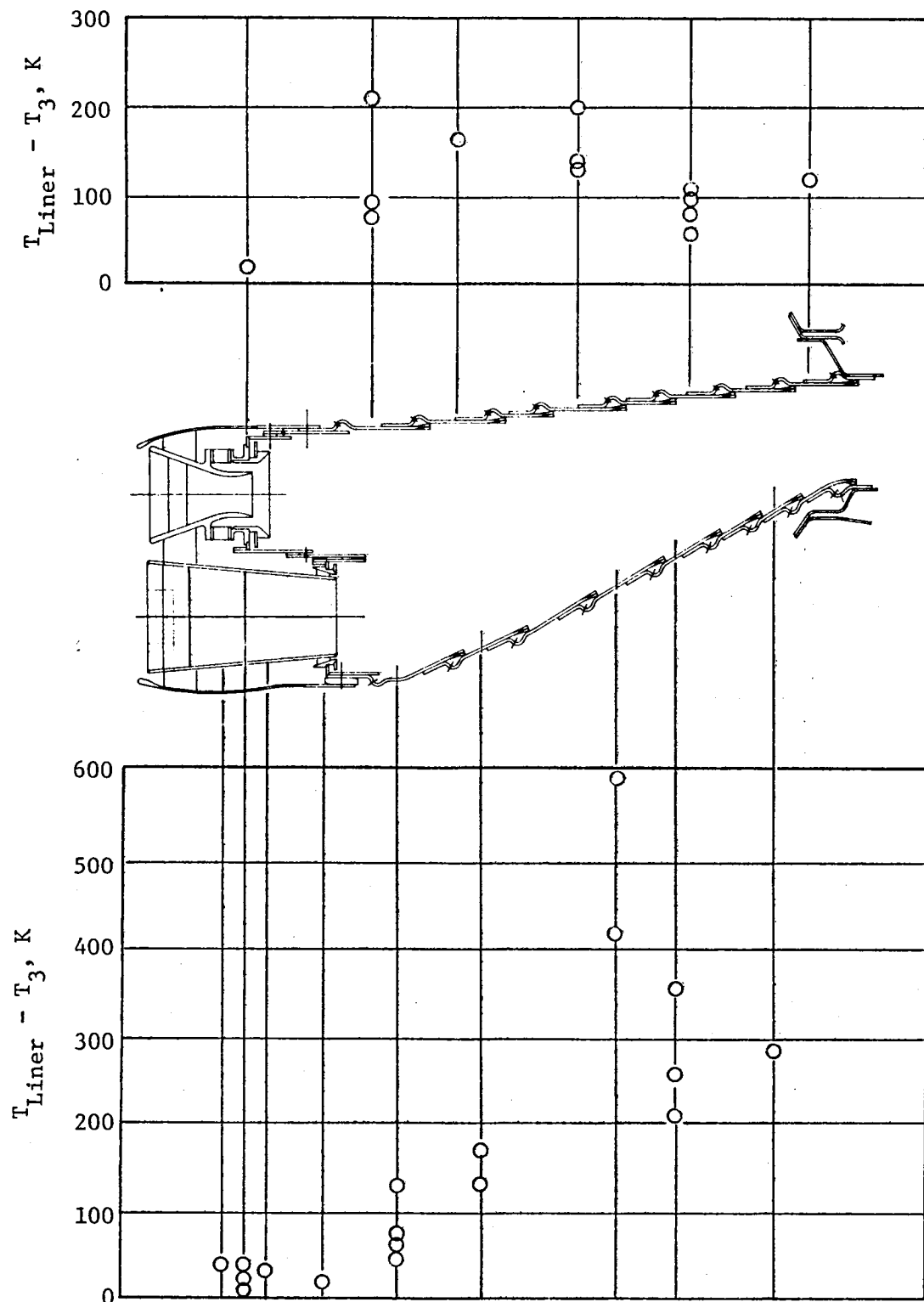
Figure 108. Liner Temperature Distribution for Parametric
Test at Cruise Conditions, f = 0.016.
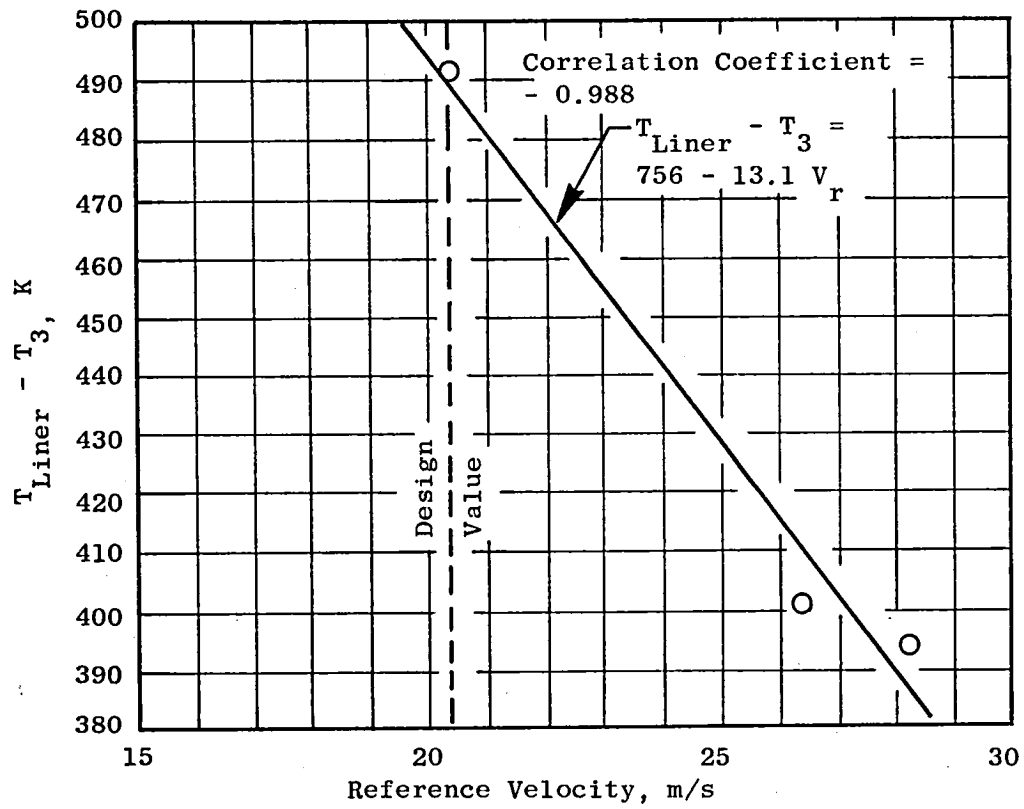
Figure 109.   Variation of Liner Temperature with Reference
Velocity in the Parametric Test at Simulated
Takeoff Conditions, f = 0.017, 12%
Hydrogen Fuel.
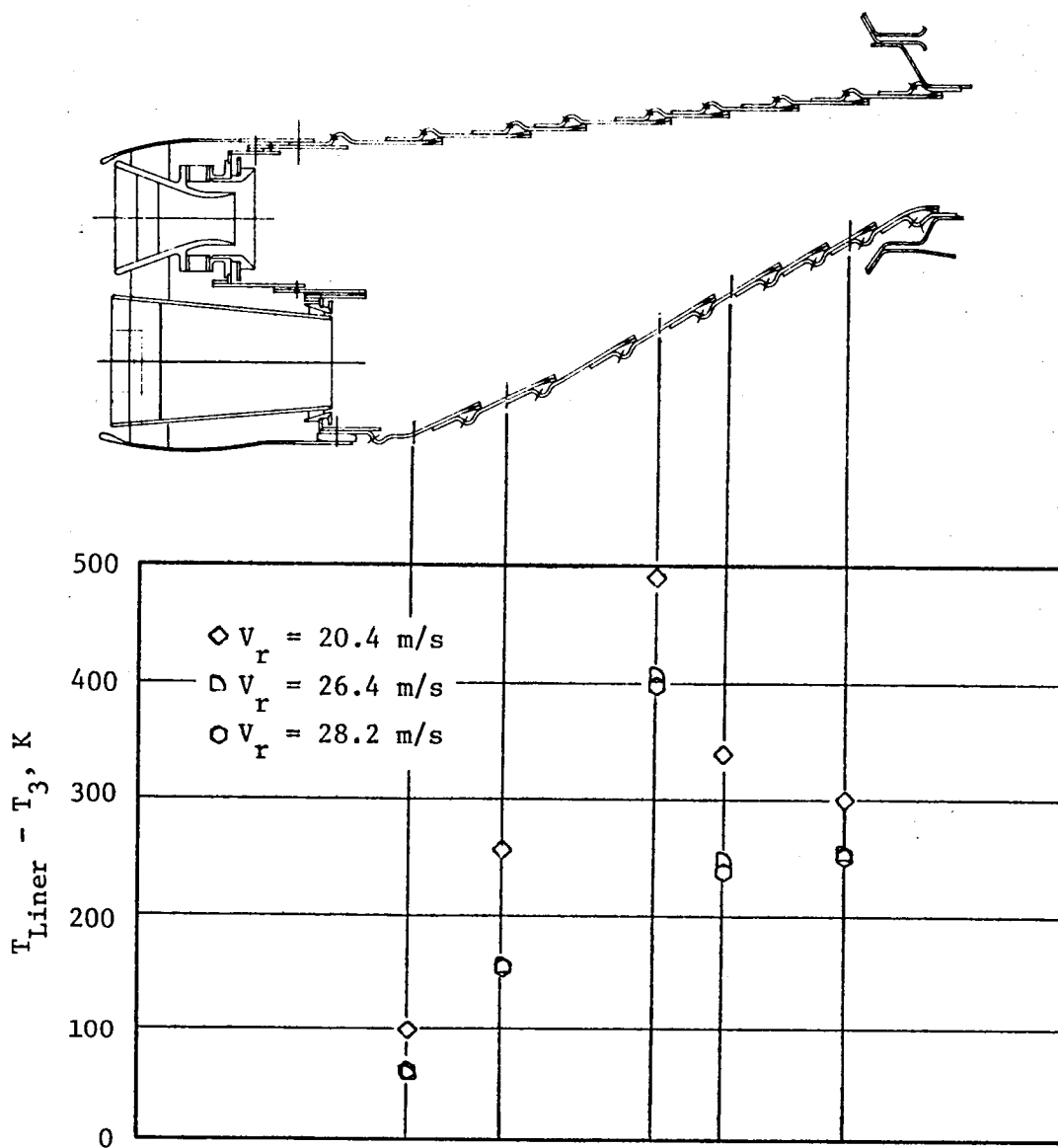
Figure 110. Parametric-Test Liner Temperature Distribution Variation with Reference Velocity.
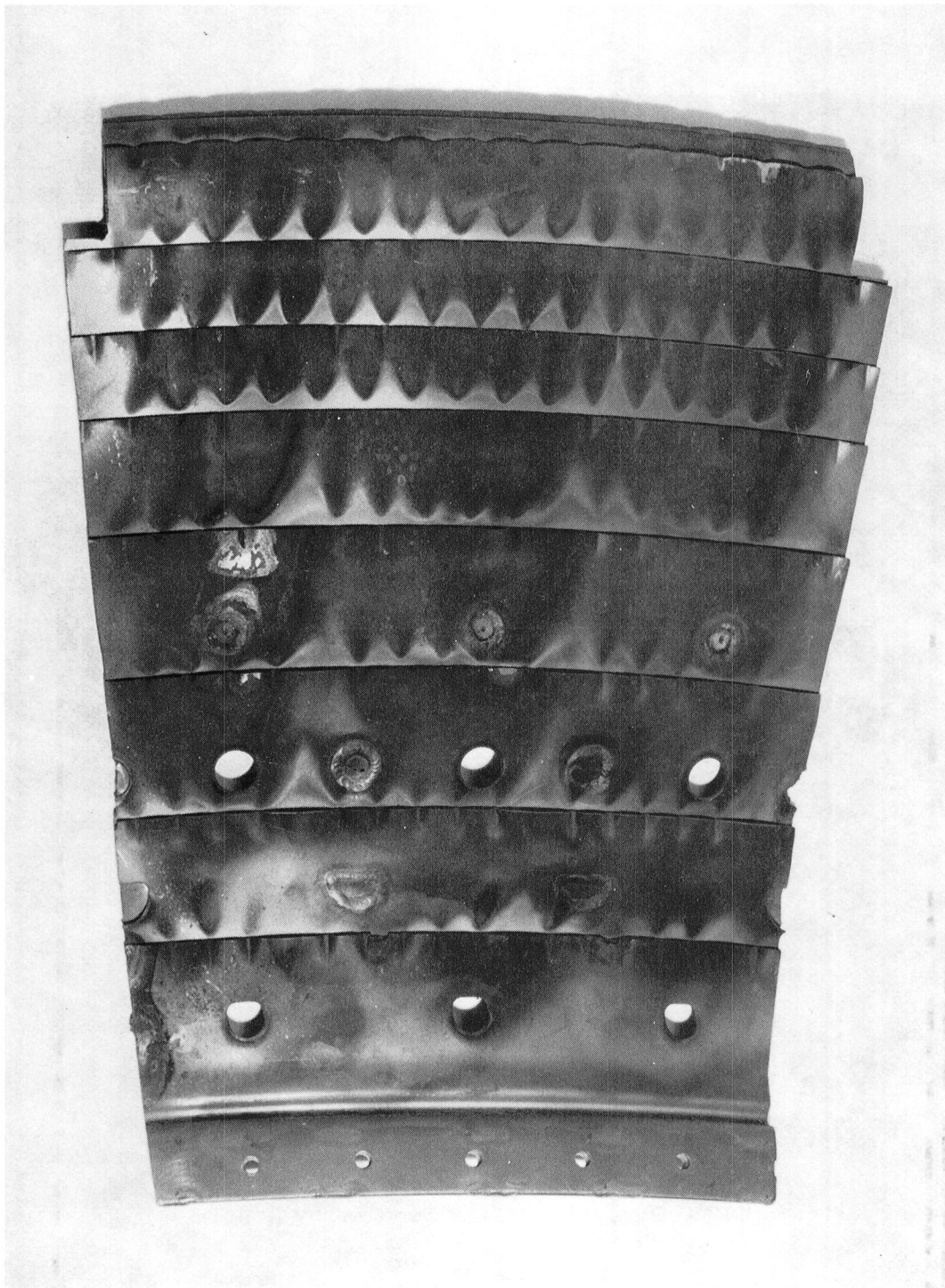
Figure 111.   Parametric-Test Inner Liner After Test.

Figure 112.   Parametric-Test Dome After Test.

Figure 113. Parametric-Test Outer Liner After Test.
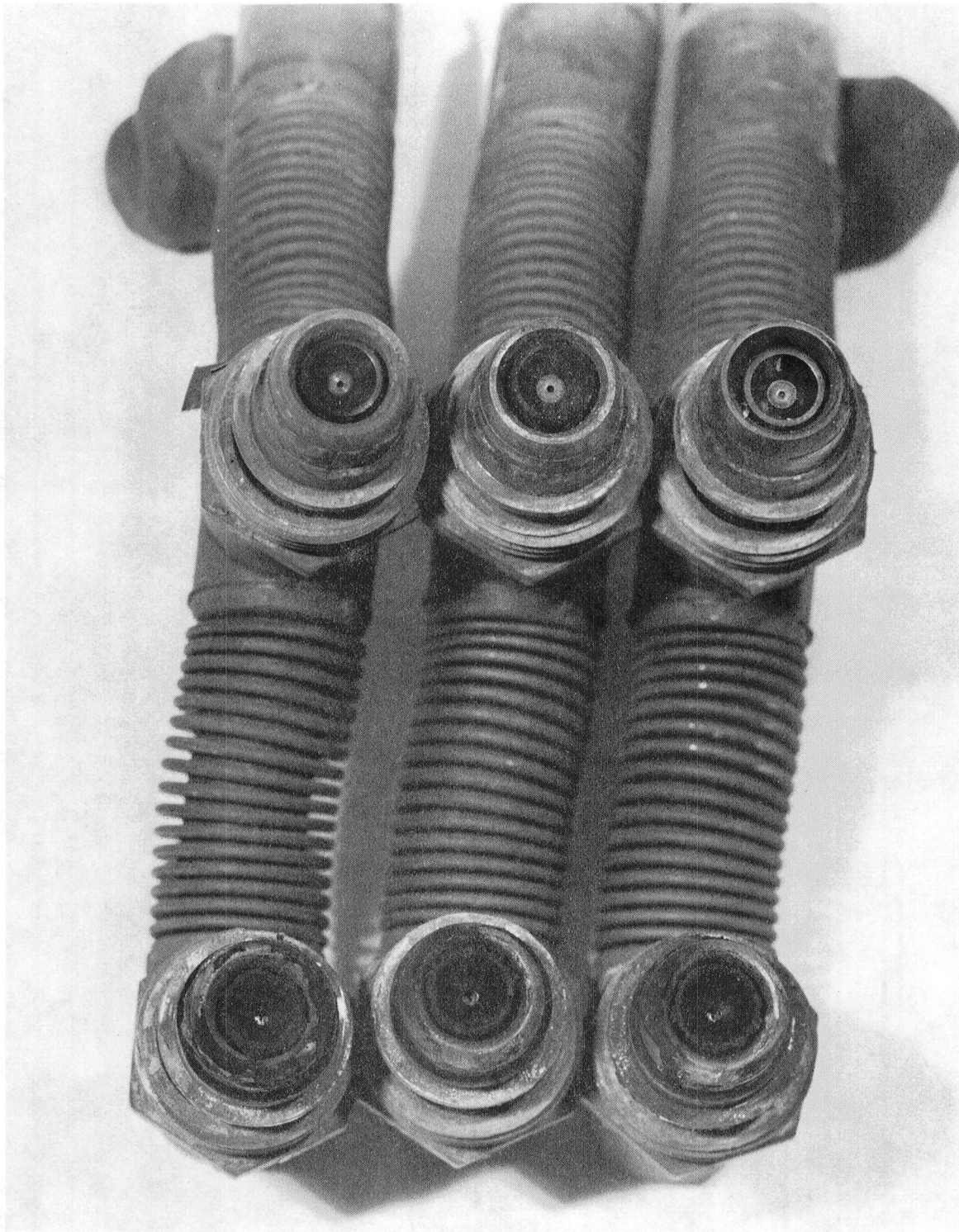
Figure 114. Parametric-Test Fuel Nozzles After Test.
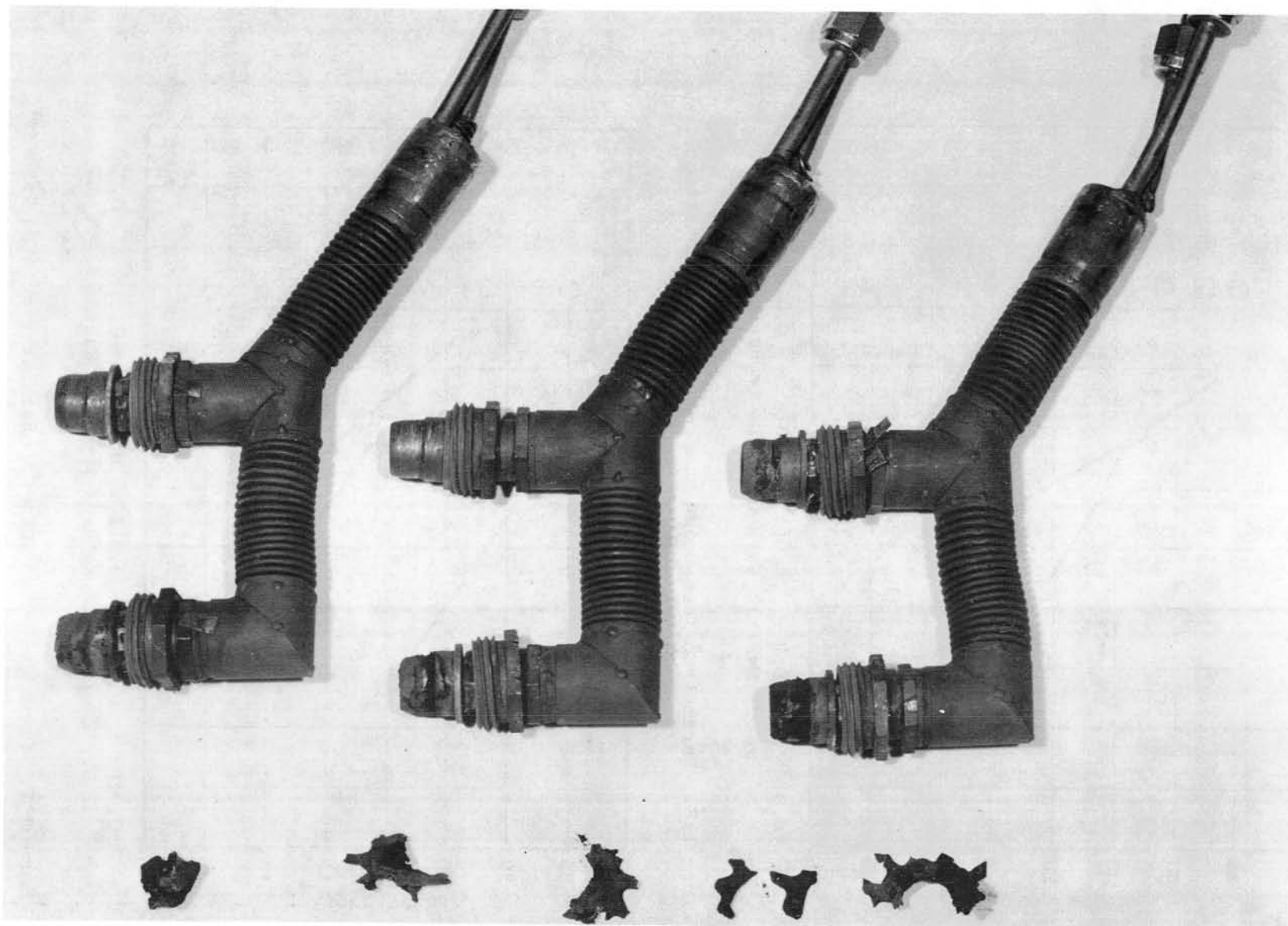
Figure 115. Parametric-Test Fuel Nozzles and Carbon Buildup from Bluff Region Between Main-Stage Swirlers and Fuel Nozzles.
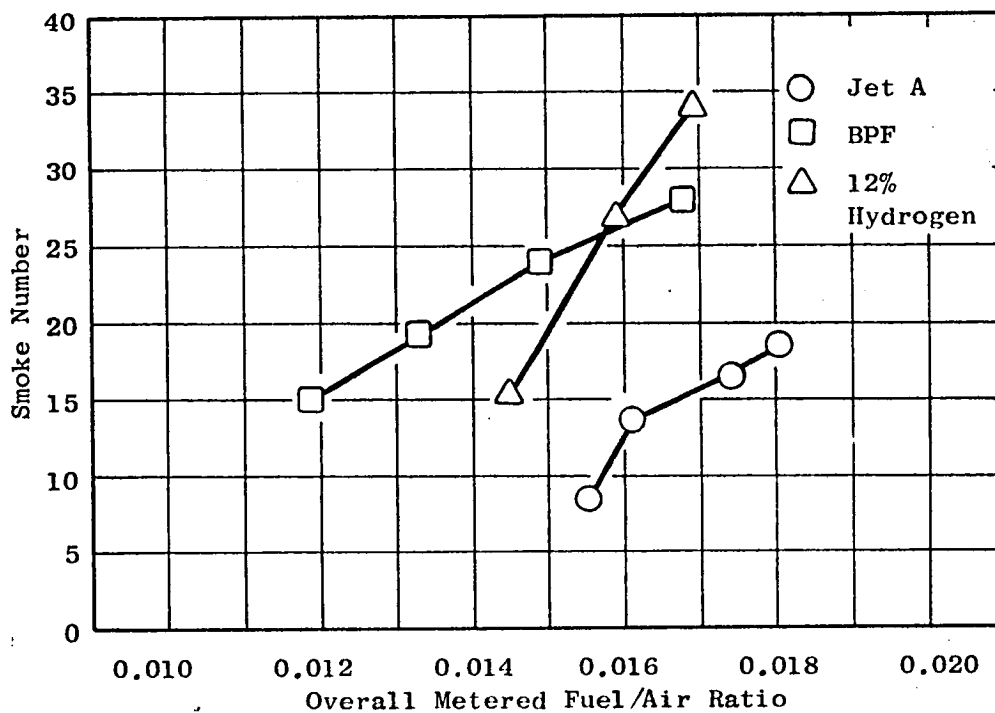
Figure 116. Parametric-Test Smoke Numbers at Cruise Conditions.
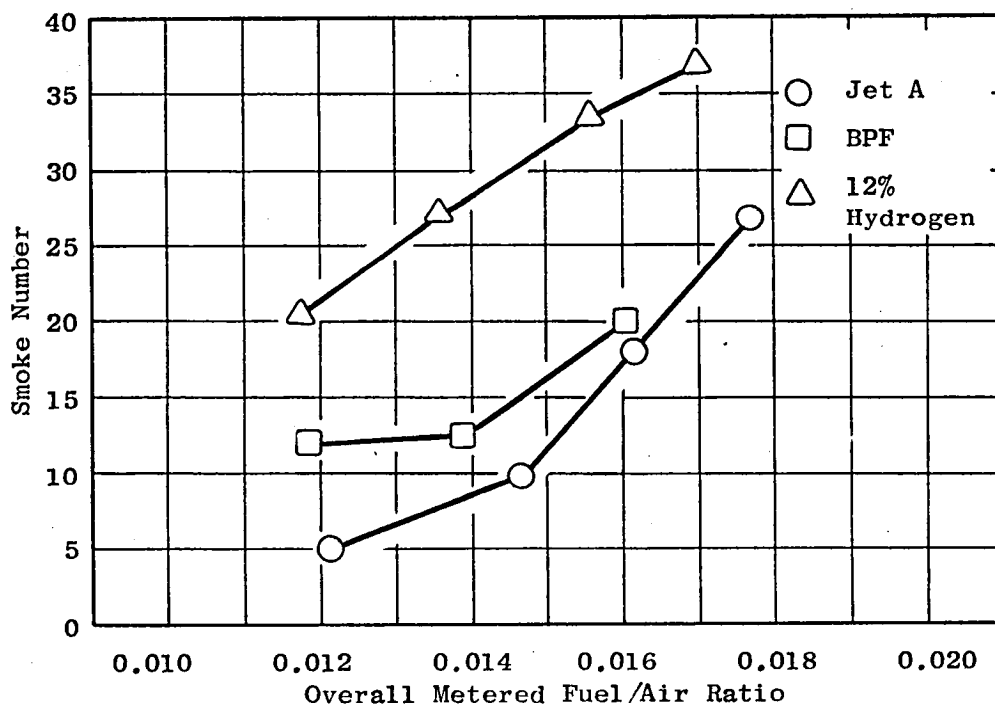
Figure 117. Parametric-Test Smoke Numbers at Simulated Takeoff
Conditions.

126
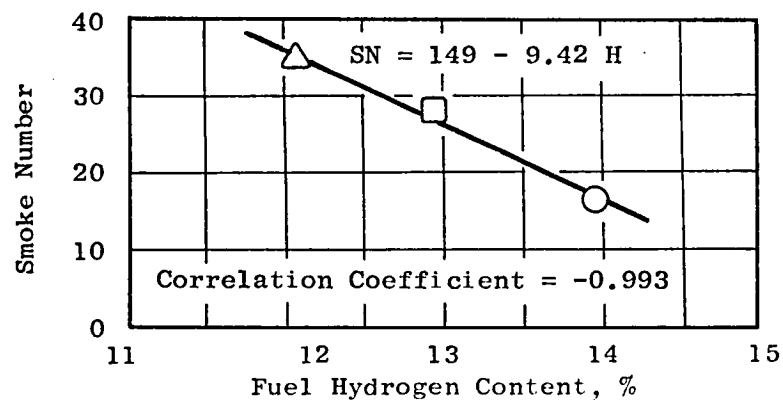
Figure 118. Variation of Parametric-Test Smoke
Number with Fuel Hydrogen Content at
Cruise Conditions, f = 0.017.
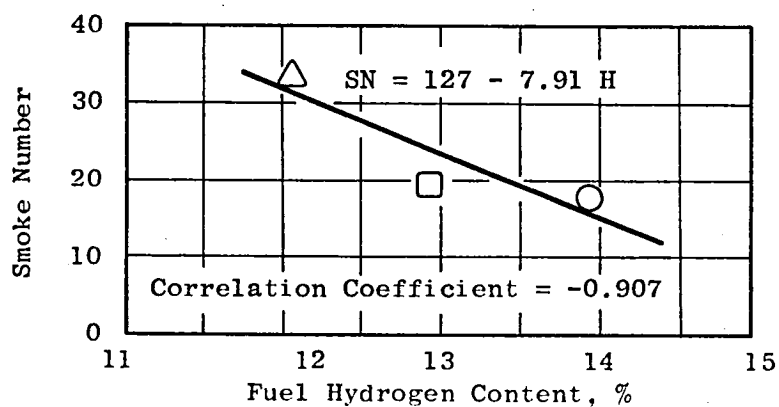
Figure 119. Variation of Parametric-Test Smoke
Number with Fuel Hydrogen Content at
Simulated Takeoff Conditions, f = 0.016.

related to the decreasing smoke number. This effect is particularly notice-able when the burner is operated on the 12% hydrogen fuel blend; that blend produced the highest smoke numbers of the three fuels tested. The insensi-tivity of smoke number to pilot/total fuel-flow ratio is shown in Figure 121.

The variation of NO_x emission index with fuel/air ratio for the three tests fuels is shown in Figures 122 and 123. Correlations with fuel hydrogen content are shown in Figures 124 and 125. The parametric test confirms that, of the burners tested, the premixing-prevaporizing design yielded the lowest levels of NO_x and the least NO_x sensitivity to fuel hydrogen content.

The variation of NO_x emission index with pilot/total fuel-flow ratio at a constant reference velocity is shown in Figure 126. This figure shows little variation in NO_x emission index below a fuel-flow ratio of 20%, but above this value the emission index increases as the pilot fuel flow is in-creased. For this combustor the design fuel-flow split is 20% pilot/total.

Figure 127 shows the decrease in NO_x emission index as reference veloc-ity increases at a constant fuel-flow ratio of 20% and fuel/air ratio of 0.017. The correlation of NO_x emission index with reference velocity confirms that NO_x decreases linearly as reference velocity increases over the range of reference velocities tested. This indicates that some modest improvement could be achieved by decreasing the residence time (increasing reference velocity).

Figures 128 and 129 show the variation of CO emission index with fuel/air ratio for the three tests fuels in the parametric test. The trends of decreasing CO with increasing fuel/air ratio are as expected for this lean-dome design. The cruise values for CO emission index are very close to those values obtained in the Concept 2 screening test and show little sensi-tivity to fuel hydrogen content. The takeoff values are lower than the cruise values, as expected, and some sensitivity to fuel properties is shown at low fuel/air ratios.

The variation of CO emission index with pilot/total fuel-flow ratio is shown in Figure 130. Comparison of this figure with the NO_x emission index variation, Figure 126, shows that the design fuel-flow ratio of 20% was the optimum for achieving minimum CO and NO_x emissions.

Figure 131 shows the increase in CO emission index with reference veloc-ity. The correlation between CO emission index and reference velocity con-firms the assumed linear relationship over the range of reference velocities tested. This assumption was made in correcting the data to a uniform set of operating conditions.

128
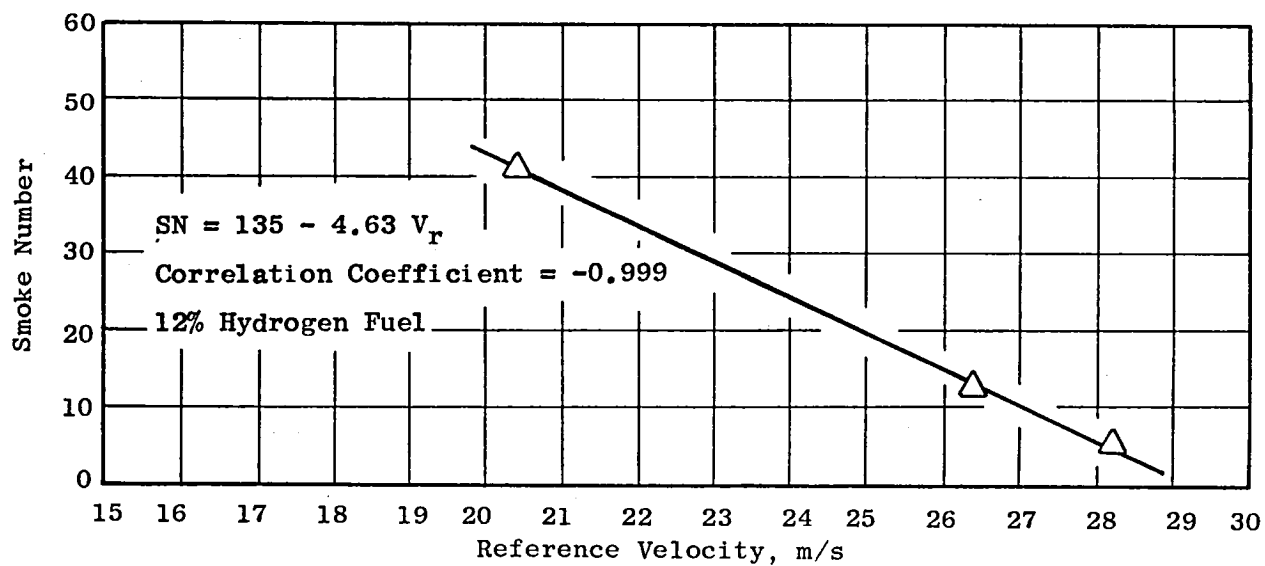
Figure 120. Variation of Parametric-Test Smoke Number with Reference Velocity at Simulated Takeoff Conditions, f = 0.017.
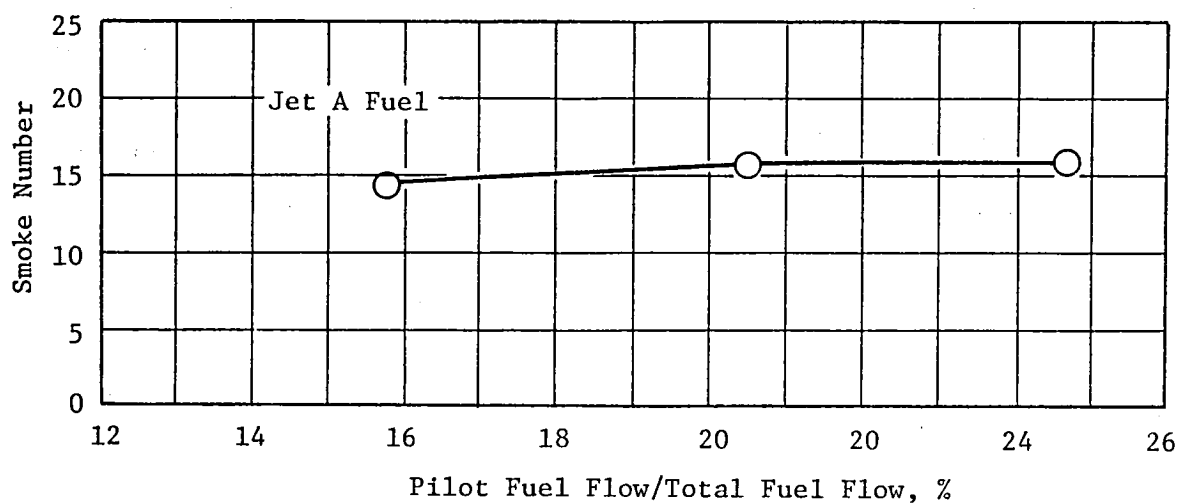
Figure 121. Variation of Parametric-Test Smoke Number with Pilot/Total Fuel-Flow Ratio at Cruise Conditions, f = 0.016.
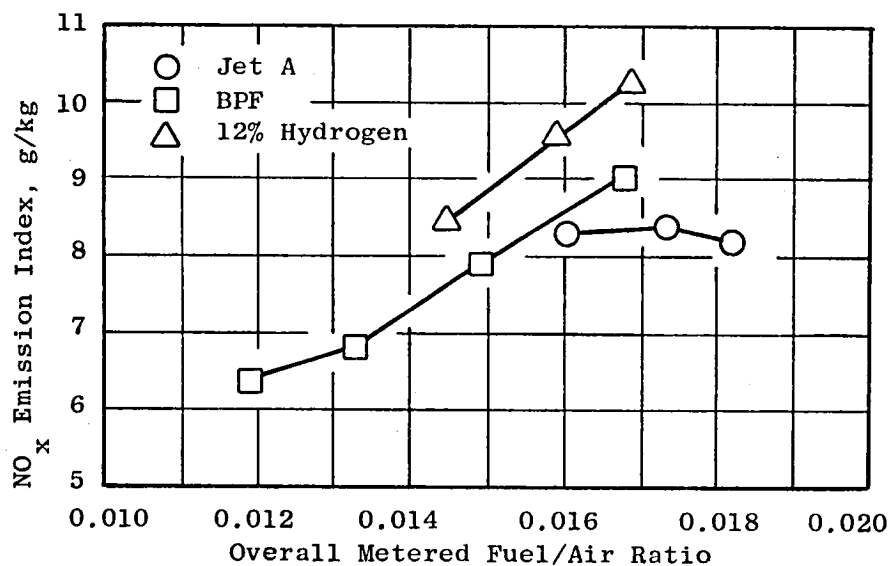
Figure 122. Parametric-Test NO_x Emission Index at Cruise Conditions.
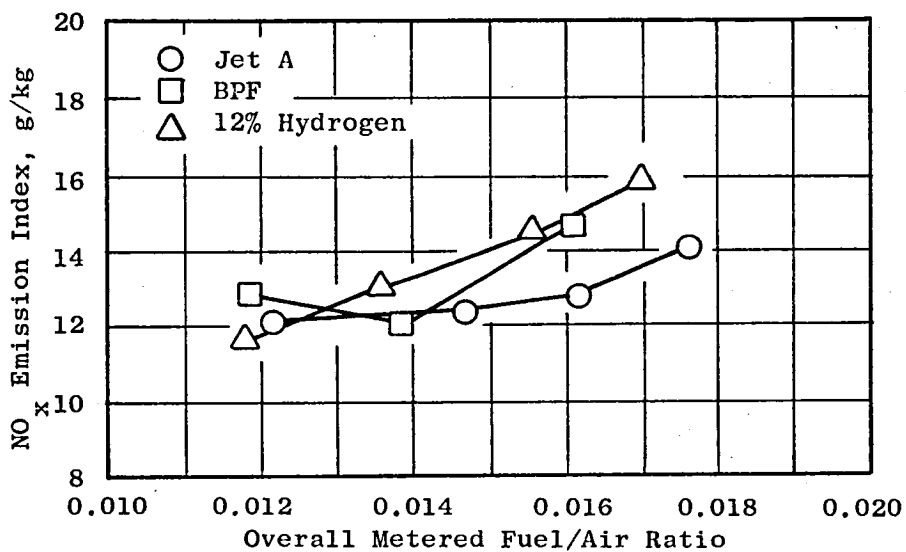
Figure 123. Parametric-Test NO_x Emission Index at Simulated Takeoff Conditions.
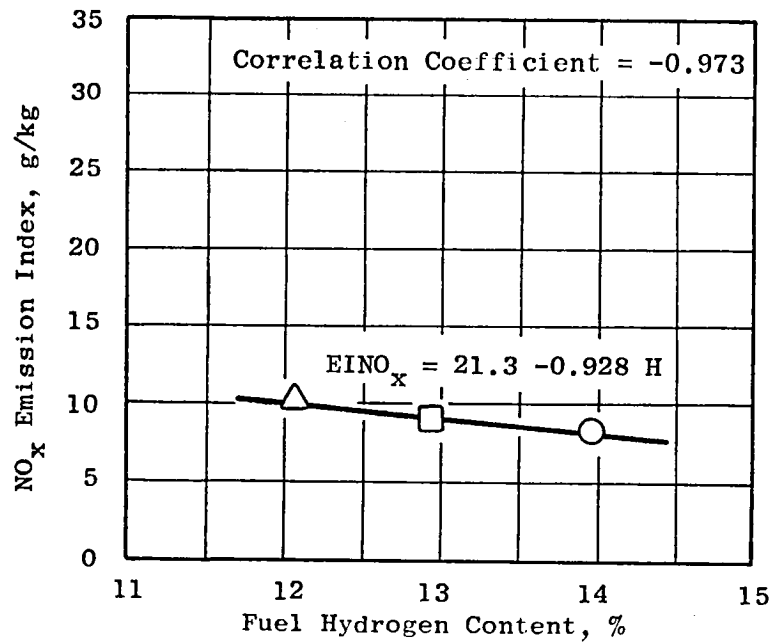
Figure 124. Variation of Parametric-Test NO_x Emission Index with Fuel Hydrogen Content at Cruise Conditions; f = 0.017.
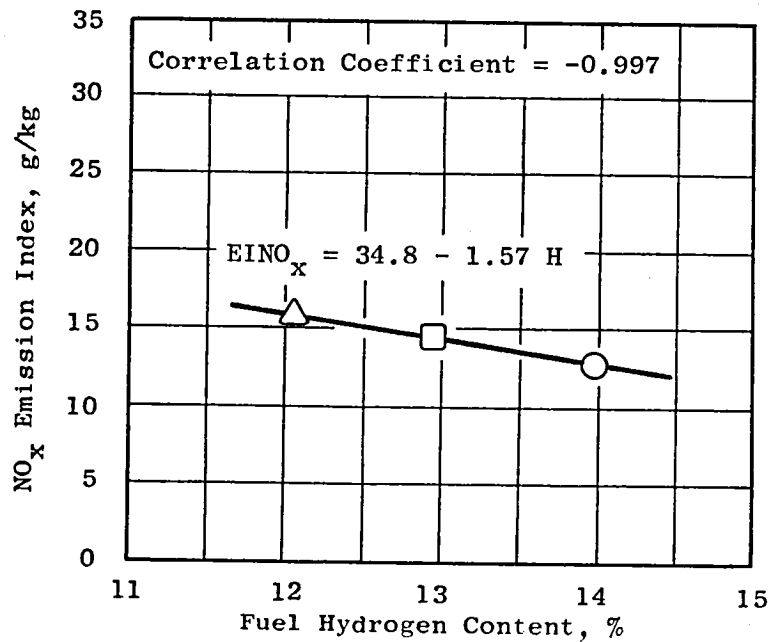
Figure 125. Variation of Parametric-Test NO_x Emission Index with Fuel Hydrogen Content at Simulated Takeoff Conditions, f = 0.016.
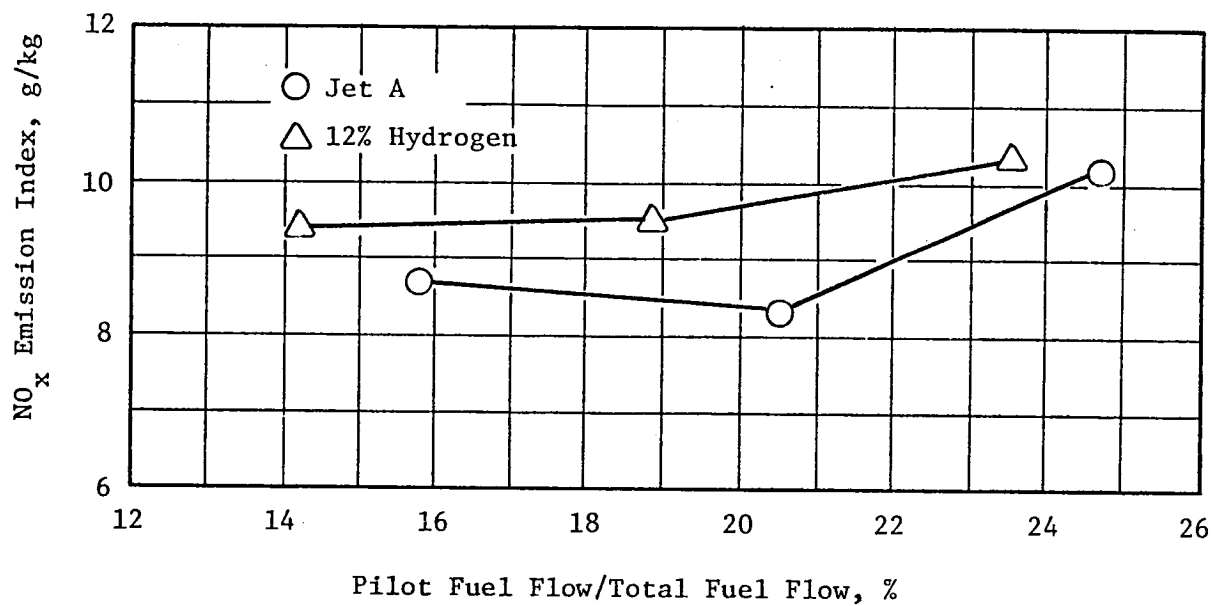
Figure 126. Variation of Parametric-Test NO_x Emission Index with Pilot/Total Fuel-Flow Ratio.
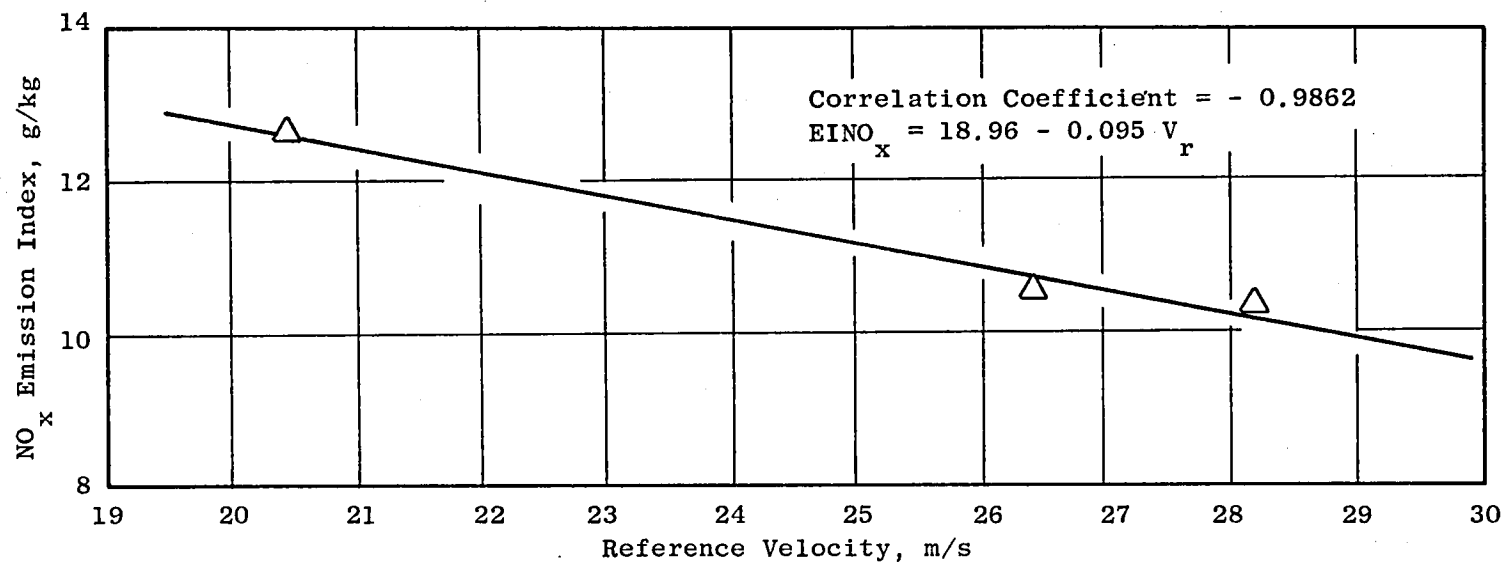
Figure 127. Variation of Parametric-Test NO_x Emission Index with Reference Velocity at Cruise Conditions, 12% Hydrogen Fuel.
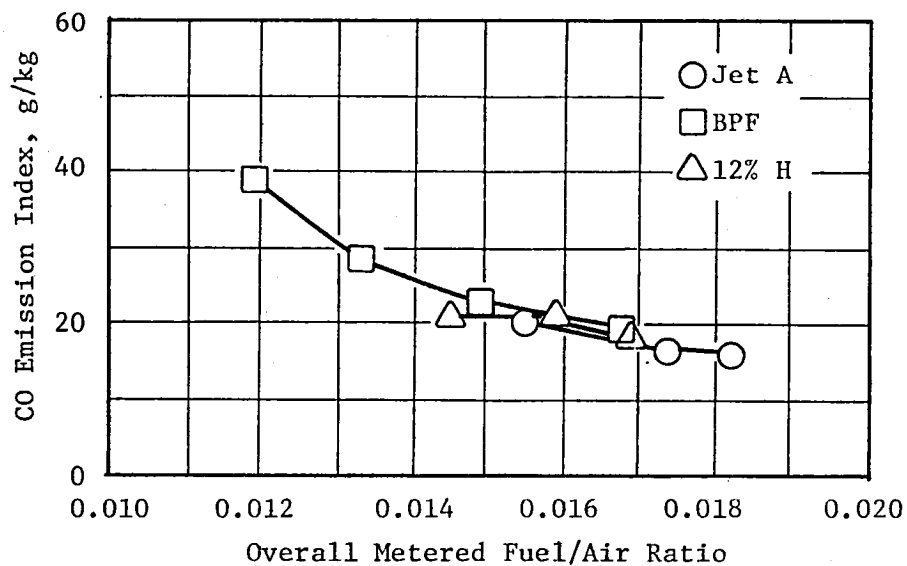
Figure 128. Parametric-Test CO Emission Index at Cruise.
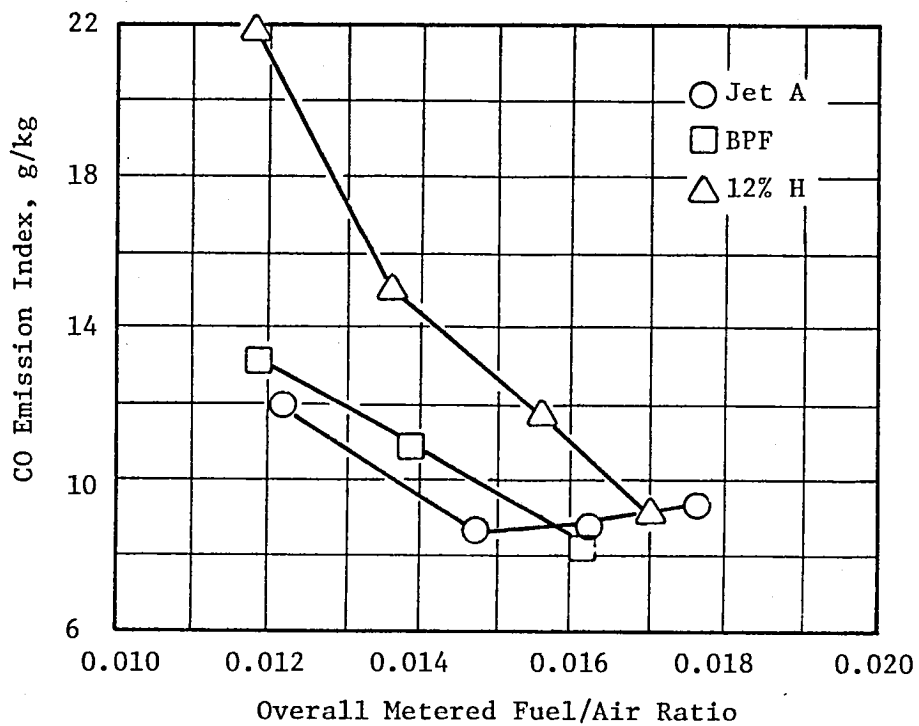
Figure 129. Parametric-Test CO Emission Index at
Simulated Takeoff.
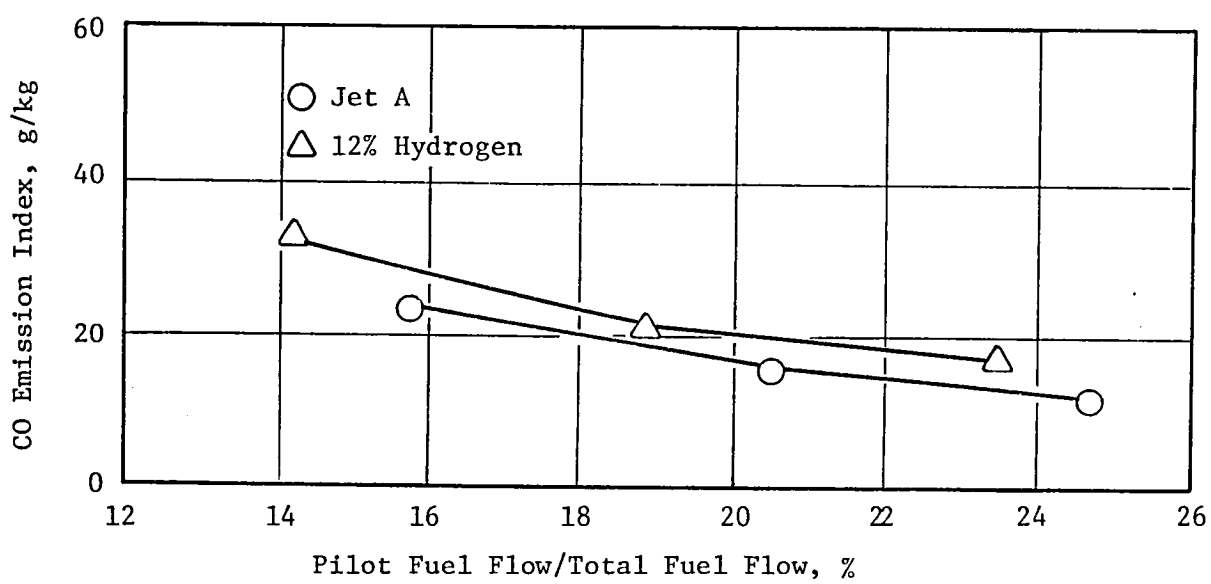
Figure 130. Variation of Parametric-Test CO Emission Index with
Pilot/Total Fuel-Flow Ratio.

CO Emission Index, g/kg (y-axis)

Correlation Coefficient = + 0.9529

EICO = 3.996 + 0.1573 V_r

Reference Velocity, m/s (x-axis)
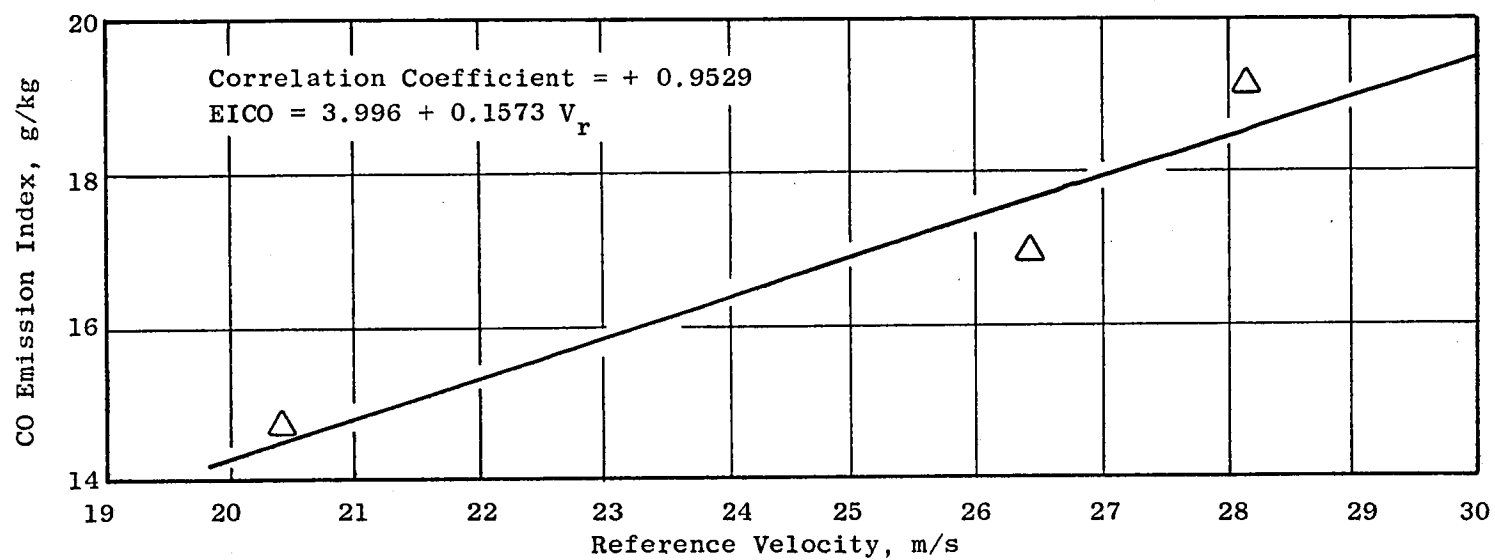
Figure 131. Variation of Parametric-Test CO Emission Index with Reference Velocity.

7.0 CONCLUDING REMARKS

Four combustor designs were tested with three types of fuel in this program. Data accumulated during this testing indicate that the variation in combustor dome design has a more significant effect on smoke and NO_x exhaust emissions than does the hydrogen content of the fuel. Dome design also has a strong effect on carboning tendencies, metal temperatures, and the sensitivity of metal temperatures to fuel hydrogen content.

The baseline CF6-50 burner test showed that smoke and CO levels for sector tests would be somewhat higher than for full-annular tests because of leakage in the rig; however, trends with operating conditions were as expected. Other test data, such as metal temperatures and NO_x levels, would not be affected. The baseline burner showed some sensitivity to fuel hydrogen content with regard to smoke, NO_x emission, and liner temperatures.

The Concept 1 burner produced low smoke levels and showed little sensitivity to fuel hydrogen content with regard to smoke levels and metal temperatures. NO_x levels were lower than CF6-50 levels but higher than Concept 2 levels. NO_x levels for this design were higher than expected based on previous tests of similar designs in the ECCP. It is suspected that these results were partially due to minor hardware problems adversely affecting combustor airflow distribution.

The Concept 2 burner had the lowest NO_x levels, a very clean dome with virtually no carbon deposits, lower smoke levels than the baseline combustor, low dome temperatures, and no combustion instability at any operating condition. Liner temperatures were low except for a region on the inner liner downstream of the premixing tubes. This liner-temperature problem would be relatively easy to remedy by the use of hole-pattern adjustments and cooling-air redistribution. Therefore, these high temperatures were not considered a major problem.

The Concept 3 burner produced the lowest smoke levels and demonstrated that the radial temperature profile could be inverted by reversing the pilot- and main-stage domes in a double-annular combustor. The NO_x levels were between those measured for the other two advanced concepts. However, this combustor encountered combustion resonance and dome flame-instability problems at some operating conditions. It is believed that, during a portion of the test, the flame was not seated in the pilot dome, as evidenced by very low metal temperatures. It is also believed that a complete set of representative data was obtained for Jet A fuel.

Concept 2 demonstrated the potential of a premixing-prevaporizing design in achieving low NO_x levels and clean liners and domes. The Concept 1 test showed that high ΔP fuel nozzles give no significant improvement over the conventional fuel nozzles tested earlier in similar combustor designs. Because of combustion-instability and resonance problems, data from the Concept 3

test were considered to be nonrepresentative of the potential of the concept. Therefore, Concept 2 was chosen for additional testing. Although no refinement or development tests to resolve problems were conducted on these advanced designs, they all appear to have potential for use with fuels with broadened specifications.

Liner temperatures tended to exhibit reduced sensitivity to fuel hydrogen content for the advanced designs. Figure 132 shows trends of liner temperature as a function of fuel hydrogen content relative to temperatures measured using Jet A fuel. As shown, the lowest temperatures were not obtained with the premixing system (Concept 2). Previous experience with double-annular combustors, including a premixing system (NASA/GE ECCP), would lead one to expect less sensitivity for a premixing system than for a double-annular combustor. It is theorized, therefore, that the fuel/air mixture at the premixing-tube exit was not as uniform as possible and that this lack of uniformity influenced the liner temperature results.

Carbon deposits in the dome regions were also significantly reduced with the advanced dome concepts. A posttest inspection of the baseline combustor revealed a light coating of soot on a large portion of the dome surface and some buildup on the trailing edges of the swirl-cup venturi. All three of the advanced designs had relatively little carbon on the pilot-dome surfaces. Concepts 1 and 3 had some carbon on the main-stage-dome surfaces, but Concept 2, with the premixed main stage, had virtually no carbon on the dome. It should be noted that all of the advanced designs used prototype fuel nozzles that had a bluff region between the fuel nozzle and the swirl cup. These bluff regions, which had carbon deposits, would be eliminated in product-engine designs.

Smoke data exhibited the expected trend toward generally increased smoke with reduced hydrogen content. Concept 2, with the premixing dome, had higher smoke levels than the other two advanced designs. This finding is also believed to be the result of less-than-uniform fuel/air mixtures at the exit of the premixing duct. Concept 3 had the lowest smoke levels measured; Concept 1 also had low smoke levels and showed the least sensitivity to fuel type. Figure 133 presents some of the smoke-data correlations for the four combustor configurations at simulated takeoff conditions.

Only general trends for radial, exit-temperature profiles are obtainable in sector combustor tests. However, it appears that Concept 3, with the inverted sequence of main to pilot stage, shifted the profile in the desired direction. For Concept 1, with the main stage on the inboard side, the profile was peaked at approximately 30% of the radial exit height (peaked inboard). For Concept 3, with the main stage on the outboard side, the profile was peaked at approximately 60% of the exit height; this is the same exit height as for the baseline combustor.

All of the advanced designs appear to have the potential for low NO_x levels. The increased-ΔP nozzles used in Concept 1 did not provide reduced NO_x relative to earlier full-annular tests of double-annular combustors

—Thermocouple
on Centerline
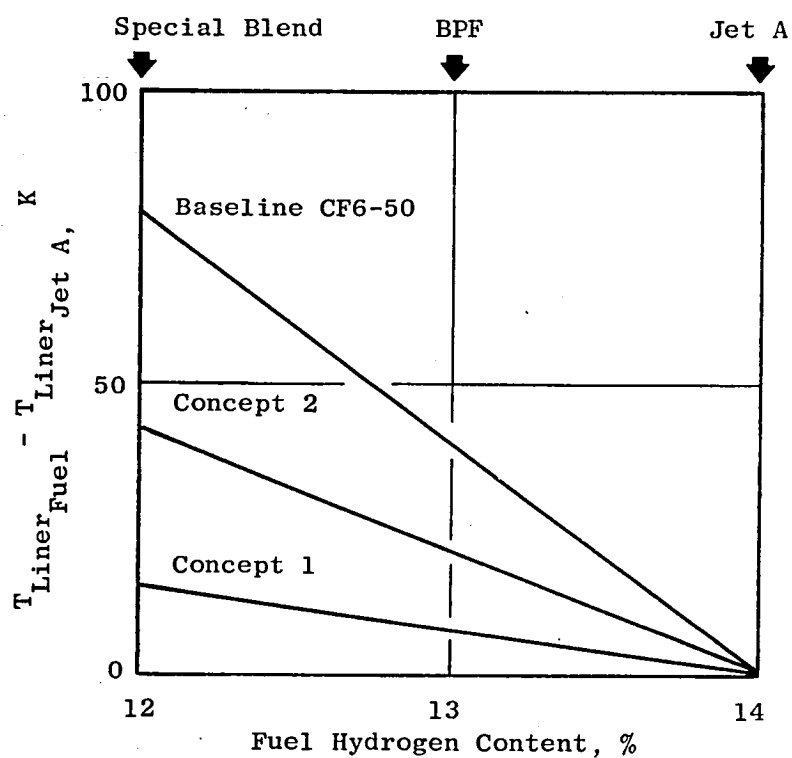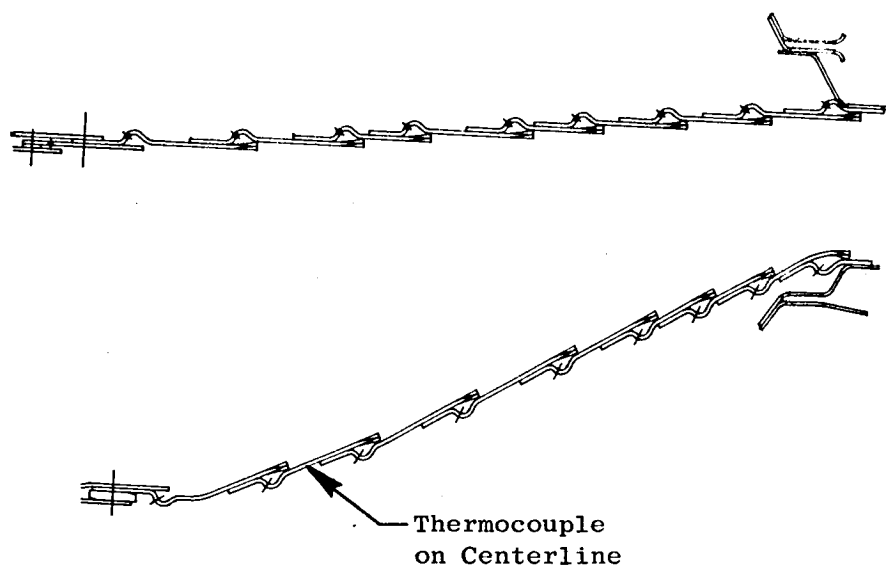
Figure 132. Variation of Local Liner Temperature
with Fuel Hydrogen Content at Cruise
Conditions, f = 0.021.

(NASA/GE ECCP). Concept 3 provided slightly lower NO_x levels than Concept 1, apparently due to reduced main-stage residence time. Concept 2, the premixing main-stage design, had the lowest NO_x levels and the least NO_x sensitivity to fuel hydrogen content, as shown in Figure 134.

The Concept 2 burner (premixing main stage) was selected for the parametric test because of low NO_x emissions levels, carbon-free dome, and very low dome temperatures that were essentially independent of fuel type. The effects of reference-velocity variation and pilot/main fuel-flow ratio on the Concept 2 burner liner temperatures and emissions were investigated in the parametric test. Fuel-flow variations showed that the NO_x emission index increased and CO emission index decreased with increasing pilot/total fuel-flow ratio. The design fuel-flow split of 20% was shown to provide a good compromise for low CO and NO_x emissions. Varying the fuel-flow ratio had no definite effect on smoke numbers. Increasing reference velocity increased the CO emission index and decreased the NO_x emission index linearly over the ranges tested. Increasing the reference velocity increased the combustor pressure drop and decreased smoke numbers. Liner temperatures decreased with increasing reference velocity.

Although the advanced combustor concepts tested in this program do not represent developed combustors, the tests indicated that significant advancements in the ability to utilize fuels with broadened specifications can be achieved by applying the technology involved in these advanced combustors. Although some problems were encountered, they appear to be relatively minor and could be resolved with modest development effort. One area that requires additional development is the fuel/air uniformity in the premixing-tube/fuel-injection system. One design that appears promising based on these results would be Concept 3 with premixing tubes. This concept would provide the advantages of a premixed design (discussed above), an improved temperature-profile, and (probably) reduced cooling difficulties on the outer liner wall since the wall would not be required to turn the high-velocity, main-stage, hot-gas stream.
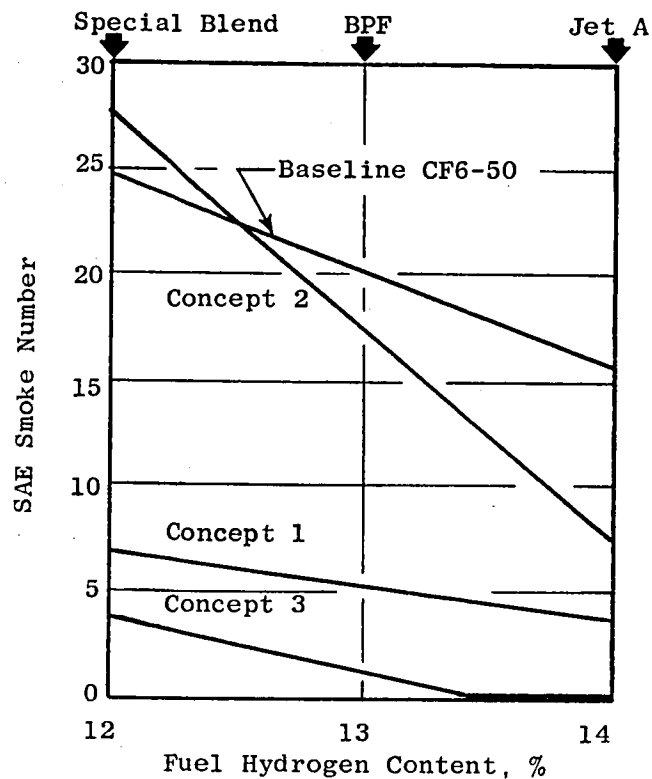
Figure 133. Variation of Smoke Number with Fuel Hydrogen Content at Simulated Takeoff Conditions.
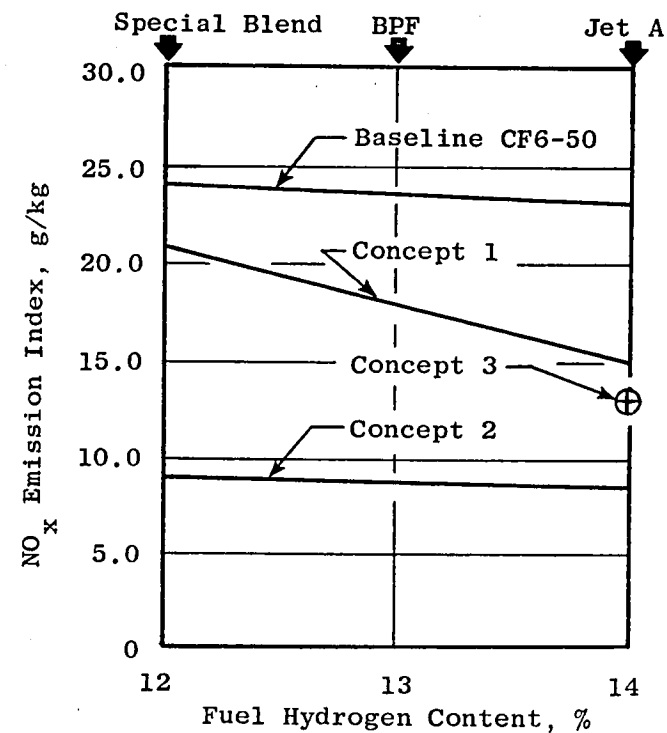
Figure 134. Variation of NO$_x$ Emission Index with Fuel Hydrogen Content at Cruise Conditions, f = 0.016.

APPENDIX A - COMBUSTOR TEST RESULTS SUMMARY

The following tabulations summarize the combustor data for the CF6-50 baseline configuration, the screening tests, and the parametric test. The following abbreviations are used in the fuel/operating condition entries:

Fuel

J   - Jet A (14% Hydrogen)

12H - Special Blend (12% Hydrogen)

B   - Broad Property (13% Hydrogen)

Test Condition

CR - Cruise

TO - Simulated Takeoff

144

CF6-50 Baseline Configuration

Reading/Test Point	1/10	2/20	3/30	5/40	6/50	8/60	11/70	12/70	13/80	14/40	15/90	16/100	17/110	18/120	19/130	20/140
Fuel/Operating Condition	J/CR	J/CR	J/CR	J/TO	J/TO	J/TO	J/TO	J/TO	J/TO	J/TO	12H/TO	12H/TO	12H/TO	12H/TO	12H/TO	B/TO
Inlet Total Pressure, kPa	1166.9	1168.0	1169.4	1585.1	1573.4	1610.6	1591.3	1588.6	1609.9	1604.4	1568.6	1572.0	1576.8	1568.6	1578.2	1578.2
Inlet Static Pressure, kPa	1090.1	1091.4	1095.6	1523.1	1498.2	1532.7	1517.5	1514.8	1537.5	1534.8	1494.7	1498.9	1501.0	1491.3	1505.8	1500.3
Inlet Total Temperature, K	721.9	726.8	729.8	811.1	822.0	822.9	822.7	823.8	824.3	824.0	823.8	824.2	824.3	824.0	822.8	820.4
Inlet Humidity, g H_2O/kg Air	3.8	3.8	3.5	2.4	2.5	2.1	2.1	2.1	2.1	2.1	2.1	2.1	2.1	2.1	2.1	2.0
Combustor Airflow, kg/s	4.997	4.982	4.934	4.962	5.369	5.450	5.440	5.490	5.411	5.335	5.354	5.360	5.341	5.365	5.343	5.555
Reference Velocity, m/s	24.0	24.0	23.9	19.7	21.9	21.6	21.8	21.9	21.6	21.2	21.8	21.8	21.6	21.8	21.6	22.3
Fuel Nozzle ΔP, Main, kPa																
Fuel Flow, Main, kg/s	0.0474	0.0605	0.0743	0.0776	0.0939	0.1119	0.1263	0.1212	0.1339	0.0759	0.0793	0.0950	0.1081	0.1236	0.1384	0.0799
Fuel Flow, Pilot, kg/s																
Metered Fuel/Air Ratio, Main	0.0095	0.0121	0.0151	0.0156	0.0175	0.0205	0.0232	0.0221	0.0247	0.0142	0.0148	0.0177	0.0202	0.0230	0.0259	0.0144
Metered Fuel/Air Ratio, Pilot																
Metered Fuel/Air Ratio, Overall	0.0095	0.0121	0.0151	0.0156	0.0175	0.0205	0.0232	0.0221	0.0247	0.0142	0.0148	0.0177	0.0202	0.0230	0.0259	0.0144
Inlet Fuel Temperature, K	299.7	299.7	298.5	297.5	297.2	297.0	297.0	297.5	297.5	297.7	298.2	298.7	297.7	297.7	298.0	297.0
Sample Fuel/Air Ratio	0.01064	0.01245	0.01483	0.01474	0.01625	0.01967	0.02090		0.02268	0.01274	0.01269	0.01508	0.01734	0.02072	0.02544	0.01408
Sample Combustion Efficiency, %	99.83	99.87	99.91	99.45	99.95	99.93	99.92		99.83	99.97	99.96	99.96	99.94	99.89	99.81	99.96
CO Emission Index, g/kg	5.4	4.1	3.1	1.0	1.3	2.1	3.3		2.2	1.0	1.2	1.5	2.2	4.4	7.6	1.2
CO_2 Emission, %	2.22	2.63	3.12	3.10	3.42	4.15	4.41		4.79	2.67	2.71	3.23	3.72	4.34	5.48	2.98
HC Emission Index, g/kg	0.4	0.4	0.2	0.2	0.2	0.2	0		0	0	0.1	0.1	0.1	0.1	0.1	0.1
NO_x Emission Index, g/kg	21.54	23.56	21.13	32.30	21.86	21.87	28.20		26.62	32.26	33.54	29.30	26.90	24.26	22.83	32.59
Smoke Number	18.4	19.8	40.7		13.6	24.6	38.8		47.9	43.4	21.5	29.4	26.3	36.8	37.4	25.2
Corrected EICO, g/kg	4.1	3.3	2.6		1.3	2.1	3.2		7.1	1.0	1.1	1.4	2.1	4.1	7.2	1.1
Corrected EIHC, g/kg	0.3	0.3	0.2		0.2	0.2	0		0	0	0.1	0.1	0.1	0.1	0.1	0.1
Corrected $EINO_x$, g/kg	26.3	28.1	24.7		22.0	22.1	29.0		26.7	32.0	34.5	30.1	27.4	25.0	23.3	34.9
Corrected Smoke Number	16.0	17.0	37.5		11.5	20.8	35.5		44.0	39.5	18.5	26.0	22.5	33.5	33.5	22.0
Maximum Liner Temperature, K	884.0	908.0	935.0	1078.0	1141.0	1204.0	1233.0	1238.0	1254.0	1093.0	1149.0	1183.0	1230.0	1265.0	1259.0	1124.0
Average Liner Temperature, K	779.0	791.0	806.0	924.0	946.0	972.0	986.0	993.0	1008.0	942.0	971.0	986.0	1002.0	1019.0	1030.0	943.0
Total Pressure Loss, %	5.23	5.44	5.46	4.02	4.06	4.18	4.22	4.54	4.44	3.95	4.22	4.52	4.73	4.89	4.71	4.56
Dome Pressure Loss, %	3.85	3.89	3.76	2.26	2.58	2.48	2.52	2.58	2.38	2.38	2.46	2.49	2.53	2.59	2.34	2.57

CF6-50 Baseline Configuration (Concluded)

Reading/Test Point	21/150	22/160	23/170	24/180	25/190	27/200	28/210	29/220	30/230	31/240	32/250	34/260	35/270	36/280	37/290	38/300
Fuel/Operating Condition	B/TO	B/TO	B/TO	B/TO	B/CR	B/CR	B/CR	B/CR	B/CR	J/CR	J/CR	12H/CR	12H/CR	12H/CR	12H/CR	12H/CR
Inlet Total Pressure, kPa	1572.7	1563.7	1575.5	1572.7	1180.4	1155.6	1148.0	1155.6	1145.9	1157.6	1154.2	1150.7	1149.4	1154.2	1148.7	1147.7
Inlet Static Pressure, kPa	1498.9	1488.6	1501.0	1501.0	1139.7	1100.4	1094.9	1101.1	1090.8	1103.9	1100.4	1097.0	1095.6	1099.7	1096.3	1093.5
Inlet Total Temperature, K	819.6	819.2	819.2	819.2	734.7	744.2	722.7	734.5	735.4	735.6	736.8	733.9	733.5	733.0	732.8	731.1
Inlet Humidity, g H_2O/kg Air	2.0	2.0	2.0	2.0	2.0	2.2	2.3	2.3	2.3	2.6	2.6	2.4	2.2	2.1	2.1	2.1
Combustor Airflow, kg/s	5.410	5.461	5.428	5.450	3.798	4.177	4.275	4.213	4.225	4.212	4.213	4.227	4.230	4.210	4.198	4.185
Reference Velocity, m/s	21.8	22.2	21.9	22.0	18.3	20.8	20.8	20.7	21.0	20.7	20.8	20.9	20.9	20.7	20.7	20.6
Fuel Nozzle ΔP, Main, kPa																
Fuel Flow, Main, kg/s	0.0938	0.1105	0.1284	0.1418	0.0511	0.0620	0.0744	0.0868	0.0977	0.0877	0.1002	0.0491	0.0632	0.0751	0.0878	0.0986
Fuel Flow, Pilot, kg/s																
Metered Fuel/Air Ratio, Main	0.0173	0.0202	0.0237	0.0260	0.0135	0.0148	0.0174	0.0206	0.0231	0.0208	0.0238	0.0116	0.0149	0.0178	0.0209	0.0236
Metered Fuel/Air Ratio, Pilot																
Metered Fuel/Air Ratio, Overall	0.0173	0.0202	0.0237	0.0260	0.0135	0.0148	0.0174	0.0206	0.0231	0.0208	0.0238	0.0116	0.0149	0.0178	0.0209	0.0236
Inlet Fuel Temperature, K	297.7	297.5	297.2	297.2	298.7	298.5	298.7	299.2	299.0	299.2	299.5	299.5	298.2	298.5	298.7	298.5
Sample Fuel/Air Ratio	0.01666	0.02084	0.02521	0.02766	0.01104	0.01278	0.01575	0.01849	0.02003	0.01854	0.02124	0.01020	0.01342	0.01622	0.01668	0.01804
Sample Combustion Efficiency, %	99.97	99.93	99.87	99.77	99.88	99.86	99.88	99.86	99.81	99.89	99.84	99.81	99.87	99.87	99.86	99.83
CO Emission Index, g/kg	1.0	2.7	5.1	9.5	3.7	4.2	3.8	4.9	6.9	3.9	6.1	6.0	4.0	3.9	4.6	5.7
CO_2 Emission, %	3.54	4.44	5.39	5.91	2.33	2.70	3.34	3.93	4.26	3.90	4.48	2.17	2.86	3.47	3.57	3.86
HC Emission Index, g/kg	0.1	0.1	0.1	0.1	0.4	0.4	0.3	0.2	0.2	0.2	0.2	0.5	0.3	0.3	0.3	0.4
NO_x Emission Index, g/kg	26.45	22.28	21.68	20.93	26.35	22.96	19.38	17.36	16.20	16.55	15.83	29.21	27.18	22.44	16.56	15.35
Smoke Number	30.2	32.3	46.6	35.0	14.6	21.0	17.2	179	23.0	24.2	19.5	10.4	18.4	18.5	20.5	24.3
Corrected EICO, g/kg	0.9	2.3	4.6	8.5	4.4	4.8	3.3	5.0	6.9	4.0	6.3	6.0	3.9	3.9	4.5	5.5
Corrected EIHC, g/kg	0.1	0.1	0.1	0.1	0.5	0.5	0.2	0.2	0.2	0.2	0.2	0.5	0.3	0.3	0.3	0.4
Corrected $EINO_x$, g/kg	27.9	23.9	22.9	22.2	22.9	21.9	20.7	17.3	16.3	16.4	15.7	29.4	27.5	22.5	16.7	15.5
Corrected Smoke Number	27.0	29.5	43.0	32.0	12.0	18.5	15.0	15.5	19.5	21.5	17.0	9.5	16.5	16.5	18.0	22.0
Maximum Liner Temperature, K	1160.0	1224.0	1251.0	1261.0	998.0	1022.0	1031.0	1103.0	1125.0	1062.0	1081.0	992.0	1036.0	1080.0	1121.0	1141.0
Average Liner Temperature, K	971.0	997.0	1011.0	1017.0	839.0	854.0	852.0	890.0	902.0	864.0	879.0	821.0	853.0	880.0	900.0	910.0
Total Pressure Loss, %	4.48	4.63	5.01			4.87	5.08	5.04	5.41	5.00	5.25	4.88	5.08	5.16	5.43	6.02
Dome Pressure Loss, %	2.61	2.56	2.46	2.45	2.16	2.90	2.83	2.88	2.85	2.86	2.81	3.03	3.01	2.82	2.85	2.79

Concept I

Reading/Test Point	1/10	2/20	3/30	4/40	9/50	6/60	7/70	8/80	10/90	11/100	12/110	13/120	14/130	16/140	17/150	18/160
Fuel/Operating Condition	J/CR	J/CR	J/CR	J/TO	J/TO	J/TO	J/TO	J/TO	12H/TO	12H/TO	12H/TO	12H/TO	12H/TO	B/TO	B/TO	B/TO
Inlet Total Pressure, kPa	1163.1	1154.2	1154.2	1598.9	1601.7	1570.6	1583.7	1588.6	1554.8	1560.3	1590.6	1567.9	1579.6	1597.5	1591.3	1594.1
Inlet Static Pressure, kPa	1112.8	1100.4	1103.9	1537.5	1539.6	1506.5	1521.7	1524.4	1487.9	1495.5	1522.4	1503.1	1516.2	1532.7	1525.8	1529.3
Inlet Total Temperature, K	723.6	718.5	717.3	767.9	772.8	771.9	772.0	772.2	780.2	781.8	782.7	780.5	782.5	775.3	774.8	784.4
Inlet Humidity, g H_2O/kg Air	7.1	7.1	2.2	2.3	2.2	2.5	2.6	2.5	2.5	2.7	2.6	2.6	3.5	1.9	1.9	1.9
Combustor Airflow, kg/s	4.129	4.178	4.185	5.271	5.275	5.260	5.240	5.304	5.264	5.198	5.284	5.306	5.256	5.361	5.385	5.396
Reference Velocity, m/s	19.9	20.1	20.1	19.6	19.7	20.0	19.8	20.0	20.5	20.2	20.1	20.5	20.2	20.1	20.3	20.6
Fuel Nozzle ΔP, Main, kPa	975.6	1592.7	2304.9	2566.9	3666.6	5411.0	5577.9	6163.9	2618.6	3752.8	5143.5	5567.5	6200.4	2560.0	3833.5	5029.7
Fuel Flow, Main, kg/s	0.0415	0.0518	0.0619	0.0612	0.0723	0.0858	0.0886	0.0930	0.0623	0.0741	0.0861	0.0896	0.0940	0.0624	0.0788	0.0896
Fuel Flow, Pilot, kg/s	0.0103	0.0129	0.0152	0.0152	0.0182	0.0212	0.0220	0.0231	0.0155	0.0186	0.0213	0.0222	0.0232	0.0156	0.0194	0.0219
Metered Fuel/Air Ratio, Main	0.01000	0.01240	0.01480	0.01160	0.01370	0.01630	0.01690	0.01750	0.01180	0.01430	0.01630	0.01690	0.01790	0.01160	0.01460	0.00166
Metered Fuel/Air Ratio, Pilot	0.0277	0.0291	0.0343	0.0269	0.0327	0.0387	0.0399	0.0413	0.0278	0.0340	0.00383	0.00397	0.00421	0.00276	0.00343	0.00390
Metered Fuel/Air Ratio, Overall	0.01227	0.01531	0.01823	0.01429	0.01697	0.02017	0.02089	0.02163	0.01458	0.01770	0.02013	0.02087	0.02211	0.01436	0.01803	0.02050
Inlet Fuel Temperature, K	295.5	294.2	293.8	295.7	299.7	297.2	299.3	300.0	299.5	300.9	301.7	301.7	302.2	297.6	298.3	298.6
Sample Fuel/Air Ratio	0.01411	0.01652	0.01840	0.01458	0.01876	0.02027	0.02226	0.02377	0.01712	0.02108	0.02865	0.02612	0.02890	0.01980	0.02494	0.0296
Sample Combustion Efficiency, %	95.64	97.25	99.64	99.73	99.89	99.85	99.85	99.83	99.80	99.86	99.83	99.80	99.84	99.82	99.89	99.86
CO Emission Index, g/kg	85.6	61.4	12.6	8.7	4.0	5.6	5.9	6.8	7.4	5.2	6.8	7.8	6.2	6.9	4.2	5.5
CO_2 Emission, %	2.79	3.35	3.87	3.05	3.95	4.27	4.70	5.02	3.66	4.53	6.19	5.63	6.25	4.21	5.33	6.35
HC Emission Index, g/kg	27.1	15.2	0.8	0.7	0.2	0.2	0.2`	0.1	0.2	0.2	0.1	0.1	0.1	0.2	0.2	0.1
NO_x Emission Index, g/kg	10.26	14.51	5.86	22.12	25.22	24.97	25.71	20.01	24.78	29.29	32.25	35.46	33.7	42.71	51.80	45.32
Smoke Number	1.9	4.3	3.11	5.02	4.64	5.02	3.45	5.04	4.27	12.1	10.9	20.2	17.0	7.1		11.1
Corrected EICO, g/kg	83.3	55.4	11.2	4.8	2.3	3.1	3.3	3.8	4.4	3.2	4.5	4.7	3.9	4.0	2.4	3.5
Corrected EIHC, g/kg	25.3	12.8	0.7	0.3	0.1	0.1	0.1	0.0	0.1	0.1	0.1	0.0	0.1	0.1	0.1	0.1
Corrected $EINO_x$, g/kg	9.9	14.6	5.9	27.0	30.2	30.8	31.2	24.4	30.1	34.7	37.6	42.8	39.5	51.7	63.4	53.5
Corrected Smoke Number	1.5	4.0	2.5	4.0	4.0	4.0	3.0	4.0	3.7	10.0	9.0	17.5	14.5	6.0		9.0
Maximum Liner Temperature, K	915.0	940.0	975.0	1005.0	1040.0	1075.0	1065.0	1088.0	981.0	1008.0	1047.0	1072.0	1112.0	1015.0	1062.0	1558.0
Average Liner Temperature, K	769.0	775.0	804.0	830.0	865.0	875.0	883.0	894.0	846.0	856.0	878.0	878.0	903.0	894.0	864.0	1212.0
Total Pressure Loss, %	4.37	4.77	4.95	4.40	4.66	5.39	5.14	5.10	5.25	4.33	4.23	3.99	4.21			
Dome Pressure Loss, %	3.69	3.92	3.91	3.57	3.32	3.75	3.53	3.45	3.47	3.60	3.50	3.65	3.57	3.37	3.44	3.49

Concept I (Concluded)

Reading/Test Point	19/170	20/180	21/190	22/200	23/210	24/220	25/230	26/240	27/242	28/241	29/250	30/260	31/270	32/280	33/290	34/300
Fuel/Operating Condition	B/TO	B/TO	B/CR	B/CR	B/CR	B/CR	B/CR	J/CR	J/CR	J/CR	J/CR	12H/CR	12H/CR	12H/CR	12H/CR	12H/CR
Inlet Total Pressure, kPa	1593.4	1605.1	1161.1	1156.9	1164.5	1163.8	1165.2	1163.1	1161.8	1162.5	1169.4	1157.6	1144.5	1159.7	1145.9	1159.0
Inlet Static Pressure, kPa	1527.9	1536.8	1109.4	1109.4	1110.7	1111.4	1117.0	1114.9	1111.4	1112.1	1118.3	1105.2	1094.9	1108.7	1094.9	1108.7
Inlet Total Temperature, K	778.2	777.9	720.7	719.8	729.7	739.6	729.2	746.0	742.0	741.0	740.8	738.8	739.5	743.2	748.2	750.8
Inlet Humidity, g H_2O/kg Air	1.9	1.9	1.9	1.9	1.9	1.7	1.5	1.0	1.1	1.3	1.1	1.1	1.2	1.2	1.2	1.2
Combustor Airflow, kg/s	5.407	5.339	4.194	4.213	4.220	4.202	4.046	4.170	4.114	4.125	4.174	4.196	4.082	4.129	4.096	4.134
Reference Velocity, m/s	20.5	20.1	20.2	20.3	20.5	20.7	19.6	20.7	20.4	20.4	20.5	20.7	20.4	20.5	20.7	20.7
Fuel Nozzle ΔP, Main, kPa	5521.3	6012.2	1025.9	1598.2	2260.1	3046.1	3918.3	3164.7	2442.8	2809.6	4032.1	1043.2	1667.2	2382.1	3171.6	5521.3
Fuel Flow, Main, kg/s	0.0935	0.0975	0.0418	0.0514	0.0608	0.0702	0.0794	0.0699	0.0611	0.0657	0.0785	0.0418	0.0520	0.0618	0.0711	0.0795
Fuel Flow, Pilot, kg/s	0.0228	0.0240	0.0110	0.0126	0.0149	0.0176	0.0198	0.0179	0.0261	0.0219	0.0202	0.0105	0.0131	0.0153	0.0177	0.0199
Metered Fuel/Air Ratio, Main	0.0173	0.0183	0.0100	0.0122	0.0144	0.0167	0.0196	0.0168	0.0149	0.0159	0.0188	0.0100	0.0127	0.0150	0.0174	0.0192
Metered Fuel/Air Ratio, Pilot	0.00450	0.00434	0.00250	0.00282	0.00335	0.00400	0.00468	0.00410	0.00613	0.00506	0.00460	0.00236	0.00306	0.00353	0.00411	0.00454
Metered Fuel/Air Ratio, Overall	0.02135	0.02264	0.01250	0.01502	0.01775	0.02070	0.02428	0.02090	0.02103	0.02096	0.02340	0.01236	0.01576	0.01853	0.02151	0.02374
Inlet Fuel Temperature, K	298.5	298.6	295.8	296.4	296.9	297.5	295.0	294.5	295.2	294.5	294.0	293.6	293.7	294.1	294.4	294.4
Sample Fuel/Air Ratio	0.03007	0.03031	0.01586	0.01901	0.02242	0.02769	0.03250	0.02810	0.02787	0.02829	0.03282	0.01619	0.02055	0.02538		
Sample Combustion Efficiency, %	99.84	99.75	99.25	99.57	99.72	99.67	99.39	99.60	99.85	99.74	99.30	99.12	99.69	99.75		
CO Emission Index, g/kg	6.6	10.4	25.9	15.9	10.8	13.3	25.4	14.2	6.4	11.3	29.7	32.2	11.8	10.0		
CO_2 Emission, %	6.45	6.49	3.32	4.02	4.76	5.91	6.93	5.93	5.91	5.98	6.91	3.41	4.39	5.45		
HC Emission Index, g/kg	0.0	0.0	1.6	0.7	0.2	0.2	0.1	0.1	0.0	0.0	0.0	1.3	0.3	0.2		
NO_x Emission Index, g/kg	44.03	20.18	12.41	17.75	18.70	18.26	18.00	16.86	18.05	0.00	0.03	0.05	0.02	0.06		
Smoke Number	8.0	8.4	5.8	4.4	2.3	2.3	4.6	4.7	3.7	2.6	5.2	4.3	2.9	3.3	4.3	18.9
Corrected EICO, g/kg	3.9	6.3	24.0	14.5	11.0	15.2	26.9	17.4	7.6	13.3	34.7	36.1	13.4	12.0		
Corrected EIHC, g/kg	0.0	0.0	1.4	0.6	0.2	0.2	0.1	0.1	0.0	0.0	0.0	1.5	0.4	0.3		
Corrected $EINO_x$, g/kg	53.3	23.9	12.3	17.8	18.0	16.9	16.6	15.8	16.2	0.0	0.03	0.05	0.02	0.05		
Corrected Smoke Number	6.5	7.0	4.5	3.8	1.7	1.7	4.0	4.0	3.2	2.0	4.0	3.8	2.0	2.8	3.5	16.5
Maximum Liner Temperature, K	1603.0	1668.0	11175.0	1273.0	1370.0	1542.0	1646.0	1572.0	1540.0	1558.0	1849.0	1242.0	1317.0	1438.0	1537.0	1690.0
Average Liner Temperature, K	1180.0	1191.0	920.0	963.0	1021.0	1082.0	1151.0	1114.0	1106.0	1104.0	1183.0	977.0	1009.0	1078.0	1147.0	1220.0
Total Pressure Loss, %																
Dome Pressure Loss, %	3.43	3.37	3.53	3.69	3.81	3.65	3.56	3.72	3.58	3.54	3.65	3.58	3.69	3.71	3.88	3.81

Concept 2 (Screening Test)

Reading/Test Point	1/10	3/20	4/30	5/240	6/241	7/242	8/260	9/270	10/280	11/290	12/190	13/200	14/210	15/220	16/220
Fuel/Operating Condition	J/CR	J/CR	J/CR	J/CR	J/CR	J/CR	12H/CR	12H/CR	12H/CR	12H/CR	B/CR	B/CR	B/CR	B/CR	B/CR
Inlet Total Pressure, kPa	1145.2	1149.4	1158.3	1150.7	1150.0	1139.7	1151.4	1150.0	1159.0	1160.4	1153.5	1141.1	1152.8	1157.6	1165.9
Inlet Static Pressure, kPa	1089.4	1093.5	1105.2	1097.0	1097.0	1085.9	1098.3	1094.9	1103.9	1108.0	1101.1	1098.3	1098.3	1105.9	1112.1
Inlet Total Temperature, K	727.6	729.1	728.4	728.3	727.6	728.2	729.5	730.3	729.7	729.9	731.0	728.9	728.4	728.8	729.1
Inlet Humidity, g H_2O/kg Air	1.3	1.3	1.7	1.7	1.7	1.7	1.8	1.8	1.8	1.8	1.8	1.8	1.8	1.8	1.8
Combustor Airflow, kg/s	4.212	4.198	4.171	4.175	4.183	4.177	4.186	4.222	4.206	4.235	4.277	4.296	4.191	4.224	4.276
Reference Velocity, m/s	20.7	20.6	20.3	20.5	20.5	20.7	20.5	20.8	20.5	20.6	21.0	21.2	20.5	20.6	20.8
Fuel Nozzle ΔP, Main, kPa	495.0	686.0	850.1	1134.2	817.0	1023.9	489.5	682.6	844.6	1117.0	455.1	632.9	808.8	1094.9	1385.8
Fuel Flow, Main, kg/s	0.0465	0.0542	0.0600	0.0692	0.0587	0.0661	0.0464	0.0547	0.0608	0.0697	0.0464	0.0543	0.0605	0.0701	0.0784
Fuel Flow, Pilot, kg/s	0.0116	0.0127	0.0146	0.0172	0.0256	0.0225	0.0115	0.0128	0.0149	0.0174	0.0110	0.0127	0.0146	0.0170	0.0188
Metered Fuel/Air Ratio, Main	0.0110	0.0129	0.0144	0.0166	0.0140	0.0158	0.0111	0.0129	0.0144	0.0165	0.0109	0.0126	0.0144	0.0166	0.0183
Metered Fuel/Air Ratio, Pilot	0.0028	0.0030	0.0035	0.0041	0.0061	0.0054	0.0027	0.0030	0.0036	0.0041	0.0025	0.0030	0.0035	0.0040	0.0044
Metered Fuel/Air Ratio, Overall	0.0138	0.0159	0.0179	0.0207	0.0201	0.0212	0.0138	0.0159	0.0180	0.0206	0.0134	0.0156	0.0179	0.0206	0.0227
Inlet Fuel Temperature, K	292.4	292.5	292.5	292.5	291.8	291.9	293.7	293.7	293.5	294.0	293.9	293.0	293.0	293.2	293.5
Sample Fuel/Air Ratio	0.0142	0.0162	0.0181	0.0216	0.0226	0.0228	0.0143	0.0174	0.0186	0.0220	0.0145	0.0163	0.0185	0.0212	0.0188
Sample Combustion Efficiency, %	99.27	99.45	99.57	99.74	99.77	99.73	99.75	99.20	99.47	99.52	99.21	99.36	99.47	99.50	99.43
CO Emission Index, g/kg	26.7	21.4	17.5	11.1	9.7	11.8	92.8	24.2	18.0	17.9	28.1	23.9	21.0	20.1	23.2
CO_2 Emission, %	2.93	3.37	3.78	4.53	4.76	4.80	2.82	3.69	3.96	4.68	3.02	3.42	3.90	4.47	3.96
HC Emission Index, g/kg	1.2	0.6	0.3	0.0	0.0	0.0	35.7	2.7	1.1	0.6	1.5	0.9	0.5	0.3	0.2
NO_x Emission Index, g/kg	7.87	8.30	8.59	9.23	13.43	11.95	6.85	8.89	10.39	10.73	5.43	5.80	6.19	6.95	8.41
Smoke Number	17.1	13.7	12.0	9.5	10.6	9.5	49.1	23.0	32.6	40.5	23.1	30.9	33.1	29.2	35.8
Corrected EICO, g/kg	24.9	20.4	16.9	10.6	9.1	11.0	89.8	23.3	17.5	17.4	27.1	22.0	20.0	19.2	22.1
Corrected EIHC, g/kg	1.1	0.6	0.3	0.0	0.0	0.0	33.9	2.6	1.1	0.6	1.4	0.8	0.5	0.3	0.2
Corrected $EINO_x$, g/kg	8.2	8.5	8.6	9.4	13.7	12.3	6.9	9.1	10.5	10.9	5.6	6.1	6.3	7.1	8.6
Corrected Smoke Number	14.5	11.5	10.0	18.0	9.0	8.0	45.5	19.5	29.0	37.0	19.5	27.4	29.6	26.0	32.5
Maximum Liner Temperature, K	1126.0	1207.0	1264.0	1352.0	1229.0	1264.0	1116.0	1191.0	1247.0	1336.0	1059.0	1135.0	1203.0	1314.0	1353.0
Average Liner Temperature, K	825.0	833.0	846.0	864.0	857.0	862.0	819.0	857.0	874.0	900.0	833.0	848.0	863.0	885.0	887.0
Total Pressure Loss, %	6.15	8.36	8.21	9.17	9.62	8.14	7.48	9.79							12.78
Dome Pressure Loss, %	3.37	3.61	3.57	3.45	3.57	3.54	3.44	3.55	3.30	3.44	3.34	3.39	3.26	3.31	3.59

Concept 2 (Screening Test) Concluded

Reading/Test Point	18/140	18/150	20/160	21/165	22/40	23/50	24/60	25/70
Fuel/Operating Condition	B/TO	B/TO	B/TO	B/TO	J/TO	J/TO	J/TO	J/TO
Inlet Total Pressure, kPa	1181.8	1190.9	1166.6	1156.3	1173.5	1175.6	1177.6	1172.8
Inlet Static Pressure, kPa	1084.5	1096.3	1070.1	1057.7	1076.3	1084.5	1085.9	1079.0
Inlet Total Temperature, K	731.8	793.7	792.9	794.4	792.5	793.2	793.1	791.9
Inlet Humidity, g H_2O/kg Air	1.8	1.8	1.8	2.0	2.0	2.0	2.0	2.0
Combustor Airflow, kg/s	5.304	5.278	5.268	5.315	5.421	5.254	5.229	5.293
Reference Velocity, m/s	25.5	27.2	27.7	28.3	28.3	27.5	27.3	27.7
Fuel Nozzle ΔP, Main, kPa	950.1	1399.6	1320.3	1044.6	901.8	1325.9	1791.3	2011.9
Fuel Flow, Main, kg/s	0.0655	0.0787	0.0766	0.0688	0.0629	0.0754	0.0874	0.0924
Fuel Flow, Pilot, kg/s	0.0149	0.0185	0.0288	0.0283	0.0152	0.0185	0.0208	0.0229
Metered Fuel/Air Ratio, Main	0.0124	0.0149	0.0145	0.0130	0.0116	0.0144	0.0167	0.0175
Metered Fuel/Air Ratio, Pilot	0.0028	0.0035	0.0055	0.0053	0.0028	0.0035	0.0040	0.0043
Metered Fuel/Air Ratio, Overall	0.0152	0.0184	0.0200	0.0183	0.0144	0.0179	0.0207	0.0218
Inlet Fuel Temperature, K	293.0	293.2	293.5	293.5	292.3	292.3	291.8	292.0
Sample Fuel/Air Ratio	0.0128	0.01394	0.02128		0.0160	0.0206	0.0229	0.0235
Sample Combustion Efficiency, %	99.47	99.42	99.63		99.44	99.53	99.22	99.06
CO Emission Index, g/kg	20.5	23.4	15.7		22.2	19.3	31.9	37.5
CO_2 Emission, %	2.67	2.92	4.51		3.32	4.31	4.76	4.88
HC Emission Index, g/kg	0.5	0.4	0.0		0.5	0.2	0.4	0.7
NO_x Emission Index, g/kg	8.89	10.71	30.71		7.75	9.78	7.56	4.83
Smoke Number	28.2	30.0	23.7		12.8	15.0	25.5	20.0
Corrected EICO, g/kg	4.6	10.6	6.5		9.4	8.4	14.8	17.1
Corrected EIHC, g/kg	0.1	0.1	0.0		0.2	0.1	0.1	0.2
Corrected $EINO_x$, g/kg	19.7	18.5	54.7		14.1	17.1	13.2	8.6
Corrected Smoke Number	25.5	26.5	20.0		10.8	13.0	22.0	17.5
Maximum Liner Temperature, K	1160.0	1439.0	1297.0	1235.0	1184.0	1259.0	1341.0	1345.0
Average Liner Temperature, K	840.0	926.0	914.0	904.0	857.0	870.0	899.0	905.0
Total Pressure Loss, %								
Dome Pressure Loss, %	5.21	5.10	5.50	5.75	5.53	5.34	5.35	5.46

Concept 3

Reading/Test Point	1/10	2/30	3/240	4/30	5/80	6/30	7/241	8/243	9/244	10/270	11/280	12/280	13/200	14/215	15/205
Fuel/Operating Condition	J/CR	J/CR	J/CR	J/CR	J/CR	J/CR	J/CR	J/CR	J/CR	12H/CR	12H/CR	12H/CR	B/CR	B/CR	B/CR
Inlet Total Pressure, kPa	1161.1	1181.1	1116.3	1162.5	1183.8	1190.7	1162.5	1180.4	1172.8	1163.1	1163.8	1172.1	1175.6	1170.0	1156.9
Inlet Static Pressure, kPa	1110.1	1133.5	1055.6	1099.7	1130.1	1137.6	1107.3	1119.7	1112.1	1101.8	1106.6	1111.4	1121.8	1112.8	1102.5
Inlet Total Temperature, K	714.3	721.0	721.9	724.0	715.2	721.4	739.2	742.8	740.5	737.4	737.6	737.4	736.7	748.5	745.9
Inlet Humidity, g H_2O/kg Air	1.5	1.5	2.7	2.7	2.7	2.7	2.7	2.7	2.7	1.6	1.6	1.6	1.6	1.6	1.6
Combustor Airflow, kg/s	4.190	4.229	4.451	4.436	4.339	4.279	4.245	4.474	4.486	4.402	4.199	4.412	4.256	4.239	4.262
Reference Velocity, m/s	20.0	20.0	22.3	21.4	20.3	20.1	20.9	21.8	21.9	21.6	20.6	21.5	20.7	21.0	21.3
Fuel Nozzle ΔP, Main, kPa	344.7	815.6	1119.0	815.6	560.5	822.5	844.6	1123.8	1154.9	565.4	819.1	823.9	534.3	882.5	680.9
Fuel Flow, Main, kg/s	0.0401	0.0603	0.0701	0.0604	0.0504	0.0601	0.0605	0.0698	0.0710	0.0514	0.0608	0.0615	0.0505	0.0640	0.0566
Fuel Flow, Pilot, kg/s	0.0111	0.0154	0.0175	0.0148	0.0126	0.0148	0.0254	0.0175	0.0177	0.0126	0.0149	0.0152	0.0125	0.0155	0.0137
Metered Fuel/Air Ratio, Main	0.0096	0.0142	0.0157	0.0136	0.0116	0.0140	0.0143	0.0156	0.0158	0.0117	0.0145	0.0140	0.0119	0.0151	0.0133
Metered Fuel/Air Ratio, Pilot	0.0026	0.0034	0.0039	0.0033	0.0029	0.0035	0.0060	0.0039	0.0039	0.0029	0.0035	0.0034	0.0029	0.0037	0.0032
Metered Fuel/Air Ratio, Overall	0.0122	0.0176	0.0196	0.0169	0.0145	0.0175	0.0203	0.0195	0.0197	0.0146	0.0180	0.0174	0.0148	0.0188	0.0165
Inlet Fuel Temperature, K	292.5	292.4	293.4	294.8	295.2	295.0	295.6	294.7	294.6	293.8	293.7	293.8	292.0	291.3	291.9
Sample Fuel/Air Ratio	0.0126	0.0206	0.0269	0.0219	0.0187	0.0237	0.0277	0.0263	0.0255	0.0166	0.0214	0.0206	0.0176	0.0237	0.0196
Sample Combustion Efficiency, %	85.88	91.47	99.21	99.40	96.50	99.52	99.81	99.78	99.75	96.57	97.17	96.96	92.31	94.10	92.89
CO Emission Index, g/kg	178.8	116.0	10.7	12.1	72.5	10.0	6.2	8.2	9.4	120.1	101.8	109.5	105.0	88.6	103.1
CO_2 Emission, %	2.13	3.83	5.67	4.60	3.73	4.99	5.86	5.57	5.40	3.33	4.36	4.17	3.34	4.65	3.76
HC Emission Index, g/kg	114.3	66.9	6.2	3.7	20.8	2.8	0.5	0.3	0.4	6.6	4.8	5.0	60.6	44.3	54.3
NO_x Emission Index, g/kg	8.20	11.32	11.36	13.32	11.14	13.71	15.27	14.51	13.83	9.42	10.79	9.71	7.79	8.14	7.30
Smoke Number	7.4	1.08	4.0	1.2	1.4	1.2	0.3	0.3	0.5	18.2	32.5	29.1	3.5	1.7	2.8
Corrected EICO, g/kg	148.2	104.5	8.4	10.6	60.1	9.2	6.7	9.0	9.9	121.7	108.4	111.7	110.5	105.7	117.5
Corrected EIHC, g/kg	86.8	57.9	4.6	3.1	16.1	2.4	0.6	0.3	0.4	6.9	5.3	5.3	65.8	57.6	66.0
Corrected $EINO_x$, g/kg	8.7	11.5	13.2	14.4	11.8	13.9	14.9	14.4	14.0	9.6	10.5	9.8	7.6	7.6	7.0
Corrected Smoke Number	6.0	1.0	3.0	1.0	1.0	1.0	0.0	0.0	0.0	15.5	29.5	26.5	2.5	1.0	1.8
Maximum Liner Temperature, K	835.0	880.0	1024.0	963.0	896.0	974.0	1250.0	1046.0	1005.0	881.0	936.0	928.0	881.0	933.0	918.0
Average Liner Temperature, K	763.0	769.0	838.0	818.0	783.0	836.0	894.0	864.0	848.0	774.0	801.0	804.0	793.0	803.0	817.0
Total Pressure Loss, %	6.21		4.44	3.94	3.49		3.67	3.87	4.27	3.83	3.54	3.83	3.54	3.62	3.72
Dome Pressure Loss, %	1.75	2.13	2.40	2.53	2.25	1.90	2.37	2.42	2.62	2.54	2.20	2.38	2.08	2.22	2.32

Concept 3 (Concluded)

Reading/Test Point	16/140	17/150	18/160	19/170	20/40	21/50	22/60	23/70	24/75	25/90	26/100	27/11	28/120
Fuel/Operating Condition	B/TO	B/TO	B/TO	B/TO	J/TO	J/TO	J/TO	J/TO	J/TO	12H/TO	12H/TO	12H/TO	12H/TO
Inlet Total Pressure, kPa	1154.9	1164.5	1168.7	1162.5	1169.4	1167.3	1170.7	1174.2	1172.8	1159.0	1179.0	1166.6	1172.1
Inlet Static Pressure, kPa	1060.4	1061.8	1063.2	1057.7	1068.0	1066.6	1072.8	1071.4	1048.7	1072.8	1077.7	1065.2	1072.1
Inlet Total Temperature, K	817.0	815.4	812.6	808.7	802.6	802.6	800.4	801.5	802.6	805.4	809.8	810.4	809.3
Inlet Humidity, g H$_2$O/kg Air	1.6	1.6	1.6	1.6	1.5	1.5	1.5	1.5	1.5	1.5	1.1	1.1	1.0
Combustor Airflow, kg/s	5.247	5.373	5.391	5.417	5.441	5.404	5.416	5.390	5.400	5.584	5.386	5.361	5.469
Reference Velocity, m/s	28.7	29.1	29.0	29.2	28.9	28.8	28.7	28.4	28.6	30.1	28.7	28.8	29.2
Fuel Nozzle ΔP, Main, kPa	870.8	1246.6	1761.6	1944.3	872.2	1291.4	1801.6	2018.8	1598.2	888.0	1301.7	1799.5	2013.3
Fuel Flow, Main, kg/s	0.0651	0.0768	0.0902	0.0946	0.0641	0.0765	0.0892	0.0940	0.0840	0.0653	0.0777	0.0902	0.0954
Fuel Flow, Pilot, kg/s	0.0159	0.0193	0.0218	0.0230	0.0162	0.0199	0.0220	0.0235	0.0321	0.0161	0.0194	0.0223	0.0236
Metered Fuel/Air Ratio, Main	0.0124	0.0143	0.0167	0.0175	0.0118	0.0142	0.0165	0.0174	0.0155	0.0117	0.0144	0.0168	0.0174
Metered Fuel/Air Ratio, Pilot	0.0030	0.0036	0.0040	0.0042	0.0030	0.0037	0.0041	0.0044	0.0059	0.0029	0.0036	0.0042	0.0043
Metered Fuel/Air Ratio, Overall	0.0154	0.0179	0.0207	0.0217	0.0148	0.0179	0.0206	0.0218	0.0214	0.0146	0.0180	0.0210	0.0217
Inlet Fuel Temperature, K	291.5	291.8	292.0	291.5	291.1	291.0	291.3	291.5	292.9	290.1	289.9	290.0	290.0
Sample Fuel/Air Ratio	0.0190	0.0224	0.0267	0.0283	0.0186	0.0237	0.0296	0.0306	0.0295	0.0183	0.0229	0.0242	0.0277
Sample Combustion Efficiency, %	92.01	93.05	94.23	94.56	90.34	92.93	95.41	95.11	94.70	93.15	93.81	94.01	95.45
CO Emission Index, g/kg	101.2	99.4	91.8	89.1	114.2	100.8	82.2	86.6	84.1	91.2	92.4	92.0	73.1
CO$_2$ Emission, %	3.61	4.32	5.25	5.59	3.41	4.52	5.86	6.04	5.80	3.57	4.50	4.78	5.61
HC Emission Index, g/kg	65.1	53.5	41.9	38.9	80.5	54.2	30.7	32.9	38.3	54.9	46.8	44.6	33.0
NO$_x$ Emission Index, g/kg	10.52	11.30	10.77	9.35	9.92	10.70	11.31	31.84	11.13	14.71	14.26	13.67	13.64
Smoke Number	1.8	1.6	0.9	1.5	0.5	0.4	0.5	1.3	1.3	1.3	9.2	14.5	5.9
Corrected EICO, g/kg	63.6	60.5	54.0	49.7	60.4	53.3	42.1	45.6	44.4	47.4	53.4	53.1	40.6
Corrected EIHC, g/kg	303.0	24.1	18.1	15.6	29.5	19.9	10.9	12.1	14.2	20.1	19.7	18.7	13.4
Corrected EINO$_x$, g/kg	17.2	18.9	18.1	16.2	17.5	18.8	20.0	55.3	19.4	26.7	23.9	23.1	23.5
Corrected Smoke Number	1.4	1.2	0.8	1.2	0.0	0.0	0.0	1.0	1.0	1.0	7.5	13.0	5.0
Maximum Liner Temperature, K	977.0	1000.0	1027.0	1044.0	951.0	980.0	1012.0	1017.0	1004.0	967.0	1014.0	1056.0	1081.0
Average Liner Temperature, K	874.0	873.0	870.0	854.0	838.0	845.0	856.0	862.0	856.0	839.0	858.0	869.0	877.0
Total Pressure Loss, %	6.12	6.42	6.42	6.49	6.34	6.15							
Dome Pressure Loss, %	4.00	3.92	4.00	4.01	3.90	3.97	3.77	3.66	3.76	4.19	3.91	3.81	3.99

151

Parametric Test

Reading/Test Point	1/10	2/20	3/10	4/10	5/10	6/20	7/20	8/30	9/40	10/50	11/60	12/80	13/90	14/100	15/70
Fuel/Operating Condition	J/CR	J/CR	J/CR	J/CR	J/CR	J/CR	J/CR	J/CR	J/CR	J/CR	12H/CR	12H/CR	12H/CR	12H/CR	12H/CR
Inlet Total Pressure, kPa	1179.0	1183.1	1167.3	1171.4	1163.8	1175.6	1172.8	1168.7	1171.4	1158.3	1161.0	1163.8	1164.5	1176.9	1156.3
Inlet Static Pressure, kPa	1128.0			1121.8	1112.1	1123.8	1118.3	1114.2	1115.6	1105.9	1107.3	1111.4	1110.7	1119.7	1109.4
Inlet Total Temperature, K	716.3	712.7	716.0	738.8	724.0	722.7	723.0	723.3	723.4	722.9	719.2	722.9	723.4	724.7	723.7
Inlet Humidity, g H_2O/kg Air	1.4	1.4	1.4	1.3	1.3	1.3	1.3	1.3	1.3	1.3	1.3	1.3	1.3	1.3	1.3
Combustor Airflow, kg/s	4.191	4.268	4.164	4.070	4.100	4.152	4.260	4.197	4.283	4.194	4.189	4.183	4.178	4.318	4.198
Reference Velocity, m/s	19.7	19.9	19.8	19.9	19.8	19.8	20.3	20.1	20.5	20.3	20.1	20.1	20.1	20.6	20.4
Fuel Nozzle ΔP, Main, kPa				1785.7	1778.8	2111.9	2034.0	2032.6	1923.6	1803.0	1723.7	1915.4	1868.5	1774.0	1963.6
Fuel Flow, Main, kg/s	0.0510	0.0605	0.0508	0.0504	0.0503	0.0603	0.0585	0.0585	0.0548	0.0512	0.0492	0.0553	0.0539	0.0503	0.0574
Fuel Flow, Pilot, kg/s	0.0130	0.0152	0.0126	0.0130	0.0130	0.0155	0.0157	0.0107	0.0141	0.0179	0.0117	0.0094	0.0127	0.0156	0.0137
Metered Fuel/Air Ratio, Main	0.0122	0.0142	0.0122	0.0124	0.0123	0.0145	0.0137	0.0139	0.0128	0.0122	0.0117	0.0132	0.0129	0.0117	0.0137
Metered Fuel/Air Ratio, Pilot	0.0031	0.0036	0.0030	0.0032	0.0032	0.0037	0.0037	0.0026	0.0037	0.0040	0.0028	0.0022	0.0030	0.0036	0.0033
Metered Fuel/Air Ratio, Overall	0.0153	0.0178	0.0152	0.0156	0.0155	0.0182	0.0174	0.0165	0.0161	0.0162	0.0145	0.0155	0.0159	0.0153	0.0169
Inlet Fuel Temperature, K	283.3	282.4	283.1	286.0	286.0	286.1	286.5	287.3	287.0	287.0	288.0	288.0	287.8	287.8	287.5
Sample Fuel/Air Ratio	0.0138	0.0178	0.0148	0.0152	0.0144	0.0179	0.0175	0.0158	0.0176	0.0181	0.0150	0.0157	0.0165	0.0163	0.0173
Sample Combustion Efficiency, %	83.14	98.55	98.37	98.63	99.27	99.43	99.41	99.17	99.46	99.59	99.22	98.79	99.26	99.44	99.41
CO Emission Index, g/kg	103.4	18.4	22.1	16.4	21.5	17.7	18.5	25.7	16.9	12.9	24.6	35.1	22.9	17.8	20.2
CO_2 Emission, %	2.32	3.71	3.04	3.14	2.98	3.74	3.64	3.27	3.67	3.78	3.17	3.28	3.49	3.45	3.67
HC Emission Index, g/kg	166.1	11.7	12.8	11.4	2.6	1.8	1.8	2.7	1.7	1.3	2.3	4.3	2.3	1.6	1.3
No_x Emission Index, g/kg	0.16	8.47	7.81	10.38	10.86	8.24	8.16	8.57	8.03	9.89	8.10	9.19	9.34	9.95	9.83
Smoke Number	8.3	15.4	10.4	6.1	9.7	20.9	19.0	14.5	15.8	15.8	17.8	23.4	30.3	22.2	38.2
Corrected EICO, g/kg	89.2	15.2	19.0	18.5	20.3	16.6	16.9	23.7	15.4	11.7	21.5	32.1	21.1	16.4	18.4
Corrected EIHC, g/kg	134.1	8.8	10.2	13.3	2.4	1.6	1.6	2.4	1.5	1.1	1.9	3.8	2.0	1.4	1.1
Corrected $EINO_x$, g/kg	0.16	8.9	8.1	9.6	10.8	8.2	8.4	8.7	8.3	10.2	8.4	9.4	9.5	10.3	10.2
Corrected Smoke Number	6.9	13.1	8.9	4.8	8.2	18.4	16.5	12.2	13.5	13.5	15.2	20.7	27.0	19.6	34.5
Maximum Liner Temperature, K	1094.0	1336.0	1218.0	1358.0	1251.0	1410.0	1381.0	1364.0	1319.0	1306.0	1271.0	1350.0	1363.0	1246.0	1379.0
Average Liner Temperature, K	795.0	834.0	804.0	878.0	848.0	874.0	869.0	860.0	859.0	861.0	868.0	875.0	880.0	869.0	886.0
Total Pressure Loss, %	3.71			3.57											
Dome Pressure Loss, %	2.92			2.85	3.05	3.13	3.14	3.21	3.15	3.07	3.05	3.05	3.16	3.19	3.12

Parametric Test (Continued)

Reading/Test Point	16/110	17/105	18/104	19/120	20/135	21/145	22/125	23/155	24/165	25/175	26/211	27/205	28/260	29/215	30/235
Fuel/Operating Condition	B/CR	B/CR	B/CR	B/CR	B/TO	B/TO	B/TO	J/TO	J/TO	J/TO	12H/TO	12H/TO	12H/TO	12H/TO	12H/TO
Inlet Total Pressure, kPa	1157.6	1168.7	1170.0	1173.5	1165.9	1170.7	1170.0	1161.1	1168.0	1168.7	1158.3	1176.2	1164.5	1179.7	1162.5
Inlet Static Pressure, kPa	1111.4	1123.2	1121.1	1125.9	1126.6	1128.0	1126.6	1123.2	1128.0	1130.1	1065.2	1099.7	1085.2	1143.2	1113.5
Inlet Total Temperature, K	731.5	732.7	733.2	734.0	821.0	813.2	811.7	811.2	812.0	813.1	801.0	799.3	799.0	800.8	801.5
Inlet Humidity, g H_2O/kg Air	0.6	0.6	0.6	0.6	0.6	0.6	0.6	1.0	1.0	1.0	1.2	1.2	1.2	1.2	1.2
Combustor Airflow, kg/s	4.111	4.040	4.235	4.230	3.894	3.935	3.913	3.857	3.956	3.812	5.256	5.022	4.853	3.876	3.789
Reference Velocity, m/s	20.1	19.6	20.5	20.5	21.2	21.2	21.0	20.9	21.3	20.5	28.2	26.4	25.8	20.4	20.2
Fuel Nozzle ΔP, Main, kPa	1620.3	1472.0	1503.1	1947.8	1581.0	1787.8	1450.0	1456.9	1601.7	1778.8	2358.0	2173.9	2046.4	1387.9	1654.0
Fuel Flow, Main, kg/s	0.0504	0.0435	0.0407	0.0565	0.0437	0.0514	0.0378	0.0377	0.0433	0.0497	0.0721	0.0668	0.0605	0.0361	0.0481
Fuel Flow, Pilot, kg/s	0.0110	0.0103	0.0095	0.0144	0.0102	0.0118	0.0087	0.0094	0.0113	0.0129	0.0181	0.0165	0.0137	0.0086	0.0109
Metered Fuel/Air Ratio, Main	0.0123	0.0108	0.0096	0.0134	0.0112	0.0131	0.0097	0.0098	0.0110	0.0130	0.0137	0.0133	0.0125	0.0093	0.0127
Metered Fuel/Air Ratio, Pilot	0.0027	0.0026	0.0022	0.0034	0.0026	0.0030	0.0022	0.0024	0.0028	0.0034	0.0034	0.0033	0.0028	0.0022	0.0029
Metered Fuel/Air Ratio, Overall	0.0149	0.0133	0.0119	0.0168	0.0139	0.0161	0.0119	0.0122	0.0138	0.0164	0.0172	0.0166	0.0153	0.0115	0.0156
Inlet Fuel Temperature, K	287.5	287.9	288.0	287.2	288.1	289.0	289.5	289.8	290.0	290.7	291.5	291.9	291.8	292.8	293.2
Sample Fuel/Air Ratio	0.0151	0.0132	0.0117	0.0171	0.0130	0.0156	0.0121	0.0117	0.0139	0.0161	0.0152	0.0149	0.0142	0.0103	0.0124
Sample Combustion Efficiency, %	99.32	99.19	98.79	99.45	99.60	99.66	99.47	99.57	99.71	99.72	99.46	99.53	99.38	96.59	97.18
CO Emission Index, g/kg	22.9	26.8	38.2	18.7	14.6	12.6	18.7	15.2	10.6	10.4	19.1	16.9	22.3	66.4	71.0
CO_2 Emission, %	3.17	2.75	2.42	3.58	2.73	3.28	2.52	2.42	2.89	3.37	3.22	3.17	3.00	2.08	2.52
HC Emission Index, g/kg	1.7	2.1	3.6	1.2	0.6	0.5	1.0	0.9	0.5	0.4	0.9	0.8	1.0	21.5	13.2
No_x Emission Index, g/kg	8.09	7.16	6.45	9.22	10.25	11.97	10.56	11.27	12.81	13.07	10.35	10.55	10.13	9.57	9.79
Smoke Number	27.0	21.5	17.8	31.4	13.8	23.4	12.9	1.9	1.9	13.5	5.6	12.2	23.2	27.9	25.0
Corrected EICO, g/kg	23.2	28.3	38.8	19.3	11.0	8.4	13.2	10.3	6.7	6.9	8.8	8.1	11.2	47.6	51.7
Corrected EIHC, g/kg	1.7	2.2	3.7	1.3	0.4	0.3	0.6	0.5	0.3	0.2	0.3	0.3	0.4	10.9	6.7
Corrected $EINO_x$, g/kg	7.9	6.8	6.4	9.0	12.1	14.6	12.9	13.8	15.9	15.5	18.0	17.3	16.3	12.0	12.2
Corrected Smoke Number	24.0	18.9	15.2	28.0	12.5	20.0	12.0	2.0	2.0	12.3	5.0	11.3	20.5	26.0	23.0
Maximum Liner Temperature, K	1221.0	1174.0	1114.0	1395.0	1235.0	1362.0	1219.0	1151.0	1255.0	1324.0	1305.0	1311.0	1301.0	1163.0	1309.0
Average Liner Temperature, K	863.0	855.0	844.0	891.0	949.0	968.0	938.0	913.0	934.0	950.0	921.0	925.0	936.0	914.0	956.0
Total Pressure Loss, %			3.54	3.53	3.55	3.42	3.18	3.27	3.36	3.19	6.61	5.28	5.74	3.45	3.62
Dome Pressure Loss, %	3.17	3.02	3.14	3.07	3.14	2.86	2.90	2.97	2.96	2.78	5.42	4.39	4.56	2.85	2.06

Parametric Test (Concluded)

Reading/Test Point	31/235	32/240	33/225	34/215	35/175	36/165	37/175	38/155	39/180
Fuel/Operating Condition	12H/TO	12H/TO	12H/TO	12H/TO	J/TO	J/TO	J/TO	J/TO	J/TO
Inlet Total Pressure, kPa	1162.5	1181.1	1158.3	1166.6	1160.4	1156.9	1163.1	1164.5	1168.7
Inlet Static Pressure, kPa	1113.5	1132.1	1121.1	1118.3	1109.4	1109.4	1115.6	1118.3	1102.5
Inlet Total Temperature, K	801.5	801.4	803.0	803.5	808.3	823.4	820.8	820.4	820.4
Inlet Humidity, g H_2O/kg Air	1.2	1.2	1.2	1.2	1.0	1.0	1.0	1.0	1.0
Combustor Airflow, kg/s	3.789	3.887	3.809	3.804	3.785	3.728	3.783	3.844	3.916
Reference Velocity, m/s	20.2	20.4	20.5	20.3	20.4	20.5	20.7	21.0	21.3
Fuel Nozzle ΔP, Main, kPa	1654.7	1829.2	1501.7	1385.8	1716.8	1551.3	1687.8	1403.1	1899.5
Fuel Flow, Main, kg/s	0.0481	0.0536	0.0422	0.0367	0.0493	0.0441	0.0493	0.0376	0.0556
Fuel Flow, Pilot, kg/s	0.0109	0.0123	0.0095	0.0082	0.0123	0.0108	0.0122	0.0093	0.0135
Metered Fuel/Air Ratio, Main	0.0127	0.0138	0.0111	0.0096	0.0132	0.0118	0.0130	0.0098	0.0142
Metered Fuel/Air Ratio, Pilot	0.0029	0.0032	0.0025	0.0022	0.0033	0.029	0.0032	0.0024	0.0034
Metered Fuel/Air Ratio, Overall	0.0156	0.0170	0.0136	0.0118	0.0164	0.0147	0.0162	0.0122	0.0176
Inlet Fuel Temperature, K	293.2	295.5	293.2	293.2	293.0	292.8	293.1	292.8	292.0
Sample Fuel/Air Ratio	0.0140	0.0160	0.0122	0.0105	0.0138	0.0136	0.0149	0.0113	0.0163
Sample Combustion Efficiency, %	99.48	99.59	99.36	99.05	99.62	99.69	99.69	99.57	99.67
CO Emission Index, g/kg	17.5	14.7	22.6	31.3	14.0	11.6	12.0	15.7	12.9
CO_2 Emission, %	2.97	3.40	2.57	2.20	2.88	2.83	3.11	2.35	3.40
HC Emission Index, g/kg	1.2	0.7	1.2	2.4	0.6	0.4	0.4	0.7	0.3
No_x Emission Index, g/kg	11.56	12.65	10.37	9.37	10.75	10.93	11.13	10.37	11.84
Smoke Number	35.8	41.2	28.9	23.0	19.9	10.5	19.9	5.5	28.9
Corrected EICO, g/kg	11.7	9.1	15.0	21.9	9.3	8.8	8.9	12.0	9.4
Corrected EIHC, g/kg	0.6	0.4	0.6	1.3	0.3	0.3	0.3	0.5	0.2
Corrected $EINO_x$, g/kg	14.4	15.8	13.0	11.6	13.1	12.4	12.8	12.1	14.0
Corrected Smoke Number	33.5	37.0	27.0	20.3	18.0	10.0	18.0	4.9	27.0
Maximum Liner Temperature, K	1309.0	1372.0	1227.0	1162.0	1273.0	1250.0	1318.0	1161.0	1392.0
Average Liner Temperature, K	956.0	973.0	937.0	918.0	931.0	949.0	959.0	925.0	971.0
Total Pressure Loss, %	3.62	3.56	3.51	3.37	3.57	3.81	3.20	3.30	3.30
Dome Pressure Loss, %	2.06	3.11	3.11	3.04	3.01	2.89	2.93	3.10	2.79

APPENDIX B - SYMBOLS

		Units
A	Area	m^2
API	American Petroleum Institute	
ARP	Aerospace Recommended Practice (SAE)	
ASME	American Society of Mechanical Engineers	
ASTM	American Society for Testing Materials	
B	Broad-Property Fuel (13% Hydrogen)	
b	Injector Spacing	
BPF	Broad-Property Fuel	
CAROL	Contaminants Analyzed and Recorded On-Line	
CO	Carbon Monoxide	
CR	Cruise Conditions	
ECCP	Experimental Clean Combustor Program	
EICO	Gas-Sample CO Emission Index	g/kg
EIHC	Gas-Sample HC Emission Index	g/kg
$EINO_x$	Gas-Sample NO_x Emission Index	g/kg
EPA	Environmental Protection Agency	
ERBS	Experimental Referee Broad Specification	
f	Fuel/Air Ratio or Overall Metered Fuel/Air Ratio	
FID	Flame Ionization Detector	
GE	General Electric Company	
H	Inlet-Air Absolute Humidity	g/kg
h	Height	m
HC	Unburned Hydrocarbons	
J	Jet A Fuel (14% Hydrogen)	
JFTOT	Jet Fuel Thermal Oxidation Test	
L	Length	m
LCO	Light Cycle Oil	
NASA	National Aeronautics and Space Administration	
NMR	Nuclear Magnetic Response	
NO_x	Oxides of Nitrogen	

		Units
P	Pressure	Pa
PM	Pensky-Martens Method Closed Flash-Point Test	
QCSEE	Quiet, Clean, Short-Haul, Experimental Engine	
SAE	Society of Automotive Engineers	
SMD	Sauter Mean Diameter	
SN	Gas-Sample Smoke Number	
T	Temperature	K
TCC	Tag Closed Cup Flash-Point Procedure	
TDR	Tube Deposit Rating	
TO	Simulated Takeoff Condition	
V	Velocity	m/s
W	Fluid Flow	kg/s
12H	Special Fuel Blend (12% Hydrogen)	
ΔP	Pressure Drop	Pa
η	Combustion Efficiency	%
ρ	Fluid Density	kg/m^3

Subscripts

1	Measured (Test)
2	Corrected or Nominal
3	Compressor Exit or Combustor Inlet
3.9	Combustor Exit
36	Combustor
c	Combustor
d	Dome
f	Fuel Flow, Fuel Injector
m	Combustor Main Stage
p	Combustor Pilot Stage
r	Reference
s	Gas Sample
T	Total

156

REFERENCES

1. Longwell, J.P., "Jet Aircraft Hydrocarbon Fuels Technology," National Aeronautics and Space Administration, CR2033, January 1978.

2. Gleason, C.C., Rodgers, D.W., and Bahr, D.W., "NASA/GE Experimental Clean Combustor Program - Phase II Final Report," National Aeronautics and Space Administration, CR134971, August 1976.

3. Bahr, D.W., Burrus, D.L., and Sabla, P.E., "Double Annular Clean Combustor Technology Report," National Aeronautics and Space Administration, CR15943, 1979.

4. Bahr, D.W. and Gleason, C.C., "Experimental Clean Combustor Program - Phase I Final Report," National Aeronautics and Space Administration, CR134737, June 1975.

5. Simmons, H.C., "Empirical Formulas for Prediction of Spray Drop Sizes," Parker-Hannifin Corporation, Technical Information Report BTA105, May 22, 1978.

6. Spadaccini, L.J., "Autoignition Characteristics of Hydrocarbon Fuels at Elevated Temperatures and Pressures," ASME Paper 76-GT-3, 1976.

7. Gleason, C.C., Oller, T.L., Shayeson, M.W., and Bahr, D.W., "Evaluation of Fuel Character Effects on F101 Engine Combustion System," U.S. Air Force Aero Propulsion Laboratories, CEEDO-TR-79-07, April 1979.

8. Prok, G.M. and Serg, G.T., "Initial Characterization of Experimental Referee Broad-Specification (ERBS) Aviation Turbine Fuel," National Aeronautics and Space Administration, TM81440, January 1980.

DISTRIBUTION LIST

<div align="right">No. of Copies</div>

NASA-Lewis Research Center
21000 Brookpark Road
Cleveland, OH 44135

Attn:			
Report Control Office	MS 5/5	1
Technology Utilization	7/3	1
Library	60/3	1
S. Himmel	3/7	1
B. Robinson	500/313	1
R. Rudey	86/5	1
C. Rosen	86/5	1
J. Grobman	86/6	1
R. Niedzwiecki	86/6	1
G. Reck	86/6	1
S. Gordon	86/6	1
D. Petrash	86/6	1
L. Diehl	86/6	1
R. Jones	86/6	1
E. Lezberg	86/6	1
J. Acurio	77/5	1.
J. Fear	86/6	1
F. Humenik	86/6	1
Major Willoughby	501/3	1
D. Weber	106/1	1
F. Torres	86/6	1
A. Smith	86/6	Remainder
Tech. Utilization	3/19	1

NASA Headquarters
600 Independence Avenue, S.W.
Washington, DC 20546

Attn:		
RJP-2/D. Poferl	1
PJG-2/H. Johnson	1
RTP-6/G. Banerian	1
R/W. Aiken	1

NASA Scientific & Technical Information Facility
Attn: Accessioning Department
P.O. Box 8757
Balt/Wash International Airport
Maryland 21240   10

Applications Engineering Office
National Space Technology Laboratories
National Aeronautics and Space Administration
Bay St. Louis, MS 39520   1

No. of Copies

NASA-Langley Research Center
Langley Station
Hampton, VA 23365
Attn: Library   1

Jet Propulsion Laboratory
4800 Oak Grove Drive
Pasadena, CA 91103
Attn: S. Kalfayan   1

II. OTHER GOVERNMENT AGENCIES

FAA Headquarters
2100 2nd Street, S.W.
Washington, DC 20591
Attn: Library   1

Environmental Protection Agency
401 Main Street, S.W.
Washington, DC 20460
Attn: G. Kittredge   1

Environmental Protection Agency
2565 Plymouth Road
Ann Arbor, MI 48105
Attn: R. Munt   1

Environmental Protection Agency
Research Triangle Park, NC 27711
Attn: J. Wasser   MS 65   1

U. S. Department of Transportation
Federal Aviation Administration
800 Independence Avenue, S.W.
Washington, DC 20591
Attn: A. J. Broderick   MS AEQ-10   1

Wright-Patterson Air Force Base
OH 45433
Attn: E. E. Bailey NASA/AFWAL-Liaison   1
        A. Churchill AFWAL/POSF   Area B, Bldg. 18D   1
        R. Henderson AFWAL/POSF   Area B, Bldg. 18D   1
        C. Delany   1
        T. Jackson   1

No. of Copies

U.S. Army Res. and Technol. Lab
Attn: E. Mularz, AVRADCOM/MS 106/2   1
           J. Acurio   1
           21000 Brookpark Road
           Cleveland, OH   44135

United States Army
Mr. Kent Smith, SAVDL/EU-TAT
Commanding Officer
Eustis Directorate - USA AMRDL
Fort Eustis, VA   23604   1

United States Army
Mr. Larry Bell
AVSCOM, AMSAV - EFP
Box 209
St. Louis, MO   63166   1

Air Force Office of Scientific Research
Bolling AFB, DC   20332
Attn: NA/Dr. B. T. Wolfson   1

Naval Air Propulsion Test Center
Trenton, NJ   03628
Attn: L. Maggitti   1

Navy Energy & Natural Resources
R & O Office, Navy Ship R & D Center
Annapolis Laboratories
Annapolis, MD   21402   1

Naval Ordinanace Systems Command
Department of the Navy
Arlington, VA   20360
Attn: J. W. Murrin   1

Institute for Defense Analysis
400 Army-Navy Drive
Arlington, VA   22202
Attn: Dr. R. C. Oliver   1

Arnold Engineering and Development Center
Arnold AF Station, TN 37389
Attn: E. L. Hively   Code D1/R   1

ARO, Incorporated
Arnold AF Station, TN   37389
160 Attn: Library   1

No. of Copies

Bureau of Mines
Bartlesville Energy Research Center
P.O. Box 1398
Bartlesville, OK 74003
Attn: R. Hurn   1

DOE
400 1st St., N.W.
Washington, DC 20545
Attn: K. Bastress   1

III. UNIVERSITIES

Massachusetts Institute of Technology
Department of Mechanical Engineering
Cambridge, MA 02139
Attn: J. Longwell   1
        G. Prado   1

University of Michigan
Department of Aerospace Engineering
Gas Dynamics Lab.
Ann Arbor, MI
Attn: A. Nichols   1
        C. Kauffman   1

University of California
Department of Mechanical Engineering
Berkely, CA 94720
Attn: Prof. R. F. Sawyer   1

Purdue University
School of Mechanical Engineering
West Lafayette, IN 47907
Attn: Prof. A. M. Mellor   1
        A. Lefebvre   1

Cornell University
Sibley School of Mechanical & Applied Engineering
Upson and Grumman Halls
Ithaca, NY 14850
Attn: Prof. F. Gouldin   1

No. of Copies

Prof. J. Odgers
Department of Mechanical Engineering
Laval University
Québec, CANADA
GIK 7P4   1

Prof. G. Scott Samuelson
Mechanical and Environmental Engineering
University of California
Irvine, CA 92717   1

Prof. F. A. Williams
Department of Applied Mechanics and Engineering Sciences, B-010
University of California at San Diego
La Jolla, CA 92093   1

Prof. C. Merkle
Department of Mechanical Engineering
203 Mechanical Engineering Building
Pennsylvania State University
University Park, PA 16802   1

Prof. Melvin Gerstein
Associate Dean of Engineering
School of Engineering
University of Southern California
Los Angeles, CA 90007   1

IV. CORPORATIONS - U.S.

Teledyne CAE
1330 Laskey Road
Toledo, OH 43697
Attn: C. Rogo   1

Detroit Diesel Allison Division
Department 8894, Plant 8
P.O. Box 894
Indianapolis, IN 46206
Attn: A. Verdouw   1
       G. Tomlinson   1

No. of Copies

Northern Research and Engineering Corporation
219 Vassar Street
Cambridge, MA   02139
Attn: E. Demetri   1

General Applied Sciences Lab
Merrick and Stewart Avenues
Westbury, NY   11590
Attn: G. Roffe   1

General Electric Company
Gas Turbine Technical Resources Operation
Bldg. 53, Room 331
One River Road
Schenectady, NY   12345
Attn: N. R. Dibelius   1

Curtiss-Wright Corporation
One Passaic Street
Woodridge, NJ   07075
Attn: S. Moskowitz   1

AVCO Corporation
Lycoming Division
550 South Main Street
Stratford, CT   06497
Attn: N. R. Marchionna   1
       G. Opdyke   1

International Harvester Company
Solar Division
2200 Pacific Highway
San Diego, CA   92112
Attn: W. A. Compton   1

The Boeing Company
Commercial Airplane Division
P.O. Box 3991
Seattle, WA   98124
Attn: P. Johnson   MS 73-07   1

Westinghouse Electric Corporation
Research and Development Center
Pittsburgh, PA   15235
Attn: Richard M. Chamberlin   1

No. of Copies

Westinghouse Electric Corporation
Gas Turbine Systems Division
P.O. Box 9175
Philadelphia, PA 19113
Attn: S. M. DelCorso   1

Douglas Aircraft Company
3855 Lakewood Blvd.
Long Beach, CA 90846
Attn: A. Peacock   MS 36-41   1

United Technologies Corporation
Pratt and Whitney Aircraft Group
Commercial Products Division
400 Main Street
East Hartford, CT 06108
Attn: A. Marsh   E1F1   1
       P. Goldberg   E2C   1
       Library   Rec. Center   1
       H. Craig   E2G3   1
       R. Lohmann   E2G3   1

United Technologies Corporation
Pratt & Whitney Aircraft Group
Government Products Division
Box 2691
West Palm Beach, FL 33402
Attn: S. A. Mosier   GPD E75   1
       J. R. Herrin   GPD E75   1

McDonnell - Douglas Company
Lambert - St. Louis Municipal Airport
P. O. Box 516
St. Louis, MO 63166
Attn: J. Snider   1

Williams Research Corporation
2280 West Maple Road
Walled Lake, MI 48088
Attn: A. Plumley   1

Ashland Petroleum Company
Ashland, KY 41101
Attn: W. A. Sutton   1

No. of Copies

Exxon Research and Engineering Company
P.O. 51
Lindon, NJ 07036
Attn: W. G. Dukek   1
       W. Blazowski   1

Texaco
P.O. Box 509
Beacon, NY 12508
Attn: Kurt H. Strauss   1

Shell Oil Company
P. O. Box 2463
Houston, TX 77002
Attn: Robert T. Holms   1

AMOCO
Research & Development Dept.
P.O. Box 400
Naperville, IL 60540
Attn: A. Couper   1

Garrett/AiResearch Company
402 South 36th Street
Phoenix, AZ 85034
Attn: J. M. Haasis   1
       T. W. Bruce   1

Batelle Columbus Laboratories
505 King Avenue
Columbus, OH 43201
Attn: Mr. David W. Locklin   1

Parker Hannifin Corporation
17325 Euclid Avenue
Cleveland, OH 44112
Attn: H. C. Simmons

United Technologies Research Center
East Hartford, CT 06108
Attn: R. Pelmas   1
       J. Keilbach   1

Southwest Research Institute
6220 Culebra Road
Post Office Drawer 28510
San Antoinio, TX 78284
Attn: Clifford A. Moses   1   165

No. of Copies

Chevron Research Company
575 Standard Avenue
Richmond, CA 94802
Attn: J. A. Bert   1